Indian Ocean Observing System (IndOOS)

Decadal Review

January 2018

Sponsored by

Table of Content

Executive summary

J. Vialard[1], L. Beal[2]

1. Laboratory of Oceanography & Climate (IRD), France

2. University of Miami, USA

Sustained Indian Ocean observations for climate: IndOOS 2020-2030

IndOOS is the sustainable ocean observing system for the Indian Ocean. The goal of IndOOS is to provide sustained high-quality oceanographic and marine meteorological measurements to support knowledge-based decision-making through improved scientific understanding, weather and climate forecasts, and environmental assessments. The current IndOOS design was established on the basis of the Implementation Plan drafted by the CLIVAR/GOOS Indian Ocean Panel (IORP) in 2006. Since then, societal and science priorities and measurement technologies have evolved and many of the practicalities of implementation have been learned. In this summary we incorporate these needs, tools, and experiences into actionable recommendations for priority observing system components moving forward, including pilot studies with new technologies. Justification for these recommendations is grounded in the chapters of this white paper, where we review the current status of IndOOS and its past successes and failures; articulate scientific and operational drivers and their societal impacts; and identify the essential ocean variables (EOVs) that address these drivers, their geographical coverage and spatio-temporal resolution.

1. Societal motivations

The Indian Ocean may be the smallest of the four major oceanic basins, but the 22 countries that border its rim gather one third of mankind. Many of these countries have developing or emergent economies, which are vulnerable to extreme weather events and climate change.

Many Indian Ocean rim countries depend on rain-fed agriculture. In India, for instance, 60% of jobs are in agriculture, which accounts for 20% of GDP, and there is a tight link between grain production and monsoon rainfall (Gadgil and Gadgil, 2006). Indian Ocean sea surface temperatures have been shown to influence these monsoon rains, as well as flooding in east African countries (Webster et al. 1999), droughts and wildfires in Indonesia (Abram et al. 2003, D'Arrigo and Wilson 2008) and Australia (Ashok et al. 2003, Ummenhofer et al. 2009a), and the strength of the Southeast Asian monsoon (Ashok et al. 2001, Hanamalai et al. 2005; Chapters 1 and 13). Recently, the Indian Ocean has been warming faster than any other basin in response to climate change (Chapter 11, Roxy et al. 2015) and as a result decreasing rainfall over eastern Africa is predicted to increase the number of undernourished people in this region by 50% by 2030 (Funk et al. 2008).

In a region where many populations are dependent on fisheries for their livelihood (Barange et al. 2014), the intense marine productivity of the northern Indian Ocean is under threat (Chapter 12, Allison et al. 2009, Roxy et al. 2015). Here, productivity is highly vulnerable to projected climate change (Allison et al. 2009), because the monsoon winds that drive upwelling and support high productivity are changing and because underneath the surface, one of the largest regions of oxygen-depleted waters in the world ocean is expanding (chapter 2). These oxygen-depleted waters are predicted to expand towards

the ocean surface and cause an increasing number of large mortality events, as has been seen in the past (e.g. Naqvi et al. 2009).

The Indian Ocean coastal population density is projected to become the largest in the world by 2030, with 340 million people exposed to coastal hazards (Neumann et al. 2015). This rapid population growth will conflate with climate-change induced sea level rise (e.g. Han et al. 2010) and increasing tropical cyclone intensity to increase vulnerability (e.g. Elsner et al. 2008; Rajeevan et al., 2013). Already, the Bay of Bengal region witnesses more than 80% of the total fatalities due to tropical cyclones (chapter 4), while only accounting for 5% of these storms globally (Paul, 2009).

Beyond its direct impact on rim countries, the Indian Ocean influences climate globally. As a whole, the basin accounts for about one fifth of the global oceanic uptake of anthropogenic CO_2 (Chapter 8; Takahashi et al., 2002), helping to buffer the effects of global warming. It is the breeding ground for the Madden Julian Oscillation (chapter 5), an atmospheric phenomenon that modulates rainfall and tropical cyclone activity across most of the tropics (MJO; Zhang, 2005). Year to year temperature variations associated with the Indian Ocean tropical dipole influence the evolution of the El Niño Southern Oscillation (ENSO) in the neighbouring Pacific Ocean (e.g. Clarke and Van Gorder 2003; Luo et al. 2010; Izumo et al. 2010), a leading climate mode with global-scale impacts. The Indian Ocean is also a tropical-subtropical gateway from the Pacific to the Atlantic Ocean, as part of the global "conveyor belt" (Chapter 7; Broecker, 1991) that drives climate variability at multidecadal and longer timescales. For instance, a redistribution of heat from the Pacific to the Indian Ocean is thought to have played a key-role in regulating global mean surface temperatures over the last decade (Tokinaga and Xie 2012; Liu et al. 2016), with rapid warming of the Indian Ocean representing about two thirds of global ocean heat gain (Chapters 10, 11 and 14; Lee et al., 2015; Nieves et al. 2015). The Indian Ocean surface warming trend has had far reaching impacts, modulating Pacific (e.g., Luo et al. 2012, Han et al. 2014, Hamlingon et al. 2014) and North Atlantic climate (e.g., Hoerling et al. 2004) and causing droughts in the West Sahel and Mediterranean (e.g., Giannini et al. 2003; Hoerling et al. 2012).

The role of the Indian Ocean in regional and global climate variability and change, and the heightened vulnerability of its rim populations, are strong incentives to better observe, understand and model this ocean, with the ultimate goal of being able to make quantitative predictions of future climate.

2. Established scientific drivers and new frontiers

Scientific interest in the Indian Ocean is not new and was initially fostered by its unique features. One of these is its geometry. A low latitude throughflow from the Pacific via the Indonesian Seas (e.g. Gordon et al. 2010) and the Asian landmass to the north (Figure 1) bring about unusual features in the Indian Ocean, such as the reversing monsoon currents and western boundary upwelling in the north, a shallow overturning circulation and semi-annual jets along the equator, and in the southern subtropics a unique poleward eastern boundary current and the strongest western boundary current of the world ocean.

Cut off to high latitudes, the Indian Ocean receives excess heat from the atmosphere and via the Indonesian Throughflow that must be evacuated towards the Atlantic and Southern Oceans. This heat export is achieved through an upper-ocean gyre circulation and a deep overturning cell (chapter 9; Ganachaud and Wunsch, 2000; Lumpkin and Speer, 2007; Hernandez-Guerra and Talley, 2016). The properties and heat content of the outflowing

waters depend strongly on mixing in the Indian Ocean, which has been estimated to be several times stronger than in the Pacific or Atlantic, with unknown causes (Lumpkin and Speer, 2007). The variability of Indian Ocean overturning and heat export and its relationship with sea surface temperatures across the basin remains unknown at any time scale, but is thought to be strongly constrained by the Agulhas Current at the western boundary (Bryden and Beal, 2001) and by the Indonesian Throughflow (Sprintall et al., 2014).

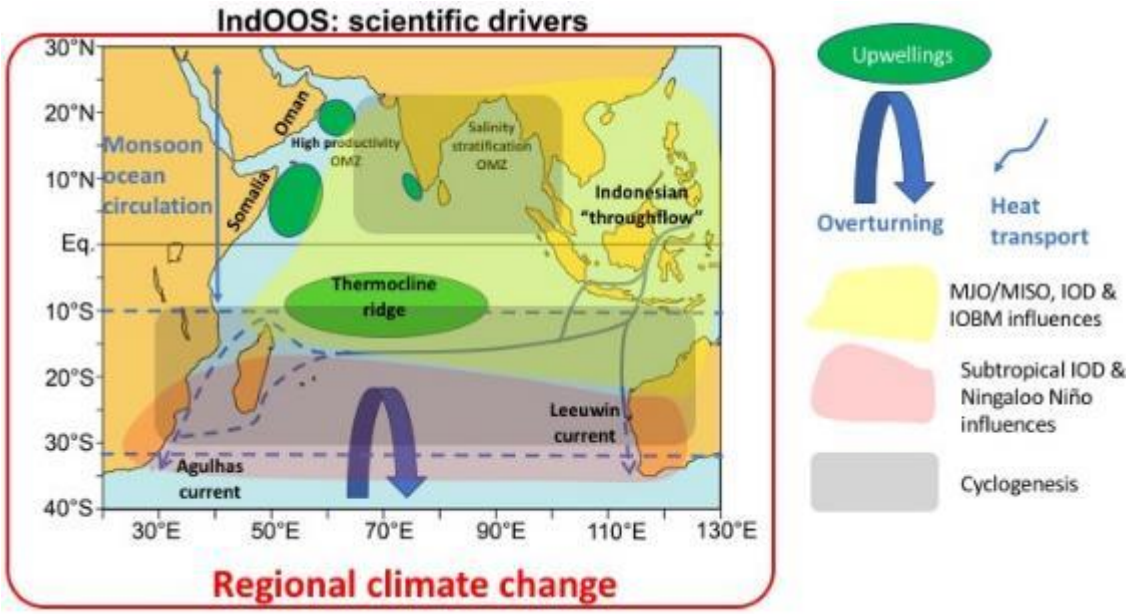

Figure 1. The region north of 10°S is strongly influenced by monsoons. The shaded regions indicate the rough area of influence of important phenomena. The green ovals indicate the main coastal or open-ocean upwellings. The thin blue arrow indicates the Indian Ocean part of the global oceanic "conveyor belt". Key regions are also named.

The presence of the Asian landmass induces a complete reversal of the winds across the northern Indian Ocean; the northeast and southwest monsoons (e.g. Schott et al. 2001). These winds drive a complex reversal of the currents north of 10°S (Figure 1), including the Somali Current at the western boundary and semi-annual eastward jets (the Wyrtki jets) along the equator that redistribute heat zonally during the inter-monsoon periods and help to establish the mean state. Many of these oceanic processes are not well reproduced by state-of-the-art climate models, with adverse impacts on predictability of the monsoons (e.g. Annamalai et al. 2016). The strong southwest monsoon winds also yield intense upwelling along the western boundary in the Arabian Sea (figure 1, chapter 3). This unique upwelling system modulates evaporation and moisture transport towards India (Chapter 1, Izumo et al. 2008), provides a globally significant source of atmospheric CO_2 (chapter SD08), and fosters intense oceanic productivity (chapter 12). This high productivity, together with low ventilation, leads to a subsurface depletion of oxygen (oxygen minimum zone, chapter 2) that is now expanding and has already led to a dramatic shift in the Arabian Sea ecosystem (Gomes et al., 2014). In the Bay of Bengal, saline stratification creates a very different habitat. Excess freshwater input from monsoon rain and river runoff strongly inhibits the vertical mixing of both heat and nutrients. This barrier layer is thought to regulate regional climate (Shenoi et al. 2002), oceanic

productivity (Prasanna Kumar et al. 2002), wet/dry spells of the monsoon (chapter 5), and cyclogenesis (Sengupta et al. 2008).

While the powerful ENSO climate mode focussed the attention of the international climate community during the 1980s, the last two decades have witnessed rising awareness of the importance of coupled climate variations in the Indian Ocean (Schott et al. 2009). The tropical Indian ocean has a large warm pool (surface temperature >27.5°C), common to the neighbouring Pacific, that maintains atmospheric convection (e.g. Graham and Barnett, 1987) and energizes the largest global atmospheric circulation cell, the Walker circulation. This Indian Ocean warm pool is modulated at the 30-90 day timescale by the Madden-Julian Oscillation (MJO) in boreal winter and by the Monsoon intraseasonal oscillation (MISO) in summer (chapters OD01 and SD05, figure 1), oscillations that are strongly coupled with Indian Ocean processes. These modes influence rainfall and cyclogenesis and, if simulated correctly, could yield enhanced predictability throughout the tropics (chapter 15). The western tropical Indian Ocean, around 5-10°S, is another important region for air-sea coupling. The thermocline dome of the tropical gyre is very shallow, making sea surface temperatures highly sensitive to atmospheric anomalies, with impacts on cyclogenesis and MJO development (e.g. Vialard et al. 2009).

At interannual time scales the tropical Indian ocean is strongly influenced by ENSO, warming uniformly during El Niño events (chapter 6) and remaining warm (e.g. Xie et al. 2009), a response known as the Indian Ocean Basin Mode (IOBM). But the Indian Ocean also has important interannual climate modes of its own, such as the Indian Ocean Dipole (IOD, Saji et al. 1999; Webster et al. 1999, chapter 6). In its positive phase, cold surface temperatures near Java-Sumatra, warm temperatures in the western tropical Indian Ocean thermocline dome, and anomalous easterly winds near the equator induce various impacts like droughts in Indonesia and Australia and floods over eastern Africa (e.g. Yamagata et al. 2004). The IOD develops through the Bjerknes feedback, similar to ENSO (Saji et al. 1999; Webster et al. 1999), with equatorial wave processes playing a central role in its evolution (Nagura and McPhaden 2010; McPhaden et al. 2015), and often co-occurs with ENSO (Yamagata et al. 2004). The Indian Ocean is also home to two subtropical climate modes. Subtropical Indian Ocean Dipole events manifest as large-scale SST anomalies spanning 15-45°S, with strong influence on South African rainfall (Reason 2001). Ningaloo Niño events are marine heatwaves off western Australia which can affect fisheries and lead to increased Australian rainfall. In 2011 a strong event caused the first recorded bleaching of the pristine Ningaloo reef (Feng et al. 2013). Some Ningaloo Niño events have predictability due to their association with ENSO (e.g. Doi et al. 2016).

The relative paucity of observations prior to the advent of IndOOS ten years ago has largely precluded studies of decadal and multi-decadal variability of the Indian Ocean (chapter 10), except through sparse repeat hydrography lines (now GO-SHIP). Hence, little is known in comparison with our understanding of the Pacific Decadal Oscillation and North Atlantic Oscillation (Han et al. 2014) and this is a serious problem when it comes to distinguishing climate change trends from patterns of natural variability (e.g. Carson et al. 2015). Even less is known about the changing biogeochemistry of the Indian Ocean at these time scales. There is, however, no doubt that the Indian Ocean, as other basins, is responding to anthropogenic climate change, with evidence of increasing surface temperatures and heat content, rising sea level, increased carbon uptake, and an intensified water cycle (IPCC 2013). The biogeochemical consequences of these changes are serious, with warming, acidification, and an expansion of oxygen minimum zones all putting serious stress on ecosystems (Bopp et al. 2013). Understanding regional patterns of change within the Indian Ocean (e.g. Han et al. 2010), the coupling and time scales of

those changes, and predicting future change to the benefit of marine management and coastal resilience for Indian Ocean rim countries is our future challenge. Only a well-planned and internationally-supported IndOOS can provide the needed data.

The outsized increase in Indian Ocean heat content over the last decade, representing 60% of the global increase (Lee et al. 2015; Vialard 2015; Nieves et al. 2015; Liu et al. 2016), is a potent illustration of the need for sustained observations: Will the Indian Ocean continue to warm more rapidly than the rest of the world ocean? What effects will this have on the Walker circulation? On upwelling, ecosystems, and fisheries? On the monsoon wet/dry spells (MISOs)? On carbon uptake and vertical mixing? On cyclone activity and storm surges? Where and how will the excess heat received by the Indian Ocean be distributed? To answer these questions and others of societal importance requires sustained measurements of essential ocean variables (EOVs): upper-ocean temperature, salinity, air-sea fluxes, and currents at hourly-to-daily time scales across the tropics, augmented with chlorophyl, nutrients, oxygen, pCO2, and pH within the Arabian Sea, Bay of Bengal, and off western Australia; weekly-to-monthly measurements of full-depth temperature, salinity, nutrients, and pCO2 throughout the subtropics; and full-depth, high spatial resolution, daily-weekly measurements of these same EOVS plus velocity within boundary fluxes, such as in the Agulhas Current and Indonesian Throughflow.

3. IndOOS components and its achievements

IndOOS (Figure 2) has been comprised of five *in situ* observing networks: profiling floats (Argo), surface drifters (GDP), a moored tropical array (RAMA), seasonal repeat temperature/salinity lines (XBT/XCTD network), and tide gauges. Augmenting these networks are remotely-sensed observations of surface winds, sea level, sea surface temperature and salinity, rainfall, and ocean colour (chapter 18).

The Research Moored Array for African-Asian-Australian Monsoon Analysis and prediction (RAMA, chapter 20, McPhaden et al. 2009) was arguably the observing network that launched IndOOS. It followed from tropical arrays in the Pacific and Atlantic Oceans, which together comprise the Global Tropical Moored Buoy Array (McPhaden et al, 2010). These arrays provide sub-daily time series of key oceanographic and surface meteorological variables in real-time (https://www.pmel.noaa.gov/gtmba/) in a region where the oceanic response to atmospheric forcing is rapid and coupled feedbacks are critical. All RAMA moorings measure meteorological surface parameters and oceanic temperature and salinity down to 500m. Some also make direct measurements of velocity, including three sites measuring deep currents along the equator, while others are “flux reference sites” with additional measurements for computation of momentum, heat, and freshwater fluxes across the air-sea interface (chapter 16), and a few sites have biogeochemical sensors (chapter 8). RAMA data have enabled the study of tropical modes of variability in the Indian Ocean, such as the MJO, MISO, and IOD, as well as the equatorial circulation and biophysical interactions. RAMA data also feed important operational applications, such as numerical weather and seasonal forecasts, gridded continuous estimates of air-sea fluxes, ocean re-analyses, and inter-calibration of successive satellite missions (chapters 15, 16, 17, 18). As one measure of its outstanding success, the original RAMA publication (McPhaden et al, 2009) has been cited 232 times as of December 2017.

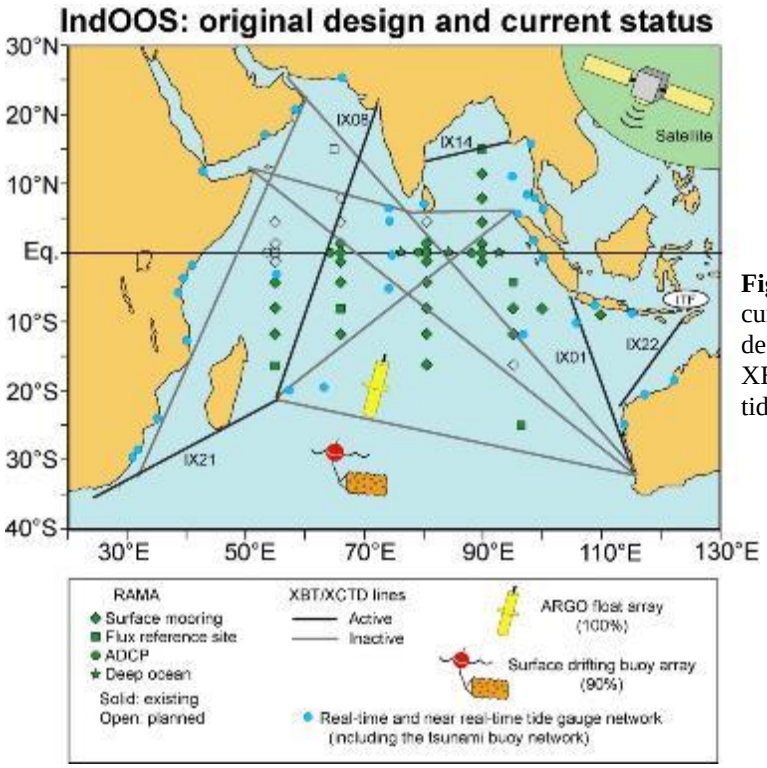

Figure 2. IndOOS original design and current state. The original IndOOS design comprises the RAMA, Argo , XBT/XCTD, surface drifting buoys and tide gauges components.

The Argo network is global (Chapter 19, Gould et al. 2004), consisting of one autonomous profiler per 3° x 3° region, each profiling the ocean (temperature, salinity, and pressure) down to 2000 m every 10 days for at least 3 years. Full coverage requires about 450 floats in the Indian Ocean north of 40°S and was first achieved in 2008. There are currently 576 active floats providing over 20,000 profiles per year. Argo data have captured the seasonal-to-interannual variability of the subtropical circulation and thermohaline structure in the Indian Ocean for the first time and were instrumental in tracking the enormous oceanic heat uptake during the "hiatus" decade (chapter 2). Argo has become a primary data source for operational oceanography (chapter 17) and for validating and initialising numerical models of the ocean and climate. A growing number of profilers (currently 48) are equipped with biogeochemical sensors to measure key processes related to plankton blooms, OMZs, and fisheries, to name a few, particularly in the Arabian Sea, Bay of Bengal, and thermocline dome region.

The voluntary observing ship eXpendable BathyThermograph (XBT) network collects temperature observations over the upper ~800 m of the ocean along regular commercial shipping routes. Prior to the advent of Argo, XBTs provided more than 50 % of all subsurface temperature observations (chapter 22). The XBT network is transitioning to monitoring phenomena poorly sampled by Argo, such as boundary currents and oceanic fronts, mesoscale variability, and volume and heat transports. For instance, the IX01 and IX22 XBT lines between Indonesia and Australia are critical for quantifying the interannual-to-decadal variability of the Indonesian throughflow (Meyer et al., 1995; Sprintall et al., 2002; Wijffels et al., 2008) and were able to capture its strengthening trend during 1984-2013 (Liu et al., 2015), which has played an important role in the redistribution of heat between the Pacific and Indian ocean over the last decade (Lee et al. 2015, Nieves et al. 2016; Vialard, 2015).

The Global Drifter program (GDP, chapter IR04) consists of surface drifters drogued to follow ocean currents at a density of one drifter per 5° x 5° region. All drifters also measure temperature and about half now measure sea level pressure, which has significantly improved numerical weather prediction (Centurioni et al. 2016). Coverage in the Indian Ocean has been about 70% since 1996 and about 90% since 2014. Surface drifters have allowed the seasonal mapping of the reversing monsoon circulation in the Arabian Sea (Beal et al., 2013). The tide-gauge network around the Indian Ocean rim provides measurements of sea-level (chapter 23) which are needed for Tsunami warnings, the monitoring and prediction of tides, the study of cyclone-induced storm surges (chapter 4), and for the understanding of basin-scale variations and trends in sea level rise (chapter 14). Tide gauges can also provide proxies for dynamical changes, such as coastally-trapped waves and the Pacific inflow along the west coast of Australia (chapter 9). Only a subset of tide gauges also monitor the level of the land, a necessary condition for a precise quantification of long term trends in sea level.

The observing networks that make up IndOOS are most effective when combined together and used with other vital observing programs, such as global satellite missions and the decadal, multi-disciplinary, hydrographic surveys of GO-SHIP. For example, Vialard et al. (2008) used a combination of RAMA, Argo, and satellite data to discover links between the thermocline dome region of the southwestern tropical Indian Ocean and the Madden-Julian Oscillation.

4. IndOOS 2020-2030: the way forward

The first decade of IndOOS has held its promise for unprecedented measurements of phenomena such as cyclones, the MJO and IOD, the equatorial circulation, and the Indonesian throughflow. **These are important measures that must be preserved in the future design.** However, IndOOS has so far fallen short of providing some critical data for the investigation of Indian Ocean biogeochemistry and fisheries, and for decadal variability and climate change.

In the Arabian Sea, where piracy and vandalism has long been a stumbling block for the completion of RAMA, **lack of measurements of the uniquely seasonal western boundary current, upwelling system, and oxygen minimum zone has stunted our understanding of biological productivity as well as monsoon variability and predictability**. With piracy receded, deployments are planned in the Arabian Sea in 2018. There have been few biogeochemical measurements as part of IndOOS (chapters 8, 19, and 2) and **hence biophysical processes and the carbon cycle remain poorly understood even in critical regions like the northern Indian Ocean oxygen minimum zones and eastern boundary upwelling cells. The subtropical Indian Ocean has also been relatively neglected** while it harbours climate modes, such as Ningaloo Niño and subtropical IOD (chapter 6), and is one of the fastest warming regions of the world ocean (chapter 11). Recent widespread interest in the “hiatus” in climate change and the associated storage of heat in the Indian Ocean has put strong emphasis on the need to be able to estimate basin-scale budgets over long time scales (chapter 7). This requires **monitoring the fluxes across the open southern boundary of the Indian Ocean, including the mighty Agulhas Current**, capturing changes in subtropical stratification, including Antarctic bottom water, and **improving surface flux estimates, particularly in the cloud-rich regions of the tropical Indian Ocean** (chapter 16).

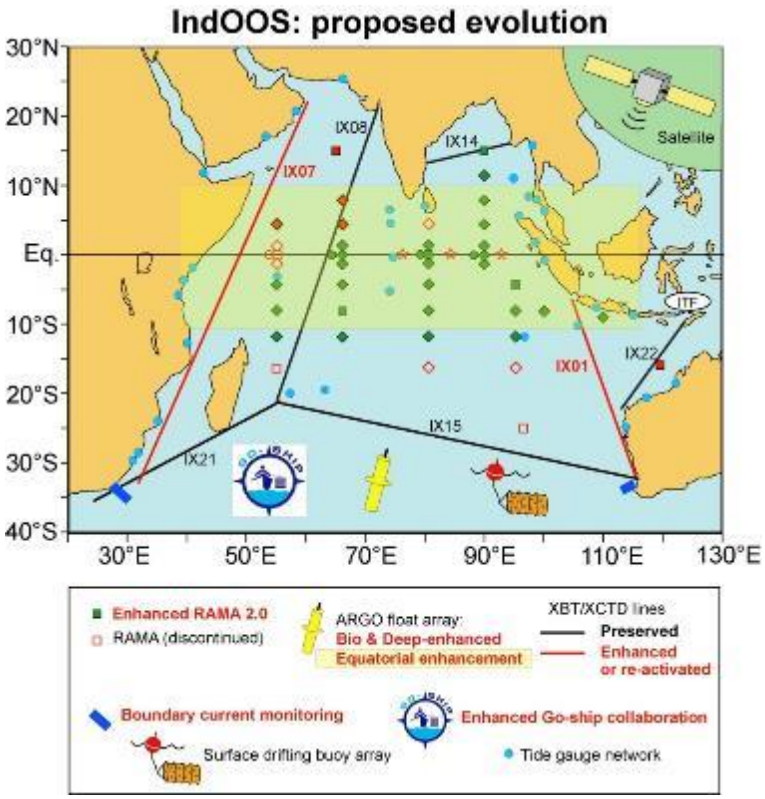

Figure 3. IndOOS original design and current state. The original IndOOS design comprises the RAMA, Argo , XBT/XCTD, surface drifting buoys and tide gauges components.

Increasing societal demand for seasonal-to-decadal climate predictability in the face of global warming makes the need for strategic, sustained observations of the Indian Ocean more urgent. At these time scales understanding the role of the ocean and its feedbacks are paramount. Here, we distill the collective wisdom from the chapters of this decadal review into a list of recommendations that can provide an Indian Ocean Observing System more capable of meeting these societal demands in the future.

Actionable recommendations:

A. **Maintain core components of IndOOS. A1:** RAMA, Argo, and surface drifter networks are the mainstays of IndOOS and must be completed and sustained. Multi-decadal records are critical, since so few long-term measurements exist, therefore **A2:** Prioritise XBT lines which have been active for 30 years or more, and **A3:** Prioritise established, long-term tide gauge measurements and add ground elevation monitoring.

B. **Expand observing system into the Arabian Sea.** The Arabian Sea is a critical region for understanding monsoon processes and predictability, and biogeochemical processes and marine productivity, yet piracy has precluded observations for almost two decades. **B1:** Deploy RAMA sites in the Arabian Sea with biogeochemical sensors. **B2:** Re-activate a portion of the IX07 XBT line with enhanced sampling in boundary current and upwelling regions. **B3:** Prioritise bio-Argo deployments in the Arabian Sea (Chlorophyll, oxygen, nutrients, pH).

C. **Eliminate redundancy and consider logistical constraints. C1: Re-e**valuate the need for XBT lines IX22, IX08, and IX14 and prioritise a sustained Argo network

in their place. **C2:** Streamline RAMA by elimination of thirteen moorings from the original design. This will ease current implementation challenges and the upcoming transition to more capable T-FLEX moorings (Figure 2 and chapter IR03).

D. Improve Indonesian Throughflow monitoring. D1: Maintain and enhance measurements of volume, heat, and freshwater transports along XBT line IX01 by including XCTDs for salinity measurements, a thermosalinograph to capture surface properties, automated XBT launchers, and a hull-mounted ADCP (chapter IR07). **D2:** A pilot project for glider deployments along IX01.

E. Measure the overturning and heat budget of the Indian Ocean. Three elements are needed, **E1**: Sustain an Agulhas Current volume, heat, and freshwater transport array (such as ASCA, chapter 24) and consider a pilot glider project. **E2:** Deploy a hydrographic end-point mooring (or CPIES) in deep water near the end of the Leeuwin current array off Australia, and **E3:** Launch a deep-Argo program in the subtropical Indian Ocean to capture the deep overturning cell (chapter 24). Finally, **E4:** Evaluate IX15 and IX21 XBT lines as possible additional constraints on transport.

F. Implement joint biophysical measurements, including chlorophyll, CO_2, oxygen, pH, and essential nutrients, beginning in key regions. **F1:** Deploy bio-Argo floats in Somali and Omani upwelling cells, Arabian Sea and Bay of Bengal OMZs, thermocline dome upwelling region, and south of Madagascar (chapter 12). **F2:** Enhance RAMA moorings with biogeochemical sensors in the Arabian Sea, Bay of Bengal, and Java upwelling regions.

G. Establish and enhance air-sea flux reference sites. G1: Implement unoccupied RAMA flux reference sites in western tropical Indian Ocean. **G2:** Establish new flux reference sites at the mouth of the Indonesian Throughflow, in the eastern equatorial Indian Ocean where various flux products strongly disagree (chapter 16), and within the Agulhas Return Current. **G3:** Enhance a subset of flux reference sites for direct flux measurements. **G4:** Improve vertical sampling to capture the diurnal cycle at selected flux reference sites in convective regimes, such as the Bay of Bengal, eastern equatorial Indian Ocean, and the thermocline dome.

H. Constrain the deep circulation and capture multidecadal timescales. Improve mapping of the deep Indian Ocean thermohaline structure and circulation. **H1:** Deploy deep-Argo in the most under-sampled regions of the deep Indian Ocean and to capture the deep overturning at ~32°S. **H2:** Increase collaboration with GO-SHIP decadal hydrographic surveys to optimize the use of ship-time and promote international participation for targeted Indian Ocean surveys.

I. Pilot project for high-resolution thermohaline monitoring in the tropics. Iridium Argo floats spend only minutes at the surface, compared to hours for the original Argos floats, allowing for improved sampling of strong and divergent currents along the equator that could complement RAMA. J1: Pilot project to double the number of Argo floats with enhanced 5-day temporal resolution within 10° of the equator.

J. Complementary satellite observations. Planned satellite missions will ensure a good continuity for EOVs such as SST, sea level, ocean winds and colour, and outgoing long-wave radiation. However, the following missions are also essential

I1: Passive microwave SST measurements to track SST signals under atmospheric convection (chapter IR01, Sengupta and Ravichandran 2001, Duvel and Vialard 2007). **I2.** Sea Surface Salinity, due to the strong role of the halocline in regulating air-sea interactions in the Bay of Bengal and equatorial Indian Ocean. **I3.** Increase the number of scatterometers (currently 2) to minimize aliasing of winds by the diurnal cycle in the equatorial Indian Ocean.

Part I: Science Drivers

1. Indian Ocean and South-Asian monsoon: upper-ocean processes relevant to monsoon annual cycle

H. Annamalai[1], Motoki Nagura[2], Kelvin Richards[1], Caroline Ummenhofer[3]
[1]International Pacific Research Center (IPRC)/Department of Oceanography, University of Hawaii, USA
[2]JAMSTEC, Japan
[3]Woods Hole Oceanographic Institution, Woods Hole, USA

In the past few decades, research has shown that the annual cycle of the South-Asian monsoon results from complex interactions among the ocean, atmosphere and land components of the climate system. At the same time, progress in improving the coupled models used to simulate and predict the monsoon has been slow (Delsole and Shukla 2002; Turner and Annamalai 2012), despite data available from multiple observational platforms (in situ, satellite, dedicated field experiments, etc.). Due to the complexity of the monsoon, identifying specific causes for the slow progress is difficult but possible conjectures include: (i) persistent model errors are not due to limitations in one particular parameterization but due to multiple processes and their interactions and (ii) current suite of observations is not adequate enough for understanding the monsoon systems, and to constrain model physics (Annamalai et al. 2017; Zhao et al. 2017). The seasonal mean monsoon rainfall largely dictates the socio-economic conditions of the small-scale farming communities in South and Southeast Asia that has a direct implication on the rice cultivation of the World. Furthermore, diabatic heating associated with the monsoon influences the global circulation. Given the global manifestation of the monsoon, understanding and modeling the processes responsible for its annual cycle remains a grand challenge of the World Climate Research Program.

In this chapter, with a focus on upper-ocean physics, we argue that, in order to improve our understanding of coupled process and to constrain model physics, specific, new and sustained observations in the tropical Indian Ocean (TIO) are needed. Based on existing knowledge of the impact of TIO processes on the mean monsoon (Section 1.1), we review essential ocean variables (EOV) that are needed to understand the processes more completely (Section 1.2). We conclude with a list of specific actions that need to be undertaken (Section 1.3). Note that this chapter does not address variability associated with the south Asian monsoon at any time scales.

1.1 Background

Previous works point toward the importance of upper-ocean processes in monsoon annual cycle (Shenoi et al. 2002; Schott et al. 2009; Seo et al. 2009; Thadathil et al. 2016; Annamalai et al. 2015; Nagura et al. 2015). Here, we review a few results in support of this idea.

ITCZ/Indo-Pacific warm pool relationship

The monsoon annual cycle is primarily driven by the seasonal displacement of the Intertropical Convergence Zone (ITCZ), which is anchored by the north-south migration of the Indo-Pacific warm pool (regions where sea surface temperature [SST] is >28°C;

Shukla and Fennessy 1994). Figures 1.1a and 1.1b plot SST (contours) and precipitation (color shading) during boreal summer and winter. During both seasons, there is intense rainfall (>8 mm/day) only in regions where SST is high (>28°C), suggesting the former is a necessary condition for the latter (e.g., Graham and Barnet 1987). The SST/precipitation relationship, however, is not one-to-one, indicating that other factors such as moisture availability in the atmosphere, tropospheric stability (Raymond 2000; Bretherton et al. 2004) and cloud-radiative feedbacks (Stephens et al. 2008) impact rainfall intensity. During the summer monsoon, orography clearly impacts precipitation, with the Western Ghats in India and Arakan Range in Myanmar causing localized heavy rainfall. During winter (summer), despite southward (northward) displacement of the thermal equator, SST over the Bay of Bengal (Equatorial Indian Ocean) remains warm with values around 28°C, suggesting the role of oceanic processes in its maintenance. Important aspects of these oceanic processes, such as upper-ocean stratification and equatorial eastward flowing Wyrtki Jets (WJs), and relevant EOVs required to understand, and model the monsoon annual cycle are discussed next.

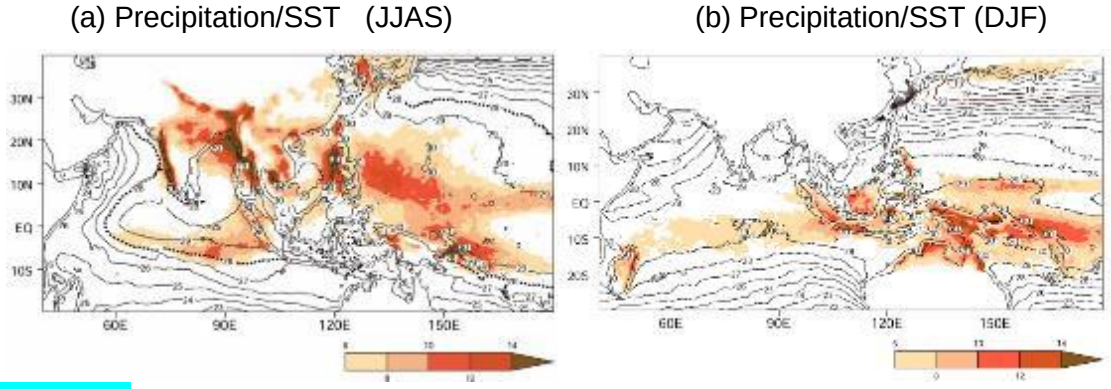

Figure 1.1: (a) Boreal summer (June-September) climatology of precipitation (shaded; mm/day) and SST (contours; °C) constructed from TRMM/TMI products (1998–2015) and (b) same as (a) but for the boreal winter (December–February) season.

Upwelling

In the northern Indian Ocean, there is a remarkable east-west asymmetry in SST and precipitation during the monsoon (Fig. 1.1a), which to a large extent results from ocean processes. Just prior to the monsoon, SST is the warmest of all the tropical oceans throughout the northern Indian Ocean (Joseph 1990). During the monsoon, there is intense upwelling of cold water along the Somali and Omani coasts driven by the cross-equatorial low-level (Findlater) jet, and SST drops to about 23–24°C (Fig. 1.1a). Subsequently, horizontal advection by ocean currents,

in conjunction with evaporative cooling, cools SST in the central Arabian Sea (e.g., McCreary et al. 1993), weakening rainfall there. These processes limit the westward extension of the warm pool (Shenoi et al. 2002). In contrast, SST over the Bay of Bengal remains high because upwelling along the east coast of India is weak or absent (McCreary et al. 1993), and rainfall is much stronger there resulting in upper-ocean stratification (Shenoi et al. 2002; Thadathil et al. 2008; Seo et al. 2009). During winter, lack of upwelling along the Somali and Omani coasts leads to SST being warmer there (Fig. 1.1b) than during the summer (Schott and McCreary 2001). Observing and modeling the fine details of the upper-ocean stratification over the Bay of Bengal, and its subsequent impact on SST evolution remain a challenge.

Salinity impacts on upper-ocean stratification

The near-surface stratification is impacted locally by the surface freshwater flux (precipitation and river run-off) and remotely through advection. The freshwater thins the surface mixed layer, and generates a barrier layer that prevents the entrainment of cold subsurface waters (Lukas and Lindstorm 1991). Furthermore, solar radiation can penetrate the mixed layer to warm the barrier layer, thereby generating temperature inversions (Sengupta and Ravichandran 2001). Two such regions in the northern Indian Ocean are the Bay of Bengal (Howden and Murtugudde 2001; Shenoi et al. 2002; Thadathil et al. 2008; 2016) and the Arabian-Sea mini-warm pool (Rao and Sivakumar 1999; Durand et al. 2004). *In these regions, are there adequate observations (spatial coverage, vertical and horizontal resolutions) to quantify processes that determine upper-ocean physics and assess their subsequent impacts on SST throughout the annual cycle?*

Bay of Bengal: During winter, cold and dry northeasterly monsoon winds are directed away from the Asian continent and SST drops to < 27^{o}C over the northern Arabian Sea but remains warm (~28^{o}C) over the Bay of Bengal (Fig. 1.1b), due to temperature inversions in the upper ocean. Results from limited observations over the northern bay suggest roughly equal contributions from precipitation and river-runoff to the freshwater-flux (e.g., Dai et al. 2009). Thadathil et al. (2008) examined seasonal variations in barrier-layer thickness over the Bay of Bengal and found that the annual mode exhibits maxima during November-December and the semi-annual mode peaks during February-March and August-September. By examining observations from RAMA buoys Thadathil et al. (2016) confirmed that the temperature inversion peaks during November-December but its existence is prominent only over the northern Bay of Bengal, and through budget analysis the authors suggested that net heat loss is the dominant process in controlling the formation and maintenance of the surface temperature inversion. Anderson and Riser (2014) examined upper-ocean measurements of temperature and salinity obtained from few Argo profiling floats equipped with auxiliary surface temperature and salinity sensors (STS) across the Bay of Bengal. These measurements with a vertical resolution of 10 cm in the top 2-4 m indicate large surface stratification with pronounced vertical gradients implying the role of heavy precipitation, and river input for the floats located in the northern Bay of Bengal. By examining fast cycle data (observed every 2 hours), they also noted large diurnal temperature amplitudes in the precipitation-dominated region of the Bay of

Bengal. Note that TMI observations (Fig. 1.1b) suggest SST values are > 28°C over central Bay of Bengal (around 15°N) during boreal winter. Is this a consequence of upper-ocean salinity stratification? Furthermore, Thadathil et al. (2007) pointed out that currents advect the barrier layer. The thick barrier layer spreads towards the interior of the bay being advected by wintertime anticyclonic circulation. It also spreads to the south being advected by the southward East India Coastal Current (EICC) in winter. Akhil et al. (2014) explicitly showed the contribution of EICC to the spreading of freshwater using a high-resolution regional ocean model. So observations on advection of salinity are needed too.

Arabian Sea mini-warm pool: The onset of the monsoon during late May–early June is characterized by a spectacular "burst of precipitation" around southern tip of India and a "sudden jump in low-level kinetic energy" over the near-equatorial western Arabian Sea. In some years during the onset, an "onset vortex" that leads to cyclonic storms forms over southern Arabian Sea. It is fueled by the presence of very warm SST over southeastern Arabian Sea (68°–77°E, 6°–15°N; the "mini-warm pool") and barotropic instability of the basic monsoon flow (Krishnamurti et al. 1981). Based on limited observations and model solutions, Durand et al. (2004), Vinaychandran et al. (2007), Mason et al. (2005) and Nyadijo et al. (2012) noted the importance of advection of low-saline waters (from the Bay of Bengal) in promoting salinity stratification and temperature inversion in the upper ocean. From case studies, a casual relationship between salinity over this mini-warm pool or its latitudinal position and monsoon rainfall (Neema et al. 2012; Sijikumar and Rajeev 2012) has been suggested, but the actual mechanisms are unclear.

Equatorial Indian Ocean

The equatorial Indian Ocean (EIO) differs from the other equatorial oceans in that it lacks trade winds, owing to the strong atmospheric convection over the eastern EIO and Maritime Continent (Figs. 1.1a-b). As a consequence, the EIO experiences semiannual westerly winds during the intermonsoon periods when the ITCZ crosses the equator, with a stress magnitude of about 0.4 N/m^2 (Fig. 1.2a). They force the eastward-flowing WJs (Wyrtki 1973), which attain velocities of the order of 80 cm/s near the surface (Fig.1.2b).

(a) EIO wind stress (b) Surface currents (3°S-3°N)

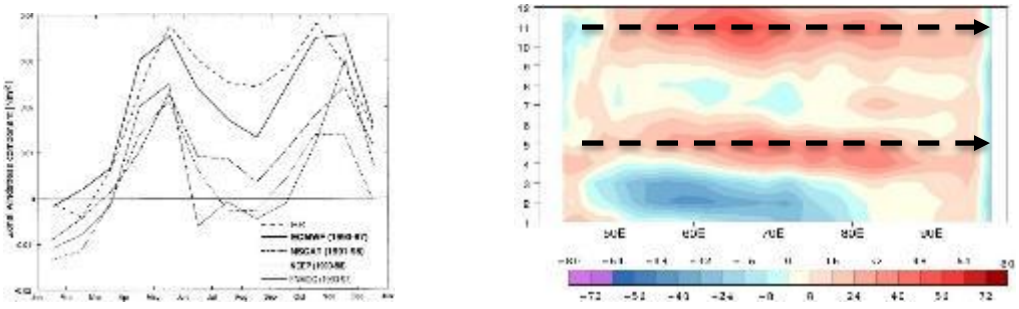

Figure 1.2: (a) Mean seasonal cycle of zonal wind stress (N/m^2) component, averaged from 60–90°E, 1°S–1°N band from various reanalysis products and observations

(from Schott and McCreary 2001) and (b) annual cycle of equatorial surface currents (cm/s) climatology obtained from OSCAR. The dotted lines in (b) indicate spring and fall Wyrtki Jets. The curves in (a) suggest "observational uncertainty".

The WJs carry mass and heat from the western to the eastern EIO and are instrumental in maintaining the warm pool over the eastern EIO (Reverdin 1987; Rao and Sivakumar 1999), so that even during boreal summer, eastern EIO experiences warm and wet conditions (Fig. 1.1a). Conversely, but less clear, they are important for draining warm, near-surface water from the western EIO, thereby decreasing the likelihood of atmospheric convection. Since 2009 as part of RAMA array, ADCP observations are maintained at 78°E, 80.5°E, 83°E and 90°E along the equator, and also at 80.5°E across latitudes 4°S–3°N. With 5-years of observations at the latter site, McPhaden et al. (2015) estimated volume transports of spring and fall WJs. Are the estimates at one longitudinal point sufficient enough to account for mass transport and heat accumulation over the eastern EIO?

The WJs are predominantly forced by the near-equatorial winds but modeling studies suggest that salinity-induced barrier layer increases the jet speed by trapping the wind momentum in a thinner-mixed layer (Han et al. 1999; Masson et al. 2003). Note that over the eastern EIO, precipitation occurs all-year around (Fig. 1.1). A few points of interest are: (i) during the annual cycle, Bjerknes' feedback (feedback loop between ocean and atmosphere; e.g., changes in SST impacts precipitation and wind leading to changes in ocean thermocline that further impacts SST) occurs along the EIO in which WJs are an important component (Annamalai et al. 2017); (ii) WJs maintain eastern EIO warm pool that promotes local precipitation that in turn results in upper-ocean stratification, a feature important to increase the WJ speed itself and (iii) it is not clear the role of westward, equatorial current during January-March (Fig. 1.2b) in the EIO processes. Are the existing Argo floats sufficient enough to study the seasonal cycle in upper-ocean stratification along central-eastern EIO? Do we need *in-situ* near-surface wind observations to construct reliable wind-stress climatology?

Southwest Indian Ocean thermocline ridge

Over the annual cycle, owing to north-south migration of the ITCZ, thermocline ridge regions experience in-situ rainfall. While at intraseasonal timescales, there is some observational evidence for the formation of salinity stratification (Vialard et al. 2009), unlike over the Bay of Bengal, at seasonal timescales, because of lack of observations role of upper-ocean stratification is unclear here. Observations during DYNAMO/CINDY field campaign suggest for advection of freshwater from eastern equatorial Indian Ocean to the ridge region (Soares et al. 2018, manuscript in preparation). Interannual variations in the monsoon onset date are linked to variations in boreal spring season SST over the ridge region through their impacts on the poleward migration of the ITCZ (Annamalai et al. 2005), particularly during years after the peak phase of El Nino when fluctuations in thermocline depth and SST are strongly coupled (Xie et al. 2002). How to measure the contributions from horizontal advection?

Systematic errors in climate models

Finally, analyses of several generations of climate models indicate that model biases in precipitation (Sperber et al. 2013), SST (Levine et al. 2013; Sandeep and Ajayamohan 2014), thermocline depth (Yokoi et al. 2009; Nagura et al. 2013), and other atmospheric/oceanic variables persist throughout the annual cycle, implying that the tropical Indian Ocean and monsoon systems are strongly coupled, with errors in one system cascading into others (Annamalai et al. 2017). Typically, researchers have sought to relate model errors to biases in the atmospheric component of the coupled models (e.g., Martin et al. 2010). Annamalai et al. (2017), however, argue that their cause is the models' near-equatorial, coupled, ocean-atmosphere processes (Bjerknes feedback) being strong, in which case oceanic, as well as atmospheric, errors are involved. Nagura et al. (2017) note that systematic errors in Bay-of-Bengal precipitation are linked to model biases in mixed-layer thicknesses and thermocline depths in the northern Arabian Sea. Sperber and Annamalai (2014) find that almost all CMIP5 models simulate a delayed monsoon onset, indicating that the delay may result from systematic coupled errors over the southwest Indian Ocean from earlier seasons in the annual cycle. *In summary, over the TIO-monsoon climate systems, large-scale model errors in ocean-atmosphere variables are prominent over the regions where upper-ocean stratification is expected to impact air-sea interactions.*

1.2 Observations needed

Based on our current knowledge (Section 1.1), here we identify regions where observations of EOVs are needed to improve understanding of the processes that shape the upper-ocean. Such an understanding is expected to improve models' physical parameterization schemes.

Fig. 1.3 shows a consolidated map of existing observations (ship measurements and profiling floats) of in-situ temperature and salinity. Current observations along the coastal regions as well as over the sensitive regions where freshwater-flux forced salinity stratification impacts on the upper-ocean processes are sparse. In regions of thin mixed-layer Argo floats do not measure temperature and salinity in the top layers (surface – 25m) where stratification is expected to impact SST. While satellite-derived sea surface salinity observations (Aquarius) are available to construct a reasonable climatology, sustained observations for assessing sub-surface salinity over regions of interest are not yet available.

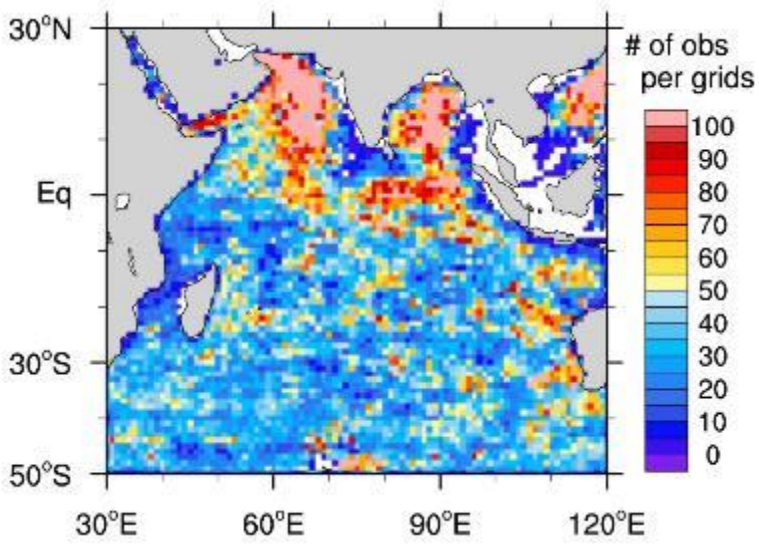

Figure 1.3: Number of in-situ observations (CTD and profiles from Argo floats) to measure temperature and salinity in the tropical Indian Ocean. (all observations since 1961 are included in constructing this map)

Upper-ocean stratification

Therefore, for a comprehensive understanding of the monsoon annual cycle, sustained three-dimensional observations of temperature and salinity over all key regions identified here are required. As of December 2017, RAMA array (https://www.pmel.noaa.gov/gtmba/rama-array-map) covers EIO, southern Indian Ocean and parts of Bay of Bengal (around 90°E). It is fair to mention that RAMA array does not cover the northern Indian Ocean, particularly upper-ocean stratification regions. Here, we focus on instruments for key regions, and suggest optimal horizontal and vertical resolutions of observations that are deemed important. Of the regions identified here, we prioritize observations for the Bay of Bengal.

Bay of Bengal: ASIRI (An Ocean-Atmosphere Initiative for Bay of Bengal), an observational and modeling program (2013-17) aimed to study the upper-ocean processes has collected unprecedented high-resolution observations from multiple instruments and have identified features in the northern Bay of Bengal where shallow, salinity-controlled mixed layers result from high river runoff and heavy rainfall (Wijesekera et al. 2016). Using field observations during November-December 2013, Mahadevan et al. (2016) suggest that mixed layers over the northern bay are of the order of ~20 m and lateral mixing due to meso-scale oceanic features contribute to upper-ocean salinity stratification. No such observations exist off the Burmese coast where high-mean precipitation occurs during boreal summer (Fig. 1.1a) and SST is > 28°C during boreal winter (Fig. 1.1b). Additionally, there is a continental shelf near the mouth of Ganges/Brahmaputra, where temperature inversion and haline stratification should be clearest, but Argo floats cannot enter there, because floats' parking depth is 1000 m, which is deeper than the bottom depth of the continental shelf. Next, we outline our recommendation for new observations.

For an extended region (12°-22°N; 80°-100°E), including the continental shelf, with a horizontal resolution of 2°x2° degree or even finer, we can aim for moored buoys in addition to Argo floats and/or equip more Argo floats with auxiliary STS sensors (~10 cm

vertical resolution in the top 2-4 m) similar to those implemented in certain regions of the Bay of Bengal (Anderson and Riser 2014). The rectangular mesh aids in the estimation of advection of salinity to and out of Bay of Bengal. To augment the reliability and in regions of very shallow mixed-layers, we also consider repeated glider sections across this region (Rainville et al. 2017) and a suite of autonomous vehicles such as SVP, and SVP-2 surface drifters (Surface Velocity Program) that are equipped with temperature and salinity sensors to measure salt fluxes associated near-surface currents and upper-ocean stratification, and other instruments such as sea-gliders implemented in SPURS (Salinity Processes in the Upper-ocean Regional Study; Fig. 1 in Lindstorm et al. 2017). *Such a multiple platform will augment the accuracy of measured fields and provide confidence in observations.*

Arabian Sea mini-warm pool: To measure upper-ocean salinity and thermal distributions over the mini warm pool (68°−77°E, 6°− 15°N), moored buoys at 10 – 20 m intervals in the vertical and at a spatial interval of 5^{o} in longitude and latitude (total of 12 buoys, preferably a rectangular mesh) with additional deployment of Argo floats with auxiliary STS sensors (at 10 cm intervals at the upper-ocean) are recommended in conjunction with ADCPs. To estimate horizontal heat advection, the rectangular mesh of buoys is necessary for temperature and salinity observations, and that of ADCPs are necessary for velocity observations. In such a configuration, for example, vertical velocity can be estimated using the continuity of mass (with a sizable error) from a rectangular mesh of ADCPs that aid in the estimation of vertical advection too.

Equatorial Indian Ocean: To assess WJ mass transports and quantify heat accumulated over eastern EIO, to further our understanding of the Bjerknes' feedback process, and to quantify accumulation of warm water (charging and discharging) ADCP observational networks need to be deployed over the eastern EIO (at 100^{o}E and 110^{o}E) and western EIO (at 45^{o}E, 50^{o}E, 55^{o}E, 60^{o}E and 65^{o}E), respectively. Over the central-eastern EIO, high vertical resolution (~10 cm) observations of upper-ocean salinity and thermal stratifications are needed and suggestions made for the Bay of Bengal region can be considered here.

Southwest Indian Ocean: Since 2009, two moored buoys (one along 55^{o}E extending from 12^{o}S-4^{o}S and another along 67^{o}E extending from 12^{o}S-Eq.) offer valuable information (but no obvious knowledge about salinity stratification) but large data gaps mask construction of a reliable climatology. Furthermore, currently no observations exist to measure salinity distribution in the upper-ocean. A feasible approach is to introduce auxiliary STS sensors on the new Argo floats, and also plan to extend RAMA bouys to few more locations (along 65^{o}E and 75^{o}E extending from 12^{o}S-Eq) yielding a rectangular mesh of bouys with the existing ones. We also recommend deployment of downward ADCP to measure velocity in the upper 40m with a vertical resolution of 0.75m to study surface Ekman flow (ref..) and examine upwelling and near-surface stratification.

Summary

In summary, ASIRI field campaign results imply that sustained observations of very high spatial (horizontal and vertical) and temporal resolutions are needed to have a comprehensive understanding of the upper-ocean physics (Wijesekara et al. 2016). In thin mixed-layer (~20 m) regions such the bay, given the fact that Argo floats could only reach up to about 25 m, and that they can't be deployed along the coastal regions, in-situ instruments are needed.

1.3 Actionable recommendations (order of priority)

(1) Over the core region of Bay of Bengal for a rectangular mesh (12^{o}N-22^{o}N, 80^o-100^{o}E), we recommend for moored buoys (2^{o}x2^o degree or even finer) in addition to Argo floats and equip more Argo floats with auxiliary surface temperature and salinity (STS) sensors. Additionally, we recommend repeated glider sections across regions of interest and a suite of autonomous vehicles as in SPURS (see Fig. 1 in Lindstorm et al. 2017), particularly over the Bay of Bengal. Vehicles such as SVP and SVP-2 drifters, and sea/wave gliders would enhance the reliability of the observations and provide the pathways for improving model parameterization schemes. Such a multi-platform is highly desirable.

(2) Over the thermocline ridge, place auxiliary STS sensors on Argo floats and extend RAMA bouys to few more locations (along 65^{o}E and 75^{o}E extending from 12^{o}S-Eq) yielding a rectangular mesh of bouys with the existing ones. We also recommend deployment of downward ADCP to measure velocity in the upper 40m with a vertical resolution of 0.75m to study surface Ekman flow and stratification.

(3) Over the EIO, ADCP networks need to be deployed over the eastern (at 100^{o}E and 110^{o}E) and western (at 45^{o}E, 50^{o}E, 55^{o}E, 60^{o}E and 65^{o}E), respectively. Over the central-eastern EIO, high vertical resolution (~10 cm) observations of upper-ocean salinity and thermal stratifications are needed and suggestions made for the Bay of Bengal region can be considered here.

(4) To measure upper-ocean salinity and thermal distributions over the mini warm pool (68°−77°E, 6°− 15°N), moored buoys at 10 – 20 m intervals in the vertical and at a spatial interval of 5^o in longitude and latitude (total of 12 buoys, preferably a rectangular mesh) with additional deployment of Argo floats with auxiliary STS sensors (at 10 cm intervals at the upper-ocean) are recommended in conjunction with ADCPs.

2. Oxygen variability and change, oxygen minimum zones

J. Wiggert and L. Resplandy

2.1.1 Deoxygenation in the Indian Ocean

Under the influence of anthropogenically driven climate change, the world's oceans are experiencing a clear trend in deoxygenation that has profound implications and impacts on ecological function that are now being revealed. Oceanic deoxygenation has been slower to gain recognition in the scientific community, relative to other high profile impacts such as warming, sea level rise and ocean acidification (Gruber, 2011). The onset and acceleration of oceanic deoxygenation is driven by global warming through both lower oxygen solubility as temperatures increase and reduced ventilation, via air-sea exchange of low O2 waters within the thermocline, as stratification increases. Reduced dissolved oxygen (DO) levels within thermocline waters then result from the oxygen demand associated with heterotrophic remineralization of sinking organic matter no longer being met by the solubility and ventilation-mediated supply of oxygen. In short, increased flux of export production (higher oxygen demand) and / or reduced ventilation due to stronger stratification (lower oxygen supply) will promote oceanic deoxygenation. In coastal waters, eutrophication due to increases in N-loading associated with use of agricultural fertilizers is a prime example of amplified oxygen demand that has led to coastal hypoxia in regions subject to extensive terrigenous runoff or riverine input (Rabalais et al., 2010).

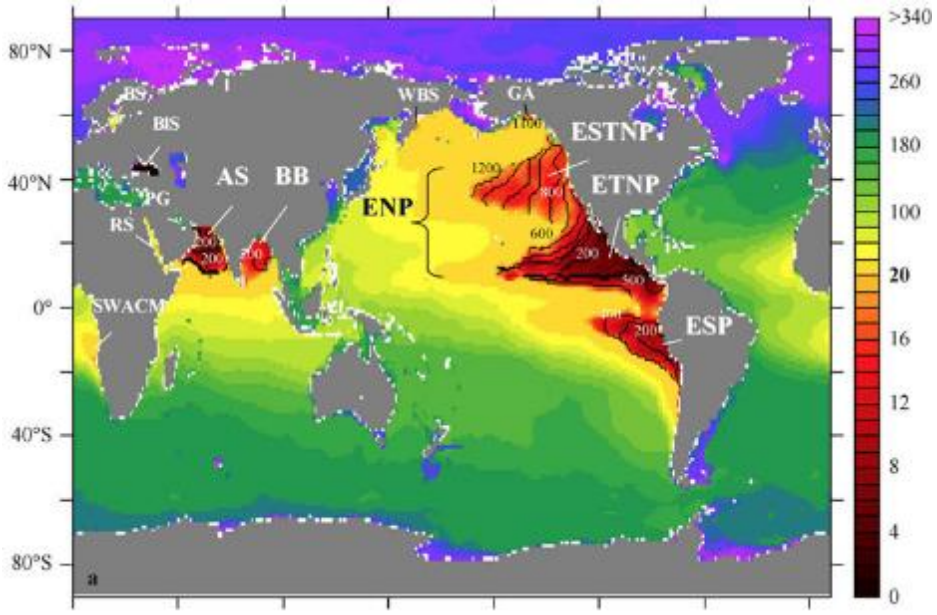

Fig. 1. O2 distribution (IM) at depth where O2 concentration is minimal, indicating the extent of the OMZs (in red) according to the WOA2005 climatology. The color bar scale corresponds to a 1 ± 2 IM interval between 0 and 20 IM, and a 20 ± 2 IM interval between 20 and 340 IM. The isolines indicate the limit of the upper OMZ CORE depth in meters with a 100-m contour interval. For OMZ acronyms, see the list at the end of the main text.

Paulmier, A., and D. Ruiz-Pino (2009), Oxygen minimum zones (OMZs) in the modern ocean, Prog. Ocean., 80(3-4), 113-128, doi:10.1016/j.pocean.2008.08.001.

Two of the most severe oxygen minimum zones (OMZs) occur in the northern Indian Ocean, namely the Arabian Sea and Bay of Bengal (Fig. 1, Paulmier and Ruiz-Pino, 2009). The Arabian Sea OMZ contributes 20% of the global mesopelagic denitrification budget

and has been identified as a hotspot of oceanic efflux of N2O, which is a greenhouse gas that factors into atmospheric ozone cycling (Bange et al., 2001; Codispoti et al., 2001; Bange et al., 2005; Naqvi et al., 2010). The intensity of the Bay of Bengal OMZ does not extend to hypoxic or anoxic conditions, hence its biogeochemical impact is less significant (Bange, 2009).

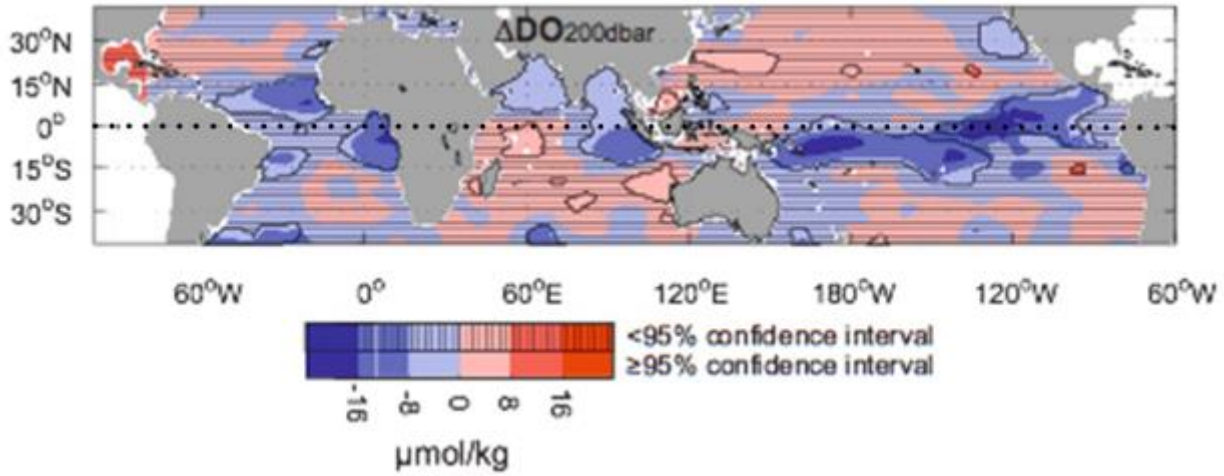

Fig. 2. Changes in dissolved oxygen (ΔDO) (mmol kg^{-1}) at 200 dbar between 40°S and 40°N between 1960–1974 and 1990–2008. Increases (decreases) in DO are indicated in red (blue), and areas with differences below the 95% confidence interval are shaded by black horizontal lines. The black dotted line demarks the equator.

Stramma, L., S. Schmidtko, L. A. Levin, and G. C. Johnson (2010), Ocean oxygen minima expansions and their biological impacts, Deep-Sea Res. I, 57(4), 10.1016/j.dsr.2010.01.005, 587-595.

Decadal trends in ocean deoxygenation at 200 dbar, based on analysis of 50-years of DO concentration measurements, reveal systematic deoxygenation in both sub-regions of the northern Indian Ocean (Fig. 2, Stramma et al., 2010). In the Arabian Sea, where thermocline hypoxia is well-established, this deoxygenation trend is consistent with the reported 63% expansion of the Arabian Sea OMZ since the 1990s (Rixen et al., 2014; Morrison et al., 1999). In the Bay of Bengal, which has low but typically non-hypoxic thermocline waters, deoxygenation may trigger a transition to permanent, wide-spread hypoxia.

State of the art Earth system models (ESMs) project consistent de-oxygenation trends at the global scale but large uncertainties remain for OMZ regions, including those in the Indian Ocean (Bopp et al., 2013). These uncertainties in future oxygenation changes arise from a compensation between a robust decrease in oxygen saturation due to warming and a robust increase in ventilation and oxygen supply of the corresponding water masses (Bopp et al., 2017). The analysis of OMZs in ESMs is however still difficult, because of large discrepancies between models and observations. Future developments in ESMs, including higher spatial resolution, will provide better insights into the future evolution of OMZs.

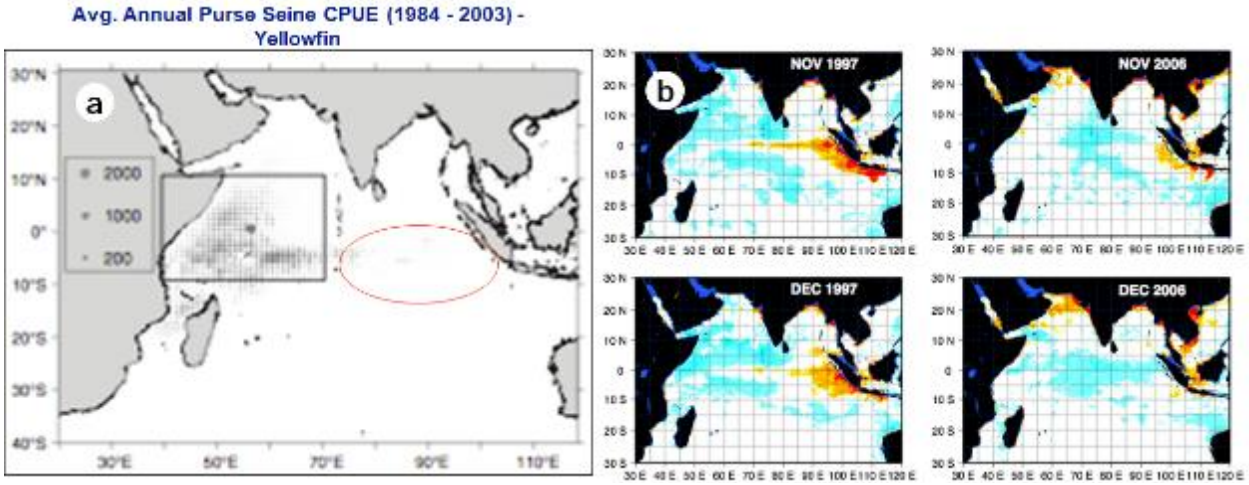

Fig. 3. a) Average annual purse seine catch per unit effort (CPUE) for Yellowfin tuna. During the 97/98 IOD, significant shift of CPUE to eastern Indian Ocean observed. b) Net primary production anomaly (NPPa, mgC m^{-2} d^{-1}) during Nov-Dec period for the IOD manifestations of 1997 and 2006.

Menard, F., F. Marsac, E. Bellier, and B. Cazelles (2007), Climatic oscillations and tuna catch rates in the Indian Ocean: a wavelet approach to time series analysis, Fish. Oceanogr., 16(1), 95-104.

Wiggert, J. D., J. Vialard, and M. Behrenfeld (2009), Basinwide modification of dynamical and biogeochemical processes by the positive phase of the Indian Ocean Dipole during the SeaWiFS era, in Indian Ocean Biogeochemical Processes and Ecological Variability, edited by J. D. Wiggert, et al., p. 350, American Geophysical Union, Washington, D. C.

In the southern tropical Indian Ocean (STIO) there is an increase of thermocline DO in the west and a decrease in the east (Fig. 2, Stramma et al., 2010), suggesting a linkage to the Indian Ocean Dipole (IOD, Saji et al., 1999), and thus a potential multi-decadal influence exerted by the IOD on biogeochemical processes. The IOD's influence on cross-basin thermocline dynamics is well-established (Webster et al., 1999), and biophysical responses have been identified across all marine trophic levels (Menard et al., 2007; Wiggert et al., 2009). The spatial coherence between long-term DO trends and the IOD signature suggests these readily observed surface biological responses link to underlying biogeochemical variability that is poorly characterized. This inference is supported by a basin scale biophysical model that demonstrates a strong positive correlation between elevated areal chlorophyll and IOD occurrence in the eastern STIO during boreal summer and fall, and a strong negative correlation in the western STIO during boreal fall and winter (Fig. 4, Currie et al., 2013). Thus in addition to reinforcing the conclusion that IOD impact on biological processes extends over the euphotic zone, these model results indicate that there is a seasonal lag in impact with the eastern STIO response leading the western STIO response.

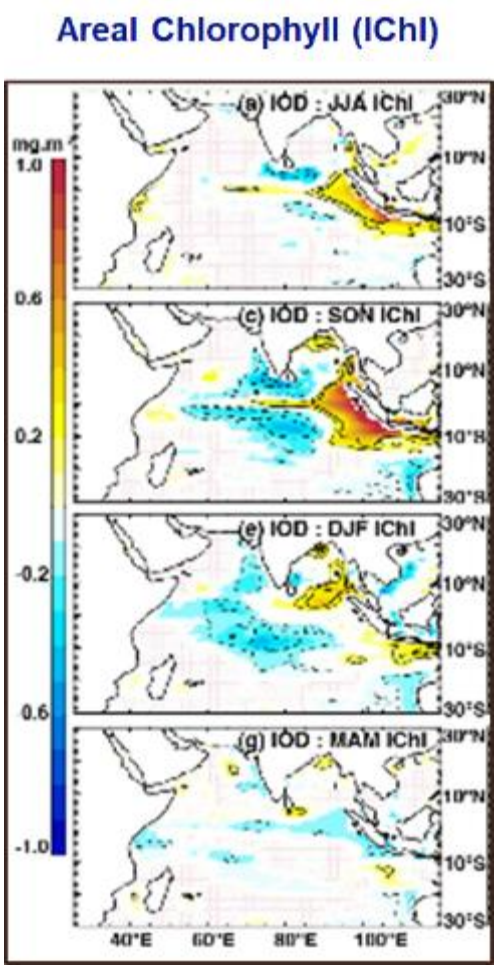

Fig. 4. The impacts of IOD on areal chlorophyll (IChl), determined using regression coefficients of IChl anomalies regressed onto the IOD index with ENSO influence removed. Regressions were computed for the 1961–2001 temporal domain.

Currie, J. C., M. Lengaigne, J. Vialard, D. M. Kaplan, O. Aumont, S. W. A. Naqvi, and O. Maury (2013), Indian Ocean Dipole and El Nino/Southern Oscillation impacts on regional chlorophyll anomalies in the Indian Ocean, Biogeosci., 10(10), 10.5194/bg-10-6677-2013, 6677-6698.

2.1.2 Ecological and societal impacts of oceanic deoxygenation

A prime distinction between the northern Indian Ocean OMZs in the Arabian Sea and Bay of Bengal, is that only the former has an extensive region of sub-hypoxia, such that there are profound biogeochemical affects of deoxygenation. The reasons for this distinction are not fully understood, but (Resplandy et al., 2012; McCreary et al., 2013) include strong contrasts in buoyancy fluxes (evaporative salinization vs. pronounced hydrologic inputs) that control contrasting stratification characteristics, the nature and extent of coastal upwelling, the impacts of seasonally reversing boundary currents (Hood et al., 2017), the degree to which mesoscale eddy activity contributes to ventilation and to lateral advection of organic matter (Resplandy et al., 2011; Lachkar et al., 2016), and terrestrial inputs of organic and inorganic nutrients and particulates (both atmospheric and river borne) that encompass desertification and increased usage of fertilizer in agricultural activities (Mahowald et al., 2006; Seitzinger et al., 2010).

The need to understand the physical and biogeochemical controls that regulate OMZ severity within the Arabian Sea and Bay of Bengal is critical to our capacity to project the consequences of anthropogenically-forced climate change. Should the OMZ in the Bay of Bengal transition to widespread hypoxia, as prevails in the Arabian Sea, then profound shifts in nitrogen cycling would be incurred, with globally significant contributions to rates

of oceanic denitrification and N2O efflux. Deoxygenation impacts all levels of the marine ecosystem, particularly in combination with global warming. As temperatures in the marine environment increase, the metabolic rates of organisms tend to rise exponentially (e.g., Eppley, 1972), leading to higher production and growth rates that necessitate higher metabolic rates that, in turn, rely on oxygen availability to satisfy increased respiratory demands (Doney et al., 2012). Faced with sub-optimal dissolved oxygen availability, marine organisms will initiate conservation responses (e.g., reduced activity and/or cellular function) or avoidance behaviors that may adversely impact growth, reproduction and survival in ways that vary greatly across species (Ekau et al., 2010). As the expected expansion of suboxic waters and associated shoaling of tropical OMZs unfolds, habitat compression of planktonic and pelagic species could necessitate enhanced foraging for large fishes (e.g., billfishes and tuna) and make them more vulnerable to exploitation by the fisheries industry (Fig. 5, Stramma et al., 2010). Deoxygenation can also lead to speciation shifts as trophic niches are impacted through the differential response of taxa to low oxygen conditions, an outcome already evidenced in the Arabian Sea with increases in specific copepods in the hypoxic water column (Wishner et al., 2008) and the appearance of Noctiluca scintillans during winter and spring (Gomes et al., 2014).

Coastal ocean regions, due to their proximity to human influences, including agricultural activity, sewage outfalls, regulation of riverine inflows, and atmospheric nitrogen deposition, are even more prone to deoxygenation. In the eastern Arabian Sea, eutrophication has led to a multi-decadal trend of coastal hypoxia along the west coast of India that has adversely affected coastal fisheries (Naqvi et al., 1998; Ram et al., 2014). The southward flowing boundary current (West Indian Coastal Current) during the SW Monsoon promotes upwelling of these hypoxic waters resulting in fish kill events(Figure 5). The coastal waters of the Bay of Bengal are similarly prone to these mechanisms (Hood et al., 2017). Projections accounting for evolving agricultural practice and human population growth indicate that the northern Indian Ocean, and particularly the Bay of Bengal, is subject to the highest eutrophication potential globally (Seitzinger et al., 2010). Finally, countries adjacent to the Bay of Bengal and eastern Indian Ocean are recognized as most dependent on fisheries for supporting their populations (Barange et al., 2014), and the economies of the Indian Ocean rim nations in general are the most vulnerable to projected climate change impacts on fisheries production (Allison et al., 2009). Thus, the potential societal impact of oceanic deoxygenation on Indian Ocean rim nations is acute and far-reaching, given that the region is home to approximately 2 billion people (~ 30% of global population).

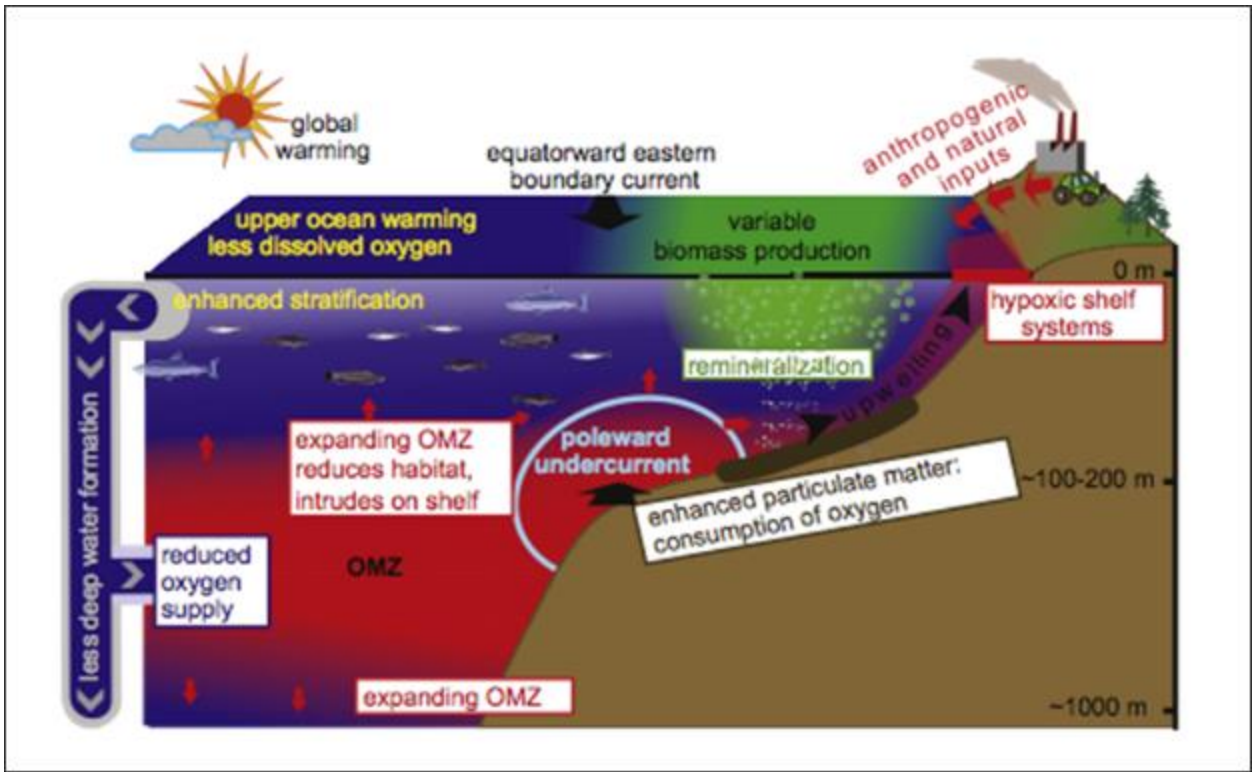

Fig. 5. Schematic of interactions of open ocean oxygen minimum zones (OMZ,red) with hypoxic shelf systems and dead zones on continental shelves of eastern ocean boundaries.

Stramma, L., S. Schmidtko, L. A. Levin, and G. C. Johnson (2010), Ocean oxygen minima expansions and their biological impacts, *Deep-Sea Res. I*, *57*(4), 587-595, doi:10.1016/j.dsr.2010.01.005.

2.2 EOVs necessary to identify state and evolution of dissolved oxygen distribution in the IO

The global database of DO measurements has clear shortcomings in spatial coverage. Observations from the 1960s-1970s have higher density than today (fig 2). A more comprehensive basinwide coverage of dissolved oxygen is needed to establish changes from the earlier period. Additionally, as oceanic deoxygenation accelerates, the need for well-resolved DO measurements will be critical for assessing the skill of climate model projections.

Broad scale observations of DO is a key first component of assessing deoxygenation over the basin and mapping the spatial domain and temporal variability of OMZ waters. However, to ascertain the degree to which an OMZ is hypoxic, and therefore whether it is contributing substantially to global N-cycling, a more comprehensive suite of observations with greater precision is required, including NO3, NO2, NH4, PO4, and δ15NNO3, which provide information about the extent and function of biogeochemical processing within a fully reducing (i.e., hypoxic / anoxic) OMZ.

2.3 Sampling recommendations for obtaining these EOVs within IndOOS framework

The expansion of the Argo program to include dissolved oxygen and nutrient sensors is a core requirement for the future evolution of IndOOS with respect to assessment of

deoxygenation trends across the basin. Bio-Argo floats with the sensor packages that can perform this sampling have been developed by a number of laboratories around the world. Limited observations to date have already afforded new scientific insights (see chapter by Ravichandran et al., this report). In order to address the spatial coverage requirement for addressing basin scale assessment of deoxygenation and defining OMZ extent, called for above, a significant expansion on the number of deployed Bio-Argo float systems is needed.

To fully characterize the biogeochemical and ecological impacts of expanding OMZs, and hence their implications for the growing human populations of Indian Ocean rim countries, close sampling in coastal waters is needed. A fleet of gliders or AUVs outfitted to measure dissolved oxygen and core nutrients could resolve these processes.

Finally, leveraging currently planned ship-based sampling opportunities (GO-SHIP, GEOTRACES) to obtain the full suite of geochemical measurements, and to perform on-board rate experiments, would provide critical information for expanding our understanding of OMZ processes. This information would also serve to advance the skill of biogeochemical modeling efforts that are vital to synthesizing the available observations and extending those to project basinwide biogeochemical and ecological function.

3. Upwelling, coastal-open ocean interactions, and ecosystems

Yukio Masumoto, Weidong Yu, Raleigh Hood, and Mike McPhaden

Upwelling is a key process in three-dimensional ocean circulation, bringing cooler and nutrient rich water up into surface layer. The surface temperature modified by the upwelling affects weather and climate over the region as well as remote areas through teleconnection pathways. The nutrient supply from the subsurface layer can enhance primary productivity in the upwelling regions (McCreary et al., 2009), thereby influencing marine food web and fishery activities (Hood et al., 2017). At the same time, the upwelling brings low oxygen and low pH water up to the surface and onto the shelf, with potentially detrimental impacts on marine ecosystems. Even though the upwelling zones are geographically confined, they represent ascending branches of basin scale circulation patterns such as the subtropical cell and cross equatorial cell (e.g., Lee, 2004). Thus, the upwelling systems should also be considered in the basin scale context, in which they are embedded.

Understanding of upwelling systems is essential for understanding regional- and basin-scale energy transport and material circulations. The upwelling manifests itself as cooler sea surface temperature (SST), lower sea surface height (SSH), and higher chlorophyll concentration in readily available satellite remote sensing products. However, our present understanding of the characteristics and mechanisms of the upwelling systems, particularly in the subsurface layer, their roles in larger systems in the ocean and climate, and their response to the climate system internal variability and anthropogenic forcing are very limited due mainly to scarcity of *in situ* observations both in physical and biogeochemical parameters.

The Indian Ocean is characterized by seasonally evolving upwelling systems associated with monsoonal winds. However, details on seasonal development and decay of each upwelling system are not well understood and need to be investigated. The seasonal evolution of the upwelling systems is disturbed and modulated by phenomena with other time scales, from intraseasonal to decadal variations that appear in the Indian Ocean (Vialard et al., 2012; Hood et al., 2015; Yu et al., 2016). The timing, duration, intensity, and spatial structure of the upwelling are determined by the relative contribution from these different phenomena. In the context of global warming, the future fate of upwelling is a subject of debate. Several studies have argued that there will be future intensification of coastal upwelling in response to the amplified land-sea pressure gradient in the warming world (Bakun, 1990; deCastro et al., 2016; Praveen et al., 2016). However, the story in the monsoonal Indian Ocean could be far more complex than in this conceptual framework.

Fisheries associated with upwelling regions are a particularly important source of protein in developing Indian Ocean rim countries, and fisheries and fish products from these regions also provide direct employment to millions of people (FAO, 2004). For example, increases in production associated with upwelling in the Java Current are linked to increases in sardine (Sardinella leumuru) catch in Bali Strait (Ghofar, 2005). IOD-driven interannual variations in the strength of this current and the intensity of upwelling give rise to dramatic interannual variations in sardine catch, which impact food supply, and also supply relative to demand and therefore market prices and income of artisanal fishers in Indonesia (Sartimbul et al., 2010). Similar phenomena are observed in other Indian Ocean upwelling systems (Hood et al., 2017). It is therefore also crucial to understand, for societal benefit, how the seasonal, intraseasonal and decadal variability in the timing and intensity of Indian Ocean upwelling systems is modulated by physical processes, and how this modulation might be altered in the future due to climate change.

3.1 Coastal upwelling systems

Fig 3.1 shows climatological horizontal distribution of surface Chlorophyll concentration in September, showing two major coastal upwelling systems off Sumatra/Java Islands and off Oman/Somali coasts. Although the two systems are located separately at the eastern and western boundary regions, respectively, they are both influenced by wind stress and its variability over the

regions and in remote areas. Fundamental forcing for the upwelling is local monsoonal winds along the coast in both regions. In addition, the Sumatra/Java upwelling region is affected by forcing further to the west in the equatorial waveguide (Iskandar et al., 2005; Chen et al., 2016), while the Oman/Somali upwelling system is influenced by wind stress curl in open oceans to the east, through westward propagating Rossby waves (Vic et al., 2017). These upwelling systems are also affected by interannual climate modes, such as the Indian Ocean Dipole (Saji et al., 1999), through associated changes in winds, causing anomalous primary productivity in the basin (Wiggert et al., 2009; Currie et al., 2013). Similarly, upwelling along the northwestern coast of Australia (Rossi et al., 2013) is affected by local monsoonal winds and signals from the Pacific Ocean, transmitted through coastal waveguides. There are other coastal upwelling systems with smaller spatial extent or less intense in magnitude, though the impact of these upwelling systems on socio-economic activities are as much as the above major ones, particularly off densely populated regions through fisheries and ecosystems. Another example is the upwelling along the southwestern coast of India (Gopalakrishna et al., 2008).

The strongest upwelling signal is concentrated within O(100km) of the coasts, while the broader spatial extent of SST cooling and high chlorophyll concentration during the upwelling season reflects the horizontal advection of cold upwelled water masses offshore, modified by air-sea heat exchanges and internal variability in the ocean, such as meso-scale eddies. In turn, meso- and submeso-scale variability in the open ocean can modify the upwelling systems. Quantitative understanding of the coastal-open ocean relations need to be improved with temporally and spatially high density data.

3.2 Open ocean upwelling systems

Figure 3.1 also demonstrates open ocean upwelling systems associated with thermocline ridge, such as the Sri Lanka Dome (Vinayachandran and Yamagata, 1998) and the Seychelles Dome (Yokoi et al., 2008; Hermes and Reason, 2009), which are excited by local wind stress curl and remotely forced Rossby wave signals. Shallow thermocline in these regions makes the SST sensitive to variability in the thermocline depth, affecting cyclone activity in the southwestern basin (Xie et al., 2002), the Asian monsoons (Annamalai et al., 2005; Izumo et al., 2008; see Chapter 1), and fisheries (Menard et al., 2007) at seasonal and interannual time-scales. The Seychelles Dome is located in a region of MJO initiations, showing the strongest intraseasonal variability in the SST in the Indian Ocean (Vialard et al., 2009; also see Chapter 1.5). It is also affected by westward propagating Rossby waves triggered by Indian Ocean Dipoles (IODs) and remote influence of ENSO in the Pacific Ocean (Xie et al, 2002). This strong variability causes the tropical Southwestern Indian Ocean to be more productive than the nearby sterile subtropical ocean. RAMA buoys and Argo floats have brought much new knowledge about its basic temporal-spatial structures (Vialard et al., 2009; Foltz et al., 2010). However, the multiscale dynamics and their implications for the biological, biochemical processes and fisheries resources have yet to be fully explored in the tropical Southwestern Indian Ocean.

3.3 Physical-biological-biogeochemical interactions

Diverse physical mechanisms in upwelling regions in the Indian Ocean lead to large uncertainties in the sources and fluxes of major and minor nutrients, thereby limiting our understanding of nutrient delivery and its ecological and biogeochemical implications, such as nitrogen fixation, cryptic (i.e. subsurface) plankton blooms, and the oxygen minimum layer. Fundamental questions remain in the Indian Ocean regarding the impact of upwelling on nutrient stoichiometry (e.g., N, Si, and Fe), associated influence on nutrient limitation controls, and the subsequent species composition of upwelling-induced phytoplankton blooms (Wiggert et al., 2006; Resplandy et al., 2011). Enhancement and transport of plankton production and distribution and variability of the plankton community, which has important implications for higher trophic levels and efficacy of the basin's artisanal and commercial fisheries (Kaplan et al., 2014), are also affected by physical processes in the upwelling systems.

3.4 Essential Ocean Variables for the upwelling systems

Detailed mechanisms of variability of the upwelling systems in the Indian Ocean, from intraseasonal to decadal and much longer time-scales associated with the global warming, are not yet well understood. For further studies, we need to obtain detailed structures of physical, biological and biogeochemical parameters at several key locations in the Indian Ocean with temporal resolution high enough to resolve intraseasonal variability. This can be achieved by a combination of moorings and frequent hydrographic observations along fixed sections for temperature and salinity down to 1000m. Argo floats add data covering wider areas and complement the moorings and hydrographic observations. Microstructure measurements are also needed to evaluate vertical mixing processes. Distributions of biogeochemical and ecological parameters, such as nutrients, chlorophyll, oxygen, pH, and CO_2, along the transects across the upwelling regions would be required seasonally, hopefully as frequent as possible, with several locations measuring plankton community structures. Bio-Argo floats are a useful new platform for sustained observations of biogeochemical parameters as well as temperature and salinity profiles. Satellite data can cover SST, ocean color, surface winds, and SSH. Since the SSH data near the coast is affected by land, tide gauge station data is also needed.

3.5 Recommended actions

The main focus of IndOOS is to obtain basin-scale data away from the boundary areas, and the open-ocean upwelling system in the southwestern Indian Ocean is captured by the observing systems. However, since most of the core regions of coastal upwelling are located within boundary regions, only the satellite data cover these regions and sustained in situ observations in the coastal upwelling hardly exist. Although the upwelling regions are geographically confined, as noted above, they should be considered as key elements in the basin scale circulations and their variability. The basin-scale sustained IndOOS observing system, therefore, is required to be maintained to provide data on background conditions and appropriate perspective of the linkages between the various components of the circulation system, including the upwelling systems. The fact that most of the boundary regions are located within EEZs of neighboring Indian Ocean rim countries may cause some difficulties in conducting research on coastal upwelling systems.

We therefore propose the following recommended actions, though they contain challenging issues, due to difficulties in political situations and logistical arrangement, for constructing observing systems in some regions in the Indian Ocean.

(1) Continue RAMA array along 8°S and in the equatorial region to obtain temperature and salinity data in the thermocline ridge region,

(2) Conduct microstructure measurements in the upwelling regions to evaluate vertical mixing processes,

(3) Extend the IndOOS observing network in the eastern tropical basin into the Sumatra/Java upwelling region, by enhancing deployment of Argo and Bio-Argo floats and/or glider sections across the region. An array of current and pressure-recording inverted echo sounders (CPIES) can monitor transports in the boundary currents associated with the coastal upwelling systems.

(4) Develop new observing platforms within the Somali/Oman upwelling region, hopefully new RAMA buoys, but Bio-Argo deployment, CPIES array, and/or glider sections can provide new physical and biogeochemical data within the upwelling region.

These observations should focus on upwelling on intraseasonal to interannual time scales and phenomena responsible for mixed-layer processes and their interactions. Relations between physical forcing and biogeochemical/ecological response and air-sea interactions are some examples of interdisciplinary research targets. In addition, focused process studies can be developed on the basis of the IndOOS sustained observing system.

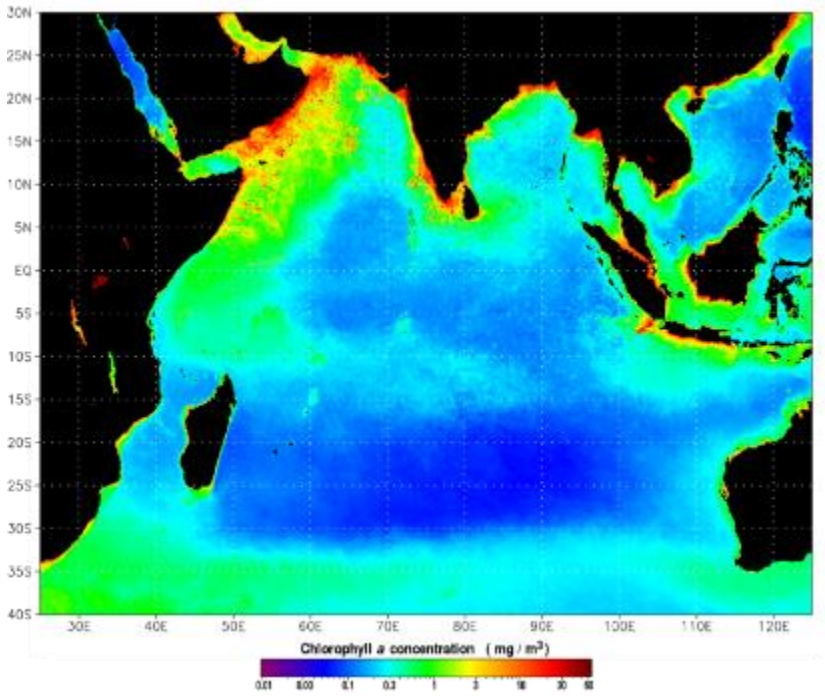

Figure 3.1: Climatological distribution of Aqua MODIS Chlorophyll concentration in September. The major upwelling regions are indicated by higher chlorophyll concentration with green/orange color shade, except for regions very close to the coasts.

4. Extreme events

Lengaigne, M., M. Feng, S. Neetu, D. Barbary, H. Ramsay, J. Vialard, K. Walsh

4.1 Motivations

The Indian Ocean (IO) region comprises one third of the world population. high population density distributed along low-lying coastal areas and poor disaster management strategies largely explain the vulnerability of countries surrounding the IO to extreme events, such as Tropical Cyclones (TCs). While the Bay of Bengal only hosts 5-6% of global TCs count, it witnesses 80-90% of TC fatalities (Paul, 2009), with 18 of the 18 deadliest TCs occurring in this region during the historical period (Needham et al. 2015). The BoB is particularly vulnerable to coastal flooding because of low-lying heavily inhabited areas and continental shelf with shallow bathymetry, which amplifies the storm surge (Antony et al. 2014). The Nargis TC in May 2008 is a dramatic example: it reached Category 4 strength and caused the worst natural disaster in Myanmar history, with more than 140,000 lives lost, one million homeless and over $10 billion in economic losses (Webster et al., 2008). Exposure to TC-induced storm surges or erosion is expected to increase overt the coming decades as a result of climate change, global sea-level rise and coastal population density increase (Karim and Mimura, 2008). Marine Heat Waves (MHWs) are also extreme events, with strong impacts on marine ecosystems. An unprecedented MHW off the west coast of Australia in early 2011 caused massive fish and invertebrate kills and coral bleaching (Pearce and Feng, 2013; Wernberg et al., 2013), resulting in a regime shift of the ecosystem in that region (Wernberg et al., 2016). These MHWs have been observed more frequently in recent decades (Zinke et al., 2014; Feng et al., 2015), considerably amplifying the effect of the gradual ocean warming and may lead to severe impacts on future marine ecosystems (Zhang et al., 2017). To their improve predictability, it is essential to better observe these events and understand the mechanisms driving them.

4.2 Tropical Cyclones

TCs track prediction has improved dramatically over the last decades but intensity forecast improvements have comparatively stalled (DeMaria et al., 2014). Various environmental atmospheric conditions influence TC intensification, such as strong vertical wind shear and high mid-tropospheric humidity. TCs primarily draw their energy from evaporation at the ocean surface, and hence enthalpy flux at the air–sea interface plays an essential role in maintaining and intensifying TCs. Because of the strong control of SST on the enthalpy flux, TC intensity is also sensitive to Sea Surface Temperature (SST): kinetic energy dissipated by friction at the air-sea interface can result in SST cooling under the TC, largely through vertical mixing (e.g. Price, 1981; Vincent et al., 2012a) and limit TC intensification (e.g. Cione and Uhlhorn 2003). This cooling can be modulated by an order of magnitude by oceanic subsurface stratification (Vincent et al. 2012b), with larger cooling in regions with a shallow thermocline, and hence a larger negative feedback on TC intensification. This has motivated the inclusion of metrics for oceanic subsurface stratification in statistical forecasts of TC intensity (e.g. DeMaria et al. 2005)

The IO is home to ~25% of global TC activity (Knutson et al., 2015). In the northern IO, they mainly occur in the western and central part of the Bay of Bengal (BoB; *Figure 4.1*) and exhibit a bimodal seasonal distribution, with preferential occurrence during the pre- and post-monsoon seasons. In the southern IO, they occur over an elongated band centred on 15°S from November to April, with enhanced TC occurrence over the southwestern IO around the islands of Mauritius, La Reunion and Madagascar (*Figure 4.1*) TC characteristics in this basin are known to be influenced by climate variability, such as the Madden-Julian Oscillation at intraseasonal timescales (Bessafi and Wheeler 2006) or El Niño at interannual timescales (Kuleshov et al. 2008). Climate change may also influence the long-term evolution of IO TC characteristics: the intensity of major TCs been suggested to increase during the post-monsoon period in the Bay of Bengal (Singh et al., 2007; Balaguru et al., 2014) and during the pre-monsoon period in the Arabian Sea (Evan et al., 2011). Recent future projections also indicate an increase in the number of the most intense TCs in the

IO (Knutson et al. 2015) but more contrasted results in terms of the TC frequency changes (Murakami et al, 2013). The specific regional characteristics of upper ocean thermohaline structure in the IO TC-prone regions may also result in a different sensitivity of TCs to ocean-atmosphere coupling compared to other basins. The BoB is indeed characterized by a strong haline stratification during the post-monsoon season in response to the summer monsoon freshwater influx, while the cyclogenesis region in the southwestern IO is one of the rare oceanic regions where warm SSTs coexist with a shallow thermocline ridge (Vialard et al. 2009). The role of subsurface oceanic conditions on TCs in the northwest Australian basin is unclear, but is likely to be less prominent there because of their smaller influence on SST variations (Vialard et al. 2012).

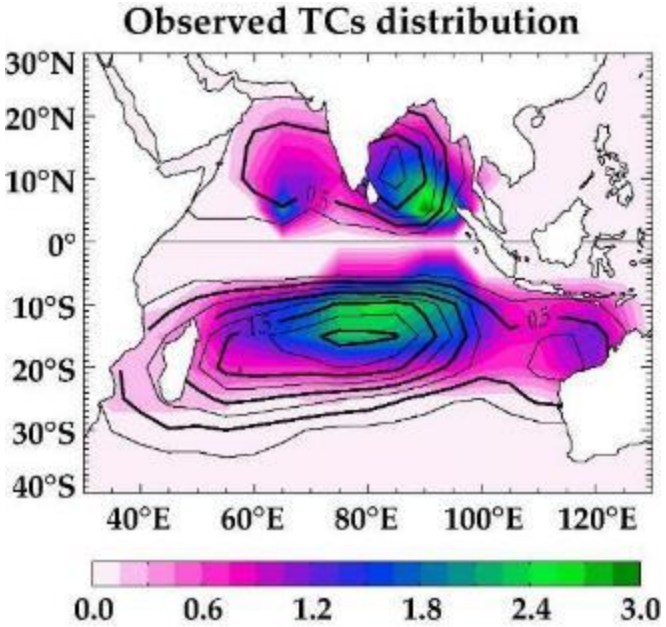

Figure 4.1**:** Observed climatological distribution of normalised cyclogenesis (colour) and TC density (contour) over the 1989-2009 period derived from the International Best Track Archive for Climate Stewardship (IBTrACS; Knapp et al. 2010).

In the BoB, moored buoy data indicated that a combination of a warm subsurface layer and strong salinity stratification played an essential role in the rapid intensification of Nargis TC (e.g. Lin et al. 2009; Yu and McPhaden 2011). At seasonal timescales, thick barrier layers induced by stronger haline stratification and deeper thermocline during the post-monsoon in this region largely explains the much weaker TC-induced oceanic cooling as compared to the pre-monsoon period (Neetu et al. 2012), which foster TC intensification in that season (Balaguru et al., 2012). At interannual timescales, the probability of TCs occurrence in the BoB decreases during El Niño events (e.g. Felton et al., 2013) and positive Indian Ocean Dipole events (e.g. Yuan and Cao, 2013). Similarly, TC activity decreases dramatically during strong El Niño events in the southwestern IO (e.g. Astier et al. 2015). Both large-scale variations of atmospheric environment (Felton et al., 2013; Astier et al., 2015) and of oceanic stratification (Xie et al. 2002; Vincent et al. 2014; Burns et al. 2016) associated with these climate modes are key drivers of this interannual modulation. TCs in the southeastern IO have also been related to ENSO (Ramsay et al. 2012) and more recently to IOD-like SST variability (Ramsay et al. 2017), but with a weaker contribution from subsurface oceanic conditions. Over the long term, surface and subsurface warming trends has also been related to an increasing trend in TCs intensity (e.g. Elsner et al. 2008; Rajeevan et al., 2013; Malan and Reason, 2013; Balaguru et al. 2014). The IO region poses a particular challenge for quantifying

long-term TC intensity trends because of the large discontinuity in satellite viewing angle when Meteosat-5 was introduced in 1998 (Kossin et al. 2013).

4.3 Marine heat waves

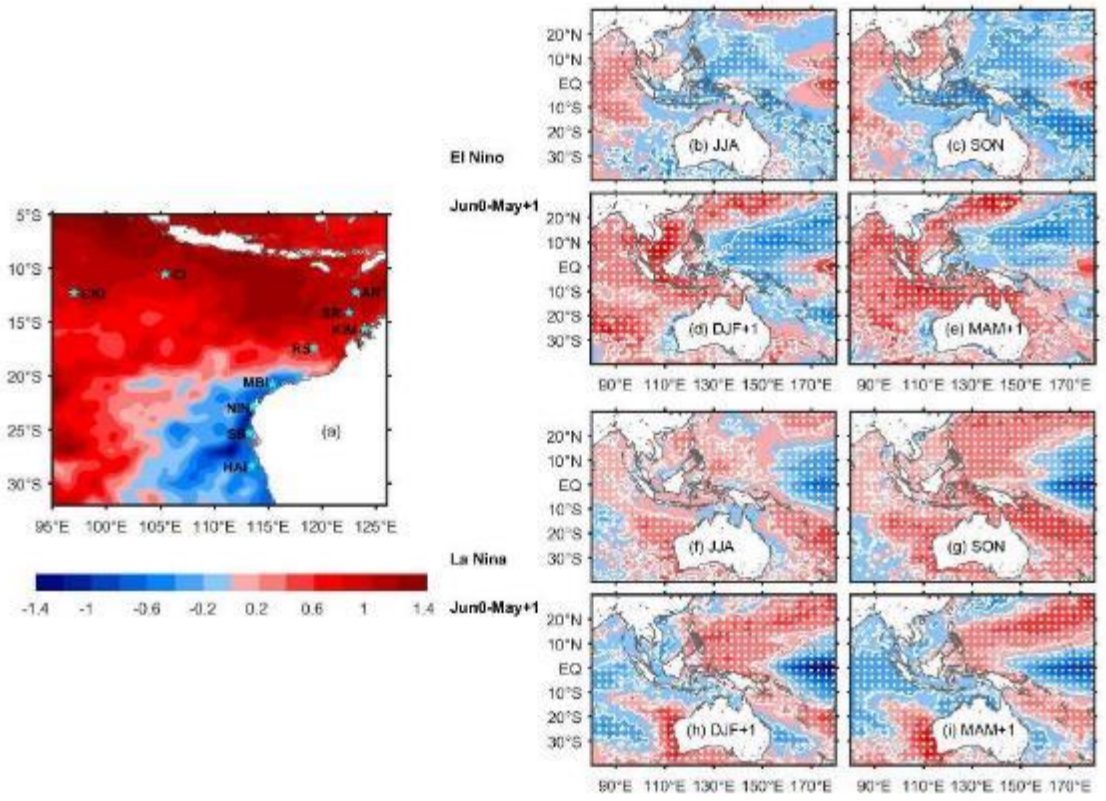

*Figure 4.2**: (a)** Averaged SST anomalies in the southeastern IO during December 2015- April 2016. Stars denote locations of representative reefs. **(b)-(e)**: composited SST anomalies for El Niño events during January 1982- April 2015 and **(f)-(i)**: for La Niña events over the same time period. The white contours and dots indicate anomalies exceeding the 95% significance level based on a two-tailed Student's t test. From Zhang et al. (2017)*

MHWs are episodic warm SST extremes that persist for days to months (Hobday et al., 2016). these extreme events cause extensive coral bleaching (Moore et al., 2012) and alter the ecosystem along the West Coast of Australia, including a reduction in the abundance of habitat-forming seaweeds (Wernberg et al., 2013) and a subsequent shift in community structure towards a depauperate state and a tropicalization of fish communities (Wernberg et al., 2016). MHWs are also associated with extreme climate variability, such as ENSO and IOD. The 2011 MHW off the west coast of Australia was instigated by an anomalously strong Leeuwin current during a strong La Niña event in the Pacific (Feng et al., 2013). The negative phase of the Interdecadal Pacific Oscillation since the late 1990s has caused more frequent similar MHWs off the coast (Feng et al., 2015). Farther north, tropical oceans off the northwest coast of Australia are more susceptible to El Niño influences and more frequent MHWs have occurred during or after the peak of strong El Niño events (Zhang et al., 2017; Figure 4.2), such as the 1997-98 and 2015-16 events which were due to reduced cloud coverage and a weakened Australian monsoon. Local air-sea-land coupling and the Madden-Julian Oscillation also facilitate the genesis of MHWs in this region (Kataoka et

al., 2014; Marshall et al., 2015; Zhang et al., 2017). These MHWs have also been observed more frequently in recent decades as a combined result of natural decadal variability and global warming (Zinke et al., 2014; Feng et al., 2015; Zhang et al., 2017).

MHWs also tend to occur in the tropical western IO due to ENSO teleconnection and IOD influences (Du et al., 2009), and in the tropical eastern IO and Maritime Continent during the negative IOD events. However, MHWs in these regions have not been well characterised. MHWs in the Agulhas Current system may be associated with the variability of the boundary currents.

4.4 EOVs for extreme events in the IO

The overall picture of IO extreme events drawn in sections 4.2 and 4.3 stresses the importance of ***sustained observations over several key regions to monitor (1) subsurface stratification and air-sea coupling under TCs and (2) MHWs.*** TC intensification is influenced by both SST and upper ocean stratification while MHWs are predominantly driven by air-sea flux anomalies and ocean boundary current variability. A better understanding and prediction of these extreme events hence requires accurate observations of:

1. Heat and momentum fluxes, sea level pressure, sea-level and waves, both in regions of cyclogenesis and along cyclone tracks with at least at hourly resolution.
2. Sea Surface Temperature in the BoB and southern IO, i.e. the TC prone regions with at least at hourly resolution: in situ measurements are of primary importance, since the cooling under the eye is not well observed, even by microwave radiometers, due to strong precipitation.
3. Upper ocean (0-200m) thermohaline background stratification in IO TC-prone regions, at least at weekly resolution
4. Upper ocean thermohaline and currents profiles at ~3hr resolution to monitor the oceanic response of TC in two contrasted TC-prone regions in the IO: the BoB characterized by a sharp salinity stratification and the southwestern IO characterized by a shallow thermocline lying below warm surface waters.
5. Boundary current systems in the IO, since they play a strong role for MHWs
6. Mixed layer processes and air-sea fluxes in the MHW hotspots, such as the southeast IO and tropical IO.

4.5 Actionable recommendations

a. Maintain satellite observations and intercalibration-work that allow the development of basin-scale wind and SST records that can be trusted in rainy/cloudy regions. This includes the use of MEGHA-TROPIQUES satellite allowing repeated scanning over the tropical regions of sea surface winds, clouds, humidity, temperature, rainfall and radiation. (addresses points 1 and 2 in section 4.4).

b. Maintain satellite altimetry and coastal tide-gauge measurements to allow monitoring storm surges especially over the Bay of Bengal. Encourage the development of high repetitive constellation of altimeter satellites in order to enhance the chances of capturing of surge signals. In complement to Jason-2 mission, the recent SARAL altimetry mission should improve coastal altimetry monitoring. The new proposed SWOT mission will also complement the standard nadir altimeter data with fine spatial coverage and high resolution (point 1)

c. Encourage the systematic deployment of drifting buoys with barometers in TC-prone regions. Experiment with drifting buoys including more surface measurements: atmospheric pressure, wind speed and direction, air and sea temperature, salinity, humidity

and waves to monitor TC surface signature and improve initialisation of TC dynamical predictions (points 1 and 2)

d. Maintain the Argo network in the IO (point 3); encourage the deployment of Iridium profilers in TC regions, which can be reprogrammed to provide higher temporal-resolution upper ocean observations near cyclones.

e. Maintain the RAMA meridional sections at 55°E and 90°E and all moorings in the southwestern IO (between 55°E and 80°E south of 5°S) as this data is critical to monitor the thermohaline stratification in the IO TC-prone regions (point 4)

f. Establish a RAMA flux mooring site in the Northwestern Australian basin (~15°S; 120°E) to be able to capture the MJO and TC evolution and dynamics in the region (points 4, 5 and 6)

g. Establish or maintain ocean boundary current observing systems (in particular the Leeuwin and Agulhas currents) in the IO (point 5)

5. Intra-seasonal air-sea coupling: Madden-Julian Oscillation and Monsoon Intra-seasonal Oscillation

Toshiaki Shinoda, Texas A&M University, USA

5.1 Introduction

This chapter discusses oceanic and atmospheric variability associated with the Madden-Julian Oscillation (MJO; Madden and Julian 1972) and the monsoon intra-seasonal oscillation (MISO; Yasunari 1980 Krishnamurti and Subrahmanyam 1982). In particular, the role of ocean and air-sea interaction in the MJO and MISO initiation and propagation over the Indian Ocean region is emphasized.

The MJO is a major source of intra-seasonal variability in the tropics, and is associated with large-scale atmospheric circulation and deep convection. It is characterized by the eastward propagation around the globe on an approximate timescale of 30-60 days. The MJO impacts the onsets and breaks of Indian and Australian monsoons (e.g., Yasunari 1979, Hendon and Liebmann 1990), the tropical cyclone activity (e.g., Liebmann et al. 1994, Maloney and Hartman 2000), climate variability in the extra-tropics through teleconnection (e.g., Weickmann et al. 1985), and interannual variability such as ENSO (e.g., Kessler and Kleeman 2000, McPhaden 1999) and the Indian Ocean dipole (e.g., Han et al. 2006, Shinoda and Han 2005).

The MISO is a dominant mode of intra-seasonal variability in the tropical troposphere during boreal summer over the Asian Monsoon region. It is characterized by 30–60 day variations of convection and low-level winds, propagating northward from the equator to South Asian and Southeast Asian region. The MISO largely influences intra-seasonal fluctuation of rainfall associated with the Indian summer monsoon and plays an important role in triggering the monsoon onset (e.g., Goswami and Ajaya Mohan, 2001; Webster et al., 2002, Lau and Yang, 1996; Annamalai and Slingo, 2001; Hoyos and Webster, 2007).

Given the strong impact of tropical intra-seasonal variability on monsoons described above, the importance of the MJO and MISO for agricultural planning and socioeconomic activities in many Indian Ocean rim countries is becoming increasingly recognized. For example, the Indian summer monsoon provides the primary water source of agriculture for South and Southeast Asian countries where millions of people live. The accurate prediction of monsoon rainfall variability caused by the MJO and MISO would thus help to make adequate agricultural decisions such as scheduling of planting and harvesting operations. Also, since intra-seasonal rainfall variability in this region often causes severe floods and droughts, better forecast of the MISO and MJO has a considerable and growing impact on many people's lives in densely populated areas.

It should be noted that there are many important scientific issues on this subject which cannot be covered in this chapter, and a recent extensive review (DeMott et al. 2015) covers many other aspects on tropical intra-seasonal air-sea interaction with a comprehensive reference list.

5.2 Air-sea coupled processes in the MJO and MISO

a. Madden-Julian Oscillation (MJO)

The MJO provides significant fluxes of momentum and heat into the tropical western Pacific and Indian Oceans (e.g., Shinoda et al. 1998), driving large upper ocean responses, including strong equatorial currents, fluctuation of mixed layer temperature, and changes of thermocline depth (e.g., Krishnamurti et al. 1988, Kessler et al. 1995, Shinoda and Hendon 1998, McPhaden 2002, Waliser et al. 2003, Moum et al. 2013). The importance of air-sea interaction for MJO development and propagation has been widely debated since the international field campaign in early 1990's (Webster and Lukas 1992) during which significant SST variations associated with the MJO were observed (e.g., Weller and Anderson 1996). A comparison of many coupled and uncoupled

numerical model experiments suggests that including air-sea feedbacks improves simulations of MJO's amplitude, period, and propagation (e.g., Kemball-Cook et al. 2002, Sperber 2004, Zhang et al. 2006, Woolnough et al. 2007, Kim et al. 2008).

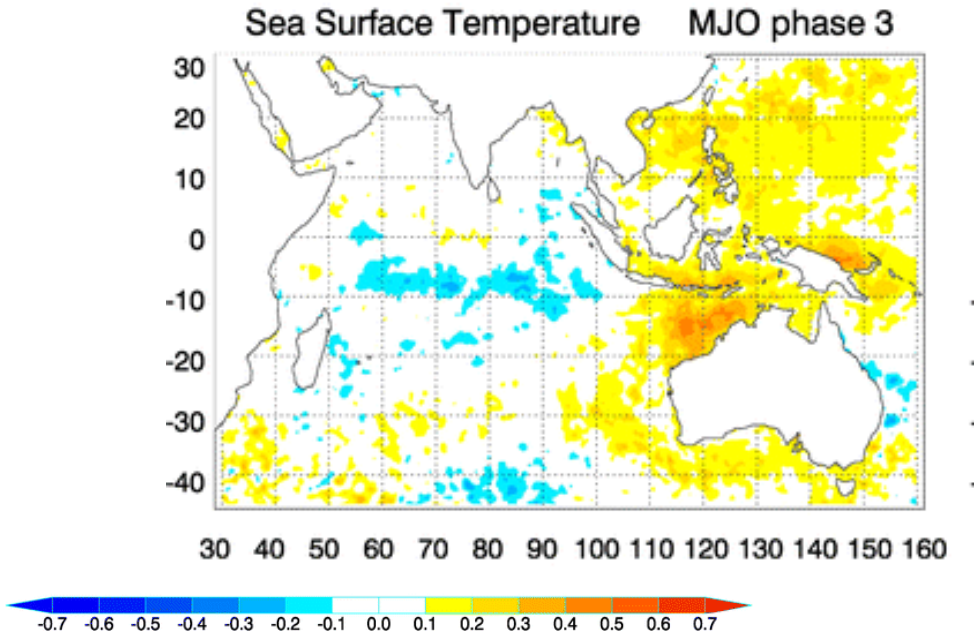

Figure 5.1 Composite SST anomalies (°C) for phases 3 of the MJO (based on Wheeler and Hendon 2004) over the November–April season calculated from POAMA (Predictive Ocean Atmosphere Model for Australia) Ensemble Ocean Data Assimilation System. Adapted from Marshall and Hendon (2014).

Processes controlling intra-seasonal SST

While surface shortwave radiation and latent heat flux primarily control the intra-seasonal variation of SST in many locations of the Indian Ocean and western Pacific warm pool (e.g., Shinoda and Hendon 1998), the contribution of ocean dynamical processes to SST can be significant in some areas, especially over the Indian Ocean. One such location is the Seychelles-Chagos thermocline ridge (SCTR; 2S-10S, 60E-80E; McCreary et al. 1993, Xie et al. 2002, Hermes and Reason 2008) region where the main thermocline is very shallow. Intra-seasonal SST variability is much larger in the SCTR region than most other areas in the tropical Indian and western Pacific Oceans.

The relative importance of surface heat fluxes and ocean dynamics in controlling intra-seasonal SST in the SCTR region is still unclear (e.g., Duvel et al. 2004, Han et al 2007, Vinayachandran and Saji 2008, Jayakumar et al. 2011, Drushka et al. 2012, DeMott et al. 2015). Recent studies (e.g., Halkides et al. 2015, Li et al. 2014) demonstrate the large spatial and temporal variability of processes controlling SST, suggesting that discrepancies in previous studies are probably due to regional differences, interannual variability, and event-to-event variability. Also, significant uncertainties in the mixed layer heat budget still exist due partly to the uncertainty of surface heat fluxes and the difficulty of quantifying vertical mixing processes including entrainment and vertical advection.

Another area of large SST variability associated with the MJO is the Timor Sea off the northwest coast of Australia (e.g., Duvel and Vialard 2007, Vialard et al. 2008, Vialard et al. 2013, Marshall and Hendon 2014) where SST anomalies induced by the MJO exceed 0.5°C (*Figure 5.1*). It appears that SST warming (cooling) in this region is driven by surface heat fluxes and coastal downwelling (upwelling) generated by easterly (westerly) wind anomalies during the supressed (active) phase of the MJO (Marshall and Hendon 2014).

However, further quantitative discussion requires better spatial and temporal coverage of the data in this region including in-situ observations.

Impact of diurnal cycle

SST warming during the suppressed phase of the MJO is largely enhanced due to a diurnal cycle of shortwave radiation (e.g., Shinoda and Hendon 1998, Shinoda 2005, Li et al. 2013). This effect could play an important role in the initiation of the MJO, since warm SSTs can enhance moisture accumulation in the troposphere which stimulates the initiation of atmospheric convection. Regional coupled model simulations demonstrated the importance of the diurnal cycle for the initiation of MJO convection for the event observed during the international field campaign of 2011/2012 (Seo et al. 2015). Further experiments as well as observations for many different cases are still necessary to confirm the role of diurnal warming.

MJO propagation through Maritime Continent

The MJO propagating eastward from the Indian Ocean often weakens over the Maritime Continent (MC) region, known as the "MJO propagation barrier". The failure of the propagation through MC occurs more often in numerical model simulations (e.g., Inness and Slingo 2006), known as the "MC prediction barrier". Several mechanisms for the MJO propagation barrier have been suggested, including a reduced surface moisture source due to the land coverage (Sobel et al. 2008), disruption of low-level winds by the island topography (Inness and Slingo 2006), and the pronounced diurnal cycle in precipitation over islands (Neale and Slingo 2003). The resolution of most numerical prediction models may not be sufficient to resolve these processes and thus could cause the MC prediction barrier. Also, many oceanic processes relevant to air-sea interaction in this region are still not well understood. For example, salinity stratification caused by a strong diurnal cycle of precipitation may potentially influence SST and heat fluxes in this region. Accordingly, understanding physical processes in the MC region may help improve the MJO prediction.

MJO diversity

During the intensive observation period of a recent international field campaign in October-December 2011 (Yoneyama et al. 2013), three active episodes of large-scale convection associated with the MJO propagated eastward across the tropical Indian Ocean. While the strength of atmospheric convection was similar for the three MJO events, a very strong ocean response to the atmospheric forcing was observed for the second event (e.g., Moum et al 2013) whereas the ocean response for the first event was much weaker. This suggests that the role of air-sea coupling in the MJO varies substantially from event to event (MJO diversity; e.g., Fu et al. 2015). Accordingly, it is crucial to maintain and enhance long-term measurements that cover many MJO events to advance our understanding of air-sea coupled processes associated with the MJO.

b. Northward propagating monsoon intra-seasonal oscillation (MISO)

Importance of air-sea coupling for MISO development and propagation has been suggested in many recent studies (e.g., Webster et al., 1998; Vecchi and Harrison, 2002; Rajendran and Kitoh, 2006; Roxy and Tanimoto, 2007; Achuthavarier and Krishnamurthy, 2011). In particular, coupled and uncoupled numerical model experiments of the MISO demonstrate that the inclusion of air-sea interaction leads to more realistic simulation and better prediction skills of the MISO (e.g., Kemball-Cook and Wang, Fu et al., 2003, Seo et al., 2007; Bellon et al. 2008, Wang et al., 2009). However, it is still unclear to what extent oceanic processes influence the MISO dynamics.

As the MISO propagates from the equator to Southeast Asia, it is thought to be influenced by underlying SSTs in the Bay of Bengal. Processes that control intra-seasonal SST variability in the Bay of Bengal have been investigated by many observational and modelling studies (e.g., Sengupta et al., 2001; Waliser et al., 2004, Duvel and Vialard, 2007, Vialard et al., 2012). While these studies indicate that shortwave radiation, latent heat flux, and ocean dynamics are all important, the relative contribution of these processes varies among the studies. The discrepancies in previous studies could partly be due to the different time period of the analysis as well as the

analysis methods and the data source. For example, there are significant year-to-year variations of the MISO associated with interannual or longer term climate variability such as Indian Ocean Dipole (e.g., Ajayamohan et al. 2008, Sabeerali et al. 2014, Karmakar et al 2015, Jongaramrungruang et al. 2017), and such variations could influence the characteristics of MISO and thus the associated ocean variability.

The Bay of Bengal receives a substantial amount of freshwater through precipitation and river runoff, creating complex upper ocean structure and dynamics including a strong halocline, temperature inversion, large diurnal variability, and frontal instabilities. In particular, strong salinity stratification causes shallow mixed layer and thick barrier (isothermal layer below the mixed layer), which tends to prohibit vertical mixing and reduces the entrainment heat flux, and in turn could influence intra-seasonal SST (Vinayachandran et al., 2002; Rao and Sivakumar, 2003; Sengupta et al., 2016). Recent studies suggest that SST variability caused by strong salinity stratification significantly influences atmospheric convection over the Bay of Bengal associated with the MISO (Li et al. 2017a, 2017b).

Despite recent advances in understanding the ocean's role in the MISO, it is still difficult for models to accurately simulate upper ocean structure and variability in the Bay of Bengal. For example, realistic simulations are severely hampered by uncertainties in estimates of river discharge which directly influences salinity variability in the northern Bay of Bengal. Long-term measurements in the northern bay, such as a surface mooring at 18°N, 90°E (Weller et al., 2016), would be very useful for understanding the overall impacts of salinity stratification on the MISO intensity and propagation.

5.3 Essential Ocean Variables (EOV)

As the atmospheric forcing associated with the MJO generate equatorial jet and equatorial waves which could in turn feedback on the MJO, monitoring upper ocean variability near the equator is crucial. Off the equator, the upper ocean structure over the Bay of Bengal should be monitored, where air-sea coupling plays an important role in the MISO development and propagation. In addition, diurnal variability in the near-surface layer needs to be resolved, given its importance for the MJO initiation. The sustained observation within the Indonesian Seas is desirable, since air-sea interaction processes in the MC region may play an important role in the MJO propagation (see the next section).

Variables

Equatorial (10°N-10°S) and Bay of Bengal temperature, salinity, velocity, SST, SSS, near-surface wind, air temperature and humidity, precipitation, shortwave and longwave radiation. Since surface fluxes are essential variables for air-sea coupling, near-surface atmospheric variables are included here in addition to ocean variables.

Resolutions

Temporal resolution: One hour to resolve a diurnal cycle

Zonal resolution: 10° in longitude (~1110 km)

Meridional resolution: 1° in latitude (~111 km) near the equator to resolve equatorial wave guide.

5.4 Recommendations

Sustained measurements are crucial for the study of intra-seasonal air-sea coupling over the Indian Ocean, and thus maintaining the current network of IndOOS especially the RAMA array and Argo program is the first priority.

Given the importance of monitoring the diurnal cycle, increasing the vertical resolution in the upper 10 m of RAMA buoy is desirable. Suggested depths of temperature and conductivity sensors are: 0.5 m, 1.0 m, 2.0 m, 3 m, 5 m, 7 m, 10 m, which can better resolve the shallow diurnal warm layer

(upper few meters) and the mixed layer deepening during night time. The enhancement of vertical resolution would be particularly useful for key regions listed in the following paragraphs.

Although the meridional resolution of the current RAMA buoy network is coarser than the desirable resolution specified in EOV, the current resolution near the equator may be acceptable given the additional coverage of satellite and Argo data. Perhaps adding new RAMA buoy sites in key areas for the MJO and MISO monitoring is the higher priority, as follows:

(1) Surface buoy in the Timor Sea at 14S, 115E

The largest SST anomalies associated with the MJO are found off the coast of northwest Australia. Hence better understanding of air-sea interaction processes in this region may lead to improving our ability to predict the MJO and the variability of Australian monsoon. The importance of this location for other climate variability and ecosystem is discussed in other chapters.

(2) Continuation of surface buoy measurements at 18N, 90E in the northern Bay of Bengal

Upper ocean and SST variability in the northern Bay of Bengal plays a crucial role in the MISO development and propagation. The buoy at this location maintained by the Woods Hole Oceanographic Institution is scheduled for termination in 2018. Continuation of this site would contribute to better understanding of the ocean's role in the MISO, and thus its prediction.

(3) ADCP measurements in SCTR

While current RAMA buoys near the center of SCTR (65E) have been monitoring temperature and salinity, the addition of velocity (ADCP) measurements to the buoy at 4°S, 65°E would provide useful information for vertical mixing processes and thus the mixed layer heat budget where equatorial Rossby waves affect the upper ocean structure.

(4) Additional buoy measurements in Maritime Continent (Indonesian Seas)

At present, long-term data from in-situ measurements within the Indonesian Seas are available only from the moorings at the Makassar Strait. One possible location for the additional buoy could be a southern part of Banda Sea where the largest intra-seasonal SST anomalies are found within the Indonesian Seas (e.g., Napitu et al. 2015).

6. Interannual variability and predictability

T. Tozuka[1, 2], T. Doi[2], and M. J. McPhaden[3]

1: The University of Tokyo; 2: Application Laboratory, JAMSTEC; 3: NOAA/PMEL

This chapter reviews progress made in the past decade on interannual variability and predictability of the Indian Ocean. We focus on four prominent modes of variability, namely the Indian Ocean Dipole (IOD), the Indian Ocean Basin Mode (IOBM), the Indian Ocean Subtropical Dipole (IOSD), and Ningaloo Niño (*Figure 6.1*). Understanding and predicting these climate modes are essential, because the first two modes have large impacts on both local and remote climate, while the latter two modes strongly influences local climate. One way or another, these climate modes are influenced by the El Niño/Southern Oscillation (ENSO); the IOBM is predominantly driven by the ENSO, whereas the other three modes are partially influenced by the ENSO. In addition, both IOSD and Ningaloo Niño are associated with modulation of the subtropical high in the southern Indian Ocean. Recommendations in terms of essential ocean variables and measurement strategies for continuing progress on understanding and predicting these variations are also presented.

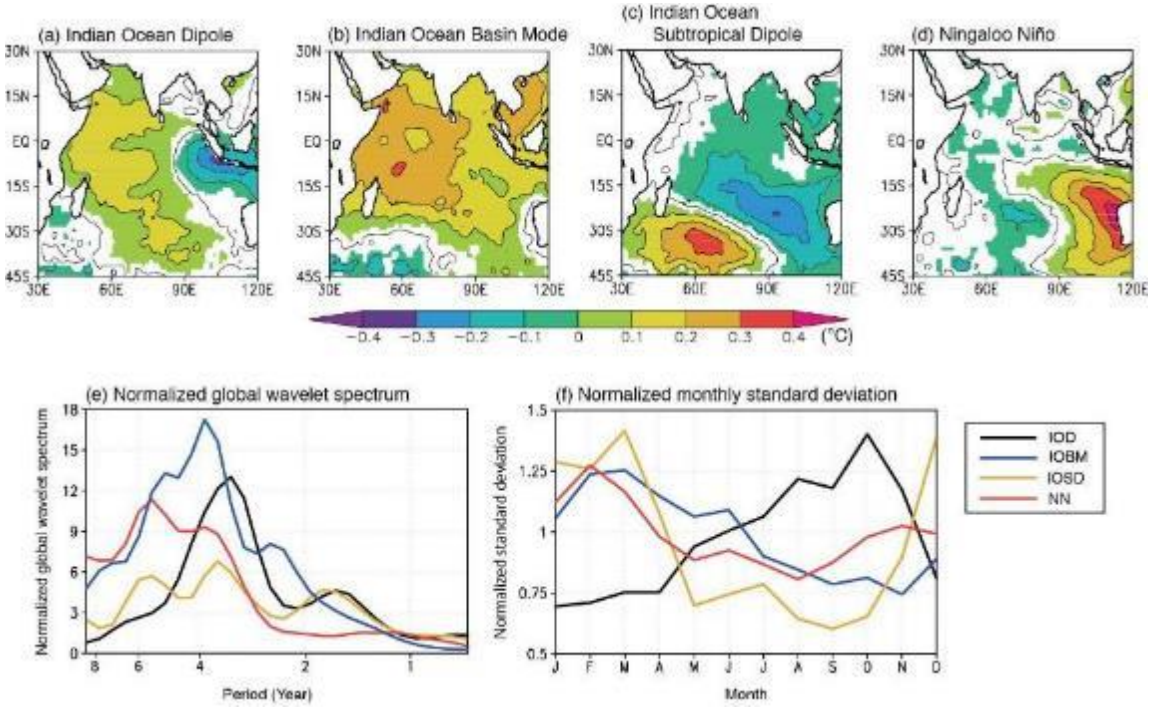

Figure 6.1 : Sea surface temperature (SST) anomalies associated with (a) the Indian Ocean Dipole, (b) the Indian Ocean Basin Mode, (c) the Indian Ocean Subtropical Dipole, and (d) Ningaloo Niño. Here, detrended SST anomalies (in °C) are regressed against their respective normalized indices. Regression coefficients significant at the 99% confidence level by a two-tailed t-test are shaded, and contour intervals are 0.2°C. Note that all months of data are used. (e) Normalized global wavelet spectrum and (f) normalized monthly standard deviation of the four indices (see the legend for the definition of colors). HadISST data (Rayner et al. 2003) is used. See the text for the definition of these four indices.

6.1 Indian Ocean Dipole

The Indian Ocean Dipole (IOD) is an interannual tropical air-sea coupled phenomenon with positive (negative) SST anomalies in the western (southeastern) tropical Indian Ocean during its positive phase (Saji et al. 1999; Webster et al. 1999) (*Figure 6.1*a, e). It is associated with easterly wind anomalies and enhanced convection over the western tropical Indian Ocean (Reverdin et al. 1987),

and phase-locked to boreal fall (*Figure 6.1*f; Saji et al. 1999). The Dipole Mode Index (DMI) is defined by the difference in SST anomalies between the western (50°-70°E, 10°S-10°N) and eastern (90°-110°E, 10°S-Equator) poles (Saji et al. 1999). The IOD develops through the Bjerknes feedback as in the El Niño/Southern Oscillation (ENSO) (Saji et al. 1999) and ocean dynamics, including equatorial wave processes, play a central role in its evolution (Nagura and McPhaden 2010; McPhaden et al. 2015). Although the IOD sometimes co-occurs with the ENSO, it can occur independently (Yamagata et al. 2004). Under global warming, it is projected that extreme IOD events increase (e.g. Cai et al. 2014) and the IOD skewness decreases (e.g. Zheng et al. 2010) (see Chapter 11 for the anthropogenic climate change in the Indian Ocean). Also, salinity and barrier layer variability plays an important role. During the positive IOD, negative sea surface salinity (SSS) anomalies appear in the central-eastern equatorial Indian Ocean, while positive SSS anomalies are observed in the southeastern tropical Indian Ocean (Zhang et al. 2013). In the subsurface, positive salinity anomalies are found near the pycnocline in the eastern equatorial Indian Ocean and negative anomalies appear over the southern tropical Indian Ocean (Kido and Tozuka 2017). These salinity anomalies result in barrier layer thickness anomalies and vertical mixing anomalies and are suggested to modify the amplitude of negative SST anomalies in the eastern pole (Qiu et al. 2012; Kido and Tozuka 2017).

Simulation of the IOD has been evaluated by several studies (e.g. Saji et al. 2006; Liu et al. 2014) and, because of its impacts on both local and remote climate (Saji and Yamagata 2003), many studies over the past decade have focused on predictability and prediction. Wajsowicz (2005) made the first attempt to assess the skill of a coupled model in predicting SST anomalies over the eastern and western poles of the IOD and Luo et al. (2008) made the first successful real-time prediction of the IOD. ENSO is a major source of predictability for the IOD through the changes in the Walker circulation in the Indo-Pacific region (e.g. Luo et al. 2007; McPhaden and Nagura, 2014; Yang et al. 2015). SST anomalies in the eastern pole show lower prediction skill compared to the western pole (Luo et al. 2007). This is because the eastern pole is partly driven by the local-air sea coupling, whereas the western pole is predominantly controlled by the ENSO. Tanizaki et al. (2017) showed that the generation mechanisms of negative SST anomalies in the eastern pole ares diverse among positive IOD events and those events in which vertical procesess play an important role tend to be better predicted. By comparing the prediction skill of several coupled models with potential predictability, Liu et al. (2017) suggested that there is potential for improving IOD prediction by 0.2-0.3 in terms of the correlation skill; the anomaly correlation coefficient currently becomes lower than 0.5 only after 3 months. See Chapter 11 for a more review on the IOD prediction.

6.2 Indian Ocean Basin Mode

The Indian Ocean Basin mode (IOBM) is associated with positive (negative) SST anomalies over the tropical Indian Ocean and usually follows an El Niño (a La Niña) event in the tropical Pacific (Yu and Rienecker 1999; Yang et al. 2007) (*Figure 6.1*b). This mode is predominantly driven by surface heat fluxes, although ocean dynamics plays an important role in the southwestern tropical Indian Ocean (Klein et al. 1999). The IOBM index is defined by the principal component of the first empirical orthogonal function mode of SST anomalies over the tropical Indian Ocean (40–110°E, 20°S–20°N) (Yang et al. 2007), which explains about 40% of the total SST variability, and it is highly correlated with ENSO indices with the IOBM index lagging about one season. As a result, the interannual frequency band is dominant (*Figure 6.1*e) and the IOBM has the monthly standard deviation peaks in February-March (*Figure 6.1*f). The IOBM has been shown to influence climate over the Indo-western Pacific and East Asia in the summer following ENSO events and the effect is known as the “Indian Ocean capacitor effect” (Xie et al. 2009, Annamalai et al. 2005; 2007).About half of the CMIP5 models capture key processes of the IOBM including its strong link with the ENSO (Du et al. 2013). Among the four climate modes identified in the Indian Ocean, the IOBM seems to be the best-predicted climate mode, because of its strong link with the well-predicted ENSO (Luo et al. 2016).

6.3 Indian Ocean Subtropical Dipole

The Indian Ocean Subtropical Dipole (IOSD) is a climate mode associated with positive (negative) SST anomalies over the southwestern (northeastern) part of the South Indian Ocean (Behera and Yamagata 2001) (*Figure 6.1*c), and peaks in austral summer (*Figure 6.1*f). It has spectrum peaks in the interannual frequency range, but the peak is not as sharp as that of the IOD and IOSD (*Figure 6.1*e). It has been suggested to influence precipitation over southern Africa (Reason 2001). The IOSD index is obtained by subtracting SST anomalies in the northeastern pole (90°-100°E, 18°-28°S) from those in the southwestern pole (55°-65°E, 27°-37°S) (Behera and Yamagata 2001). The mixed layer warming by the shortwave radiation is enhanced (suppressed) as a result of negative (positive) mixed layer depth (MLD) anomalies over the southwestern (northeastern) part, and these MLD anomalies are induced by anomalous winds associated with changes in the Mascarene High (Morioka et al. 2010). Although many coupled models simulate the IOSD relatively well, the location and structure of the SST anomaly vary among models (Kataoka et al. 2012).

Yuan et al. (2014) evaluated the prediction skill of the IOSD in a coupled model. It was found that the prediction skill is not much different from the persistence, partly because of the low predictability of the SST anomalies in the southwestern pole. However, some strong IOSD events were successfully predicted one season ahead. The low prediction skill may be related to difficulty in predicting interannual variability of the Mascarene High, although increased observations of MLD and the upper ocean stratification may be helpful to improve the prediction skill.

6.4 Ningaloo Niño

An unprecedented marine heat wave in early 2011 led to the identification of a new climate mode called “Ningaloo Niño” (Feng et al. 2013, 2015b; see chapter 4 on extreme events for more details). This recently-identified phenomenon is associated with positive SST anomalies off the west coast of Australia (*Figure 6.1*d) and its strength is defined by the Ningaloo Niño Index (area-averaged SST anomalies in 108°E-coast, 28°S-22°S). Both local ocean-atmosphere positive feedback and remote forcing from ENSO via atmospheric and oceanic teleconnections contribute to its development (Feng et al. 2013; Kataoka et al. 2014, 2017; Marshall et al. 2015). This climate mode peaks around austral summer (*Figure 6.1*f) and the power spectrum shows a broad peak for 4-6 years period (*Figure 6.1*e). Salinity variability is also important for Ningaloo Niño; Feng et al. (2015) showed that low-salinity anomalies contributed to about 30% increase in the southward Leeuwin Current and thus the unprecedented warming event in 2010-2011. The increased occurrence of Ningaloo Niño since the late 1990s may be related to the negative phase of the Interdecadal Pacific Oscillation (Feng et al. 2015a). Because of its impacts on local precipitation (Tozuka et al. 2014) and marine ecosystems (Depczynski et al. 2013; Wernberg et al. 2013, 2016), advancing our understanding of this phenomenon is a priority for the coming decade. Kido et al. (2016) evaluated the ability of coupled models to simulate Ningaloo Niño/Niña and found that further improvements in resolving this climate mode are required in many coupled models.

Doi et al. (2013) were the first to evaluate predictability of Ningaloo Niño/Niña. Although Ningaloo Niño (Niña) events that co-occur with La Niña (El Niño) events were relatively well predicted by a coupled model (e.g. the extreme 2011 event was successfully predicted in hindcast experiments 9 months in advance) owing to the high prediction skill of ENSO events, those developing independent of ENSO events could not be predicted. Resolving the Leeuwin Current with a higher horizontal resolution in the ocean component of coupled models may lead to improved prediction skill (e.g. Doi et al. 2016). Also, since mixed layer process plays a key role in the evolution of Ningaloo Niño/Niña, a RAMA mooring and/or denser observation in the Ningaloo Niño/Niña region of maximum SST anomalies will be helpful for better understanding and prediction of Ningaloo Niño/Niña.

6.5 Required Essential Ocean Variables (EOVs) and actionable recommendations for collection of these EOVs

The required EOVs for better understanding and improved prediction of these climate modes are ocean surface stress, sea surface height, SST, subsurface temperature, surface and subsurface currents, sea surface and subsurface salinity, and ocean surface heat flux. Considering that coastal currents and upwelling in the eastern basin play an important role in the development of the IOD (Halkides and Lee 2009; Tanizaki et al. 2017) and Ningaloo Niño/Niña (Marshall et al. 2015), it is desirable to obtain the above variables with a horizontal resolution of 0.5° or higher in these regions. Also, daily data are required especially for the IOD and Ningaloo Niño/Niña, because intraseasonal variations including the Madden-Julian Oscillations significantly influence evolution of these climate modes (Rao and Yamagata 2004; Marshall and Hendon 2014). Furthermore, subsurface data in addition to surface data is valuable for improved prediction of these climate modes (e.g. Horii et al, 2008; Doi et al. 2017).

Based on the above, the actionable recommendations on the current Indian Ocean Observing System (IndOOS) design is as follows:

1) Sustain the existing satellite and in situ measurements from the IndOOS as well as the Argo network in the entire Indian Ocean to advance our understanding of and ability to predict these climate modes.

2) Complete and maintain the RAMA buoy network. Deployment of the RAMA buoy in the western tropical Indian Ocean allows us to better understand the dynamics and thermodynamics of the western pole of the IOD. The RAMA buoys in the eastern pole of the IOD are essential for further understanding of the IOD as well as improved prediction of the IOD.

3) Near-coastal enhancement of IndOOS in the eastern pole of the IOD and in the formation region of the Ningaloo Niño would also be desirable.

4) Maintain the IX01 XBT line with a monthly resolution. This will be helpful for monitoring the Pacific influence on the Ningaloo Niño/Niña via the oceanic channel.

7. IndOOS Review Chapter: Indian Ocean heat budget

Lisa Beal[1], Elaine McDonagh[2]

1.RSMAS/OCE, University of Miami, USA;
2. National Oceanography Center, Natural Environment Research Council (NERC), UK

7.1 Current Understanding and Societal Impact

To date, the world's oceans have absorbed 93% of the global heat gain due to anthropogenic increases in greenhouse gases over the last 150 years (Cheng et al., 2017). The oceans are acting as a buffer to global warming. Although the Indian Ocean is the smallest of the world's oceans, it has accounted for more than one quarter of global ocean heat gain over the last twenty years (Lee et al., 2015; Cheng et al. 2017) and perhaps as much as 45% over the upper 700 m in the last ten years (Desbruyeres et al., 2017). Since 1950 it has warmed about 1°C at the surface, compared to a global average of 0.6°C, possibly due to a faster response to climate change, or to natural decadal variability (Lau and Weng 1999; Alory et al. 2007; Roxy et al. 2014). Oceanic heat content and its distribution influences the climate of Indian Ocean rim countries through its feedback on winds, rainfall, storm intensity, and sea level rise (Han et al., 2014; Chapter OD-02). And can influence fisheries and marine ecosystems due to associated changes in stratification, oxygen, and nutrient levels (Roxy et al., 2016). Funk et al. (2008) estimate a 50% increase in undernourished populations of East Africa owing to long term decreases in rainfall due to warming trends in the equatorial Indian Ocean. Sea level rise has accelerated along the coasts of India and Australia since the late 1990s and greater than global increases have been estimated along the coasts of Indonesia, Sumatra, Oman, and Madagascar (Han et al., 2010, Watson, 2011).

Heat content and its variability throughout the Indian Ocean depend on the inflow and outflow of heat across its borders (Roberts et al., 2017). In contrast to the Atlantic and Pacific Oceans, the Indian Ocean is insulated from surface heat loss at cold northern latitudes by the Asian continent and receives an influx of warm tropical waters via the Indonesian Throughflow. As a result, there is large heat gain which is balanced by an export across its open southern boundary, estimated to be as much as 1.5 PW (Figure 1; Ganachaud and Wunsch, 2000; Lumpkin and Speer, 2007; Hernández-Guerra and Talley, 2016). This Indian Ocean heat export plays the biggest role in balancing heat loss in both the Atlantic and Southern Oceans (Talley, 2013). It is carried predominantly by an overturning circulation, with the transport of warm outflowing surface waters within the Agulhas Current balanced by deep inflows of cold Antarctic waters, although the circulation may best be described by separate upper gyre and deep overturning cells (McDonagh et al., 2008). Some 30% of Indian Ocean heat export is thought to be carried by the gyre circulation (Talley, 2008). The properties and heat content of the outflowing waters depend strongly on mixing and diffusion in the Indian and Pacific Oceans.

Estimates for Indian Ocean overturning range between 8 and 25 Sv, with an even larger range for the heat export, of between 0.1 and 1.5 PW (Sultan et al., 2007; Hernández-Guerra and Talley, 2016). Diapycnal mixing at the bottom of the thermocline has been estimated to be several times stronger than in the Pacific or Atlantic, with unknown causes (Lumpkin and Speer, 2007). All these estimates have been underpinned by hydrographic (GO-SHIP) data collected across the Indian Ocean along nominal latitude 32°S, combined with Indonesian Throughflow and surface flux observations. There have been three occupations at this latitude over the last thirty years; in 1987, 2002, and 2009. To estimate mean absolute fluxes the circulation is assumed to be steady and geostrophic, and conservation of mass, salt, and other properties are used as constraints. Four estimates have been derived using global hydrography and constraints (e.g. figure 7.1), yielding Indian Ocean overturning between 10 and 17 Sv and heat exports of 1.45-1.55 PW (McDonald, 1998; Ganachaud and Wunsch, 2000; Lumpkin and Speer, 2007, Talley, 2008). The temporal variability of Indian Ocean overturning remains unknown at any time scale and could be as large as 20 Sv peak-to-peak and 5 Sv at seasonal scales, if similar to the Atlantic overturning (Kanzow et al., 2010).

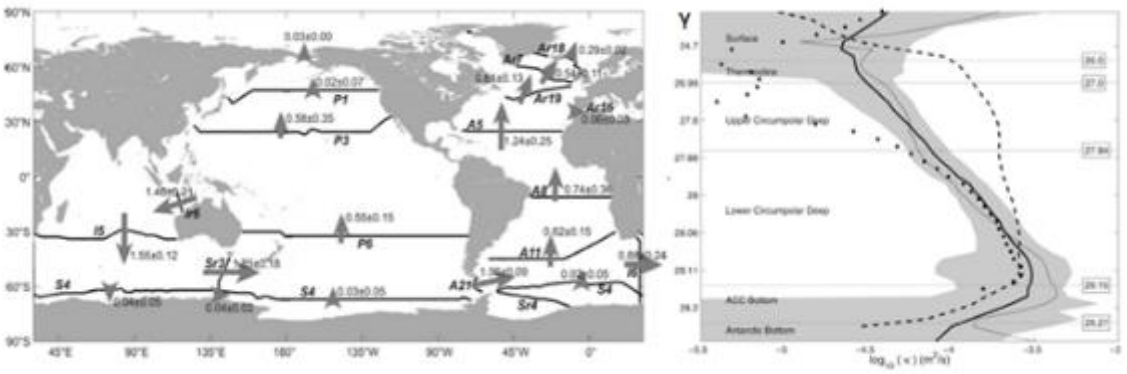

Figure 7.1: The largest oceanic heat transports are estimated in the Indian Ocean (left, PW), where diapycnal mixing at the base of the thermocline may be five times stronger than the Pacific and Atlantic Oceans (right, m^2/s). Heat transports are from a global inverse model. Effective diapycnal diffusivities are shown as a function of neutral density (γ) for the global average (thick line with standard error shaded), Atlantic (thin solid), Indian (dashed), and Pacific (dotted) boxes, all between 32°S–48°N. Horizontal lines indicate water mass divisions (Orsi et al. 2002). From Lumpkin and Speer (2007).

Overturning and heat export are thought to be strongly constrained by the strength and depth of the Agulhas Current at the western boundary (Bryden and Beal, 2001) and by the Indonesian Throughflow (Sprintall et al., 2014), although the exact dependencies are highly uncertain (McDonagh et al., 2008). The Agulhas Current appears to have broadened over the past twenty years with little change in its transport despite strengthening Westerlies (Beal and Elipot, 2016), while the Throughflow is currently shoaling and strengthening along with strengthening of the Pacific Trade winds (Wijffels et al., 2008; Feng et al., 2011; Sprintall and Révelard, 2014). Over the long-term the Agulhas is expected to strengthen and the Throughflow to weaken with climate change (Yang et al., 2016; Feng et al., 2017). The vertical structure of Indian Ocean overturning is less robust than estimates for the Atlantic and Pacific, with net flow direction in the thermocline and intermediate waters appearing to change between occupations (Hernández-Guerra and Talley, 2016). This may be related to decadal variability in Indian Ocean thermocline waters which have reversed from freshening (Bindoff and McDougall, 2000) to now becoming saltier (McDonagh et al., 2005), while the subtropical gyre may have been strengthening 1987-2002 (Palmer et al., 2004), as also indicated by oxygen changes (McDonagh et al., 2005). Long-term warming of upper Indian Ocean waters is concentrated in the southern Indian Ocean (Alory et al., 2007) and throughout the Agulhas system (Wu et al., 2012) and may be related to a poleward expansion of the subtropical gyre. Abyssal ocean warming below 4000 m (Purkey and Johnson, 2010; Desbruyeres et al., 2017) and a possible reduction in Antarctic bottom water formation may have contributed to a reduction in Indian Ocean overturning since 2002 (Katsumata et al., 2013; Hernández-Guerra and Talley, 2016). The contribution of eddies to heat transport is difficult to capture (Johns et al., 2011) and undetermined in the Indian Ocean.

There is much to be gained through monitoring of Indian Ocean overturning and heat fluxes as a component of the Indian Ocean Observing System. In the past decade of IndOOS most targeted assets have been concentrated within the equatorial region, yet Banks and Wood (2002) suggest that subsurface temperature and salinity in the southern Indian Ocean are a good place to look for climate change signals. The greatest rates of heat content changes have been in the Southern Indian Ocean, thought to be due to a shift and intensification of the Westerly winds and spin-up of the Southern hemisphere supergyre (Cai et al., 2007; Wu et al., 2012; Alory et al., 2007; Yang et al., 2016). At the same time, a reduction in Antarctic bottom water formation may have weakened the overturning while strengthening the export of heat (Katsumata et al., 2013; Hernández-Guerra and Talley, 2016). We need to better understand how sea surface temperature, heat content, the Agulhas Current, and heat export are linked in order improve predictability of interannual to decadal climate variability over the Indian Ocean basin and rim countries.

7.2 Required Essential Ocean Variables

To gain a better understanding of how wind and circulation changes impact the Indian Ocean heat budget and vice versa we need to measure variability and change in Indian Ocean overturning and heat flux. This requires the collection of temperature, salinity, pressure, velocity, and where possible oxygen data in both the upper and deep oceans along the open southern boundary of the basin, latitudes ~32°-34°S (figure 7.2). Daily observations of these EOVs at 10 km (inshore)—50 km (offshore) horizontal resolution, and 100 m (upper)—1000 m (bottom) vertical resolution are needed to capture the intense Agulhas Current and its heat flux at the western boundary. At the eastern boundary, full-depth (>4000 m), daily observations at a fixed point near the foot of the continental slope are needed to provide, in combination with the western boundary array, a time series of basin-wide geostrophic fluxes for the overturning. The Leeuwin Current is small and shallow and currently lies within error bars, but capturing it too would improve estimates. Across the interior, deep profiles (6000 m) of EOVs T,S,p,O2 at monthly resolution are needed to capture eddy fluxes, inflows of deep and bottom waters, and constrain gyre circulation. Periodic GO-SHIP sections, which include the collection of silicates and other properties, are required to provide important constraints on circulation and heat flux estimates. These in situ observations must be augmented by sustained, consistent satellite observations of sea level and wind stress to obtain barotropic fluxes and meridional Ekman transport.

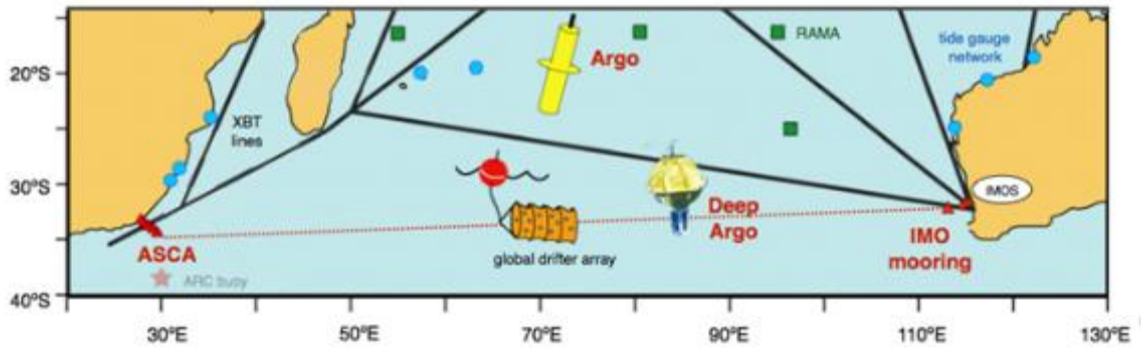

Figure 7.2: Recommendations for targeted observing system elements to capture Indian Ocean overturning and heat transport. Western boundary observing system (ASCA), eastern boundary hydrographic mooring (IMO: Indian Meridional Overturning), and deep Argo. Sustained satellite observations (sea level, temperature, winds), Argo, surface drifters, and measurement of the Indonesian Throughflow are also essential.

7.3 Actionable Recommendations

1) Sustained Agulhas array, including a deep western hydrographic “end-point” mooring (> 4000 m).
2) Establishment of a deep eastern hydrographic “end-point” mooring in waters > 4000 m near Western Australia and the existing Leeuwin Current array.
3) Sustained Indonesian Throughflow volume and heat flux monitoring.
4) Deep Argo float deployments throughout the south Indian Ocean subtropical gyre.
5) Decadal repeat of GO-SHIP line I5.

8. Carbon cycle, acidification, and ecological impacts (R. Hood)

8.1 Current understanding and societal Impact

The oceanic uptake of atmospheric CO_2 is estimated to be 2.6 Gigatonnes (Gt) of carbon per year, which is nearly comparable to the uptake by land (LeQuere et al., 2015). As such, the oceanic sink plays an important role in the global carbon cycle acting to slow the increase of atmospheric CO_2 (Sabine et al., 2004; Takahashi et al., 2009) and therefore also global climate change. Thus, it is important to accurately quantify the oceanic sink and understand the factors that drive it's spatial and temporal variability in order to accurately project future atmospheric CO_2 levels and global climate change (Takahashi and Sutherland, 2013).

It has been estimated that the Indian Ocean as a whole accounts for ~1/5 of the global oceanic uptake of atmospheric CO_2 (Takahashi et al., 2002). The Arabian Sea is a source of CO_2 to the atmosphere because of elevated pCO_2 within the Southwest Monsoon-driven upwelling (*Figure 8.1*; see also Takahashi et al., 2009; 2014). Overall, the Indian Ocean north of 14°S loses CO_2 at a rate of 0.12 PgC/yr. Takahashi et al., 2002; 2009; 2014). Whether the Bay of Bengal is a CO_2 source or sink remains ill-defined due to sparse sampling in both space and time (*Figure 8.1*; Bates et al., 2006a). The southern Indian Ocean appears to be a strong net CO_2 sink (-0.44 PgC/yr in the band 14°S-50°S; *Figure 8.1*). The biological pump (sum of all the biologically mediated processes that export carbon) and the solubility pump (dissolution of CO_2 and its physical transport) are estimated to contribute equally to the CO_2 flux in the South Indian Ocean region (Valsala et al., 2012), but the factors that maintain this sink are unclear. Cold temperatures certainly increase CO_2 solubility in the austral winter, but there is also evidence that chemical and biological factors are important (Piketh, Tyson, and Steffen 2000; Wiggert, Murtugudde, and Christian 2006).

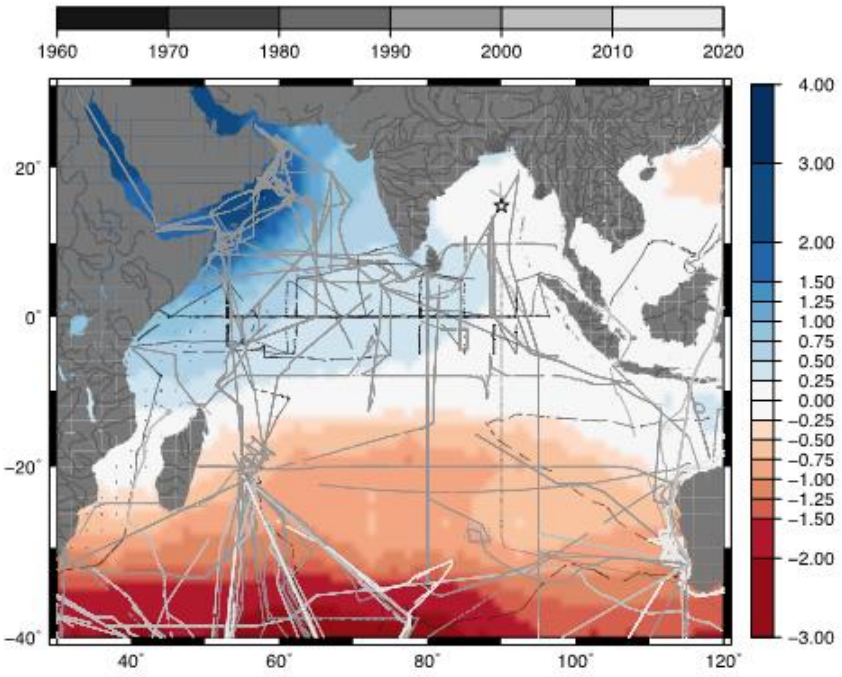

Figure 8.1 Annual CO_2 flux (mol C m^{-2} yr^{-1}) referenced to the year 2000 (Takahashi et al., 2009) over the Indian Ocean. Data points colored by year of collection (Takahashi & Sutherland, 2016) are overlaid as points. Major rivers are also delineated over the continents.

A synthesis of the seasonal, annual and interannual air-sea CO_2 fluxes based on both observations (Takahashi et al., 2009) and models (ocean, atmospheric inversions), shows that the sea-air CO_2 uptake derived from models (-0.37 PgC/yr) is not inconsistent with the estimates from observations (-0.24 PgC/yr), given the uncertainties (Sarma et al., 2013). However, models underestimate the flux in the northwestern region and overestimate the flux in the Bay of Bengal. This suggests that the atmospheric inversions are not well constrained due to lack of CO_2 time series. Observations of ocean carbon flux are very important to constrain these models. Compared to other oceans there have been few observations in the Indian Ocean (north of 20S) in recent years (Figure 8.1; Bakker et al., 2014, see also www.socat.info).

The uptake of anthropogenic CO_2 by the global ocean induces fundamental changes in seawater chemistry that could have dramatic impacts on upper ocean ecosystems. Estimates based on the Intergovernmental Panel on Climate Change (IPCC) business-as-usual emission scenarios suggest that atmospheric CO_2 levels could approach 800 ppm near the end of this century (Feely et al., 2009). The associated global trend of increasing oceanic CO_2 concentrations will lead to lower pH and acidification of the Indian Ocean over the coming decades, with potential negative impacts on coral reefs and other calcifying organisms (Doney, 2010). The average surface pH values for the northern (20°E-120°E, 0°-24.5°N) and southern Indian (20°E-120°E, 0°-40°S) oceans in 1995 were 8.068 +/- 0.03 and 8.092 +/- 0.03, respectively (Feely et al., 2009, the lowest of the major ocean basins. The causes for these differences are not understood (Takahashi et al. 2014). Seasonally occurring very low surface pH (<7.9) off the Arabian Peninsula results from upwelling of (more acidic) subsurface waters during the SW monsoon (Takahashi et al., 2014). There are only a few studies on the temporal evolution of surface ocean acidification because of the lack of time-series measurements. The results of a recently published study from the eastern Bay of Bengal indicate a decrease in pH of 0.2 in the period from 1994 to 2012 (Rashid et al., 2013), which is much faster than the global rate of 0.1 over the last 100 years (IPCC 2007).

The large-scale coral bleaching events of 1998, 2005 and 2011 caused by high sea-surface temperatures highlight the susceptibility of the Indian Ocean to warming (McClanahan et al., 2007; Moore et al., 2012; see also section 3 of chapter 4 on the 2011 marine heat wave off Western Australia), and ocean acidification has the potential to exacerbate these negative impacts on coral reef areas. For example, the 1998 bleaching event influenced higher trophic levels by altering the age distribution of commercially harvested fish (Graham et al. 2007). Coral reef ecosystems may be at greater risk than previously thought because of the combined effects of acidification, human development and global warming (Hoegh-Guldberg et al., 2007). In addition, some commercially fished species (e.g., shelled mollusks) are directly vulnerable to ocean acidification (Hoegh-Guldberg et al., 2014). A study on modern planktonic foraminifera off Somalia suggests that human-induced ocean acidification reduced the rate at which foraminifera calcify, resulting in lighter shells (de Moel et al., 2009). The Southern Ocean sector of the Indian Ocean could experience major disruptions in upper levels of pelagic food webs due to the effects of acidification on calcifying pteropods, which are preyed on by many higher trophic level organisms (Bednarsek et al., 2012).

In addition to the direct impacts of acidification, increasing CO_2 in the upper ocean could lead to increased primary productivity for some species (e.g., diazotrophs; Hutchins et al., 2007), altering rates of nitrogen fixation and therefore the biogeochemistry of particulate organic matter formation and remineralization. Decreasing pH also shifts the chemical equilibrium from ammonia (NH_3) to ammonium (NH_4^+), which may alter key biological processes such as microbial nitrification and nitrogen assimilation by phytoplankton (Gattuso and Hansson, 2011).

Clearly, understanding current carbon uptake by the Indian Ocean is critical for understanding how the global carbon cycle and climate are evolving under the impact of human activities. Understanding and predicting rates of carbon uptake and ocean acidification are also fundamental to understanding the biogeochemical and ecological evolution of the Indian Ocean

8.2 Required EOVs, their spatial coverage and temporal/spatial resolution

The observations required to constrain the carbon system at a point in space and time are any two of Dissolved Inorganic Carbon (DIC), Total Alkalinity (TA), partial pressure of carbon dioxide (pCO_2) and pH, plus temperature and salinity. The products that can be derived from these carbon system measurements include saturation state (aragonite, calcite), dissolved carbonate ion concentration, air-sea flux of CO_2, anthropogenic carbon, and the change in total carbon.

The carbon cycle research community has set a goal of being able to constrain the regional fluxes to 0.2 Pg C $year^{-1}$, which translates into measuring the atmospheric fCO_2 (fugacity to CO_2 which is similar to partial pressure) to within 0.1 µatm and the seawater fCO_2 to within 2 µatm (Pierrot et al., 2009). These observations can be obtained from ships and moorings, with ships providing infrequent large-scale spatial transects and moorings providing complimentary continuous measurements at specific locations.

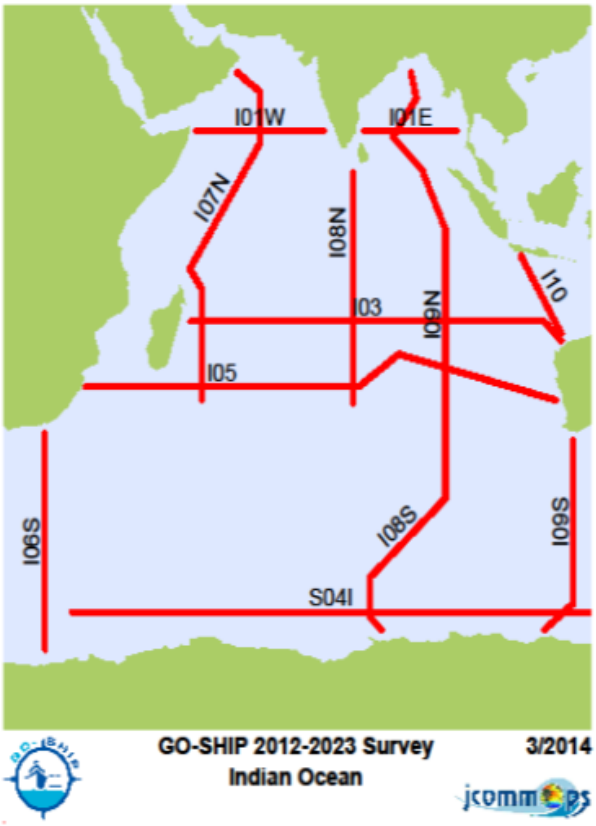

Figure 8.2 GO-SHIP sections in the Indian Ocean.

The GO-SHIP program is working to develop a globally coordinated network of sustained hydrographic sections as part of the global ocean/climate observing system including physical oceanography, the carbon cycle, marine biogeochemistry and ecosystems. GO-SHIP provides approximately decadal resolution of the changes in inventories of heat, freshwater, carbon, oxygen, nutrients and transient tracers, covering the ocean basins from coast to coast and full depth (top to bottom), with global measurements of the highest required accuracy to detect these changes. GO-SHIP has several lines in the Indian Ocean that are part of the global decadal survey (Figure 8.2). Several of these lines have national commitments for occupation over the next 5 – 10 years. These surveys will be crucial for filling in the current large spatial gaps in carbon system measurement in the Indian Ocean (Figure 8.1, for more details on the GO-SHIP program see chapter 25).

The development and deployment of Moored Autonomous pCO_2 ($MAPCO_2$) systems have dramatically improved our ability to characterize the temporal variability in the carbon system, sea–air gas exchange, and biogeochemical processes (Sutton et al, 2014). The $MAPCO_2$ system provides high-resolution data that can measure interannual, seasonal, and sub-seasonal dynamics and constrain the impact of short- term biogeochemical variability on CO_2 flux. Overall uncertainty of the $MAPCO_2$ using in situ calibrations with certified gas standards and post-deployment standard operating procedures is < 2 µatm for seawater partial pressure of CO_2 (pCO_2) and <1µatm for air pCO_2. The $MAPCO_2$ can maintain this level of uncertainty for over 400 days of autonomous operation and the measurements are consistent with ship- board seawater pCO2 measurements. The MAPCO2 system also provides direct measurements of pH.

The deployment of a $MAPCO_2$ system at the Bay of Bengal Ocean Acidification (BOBOA) mooring site, established at 15°N, 90°E on 23 November 2013, is providing the first continuous surface water carbon system measurements along with physical measurements in the northern Indian Ocean. Data from the time series reveal strong seasonal variations in pCO_2 in the surface water relative to the air, which are associated with the monsoon seasonal cycle, with a slight predominance of ingassing over the annual cycle (*Figure 8.3*; Hood et al., 2017). Multiple deployments of $MAPCO_2$ systems on RAMA moorings could fill in the current large temporal gaps in carbon system measurement in the Indian Ocean that cannot be addressed by the infrequent large-scale GO-SHIP surveys.

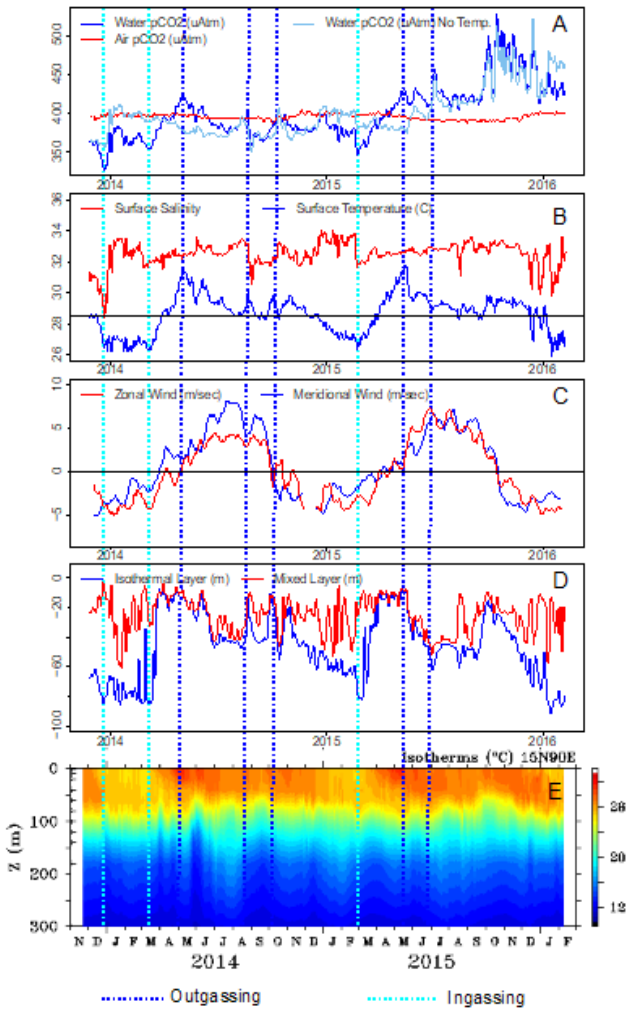

Figure 8.3 Time series plots from the BOBOA mooring of: (A) pCO_2 in the water (dark blue), in the air (red) and with the temperature effect removed (light blue); (B) surface temperature (blue) and salinity (red); (C) zonal (red) and meridional (blue) wind speed; (D) isothermal layer (blue) and mixed layer (red) depth; and (E) water column temperature down to 300 meters depth.

8.3 Recommendations for collection of these EOVS in the context of IndOOS

IndOOS should seek additional resources to enable deployment of $MAPCO_2$ systems on RAMA moorings. The RAMA mooring array design/deployment team has identified 8 sites for air-sea observatories (Flux Reference Sites, Figure 8.4 and Table 8.1). These sites should be targeted for deployment of the $MAPCO_2$ systems (one per mooring) because they provide all of the additional atmospheric and physical oceanographic measurements that are needed to calculate the derived products mentioned above and, in particular, air-sea flux of CO_2.

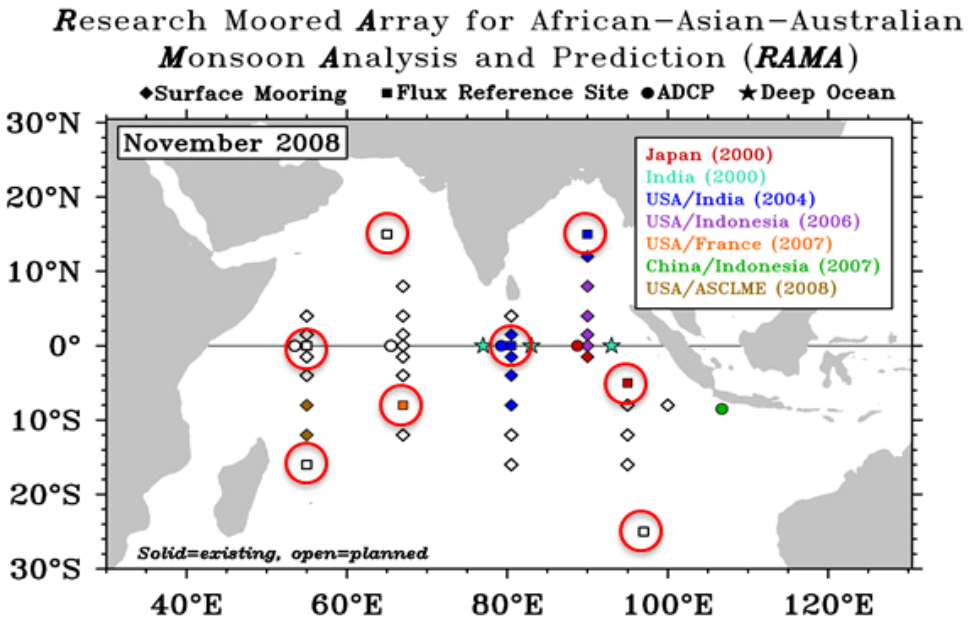

Figure 8.4 The RAMA mooring array Flux Reference Sites (circled in red).

In addition, collaboration between GO-SHIP and IndOOS provides a potential opportunity to add large-scale carbon system measurements to IndOOS. GO-SHIP should become an integral component of IndOOS, providing high-quality carbon system measurements, along with heat, freshwater, oxygen, nutrients and transient tracers in the Indian Ocean along dedicated repeated hydrographic lines.

9. Oceanic fluxes: Boundary currents and Indonesian Throughflow

Ming Feng, CSIRO Ocean and Atmosphere, Perth, Western Australia, Australia
R. Dwi Susanto, University of Maryland, Maryland, USA, & Bandung Institute of Technology, Indonesia
Helen Phillips, University of Tasmania, Hobart, Tasmania, Australia
Lisa Beal, University of Miami, Florida, USA

9.1 Motivation

Ocean boundary currents of the Indian Ocean, including western boundary currents and eastern boundary currents, are narrow and fast-flowing currents along boundaries of the ocean basin, are important for heat transport, nutrient distribution and marine productivity, and ocean climate on regional and basin scales. The enclosed northern Indian Ocean boundary, seasonally-reversing monsoonal forcing, and the connection with the Pacific engender some of the unique oceanography features of the Indian Ocean. Most notable is the low-latitude connection to the Pacific Ocean through the Indonesian Seas, the Indonesian throughflow (ITF), providing a pathway from the large heat store of the Western Pacific warm pool into the tropical Indian Ocean. The magnitude and variability of the ITF are important to the basin budgets of both Pacific and Indian Oceans. The ITF and the Agulhas Current form the warm route of the global overturning circulation, which regulates global climate on multi-decadal and centennial time scales. On average, 15 Sv from Agulhas leaks into Atlantic as surface arm of Atlantic Meridional Overturning Circulation (AMOC, Beal et al., 2011). Strength of Agulhas and ITF are largest components of the Indian Ocean heat budget, but their contribution to the variability of basin scale heat budget is still not well quantified (chapter 1.7).

Globally, subtropical western boundary currents are the fastest warming regions of the world ocean (Wu et al., 2012); they integrate changes from across the basin and carry vast amounts of heat poleward, influencing the overlying atmosphere (Figure 9.1). Models and reanalyses have suggested that western boundary currents are strengthening with climate change (Wu et al., 2012), yet direct observations point to an increase in their eddy kinetic energy instead (e.g. Beal and Elipot, 2016). The Agulhas leakage is expected to increase with climate change (Biastoch et al., 2013) and could weaken AMOC (Weijer et al., 2002). The ITF is observed to have strengthened during the climate change hiatus in recent decades (Liu et al., 2015), reversing a previous declining trend (Wainwright et al., 2008). The ITF is projected to weaken under the influence of human-induced climate change (sen Gupta et al., 2016; Feng et al., 2017). There are still substantial uncertainties in the decadal and centennial changes of the ITF and the boundary current systems in the Indian Ocean in both observations and numerical models, with neither yet able to fully resolve these narrow, dynamic systems.

Almost all the countries in the Indian Ocean region are developing countries which are often densely populated. In general, ocean boundary currents of the Indian Ocean have not been well observed under the IndOOS program due to severe lack of resources from the bordering countries. The narrow, intense nature of boundary currents requires finely spaced instrumentation to observe their structure and variability. The environment is challenging because the instruments are susceptible to human interference and require robust engineering to manage long-term deep deployments. Sustained observations of these boundary currents are crucial to quantify their contribution to the basin scale heat and freshwater balances and to better constrain future climate projections of the Indian Ocean circulation and climate.

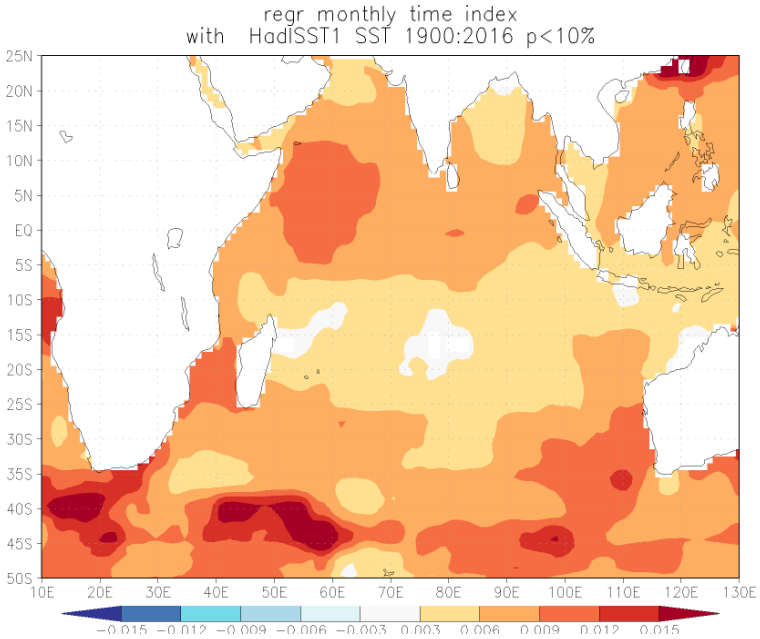

Figure 9.1 Linear trend of sea surface temperature the Indian Ocean during 1900-2016 (unit: K/year)./ HadISST1 data are used to derive the trend. Generated from Climate Explorer.

9.2 Background

9.2.1 Indonesian Throughflow

The ITF conveys volume, heat, and freshwater fluxes from the tropical Pacific into the southeastern Indian Ocean through the complex topography and narrow passages of the Indonesian Seas. There are three main pathways of the ITF: the Karimata Strait, Makassar Strait, and Lifamatola passage. The ITF exits into the Indian Ocean mainly through the Timor passage, Ombai Strait, Lombok Strait, and the Sunda Strait, with an average transport of 15 Sv (Figure 9.2; Sprintall et al., 2009; Susanto et al., 2016). Tidal mixing and air-sea interaction in the Indonesian Seas strongly modify the ITF water properties (i.e Ffield and Gordon, 1996; Alford et al., 1999; Hatayama, 2004; Koch-Larrouy et al., 2007; 2010; 2015; Nagai and Hibiya, 2015; Ray and Susanto, 2016). The ITF variability is influenced by El Niño Southern Oscillation (ENSO) and Inter-decadal Pacific Oscillation (IPO) from the Pacific and by the Indian Ocean Dipole (see chapter 1.6) variability (e.g. Deckker, 2016; Lee et al*.,* 2015; Sprintall et al*.,* 2014; Liu et al*.,* 2015). Climate models project a significant decline of the ITF transport in the future, mostly associated with weakening of the deep upwelling in the Pacific and the slowdown of the global overturning circulation (sen Gupta et al., 2016; Feng et al., 2017). With the increase in the intensity of ENSO variability under a warming climate (Cai et al., 2014; 2015), the ITF variability may also increase.

Sustained *in situ* measurements of the ITF are logistically challenging and expensive. The longest-running time series of 30 years is from the IX1 XBT line between Fremantle, Australia and Sunda Strait, Indonesia, currently occupied bi-weekly (chapter 2.3). This line captures the upper ocean geostrophic structure of the ITF outflow as it first enters the Indian Ocean (Meyers et al. 1995, Wijffels et al. 2008). These observations have also revealed that ITF geostrophic transport is strong during La Nina, and weaker during El Nino, Meyers 1996), and that it has been increasing at a rate of 1 Sv per decade over the past 30 years (Liu et al., 2015). Measurements in all major ITF passages were taken simultaneously for the first time from 2003 to 2007 (Gordon et al*.,* 2010; Sprintall et al., 2009; Susanto et al*.*, 2012; Van Aken et al., 2009), revealing a total ITF transport of 15 Sv. Subsequently, the South China Sea throughflow in the Karimata and Sunda Straits was measured from 2007 to 2016 (Fang et al*.,* 2010; Susanto et al*.*, 2010; 2013; Wei et al., 2015). Major results from the analysis of these observations and associated modelling work reveal that

the ITF has maximum velocities near 100 m depth, with less volume carried in surface waters than previously thought; El Nino causes a shoaling and slowing of the ITF; and intense vertical mixing produces upwelling and cooling of surface waters in the Indonesian Seas that affects regional precipitation and wind patterns (Sprintall et al. 2014).

Whereas the IX1 XBT line relies on a reference depth to derive the upper ocean geostrophic transport and doesn't resolve processes below 700m, the direct mooring observations were only for a much shorter period. Techniques for developing a proxy-ITF monitoring system are ultimately needed in order to ensure cost-effective, long-term ITF transport information. Proxies, such as from satellite sea surface height observations work well for the case where ITF transport is concentrated only in the upper layer (Potemra et al., 1997; Potemra 2005; Sprintall and Revelard, 2014; Susanto et al*.,* 2007; van Aken 2009). A combined geostrophic-hydraulic formulation to estimate the full-depth ITF transport, which draws upon altimetry sea surface height for the surface layer (geostrophic balance) and ocean bottom pressure for the deeper-layer (hydraulic control) (Susanto and Song, 2015), provides a two-layer proxy framework.

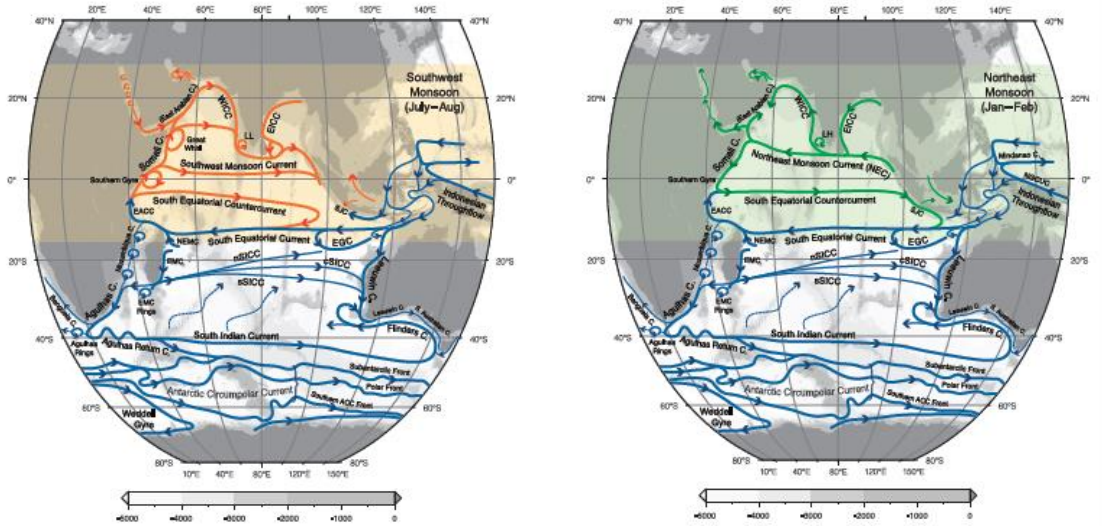

Figure 9.2 Surface circulation of the Indian Ocean in boreal summer and winter. Adapted from Talley et al. (2011), with Southern Indian Ocean interior circulation after Menezes et al. (2013; 2014). Art work: Louise Bell.

9.2.2 Eastern boundary current systems

The meridional pressure gradient in the southeast Indian Ocean provides the driving force for the Leeuwin Current, and also supports broad eastward currents that feed into the Leeuwin Current (Figure 9.2; Thompson 1984; McCreary et al. 1986; Furue et al. 2017). The Leeuwin Current transports warm, fresh tropical waters southwards and is important for the upper ocean heat and freshwater balances in the southeast Indian Ocean (Domingues et al., 2007; Feng et al., 2008). The Leeuwin Current also hosts broad-scale downwelling (Furue et al. 2017, Liang et al. 2017) of the eastward surface currents into the depths of the Leeuwin Undercurrent (200-1000m) to create a zonal overturning cell in the upper 1000m of about 4 Sv (Furue et al. 2017). The Leeuwin Undercurrent carries waters of Subantarctic origin along the western Australian coast (Woo and Pattiaratchi 2008), leaving the coast near 22°S contributing the lower limb of the zonal overturning (Furue et al. 2017). Theories around the Leeuwin Current dynamics predict the surface current will strengthen southward in response to the zonal inflow of mass (Furue et al. 2013, Benthuysen et al. 2014), however, this strong downwelling at the coast counters these ideas and is likely a key to the not yet understood dynamics of the Leeuwin Undercurrent.

The Leeuwin Current system channels Pacific influences such as ENSO and IPO into the Indian Ocean through the planetary waveguides (Feng et al., 2003; Wijffels and Meyers 2004). The

Leeuwin Current is strong during La Nina and negative Inter-decadal Pacific Oscillation (IPO) phase. An unseasonably strong Leeuwin Current during the 2010-11 La Nina event in the negative phase of IPO instigated an unprecedented marine heat wave off the west coast of Australia (Feng et al., 2013), damaging the marine ecosystems (also see chapter 1.4.3). IPO anomalies transmitted through the Pacific-Indian waveguide have been suggested to influence decadal variations of Indian Ocean thermocline depth (Han et al., 2014) and the shallow overturning circulation (e.g. Zhuang et al., 2013).

Measurements of the Leeuwin Current have been patchy. Since 2009, the Australian IMOS program has been monitoring the Leeuwin Current system using ADCP and thermistor moorings and monthly/quarterly glider surveys. The mooring observations have been confined to the shelf within the 500 m isobath. The southern end of the IX1 XBT line does not provide sufficient data resolution to capture the interannual variations of the Leeuwin Current. So far, most of the interannual and decadal variations of the Leewin Current have been inferred from the Fremantle sea level observation in the IndOOS tide gauge network (Feng et al., 2003; Feng et al., 2011; chapter 2.6).

The South Java Current system provides an important oceanic waveguide for communicating tropical Indian Ocean climate variability into the Indonesian seas (Wijffels and Meyers, 2004; Sprintall et al., 2014). The region hosts strong coastal upwelling (Susanto et al., 2001; Susanto and Marra, 2005; see chapter 1.3) and is a key region for the development of the coupled atmosphere-ocean instability of the Indian Ocean Dipole (chapter 1.6).

RAMA moorings off the Sumatra-Java coast have been monitoring the coupled atmosphere-ocean processes of the boundary current system (chapter 2.3). Variability of the South Java Current has been partly surveyed by the IX1 XBT line, as a component of the total ITF transport variability. No designated observing program has been implemented for the South Java Current system.

9.2.3 Western boundary currents

The bulk of the ITF waters is carried westward in the South Equatorial Current and feed the Agulhas Current through the Mozambique Channel or the southern tip of Madagascar (Figure 9.2; Quartly et al., 2006, Nauw et al., 2008; Ridderinkhof et al., 2013). Agulhas system is a hotspot for air-sea interaction, pumping moisture into the atmosphere and accelerating winds (Rouault et al., 2003; Small et al., 2008). Rising sea surface temperatures over the Agulhas system (Figure 9.1; Wu et al., 2012) are expected to enhance coupling with the atmosphere, altering regional wind and rainfall patterns, and may act to dry the adjacent southern African continent (Rouault et al., 2010; Neukom et al., 2014). Ocean reanalyses suggest that warming of the Agulhas system is related to an intensification and poleward shift of the currents (Wu et al., 2012; Yang et al., 2016), driven by an intensification and poleward shift of the westerlies which is projected to continue over the twenty-first century under anthropogenic forcing (Cai, 2006; Sen Gupta et al., 2009; Biastoch & Boning, 2013). In situ observations combined with satellite altimetry point instead to an increase in eddy kinetic energy throughout the system, such that the Agulhas Current has broadened but not strengthened over the past 25 years (Beal & Elipot, 2016). About 10% interannual variance of Agulhas teleconnected to ENSO, with resultant SST anomalies possibly linked to rainfall over Southern Africa (Rouault et al., 2010; Putrasahan et al., 2016; Dieppois et al., 2015; Elipot & Beal, in review).

The Mozambique Channel has emerged as a major thoroughfare of tropical/subtropical exchange (Ridderinkhof et al., 2010). Observations of Mozambique Channel inflow from 2003 to 2012 measured a mean transport of 16.7 Sv with a maximum in austral winter, and IOD-related interannual variability of 8.9 Sv (Ridderinkhof et al., 2010). During 2010-2013 the Agulhas Current Time-series project measured the variability of the western boundary current proper using an array of moorings beneath a satellite altimeter ground track at around 34°S off South Africa. The transport was found to be 85 Sv in the mean, including about 25 Sv of ITF and overturning transport. The transport varies by 10 Sv throughout the year, with a maximum in austral summer (Figure 9.3; Beal et al., 2015), opposite to that in the Mozambique Channel. The pilot of a sustained array in the

Agulhas Current as part of IndOOS, the Agulhas System Climate Array (ASCA), began in April 2016 through collaboration between South African, US, and Dutch scientists. ASCA consists of full-depth current, temperature, and salinity measurements, with offshore CPIES able to capture the flow during meander events (Figure 9.3).

During boreal summer monsoon, the East African Coastal Current overshoots the equator to supply the northward Somali Current along the boundary (Schott and McCreary 2001, Beal et al., 2013). Its strength builds from about 5 Sv in June to 37 Sv in September (Beal and Chereskin, 2003). During boreal winter monsoon, the Somali Current is weaker and flows southward. The Somali Current is important in the shallow overturning circulation of the Indian Ocean, supplying water to the upwelling along the western boundary and compensating the cross-equatorial Ekman transport (Schott et al. 2009). Roles of the Somali Current in upwelling, monsoon rainfall, and Arabian Sea heat balance are poorly understood, but expected to be rather important given its up to 40 Sv transport (e.g. Beal and Chereskin, 2003).

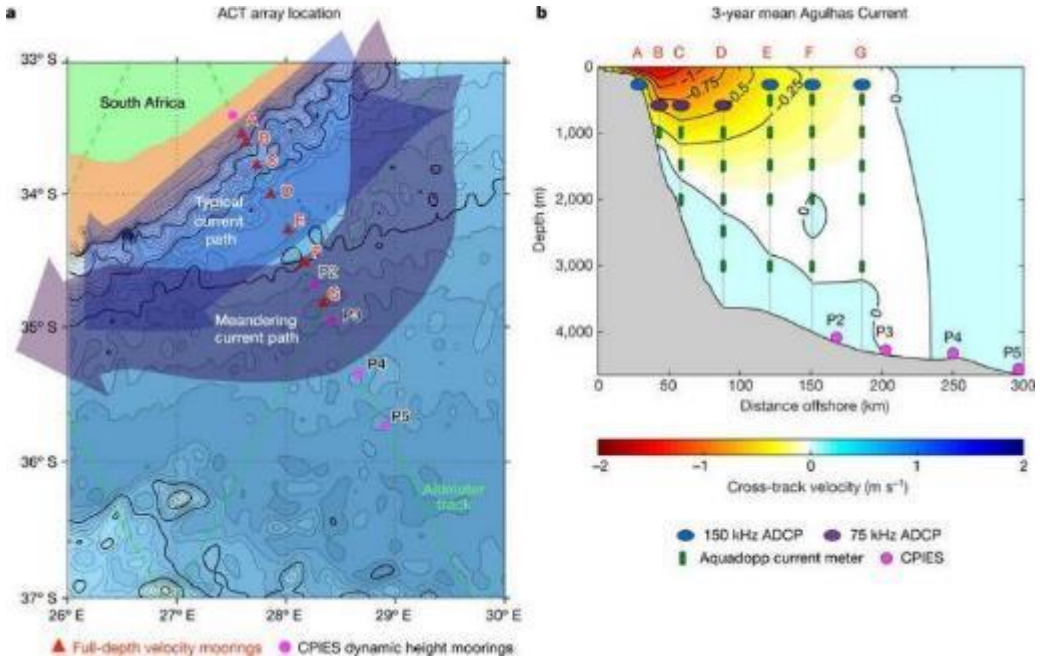

Figure 9.3: Geographical location of ACT mooring array (a) and Vertical section of the mooring array superposed on the 3-year mean cross-track velocity. From Beal and Elipot, 2016.

9.3 Essential Ocean Variables (EOV)

It is essential to capture decadal variations of the Indian Ocean's boundary currents and the ITF in order to understand their roles, as capacitors for Pacific variability and as carriers of heat and freshwater, in driving decadal climate variability and rapid warming trends in the Indian Ocean. Sustained observations of boundary currents have been a priority for international CLIVAR/GOOS for almost a decade, as articulated in an OceanObs09 white paper. Yet currently there is no framework in place for systematic coverage of any of the boundary currents of the Indian Ocean. Sustained observing of the following EOVs are needed:

- Velocity, temperature, salinity, and pressure at daily to weekly resolution at the Indonesian throughflow inflow and outflow channels.
- Upper ocean temperature measurements at 50-100 km, at weekly-monthly resolution between Australia and Indonesia and between Australia and the Red Sea, with enhanced salinity measurements from Argo floats.

- Full-depth velocity, temperature, salinity, and pressure in key western boundary current systems, including the Somali Current and Agulhas Current, at daily to weekly resolution, dependent on regional tides and variance.
- Upper ocean velocity, temperature, salinity, and pressure measurements in key eastern boundary current systems, such as the Leeuwin Current and the South Java Current; it is desirable to integrate the physical measurements with nutrient, plankton biomass and carbon measurements.

9.4 IndOOS recommendations

Maintain the frequently repeated IX1 XBT section across the ITF, and enhance the section with additional salinity measurements by using XCTDs and/or by increasing the density of Argo floats around IX1; There is a need to have more emphasis on the end point measurements of the IX1 section, especially at the northern end of the Sumatra-Java coast to resolve the South Java Current.

Maintain the frequently repeated IX12 XBT section across the Somali Current system.

Establish an international alliance to coherently monitor the ITF volume and heat transport as well as biogeochemical fluxes in different inflow and exit channels, to aid the interpretation of the geostrophic transport estimates from the IX01 XBT section.

Maintain the ASCA mooring array for the Agulhas Current system; Integrated observing systems maintained through regional alliances and combining moorings, gliders, and periodic ship measurements are optimal.

Establish a boundary current array for the Leeuwin Current to monitor the coastal waveguide along the Australian coast to assess the influences of decadal Pacific climate on the Indian Ocean, and combined mooring and gliders observations will be optimal.

Maintain the existing network of island and coastal sea level stations and ensure open accessibility of sea level data from this network, so that historical boundary current transports such as the Leeuwin Current as well as the ITF can be estimated using sea level proxies – Fremantle sea level records have been crucial to monitor the Pacific influences on the interannual and decadal variability of the Leeuwin Current and their impacts on the interior southern Indian Ocean, as well as evaluating numerical model performance.

Maintain satellite altimeter missions to characterize long term variations of mesoscale eddy energetics in the ocean boundary currents in the Indian Ocean.

10. Decadal variability and predictability

Vialard, J.[1], W. Han[2], M. Feng[3], T. Tozuka[4], M. McPhaden[5], M.K. Roxy[6], M. Lengaigne[1], A.G. Nidheesh[1]
[1]IRD, France; [2]Univ. Colorado, USA; [3]CSIRO, Australia; [4]Univ. Tokyo, Japan; [5]NOAA, USA; [6]IITM, India

10.1 Motivations: Indian Ocean contribution to decadal climate predictability

Modes of decadal internal climate variability have been clearly identified in the Pacific (the IPO or Interdecadal Pacific Oscillation, e.g. Alexander 2010; Liu 2012) and Atlantic (the Atlantic Meridional Oscillation or AMO, e.g. Liu 2012). This is not the case for the Indian Ocean: the lack of data and dedicated studies make decadal variability in this basin a "grey area" (Han et al. 2014a). This is a problem for attributing climate change signals in this basin. For instance, is the rapid ~1°C Indian Ocean surface warming between 1950 and 2015 (compared to the ~0.6°C global average) due to a faster response to climate change in this basin or natural decadal climate variability (Lau and Weng 1999; Alory et al. 2007; Roxy et al. 2014)? Indian Ocean decadal variability may also have played an important role in the recent global warming "hiatus". A negative IPO phase during the 2000-2010 decade has promoted a colder Pacific ocean that has pumped more heat than usual from the atmosphere, hence yielding a slowdown of global warming (e.g. Kosaka and Xie 2013). The Indian Ocean recent fast warming appears to have contributed to this negative IPO phase by enhancing the Walker circulation (Luo et al. 2012; Han et al. 2014b; Hamlington et al. 2014; Li et al. 2015). A significant fraction of the Pacific heat uptake has also been pushed to the Indian Ocean via the Indonesian throughflow (Lee et al. 2015; Nieves et al. 2015; Liu et al. 2016). Whether this extra heat in the Indian Ocean will re-surface or stay at depth during the coming decades could influence the evolution of the global surface temperature (Vialard, 2015), hence making the Indian Ocean a potentially important region for decadal climate predictions. The Indian Ocean is also the region of highest skill for decadal surface temperature predictions, due to a relatively weak internal variability there (Guemas et al. 2012), offering potential prospects for decadal regional climate projections. **There is hence a strong need to characterize natural decadal Indian Ocean variability in order to attribute climate change signals in this region, and predict the global climate evolution over the coming decades.**

10.2 What is known about IO decadal variability?

The Pacific and Indian Oceans are closely connected through their common warm pool, which energizes the planetary-scale Walker circulation. This results in a close connection of the two basins at the interannual time-scale. The eastward shift of the Walker circulation during El Niño events induces subsidence over the Indian Ocean, leading to a basin-scale warming through enhanced solar fluxes and local air-sea feedbacks (e.g. Klein et al. 1999; Xie et al. 2009). El Niño events also tend to trigger positive IOD events (e.g. Annamalai et al. 2003). A close connection between the two basins is hence expected at decadal timescales.

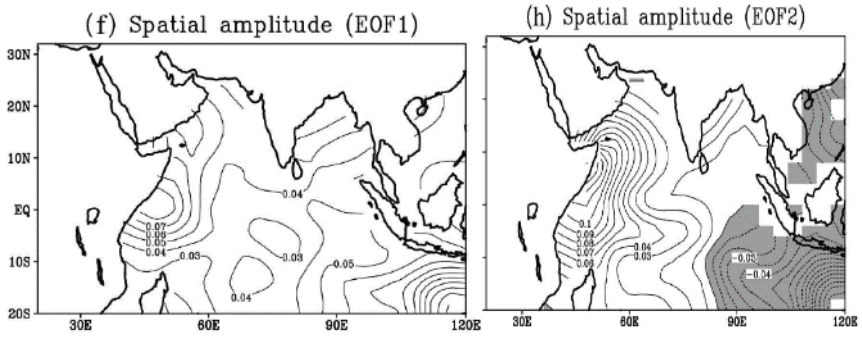

Figure 10. SEQ Figure_10. * ARABIC 1 Spatial patterns (f,h) of the first (37% of total variance) and second (14% of total variance) Empirical Orthogonal Function of decadal (9-35 years) observed SST (ERSST product). Adapted from

The leading mode of decadal Indian Ocean SST variability is associated with a relatively homogenous basin-scale signal (*Figure 10.1*), referred to as the decadal Indian Ocean Basin-mode (decadal IOB). The decadal IOB is in phase with the IPO (Tozuka et al. 2007, Han et al. 2014b, Dong et al. 2016). "Pacemaker" experiments with specified SST in the equatorial Pacific are able to reproduce the observed decadal IOB phase, demonstrating that the decadal modulation of ENSO is its primary driver, essentially through zonal shifts in the Walker circulation, similarly to what happens at the interannual timescale (Dong et al. 2016). Han et al. (2014b) however remarked that the phase agreement between the IOB and IPO has broken down since the 1980s, with a negative IPO phase coinciding with an anomalously warm Indian Ocean over the 2000-2010 decade. This may be a consequence of a faster warming trend of the IO relative to the Pacific on inter-decadal time-scales (Luo et al. 2012; Han et al. 2014b; Dong and McPhaden 2017) and volcanic eruptions on decadal time-scales (W. Han, pers. Comm.). The resulting unique SST pattern (cold Pacific, warm Indian Ocean) may have contributed to enhance Pacific easterlies (Dong and McPhaden 2017), resulting in an unprecedented sea-level rise in the western Pacific (Han et al. 2014b) and heat transfer to the Indian Ocean over the last decade (Lee et al. 2015, Nieves et al. 2016).

The second mode of decadal tropical Indian Ocean SST variability is associated with an east-west SST dipole (*Figure 10.1*) which has been interpreted as a decadal modulation of the Indian Ocean Dipole (Ashok et al. 2004, Tozuka et al. 2007). Positive IODs are associated with a large sea-level signal in the southern tropical Indian Ocean, while the sea-level signal associated with ENSO is much weaker (e.g. Yu et al. 2005). There is unfortunately a large spread in the decadal sea-level variability reconstructed from observations in this region (*Figure 10.2*, Nidheesh et al. 2017; see chapter 14 for a more detailed discussion of decadal Indian Ocean sea-level variations). While some products (Nidheesh et al. 2017) or the short altimetry record (Lee and McPhaden 2008) suggest coherent variations with those associated with the IPO in the Pacific, other studies suggest that the IOD decadal modulation is relatively independent from the IPO (Ashok et al. 2004, Tozuka et al. 2007; Nidheesh et al. 2013). The large uncertainties on the observed decadal Indian Ocean sea level (Nidheesh et al. 2017) and wind (Nidheesh et al. 2013) variability however prevent a thorough assessment of decadal IOD-IPO coupling through the Walker Circulation.

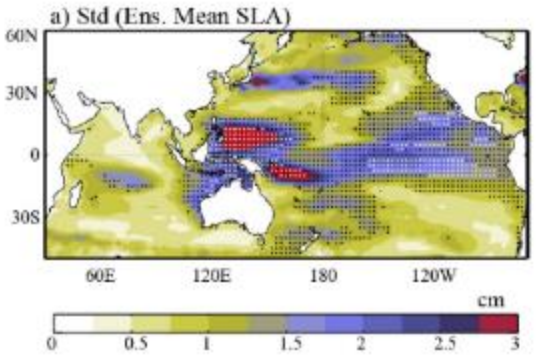

Figure 10. SEQ Figure_10. * ARABIC 2 Standard deviation of the ensemble-mean decadal sea-level variability from ten gridded, observationally-derived sea-level products over the 1960-2010 period. Black (resp. white) dots indicate regions where the inter-product spread is smaller (resp. twice smaller) than the standard deviation of the ensemble-mean, i.e. where sea-level decadal variability is well constrained by available-products. This figure illustrates that decadal sea-level variability is much more uncertain in the Indian Ocean than in the Pacific. It also suggests two regions of strong variability near the west coast of Australia and in the South-western tropical Indian Ocean.

The subtropical Indian Ocean dipole is a meridional SST dipole, peaking in austral summer, and associated with fluctuations in the Mascarene anticyclone intensity (Behera et al. 2001). Yamagami and Tozuka (2015) have shown in ocean modelling experiments that this subtropical SST dipole is decadally modulated, as a result of decadal fluctuations of oceanic mixed layer depth in the subtropical Indian Ocean: there is however no mixed layer data available to further study decadal fluctuations in this region.

In addition to the Walker circulation atmospheric bridge described above, the Indian Ocean is also connected to the Pacific via the Indonesian throughflow. There is an average mass, heat and freshwater transport from the Pacific to the Indian Ocean via the throughflow (e.g. Gordon et al. 2010). This mass and heat transport is increased during La Niña events, with a clear sea level rise signal along the west coast of Australia and Leeuwin current strengthening as a result (e.g. Feng et al. 2003). At the decadal timescale, negative IPO phases also induce positive sea-level signals off the west coast of Australia (Feng et al. 2004), which are robust in most of the available observationally-derived sea-level datasets (*Figure 10.2*, Nidheesh et al. 2017). The negative IPO phase since the 1990s has favored more frequent warm events with large ecosystem consequences along the west coast of Australia (Ningaloo Niños, Feng et al. 2013, Feng et al. 2015). The modulation of the eastern equatorial Indian Ocean heat content by the IPO through the oceanic bridge also appears to influence the IOD, with more frequent positive IODs during positive IPO phases (Ummenhofer et al. 2017), although those changes may have occurred through the atmospheric bridge. Finally, as noted earlier, an important fraction of the heat uptake in the Pacific during the last decade negative IPO phase was transferred to the Indian Ocean following this pathway (e.g. Lee et al. 2015; Nieves et al. 2015). Whether this heat will re-surface or not once in the Indian Ocean has important implications for the future evolution of global surface temperature.

Recent studies have suggested a decadal regional sea-level rise in the northern Indian Ocean, partly attributed to decadal fluctuations in the cross equatorial cell (CEC, Schott et al. 2002) intensity (Thompson et al. 2016), with a possible role of air-sea fluxes (Srinivasu et al. 2017). Dong and McPhaden (2016) have suggested that, despite this sea level rise signal, the heat content has increased more in the southern than in the Northern Indian ocean over the last decade (i.e. most of heat input from the throughflow remains south of the equator), leading to a decadal interhemispheric SST gradient change, presumably through a reduction in the vertical turbulent transport of heat from the surface layer the deep ocean. Large uncertainties in this region (*Figure 10.2*) however currently prevent a thorough assessment of the decadal mass and heat content changes in the northern Indian Ocean.

10.3 EOVs for Indian Ocean decadal climate variability and predictability

As was underlined in section 10.1, better describing Indian Ocean decadal climate variability is a must for detecting climate change signals in this under-sampled basin & for global decadal climate

projections. The overall picture of natural decadal Indian Ocean climate variability is however very incomplete, with many questions that have yet to be resolved. For instance, is the recent apparent decoupling between the IPO and decadal IOB a result of external forcing (rapid Indian Ocean warming associated with anthropogenic climate change and/or decadal SST variability due to volcanic eruptions), and did this contribute to the unusually fast sea level rise in the western Pacific and heat transfer to the Indian Ocean over the 2000-2010 decade? Is decadal IOD modulation partially coupled with the IPO through the Walker circulation or through the Indonesian throughflow (Ummenhofer et al. 2017), or is it independent as initially suggested by Ashok et al. (2004) and Tozuka et al. (2007)? Is the northern Indian Ocean sea-level and heat content decadally modulated through changes in the CEC strength? What are the impacts on the monsoons of the decadal interhemispheric SST gradient variations as a result of the decadal modulation of the Indonesian throughflow (Dong and McPhaden, 2016)? Are there other modes of decadal climate variability intrinsic to the Indian Ocean? What combination of physical processes, e.g. air-sea heat exchange, changes in ocean circulation and upper ocean heat content, planetary waves etc., give rise to the observed decadal time scale variations? Our limited ability to answer these questions based on the existing Indian Ocean observational record stresses the utmost importance of ***sustained basin-scale observations over several decades in key regions for decadal climate variability quantification, with a at least ~monthly resolution.*** These observations include:

1. The transport of mass, heat and freshwater into the Indian Ocean through the Indonesian throughflow.
2. Sea surface temperature, with special emphasis on key regions like in the eastern equatorial Indian Ocean (the dynamical core of IOD variability).
3. Consistent, multi-decadal ocean surface wind stress vector, with special emphasis in the central equatorial and southern-tropical Indian Ocean (where IOD wind signals are strongest).
4. Sea-level and upper ocean heat content, with special emphasis on a) the southern tropical Indian Ocean (both off the west coast of Australia where signals are large and coherent across datasets but also in the southwestern tropical Indian Ocean where existing products suggest large but inconsistent signals); and b) the northern tropical Indian ocean (where a recent, unprecedented sea level rise has been observed).
5. Volume and heat transports in key regions: cross-equatorial cell (including the Somali boundary current), transport across 32°S (including the Agulhas and Leeuwin boundary currents).
6. Net surface heat and constituent turbulent and radiative components.

10.4 Actionable recommendations

Based on the suggested Essential Ocean Variables listed above, the actionable recommendations on the current IndOOS design follow:

a. Maintain the IX01 XBT line with a monthly resolution at least: allows monitoring geostrophic mass and heat transport at the throughflow exit and crosses the region of strong decadal sea-level signal off the west coast of Australia (points 1 and 4 above). Experimental glider doubling of the IX01 line.

b. Complete and maintain RAMA for observing and diagnosing surface and upper ocean variability in key regions and to ensure the inter-calibration of successive satellite missions, which is essential for producing a decadal record (points 2-6 above)

c. Maintain the Argo network in the entire Indian Ocean (points 4 and 5 above)

d. Maintain satellite observations and intercalibration-work that allow the development of basin-scale wind and SST records that span several decades and can be trusted in rainy/cloudy regions (points 2 and 3 above)

e. Maintain the existing network of island and coastal sea level stations and ensure open accessibility of sea level data from this network.

f. Develop collaborations with the paleo-proxy community to provide long records of the SST variability in the IOD eastern pole and sea level variability near the west coast of Australia (e.g. Zinke et al. 2015), Chagos archipelago and Mascarene Islands (point 4 above).

11. Anthropogenic climate change in the Indian Ocean

Roxy, M.K.[1], L. Cheng[2], T. Zhou[2], P.J. Durack[3], W. Han[4] and J. Vialard[5]

1.IITM, India; 2. IAP, China; 3. LLNL, USA; 4. Univ. Colorado, USA; 5. IRD, France

11.1 Background

The Indian Ocean is responding quickly to anthropogenic climate change, in terms of increasing surface temperatures and heat content, rising sea level and an intensified water cycle (IPCC 2013). This has important consequences for the climate system and impacts the food, water and energy security of Indian Ocean rim countries, which host one third of the world population. Changes in the Indian Ocean can affect the monsoon system, resulting in extreme droughts, rainfall and high sea level events (Roxy et al. 2015; Kay et al. 2015). Recent studies show that the warming trend of the Indian Ocean has far reaching impact, modulating the Pacific climate (e.g., Luo et al. 2012, Han et al. 2014, Hamlingon et al. 2014), affecting the North Atlantic Oscillation (e.g., Hoerling et al. 2004), and causing the West Sahel and Mediterranean droughts (e.g., Giannini et al. 2003; Hoerling et al. 2012). In light of these impacts, it is of immediate urgency that we should understand the extent and mechanisms of the changes in the Indian Ocean in a comprehensive manner, so as to respond effectively by taking the right measures for climate change adaptation and mitigation.

11.2 Detection and attribution of long-term changes in the Indian Ocean

11.2.1 Warming in the Indian Ocean

Approximately 93% of the heat due to anthropogenic global warming has gone into the oceans since the 1950s (Glecker et al. 2012; Pierce et al. 2012; IPCC 2013; Gnanaseelan et al. 2017; Cheng et al. 2017). The Indian Ocean exhibits a basin wide warming in sea surface temperature (SST) during this period (Figure 1a; Lau and Weng 1999; Alory et al. 2007; Ihara et al. 2008; Du and Xie 2008; Rao et al. 2012; Roxy et al. 2014, Dong et al. 2014a,b). While the global mean SST warming is about 0.67°C and the tropical SST warming is about 0.83°C during 1950-2015, the tropical Indian Ocean SST has warmed by 1.04°C (numbers from ERSST v4 data).

The Indian Ocean basin-mean temperature has experienced consistent warming from the surface to 2000 m during recent decades, and most of the warming has occurred in the upper 300 m (Pierce et al. 2006; Cheng et al. 2015), with a substantial increase in ocean heat content (OHC) in the upper 700 m of the south Indian Ocean (Levitus et al. 2012). The upper 2000m OHC increase in the Indian Ocean (north of 34°S) is 0.41 x 1022 Joules per decade from 1960 to 2015, based on a new historical OHC estimate (Cheng et al. 2017). Particularly, the Indian Ocean upper 700m OHC increased abruptly after 1998 (Figure 1b), at a rate of about 1.60 x 1022 Joules per decade, accounting for more than 28% of the global ocean heat gain, despite only representing ~12% of the global ocean area. This suggests that the Indian Ocean has recently been an important heat sink, offsetting accelerating anthropogenic global warming over the two last decades.

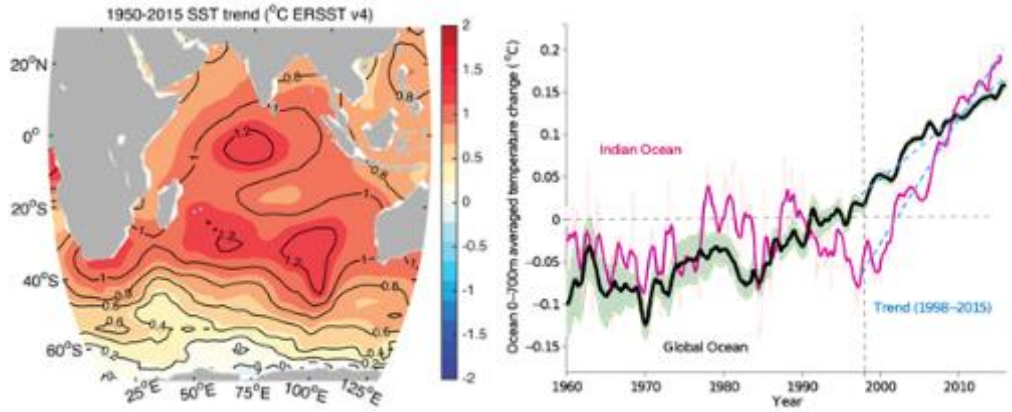

Figure 11.1. a) 1950-2015 SST trend (ERSST v4) represented by total change in 66 years, and b) 12-month running mean time series of the 0-700m averaged temperature for the Global Ocean (black) and Indian Ocean (purple). For the global ocean, the green shading displays the 95% confidence interval. For the Indian Ocean, the thin purple line shows the monthly time series. The 1998 to 2015 linear trends for both series are displayed as blue dashed lines. The data are from IAP-Gridded dataset (Cheng et al. 2017).

Despite these inferences, there are substantial uncertainties in long-term changes in OHC due to insufficient data coverage (Wang et al. 2017). Some analyses indicate that global ocean warming is underestimated in some ocean datasets due to poor sampling of the Southern Hemisphere (Gille 2008, Durack et al. 2014) and limitations of the objective analysis methods used to fill in data gaps (Cheng et al. 2017, Wang et al. 2017). Only 60% of Argo floats successfully reached profiling depths of 2000 m in 2010 (Schuckmann and Le Traon 2011) and hence, the data coverage is still a major challenge for reliable detection of deep ocean changes below 1500 m. The absence of observations in the Indonesian Throughflow (ITF) region may also cause bias for the global and regional scale OHC changes (Schuckmann and Le Traon 2011).

Climate model experiments indicate that anthropogenic forcing accounts for about 90% of the surface warming in the Indian Ocean (Dong et al. 2014a,b). The basin-wide warming trend is primarily attributed to atmospheric forcing via radiative and turbulent fluxes associated with anthropogenic GHG forcing (Barnett et al. 2005; Pierce et al. 2006; Knutson et al. 2006; Du and Xie 2008; Dong et al. 2014b), while anthropogenic aerosols have regional cooling effects (Figure 2; Dong et al. 2014a). Simulated basin-wide warming is not spatially uniform, but with a maximum occurring in the tropical west-central Indian Ocean and a minimum in the south-eastern basin. Analyses of climate model results indicate that local air-sea interaction (e.g., Liu et al. 2015, Rahul and Gnanaseelan 2016, Yao et al. 2016) and ocean dynamics (Dong et al. 2014b, Rahul and Gnanaseelan 2016, Luo et al. 2016) are responsible for the inhomogeneous warming over the tropical Indian Ocean. Ocean dynamics results in the positive dipole-like warming pattern via anomalous warm water advection, due to the surface easterly wind anomaly along the equator, which is mainly associated with anthropogenic GHG forcing (Dong et al. 2014b). Though future projections indicate an IOD-like pattern of mean changes, many of these model simulations have large biases in the mean state and interannual IOD variance, and hence the warming patterns could also be due to artifacts of model errors (Li et al. 2016).

In contrast to these simulated results, observations (Yu et al. 2007, Rao et al. 2012, Ummenhofer et al. 2017) show a negative surface heat flux trend over the Indian Ocean (for the period 1984-2007, Rao et al. 2012), which therefore cannot explain the observed surface warming. Considerable uncertainty exists about the sign of the net heat flux into or out of the Indian Ocean in some parts (Yu et al. 2007), and the surface fluxes over the global ocean are the most uncertain geophysical measurement in the global ocean observing array at present. See Chapter 2 for more details on air-sea fluxes.

Superimposed on the anthropogenic trend, Indian Ocean SSTs display considerable decadal variations (see chapter 10 for more details). Although the external forcing accounts for most of the

warming trend over the 1958-2005 period (Dong et al. 2014b), decadal variability induced by the Interdecadal Pacific Oscillation (IPO) weakens the trend by about 50% over the Indian Ocean during IPO's cold phase, and vice-versa during the warm phase, contributing about 10% to the global warming hiatus since 1999 (Dong et al. 2016). This negative IPO phase also increased Indian Ocean heat content in the recent decades (2003-2012), linked to an increase in the heat transport from the Pacific via the ITF (Lee et al. 2015). Ummenhofer et al. (2017) further suggest that this IPO control of multidecadal Indian Ocean heat content via the ITF operates over the entire 1958-2007 period.

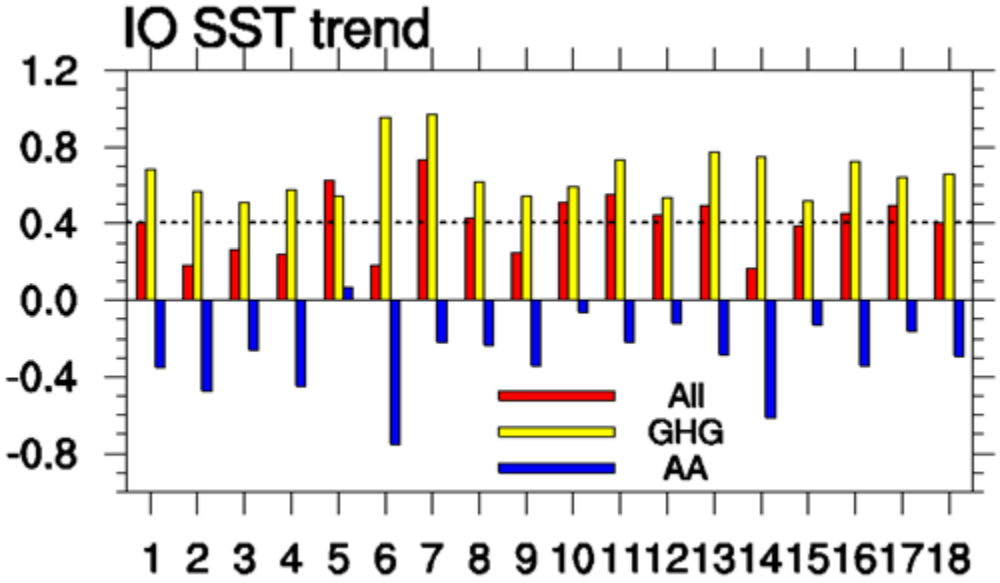

Figure 11.2. The SST trends during 1870-2005 averaged in Indian Ocean (40°S-15°N, 40°E-100°E) under all forcing runs, GHG-only forcing runs, and AA-only forcing (historical-historicalGHG-historicalNat) from 17 CMIP5 models and the MME of them (number 18). The dashed line represents the trends in observation. Units: K (100-year)-1 (Dong and Zhou 2014a).

11.2.2 Sea level changes

The anthropogenic change in ocean temperature affects sea level change (SLC), with thermal expansion accounting for 35% of the global sea level rise during 1993-2010 (IPCC 2013). While SLC averaged over the entire Indian Ocean (30°E–120°E, 30°S–30°N) is 5.6 mm/year during 2004-2013, as shown by satellite altimeter data, the rise in the northern Indian Ocean (30°E–120°E, 5°S–30°N) is at a rate of 6.1 mm/year (Srinivasu et al. 2017), dominated by thermosteric effects (Thompson et al. 2016; Srinivasu et al. 2017). The northern and eastern coasts of the Bay of Bengal experience the largest trends (Unnikrishnan et al., 2015) for the altimetry period of 1993-2012. Some studies relate the fast 2004-2013 SLC over the northern Indian Ocean to superimposition of natural decadal variability (e.g., Srinivasu et al. 2017). Whether this is the entirely the case or a regional signature of global warming, however, deserves more investigation.

Distinct spatial patterns of SLC since the 1960s have been detected using tide gauge data and OGCM simulations, with rising sea level along most of the coastal regions of the Indian Ocean rim countries (e.g., Mumbai, Kochi, Vishakhapatnam on the Indian coast, Durban in South Africa, and Fremantle and Port Hedland along the Australian coast) and falling sea level in the southwest tropical basin (Han et al. 2010). An enhancement of the Indian Ocean regional Walker and Hadley cell (along with changes in the Somali jet), partially attributed to anthropogenic warming, is shown to be the major cause for the basin-wide patterns of sea level trend discussed above (Han et al. 2010).

11.2.3 Changes in salinity

The strong salinity contrast between the Arabian Sea (where evaporation dominates) and the Bay of Bengal (where precipitation and runoff dominates) has been amplified since 1950, based on in situ measurements, with an increase in sea surface salinity over the Arabian Sea and a freshening trend over the Bay of Bengal (Hosoda et al., 2009; Durack and Wijffels 2010). Outside the marginal seas, the Indian Ocean has a strong near-surface salinity trend in the subtropical gyre which extends to the depth of the thermocline (Hosoda et al., 2009; Durack & Wijffels, 2010; Skliris et al., 2014) and a very large and consistent freshening below, which is associated with subduction of Subantarctic Mode Water (SAMW) south of Australia (Sallee et al., 2009). This feature is one of the largest magnitude freshening signatures ofthe global ocean (Durack and Wijffels, 2010; Helm et al., 2010; Skliris et al., 2014). A freshening plume aligned with the low salinity ITF waters from the North Pacific is also visible, and extends from the east along 12°S and in the central region south of the equator. At depth, saline Red Sea Waters (RSW) lead to an enhanced salinity signature in the Northern Indian Ocean, particularly in the Arabian Sea intermediate waters, extending to 1000 m depth. When considering these Indian Ocean salinity changes together with those in the Pacific and Atlantic Oceans, these suggest a clear enhancement of both horizontal and vertical salinity gradients – a signature of fresh regions becoming fresher, and salty regions becoming saltier (Fig. 11. 3).

Studies focused on salinity, temperature and these changes together have successfully attributed observed changes to anthropogenic influence over the three ocean basins, Indian, Pacific and Atlantic (e.g. Stott et al., 2008; Gleckler et al., 2012; Pierce et al., 2012; Terray et al., 2012; Durack et al., 2014, Fig. 11.3). Warming induced stratification (Fig. 11.3) has lead to a decrease in the transport of dissolved oxygen from surface to subsurface waters, leading to increased deoxygenation in the Indian Ocean (Stramma et al. 2010). Thermal stratification has also lead to a reduction in marine phytoplankton (30% during 1998-2013 based on observations, 20% during 1950-2005 based on CMIP5 model historical simulations) in the western Arabian Sea (Roxy et al. 2016).

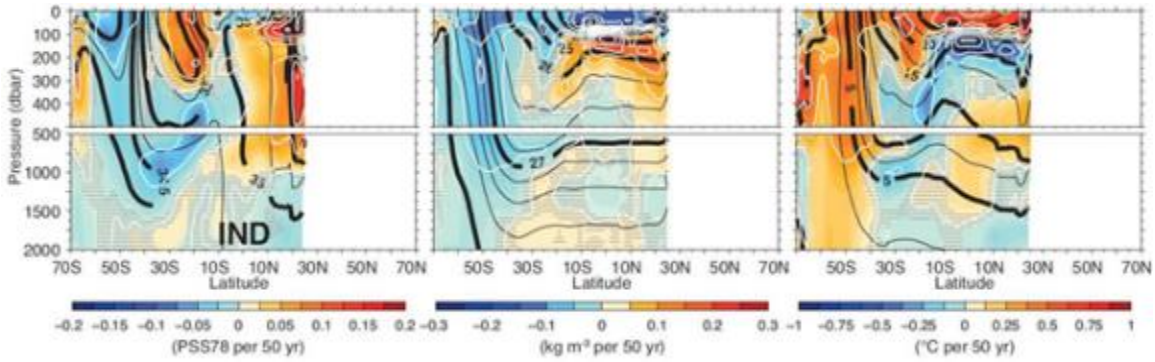

Figure 11.3. Zonally-averaged linear trend of salinity changes (left), neutral density changes (middle), and potential temperature changes (right), for the Indian Ocean during 1950 to 2000. Mean fields are shown as black lines. Regions where the resolved linear trend is not significant at the 90% confidence level are stippled in grey (IPCC 2013).

11.3 EOVs for the long-term changes in the Indian Ocean

Long term changes in Indian Ocean SST, heat content, salinity, and sea level are occurring, among others (changes in heat content and transport are discussed in Chapter 7 and changes in upwelling is discussed in Chapter 3). However internal climate variability can obscure the attribution of those signals to anthropogenic drivers. It is however difficult to distinguish the climate change signal from internal climate variability without long-term observations. The key is thus to maintain sustained observations of key-variables over a long period.

Those variables include:

1) In situ data to monitor the SST trend at the basin-scale, e.g. to confirm the large and quick warming in the western Indian Ocean.
2) Improved monitoring of mass, heat and salt transport at the key Indian Ocean entrances (ITF) and exits (section along 32°S, including the Leeuwin and Agulhas boundary currents), as a tool for basin-scale budget studies.
3) Improved long term time series of air-sea heat fluxes and constituent turbulent and radiative components across the basin, which are currently not consistent with SST trends, as a tool for basin-scale budget studies.
4) Basin scale measurements of subsurface temperature and salinity, in order to provide reliable estimates of the long-term heat and salt content trends
5) Sea level measurements at the basin-scale, in order to maintain a close monitoring of regional sea level signals, which can also provide indications on long-term wind changes.
6) Surface wind and wind stress measurements at the basin scale, in particular along the equator to monitor the Indian Ocean part of the Walker circulation, in the Somali jet that plays a strong role for the southwest monsoon, and in the south-western Indian Ocean where changes in wind stress curl are believed to induce a sea level decrease.

11.4 Actionable recommendations

Based on the suggested Essential Ocean Variables listed above, the actionable recommendations on the current IndOOS design follow:

1) Maintain and complete the RAMA array, which provides sustained, high-frequency observations of, in particular, SST, winds, subsurface temperature, air-sea fluxes in key regions of the tropical Indian Ocean. In particular, expand the array into the Arabian Sea and western Indian Ocean – where the uncertainties regarding air-sea fluxes are large.
2) Maintain the current Argo coverage in the Indian Ocean, but: a) Enhance the coverage near the ITF exit and b) favour the development of deep Argo (Johnson et al. 2015), in particular in the Southern subtropical Indian Ocean, e.g., along ~32°S. Explore the technical feasibility of enhancing Argo observations in the ITF region. Explore the technical feasibility of a long-distance glider line along 32°S.
3) Maintain the GO-SHIP array of repeat hydrographic sections in the Indian Ocean (sections: IO7S, IO5, IO7N, IO1W, IO5, IO8N, IO3, IO8S, IO9N, IO1E, I10, IO9S) to ensure that long-term, full-depth measurements are available to quantify ongoing change and provide important regional calibration targets for deep Argo in the region
4) Maintain the IX01 XBT line to monitor the geostrophic volume and heat transport at the exit of the ITF. Experimental doubling of the IX01 line by gliders.
5) Maintain basin-scale satellite observations of SST, SSS, Sea level, Winds, that are inter-calibrated between various missions in order to reach climate-grade quality. Ensure that the ongoing satellite missions providing these important measurements are acknowledged as being an important part of the Indian Ocean observing network, and this information is conveyed to the agencies responsible for maintaining and renewing these satellite missions
6) Maintain and augment (in particular in south-western tropical Indian Ocean Islands & Madagascar) the existing tide-gauge network, and ensure open distribution and common processing of the data. Ensure that all contributing stations begin capturing geodetic information relevant to the site, so that sea-level data quality can be ensured.

12. Ocean primary productivity variability, predictability and change

Peter G. Strutton

Institute for Marine and Antarctic Studies, University of Tasmania, Hobart, Tasmania, Australia
And Australian Research Council Centre of Excellence for Climate Extremes

12.1 Introduction

The Indian Ocean is a basin of considerable primary productivity variability in both space and time. The boundary currents, particularly in the west, are extremely productive and support fisheries of local and global importance (Lee et al., 2005). The upwelling system in the northwest, despite high biological productivity, is a very strong source of CO_2 to the atmosphere, while the southern Indian Ocean is a weak sink (Takahashi et al., 2009). The Leeuwin current in the east supports moderate productivity and spawns long-lived eddies that travel west, sometimes as far as Madagascar (Gaube et al., 2013). The productivity of the equatorial band and the northern basin is strongly modulated by the monsoons and wind reversals (Hood et al., 2017; Strutton et al., 2015). The surface Indian Ocean is rapidly warming (Roxy et al., 2014) and there is evidence for long term change in the productivity of the basin, particularly in the west (Roxy et al., 2016). The Indian Ocean's role in ecologically and economically important fisheries, air-sea CO_2 exchange, and the emerging sensitivity to climate change mean that it is important to accurately and comprehensively observe the system.

In addition to long term climate change, the Indian Ocean is also strongly influenced by both the Indian Ocean Dipole (IOD) and the El Niño Southern Oscillation (ENSO). Several studies have investigated the impact of these climate modes on the primary productivity of the basin (Currie et al., 2013; Keerthi et al., 2016; McCreary et al., 2009; Wiggert et al., 2009. See also Wiggert, this volume). From this work it seems that the IOD is the dominant mode, except in the Somali upwelling system, where El Niño can suppress upwelling and therefore productivity. A positive IOD increases productivity in the eastern tropical Indian Ocean, around Sumatra, and slightly decreases productivity in the central tropical Indian Ocean.

Compared to the Pacific and Atlantic, the Indian Ocean is very poorly sampled with respect to biogeochemistry in general and ocean productivity in particular. For example, the Vertically Generalized Productivity Model (VGPM; Behrenfeld and Falkowski, 1997) was developed using a global database of 1698 primary productivity stations. Only 26 of those stations were in the Indian Ocean sector, from south of 40°S near Kerguelen Island. No data from the temperate or tropical Indian Ocean went into the development of the satellite productivity algorithm that has become the gold standard for estimating global ocean primary productivity and its change over time. This example serves to illustrate the lack of coverage relative to other basins and also raises doubts about the accuracy of satellite algorithms in the Indian Ocean.

The lack of biogeochemical measurements in the Indian Ocean presents both a problem and an opportunity for the future of the observing system. The opportunity is obvious, but the problem is that in many areas of the basin, there are insufficient observations to inform the spatial distribution of platforms and sensors. This chapter reviews some of the existing knowledge, suggests regions that are obvious candidates for future attention, and recommends an approach to instrument these areas.

12.2 The seasonal cycle and major primary productivity features

Basin scale patterns

The primary productivity of the Indian Ocean is strongly forced by the monsoons, the equatorial jets and the stratification of the south Indian Ocean Gyre. Figure 12.1 shows the climatology of

seasonal variability in Indian Ocean chlorophyll, where the seasons are defined by months that correspond with the monsoons.

In June through September (Figure 12.1(a)), the southwest monsoon drives the Arabian Sea upwelling and productivity there is at its seasonal maximum. The band of coastal high chlorophyll at the southern tip of India and around Sri Lanka is also at its maximum. Equatorial productivity is low, but the spatial extent of the lowest chlorophyll there is reduced because of the expansion of the high chlorophyll region in the Arabian Sea. Winter mixing in the southern hemisphere likely enhances productivity in the subtropical gyre slightly, and the size of this chlorophyll desert shrinks to its seasonal minimum.

In October-November (Figure 12.1(b)), the northeast monsoon stimulates some productivity in the Arabian Sea. The equatorial jets intensify and stimulate productivity there, and the size of the oligotrophic subtropical gyre expands.

In December through March (Figure 12.1(c)), there is still high productivity in the central Arabian Sea, which may be related to convective overturning as opposed to upwelling, but chlorophyll along the Somali coast is at its annual minimum. The size of the oligotrophic subtropical gyre is at its maximum and productivity along the equator is decreasing.

In April-May (Figure 12.1(d)), productivity across the basin is low. The Arabian Sea upwelling is absent, equatorial productivity is low and the size of the oligotrophic subtropical gyre in the south is near its (austral) summer maximum spatial extent.

The following sections describe some regional features in more detail.

Bay of Bengal

Vinayachandran (2009) described three important bloom features in the Bay of Bengal. First, rivers elevate productivity near the coast and the blooms there coincide with the seasonal maximum in discharge around August and September (Yaremchuk et al., 2005). Second, the northeast monsoon drives Ekman transport and a bloom in the southwest of the bay in northern hemisphere autumn. Third, the summer monsoon causes a large bloom around the south of India, that reaches into the Bay of Bengal to the east of Sri Lanka. In addition to these regular, seasonal features, the bay is also impacted by cyclones, that can generate nutrient mixing and elevated chlorophyll. This effect is reduced in the northern part of the bay due to stronger stratification there.

Arabian Sea

McCreary et al. (2009) distinguish the productivity in the Arabian Sea as being driven by two different processes. First, textbook seasonal upwelling during the southwest monsoon, from about July through September, drives blooms along the coast of Somalia, Oman and western India. These have been well-studied during experiments in the 1990s (Barber et al., 2001). Second, in the central Arabian Sea, blooms driven by either entrainment of a subsurface chlorophyll maximum, or detrainment (stratification) occur during both the southwest and northeast monsoon. While this region of the Indian Ocean is in some ways better studied than others, questions remain regarding the role of zooplankton grazing and potential iron limitation in regulating the bloom. This is also thought to be a region where nitrogen fixation could play a significant, yet poorly quantified role in ocean productivity.

The equatorial Indian Ocean

Productivity is low on the equator during the boreal spring intermonsoon period (March to May, Fig. 12.1c,d). Chlorophyll increases to the north and concentrations are very low to the south in the subtropical gyre. The southwest monsoon (Fig. 12.1a) drives upwelling and mixing as described above, and chlorophyll concentrations increase dramatically in the northern Indian Ocean and in western equatorial waters. Central equatorial chlorophyll remains low, less than 0.5 mg m^{-3}, just south of high concentrations off of southern India and Sri Lanka. In boreal autumn, island wake effects advect high-chlorophyll water eastward along the equator from the Chagos-Laccadive Ridge at 73°E (Fig. 12.1b), reversing and sweeping westward in late winter (Fig. 12.1c). Intermittent high chlorophyll has been observed at the equator at 80°E in boreal autumn (Strutton et al., 2015)

and has been attributed to (1) local entrainment of nutrients or chlorophyll, or both and (2) southward advection of the island wake band of high chlorophyll by undulating Wyrtki jets.

The southwest Indian Ocean

South of Madagascar in late Austral summer, a large bloom develops that covers about 1% of the ocean surface (Figure 12.1c and d). Srokosz et al. (2015) suggested that the bloom is fertilized by iron that originates from the island of Madagascar and is advected east in eddies. There is considerable interannual variability in the extent of the bloom, and Srokosz et al. (2015) linked this variability to interannual differences in the number of eddies.

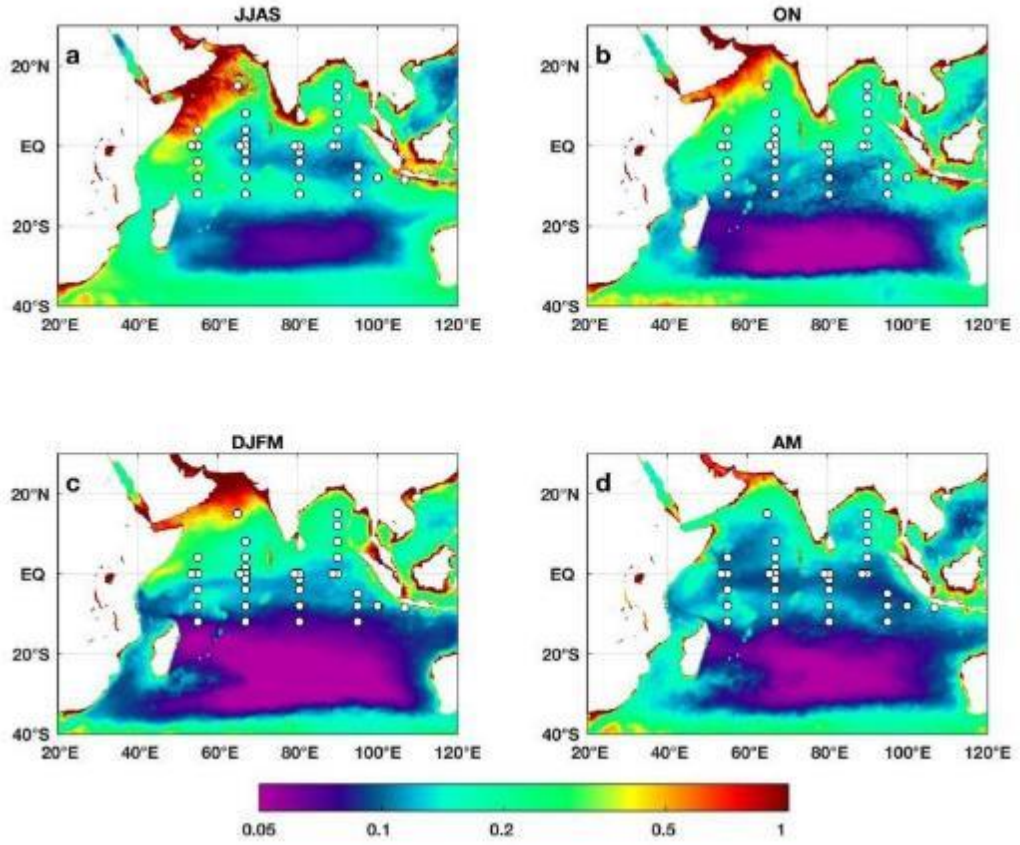

Figure 12.1: Seasonal variability in Satellite-derived surface chlorophyll [mg m^{-3}]. The seasons are defined to correspond closely with the monsoons, as suggested by Jerome Vialard: (a) June through September, (b) October-November, (c) December through March and (d) April-May. The maps are compiled from climatological monthly means from the SeaWiFS satellite. Circles are the currently occupied and proposed Research Moored Array for African-Asian-Australian Monsoon Analysis and Prediction (RAMA) mooring sites, courtesy of Michael McPhaden and Dai McClurg.

12.3 Current productivity observations

Like the tropical Pacific and Atlantic observing systems, sustained productivity observations in the Indian Ocean are limited to one very important data stream: Satellite ocean color. This data record consists of the Coastal Zone Color Scanner (CZCS, 1978-1986), Ocean Color Temperature Scanner (OCTS, 1996-1997), the Sea-viewing Wide Field-of-view Sensor (SeaWiFS, 1997-2010), the Moderate Resolution Imaging Spectroradiometer (MODIS, 2002-) and more recently VIIRS and

Sentinel. In the northern Indian Ocean, the coverage of ocean color measurements is sometimes limited by cloud cover. The CZCS pigment measurements are not directly comparable to the chlorophyll measurements of later satellites and are not quite global in coverage, which limits the length of the climate data record. Since the launch of SeaWiFS in 1997, the data set is robust and has been used to document a long term decrease in Indian Ocean productivity (Roxy et al., 2016).

Historical ship-based productivity measurements do exist (Zeitzschel, 1973). These data cover not just phytoplankton primary productivity, but also abundance and rate observations for bacteria and grazers. These data serve as historical baselines but also as indicators of regions that merit closer monitoring, as discussed for nutrient limitation versus grazing in the Arabian Sea, above. There is no coordinated program of bio-optical or nutrient sampling on Indian Ocean moorings, but ad hoc deployments have revealed interesting dynamics associated with seasonal and shorter time scale processes (Strutton et al., 2015).

Bio-optical and biogeochemical deployments on profiling floats have the potential to answer questions regarding large scale spatial patterns and seasonal to long term trends, but also more targeted features such as the role of eddies in nutrient fluxes and sub-surface chlorophyll patterns (Dufois et al., 2017; Gaube et al., 2013). At the time of writing there have been at least five bioArgo deployments in the southern Indian Ocean (https://research.csiro.au/iobioargo/data-access/). A pathway to global coverage now exists in the form of an implementation plan for a biogeochemical Argo float program (Johnson and Claustre, 2016).

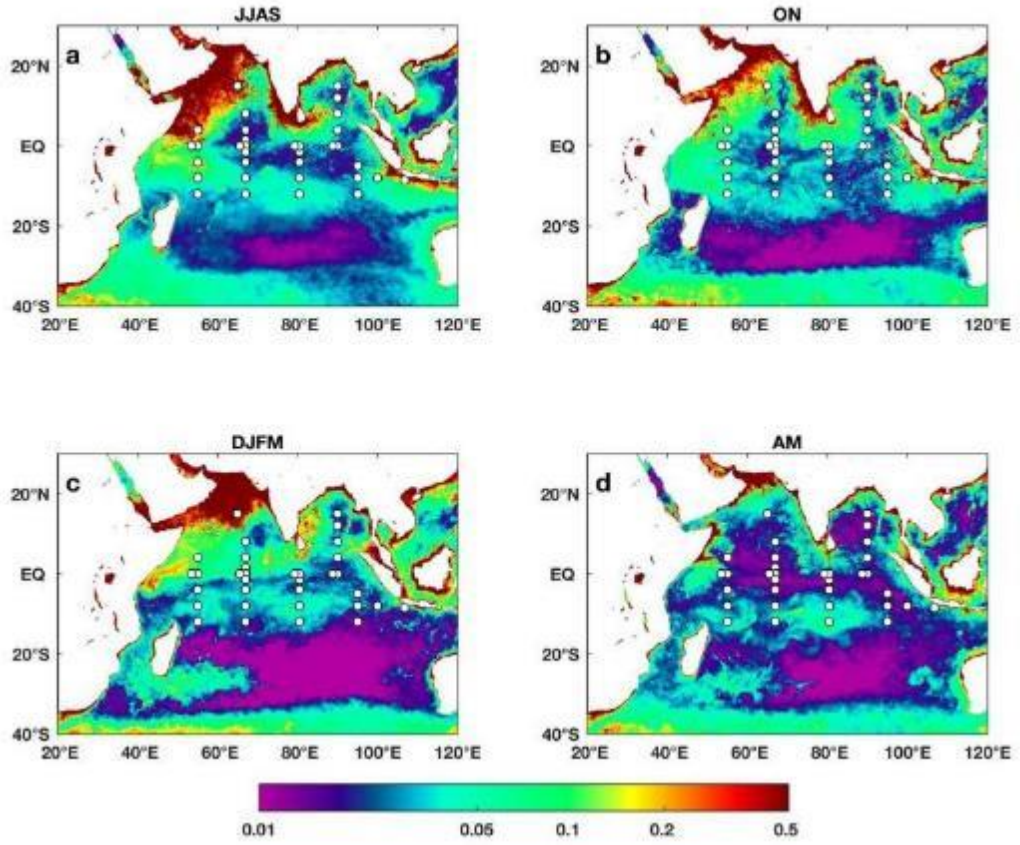

Figure 12.2: A representation of chlorophyll variability in the Indian Ocean. The seasons in the four panels are defined as for Figure 12.1 to correspond with the monsoons. Each panel is calculated as the standard deviation of chlorophyll [mg m^{-3}] from MODIS-Aqua monthly mean maps spanning 2002 to 2016.

12.4 Relevant essential ocean variables (EOVs)

Requirements for understanding carbon chemistry and oxygen distributions are covered in chapters by Hood and Wiggert, respectively. The Global Ocean Observing System defines **nutrients, ocean color and phytoplankton biomass and diversity as the relevant EOVs for ocean primary productivity** (http://www.goosocean.org).

Figure 12.2 shows the variability in satellite chlorophyll, calculated as the standard deviation of monthly ocean color data at each pixel. These maps contain elements of intraseasonal and interannual variability because they are calculated from monthly data across all years of MODIS-Aqua satellite chlorophyll data. For example, panel 2a is calculated from 60 months of satellite data (15 years of June, July, August, September). Not surprisingly, the regions with moderate to high chlorophyll concentrations in Figure 12.1 have moderate to high chlorophyll variability, and the South Indian Ocean gyre has very low chlorophyll variability. The maps show that in general, the RAMA mooring locations have the potential to provide important data in the regions of greatest variability in primary productivity, except for the near-coastal parts of the Arabian Sea upwelling system in the northwest of the basin and the Madagascar bloom.

However, obtaining nutrient and chlorophyll measurements from moorings at appropriate depths and with sufficient resolution of vertical variability represents a challenge. To do so would require accurate knowledge of the vertical scales or features that need to be resolved. We do not have this information for the Indian Ocean. A similar statement could be made for dissolved oxygen – mapping features such as oxygen minimum zones (OMZs) from moorings would require large numbers of sensors located at depths we can only guess at. For these reasons, oxygen, nutrient and bio-optical measurements on Argo floats would likely be the best way to observe EOVs in the Indian Ocean, and this view is shared by Wiggert in the chapter on oxygen. However, autonomous nutrient measurements of nutrients are currently limited to nitrate. To obtain the full suite of nutrients (nitrate, phosphate, silicic acid, ammonium) requires ship-based sampling and this could be achieved during GO-SHIP occupations of the established Indian Ocean lines. These voyages also represent the best opportunity to collect data on phytoplankton community structure.

12.5 Recommendations

Based on the seasonal cycle (Figure 12.1) and intraseasonal and interannual variability (Figure 12.2) of satellite ocean color, the main regional productivity features that an observing system must quantify are:

1. The intensity and spatial extent of the Arabian Sea upwelling bloom, mostly during the southwest monsoon, in the latter part of the calendar year.
2. The central Arabian Sea, where high productivity begins with the southwest monsoon but extends into northern hemisphere winter.
3. The Somali coast.
4. The signal along the equator, linked to the seasonal variability of the Wyrtki jets.
5. The Bay of Bengal, coastal India and Sri Lanka.
6. The spatial extent of the oligotrophic gyre and the (low) levels of productivity there.

Satellite ocean color provides the surface-only, broad scale information on variability of primary productivity, and the Indian Ocean observing community should continue to advocate for satellite ocean color missions. Some existing and proposed RAMA mooring locations could host biogeochemical sensors to capture these processes and features. Candidate locations include the northern-most mooring in the Arabian Sea (65°E, 15°N), the three moorings in the Bay of Bengal (90°E line), the mooring closest to Sri Lanka (80.5°E line), the southernmost mooring on the 80.5°E line and the 100°E, 27°S for the gyre, and the equatorial moorings. However, as mentioned above, comprehensive observations of vertical variability in nutrients and chlorophyll will require large numbers of well-targeted sensors. For this reason, and especially in areas impacted by piracy, such

as the western basin and the northern Arabian Sea, autonomous platforms such as Argo floats will likely be the only feasible platform for the near future.

The **recommended next steps** for implementation of productivity-related measurements are:

1. Maintain support and advocacy for satellite ocean color missions.
2. Maintain nutrient measurements on GO-SHIP lines and incorporate observations of phytoplankton community structure where possible.
3. Develop a plan in consultation with the global bio-Argo community, for observations of nutrients, bio-optics and oxygen on Argo floats in the Indian Ocean. This should include identifying areas of significant nitrogen cycle activity, and prioritize these areas for nutrient sensor deployments.
4. Using the results in Figure 12.2 as a starting point, perform an analysis of existing data or model outputs, or both, to determine the locations of strongest productivity variability that needs to be captured by observations.
5. Target bio-Argo deployments in these locations, and in areas known to be important for the nitrogen cycle, such as OMZs..
6. Given the lack of Indian Ocean data that has contributed to global satellite ocean color and productivity algorithms, perform a data mining exercise to create matchups of satellite and in situ chlorophyll and productivity. With these matchups, quantify the accuracy of satellite algorithms from SeaWiFS forward. Consider development of a regionally tuned Indian Ocean algorithms.

13. The Indian Ocean's Influence on Regional Hydroclimate

C. Ummenhofe, Woods Hole Oceanographic Institution

13.1 Introduction

The importance of upper-ocean conditions in the Indian Ocean for modulating rainfall variability in surrounding countries is receiving increasing recognition. Indian Ocean SST variability has been implicated in widespread changes in hydroclimate, such as enhanced rainfall and flooding in East Africa (Webster et al. 1999), droughts, wildfires, and river streamflow in Indonesia (Abram et al. 2003, D'Arrigo and Wilson 2008), Australian rainfall and droughts (Ashok et al. 2003, Ummenhofer et al. 2009a), and monsoon rainfall in Southeast Asia (Ashok et al. 2001; Chapter 1).

As upper-ocean conditions in the Indian Ocean are experiencing robust changes across a range of timescales (Chapters 6, 10, 11; and references therein), a better understanding of the mechanisms by which Indian Ocean variability and change modulate regional hydroclimate is warranted. This has major implications for seasonal rainfall forecasting and, ultimately, for effective water and agricultural management in vulnerable societies in Indian Ocean rim countries. The Indian Ocean region in particular stands out globally as an area with the highest predictive skill in the 2-9yr range (Guemas et al. 2013). Improved understanding of drivers of low-frequency Indian Ocean variability could thus help advance decadal forecasting capabilities in the region.

13.2 Influence of the Indian Ocean on regional hydroclimate

Upper-ocean conditions in the Indian Ocean influence regional hydroclimate across a range of timescales, from sub-seasonal to decadal and beyond. On sub-seasonal timescales, both northward and eastward propagating intraseasonal oscillations (ISOs) are active in the Indian Ocean (Schott et al. 2009). The Madden-Julian-Oscillation (MJO; Zhang 2005, 2013; see Chapter 5) is associated with eastward propagating large-scale atmospheric circulation and deep convection features that interact with the warm underlying SST over the Indian Ocean and Maritime Continent. Several major flooding events in Indonesia and Malaysia in 2006/2007 have been associated with strong easterly winds over the eastern Indian Ocean near Java associated with a Rossby wave-type response to the MJO that allowed for anomalous southward penetration of northeasterly winds from the South China Sea and strong low-level convergence over the region (Aldrian 2008, Tangang et al. 2008). Observing the convectively coupled waves especially during the convectively active MJO phase at sufficient spatiotemporal resolution with *in situ* measurements, such as upper-air soundings, is important and the limited number of available soundings in the tropical Indian Ocean region can have adverse effects on estimated rainfall rates or heat and moisture budgets (Katsumata et al. 2011). Conversely, the skill of representing and predicting ISOs is larger in ocean-atmosphere coupled models compared to stand-alone atmospheric models, highlighting the importance of the feedback between air-sea interactions and upper-ocean structures on intraseasonal timescales (Mahadevan et al. 2016a).

Northward propagating ISOs over the Indian Ocean are associated with active and break periods in the monsoon and thus impact summer rainfall across southern Asia from India to the Philippines (Annamalai and Sperber 2005, Schott et al. 2009). Central equatorial Indian Ocean SST centred on 70-90°E are found to interact with northward propagating mesoscale instabilities in the atmosphere to affect Indian summer monsoon precipitation (Zhou et al. 2017). A persistence of warm SST anomalies over the shallow thermocline region of the Seychelles-Chagos Thermocline Ridge (SCTR) can delay the north-northwest migration of the intertropical convergence zone into the northern Indian Ocean and thus postpone the monsoon onset over southern India (Vecchi and Harrison 2004, Annamalai et al. 2005a, Vialard et al. 2009). Over the SCTR region 5-10°S, strong intraseasonal SST signals were associated with active phases of the MJO in 2007/2008 (Vialard et al. 2008).

The Bay of Bengal is an area of particularly active northward propagating ISOs; this is reflected in strong coupling between SST and intraseasonal summer monsoon rainfall variability (e.g.,

Wijsekera et al. 2016 and references therein), with SST warming in the northern Bay of Bengal leading the onset of intraseasonal rainfall by 5 days. The rainfall-SST relationship, through latent heating, is strengthened in years with anomalously warm SST in the Bay of Bengal, resulting in stronger low-level moisture convergence, as occurs during the negative phase of the Indian Ocean Dipole (IOD; Ajayamohan et al. 2008, Jongaramrungruang et al. 2017).

The IOD (Chapter 6; Saji et al. 1999, Webster et al. 1999) is the Indian Ocean's leading mode of variability on interannual timescales and widely impacts climate in surrounding countries (Saji and Yamagata 2003): this includes rainfall and flooding in East Africa (Behera et al. 1999, Birkett et al. 1999, Webster et al. 1999, Black et al. 2003, Ummenhofer et al. 2009b, Manatsa et al. 2012; Manatsa and Behera 2013), droughts, wildfires, and streamflow in Indonesia (Abram et al. 2003, Hendon 2003, D'Arrigo and Wilson 2008, D'Arrigo et al. 2011), Australian rainfall and droughts (Ashok et al. 2003, Cai et al. 2009a,b, Ummenhofer et al. 2008, 2009a,c, 2011b), and Indian Ocean SST modulate the well-known teleconnection between the El Niño-Southern Oscillation (ENSO) and the Asian monsoon systems (Ashok et al. 2001, 2004, Gadgil et al. 2004, Ummenhofer et al. 2011a). Furthermore, SST in the subtropical southern Indian Ocean in a characteristic dipole pattern (see Chapter 6) affects southern African rainfall during austral summer, with warm (cool) SST in the southwest (southeast) Indian Ocean associated with enhanced low-level moisture advection onto southern Africa (Behera et al. 2001, Reason 2001, 2002).

In a series of atmospheric general circulation model experiments, Indian Ocean SST anomalies were found to modulate low- to mid-latitude precipitation over Indian Ocean-rim countries (Ummenhofer et al. 2008, 2009b,c). SST anomalies closely resembling both tropical and subtropical Indian Ocean dipoles induce a basin-wide re-organization of the atmospheric circulation, resulting in significant rainfall changes over the surrounding landmasses (**Figure 13.1**). Precipitation over southwestern Australia is modulated by variations in the *meridional* temperature gradients in the eastern Indian Ocean, which affect thermal winds and moisture flux, as well as baroclinicity over the region (Ummenhofer et al. 2008, 2009c). Over East Africa, years with an anomalously wet 'short rain' season (September – November) were primarily due to increased onshore moisture transport convergence driven by local warm SST in the western Indian Ocean (Ummenhofer et al. 2009b), rather than a strengthened zonal SST gradient across the equatorial Indian Ocean associated with the IOD (Saji et al. 1999, Webster et al. 1999, Black et al. 2003).

The Indian Ocean is particularly influential for regional hydroclimate on decadal timescales, as found for droughts and wet spells in eastern Australia and East Africa (Ummenhofer et al. 2009a, 2011b, 2017b). Changes in the tropical atmospheric circulation across the Indo-Pacific on multi-decadal timescales (Vecchi and Soden 2007, L'Heureux et al. 2013) modulate the relationship between Indian Ocean SST and regional rainfall: When the Pacific Walker cell weakened, while the Indian Ocean cell strengthened after 1961, the East African short rains became more variable and wetter (Nicholson 2015). Similarly, there was a strengthening in the relationship between the IOD and East African rainfall post-1961, with 73% of short rain variability in East Africa explained by the IOD, up from 50% in previous decades (Manatsa and Behera, 2013). After 1997, this increased further to 82%, explaining spatially coherent rainfall extremes across the region (Manatsa and Behera 2013). The correlation between Indian Ocean SST and East African rainfall is most pronounced during the short rains, though Williams and Funk (2011) argued that warming Indian Ocean SST in recent decades were also associated with reduced long rains for the March-June season in Ethiopia and Kenya. In contrast, increasingly wetter short rain seasons in East Africa may be related to recent warming trends in the western Indian Ocean (e.g., Liebmann et al. 2014).

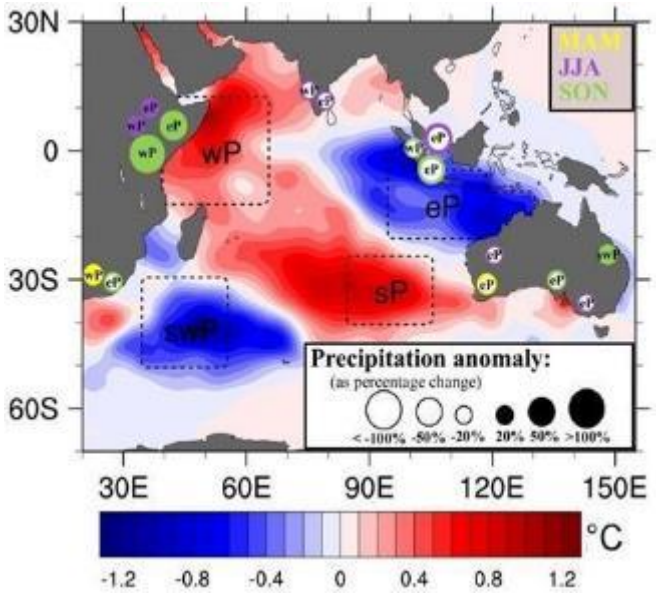

Figure 13.1: Schematic highlighting the influence of Indian Ocean SST anomalies on regional precipitation for the March-May (MAM), June-August (JJA), and September-November (SON) seasons, using atmospheric general circulation model simulations. SST anomalies (° C) are shown as the March-November average. Specific regions with SST anomalies characteristic of tropical and subtropical Indian Ocean dipoles are employed in the simulations, with the poles indicated by the dashed boxes. The anomalous rainfall associated with these regions of SST anomalies is shown by circles in Indian Ocean rim countries. Filled (empty) circles denote an increase (decrease) in precipitation (as percentage change), with the size of the circle reflecting the magnitude of change and the color the season. (Adapted from Ummenhofer et al. 2009d).

Changes in the eastern Indian Ocean thermocline depth on decadal timescales can potentially impact the frequency and strength of the IOD (Annamalai et al. 2005b). Investigating the rare occurrence of three consecutive positive IOD events observed in 2006–2008, Cai et al. (2009c) found that subsurface oceanic conditions may be the key triggering mechanism. An anthropogenic contribution was also proposed, since positive IOD events became more frequent over the period 1950–1999 in the CMIP5 models, which also project an increase in extreme positive IOD events (Cai et al. 2014). Some decadal IOD variability has been linked to the Pacific Decadal Oscillation (Krishnamurthy and Krishnamurthy 2016). Low-frequency changes in the eastern Indian Ocean thermocline depth (0-10°S, 90-100°E), in response to multi-decadal variations in Pacific wind forcing, were associated with decadal variations in the frequency of IOD events (Ummenhofer et al. (2017a). Positive IOD events were unusually common in the 1960s and 1990s with a relatively shallow thermocline, while the deeper thermocline depth in the 1970s and 1980s was associated with frequent negative IOD and rare positive IOD events (Ummenhofer et al. 2017a). Hence it is important to better understand how slowly evolving upper-ocean thermal properties on multi-decadal time scales could affect IOD events that influence regional hydroclimate. This could help decadal forecasting capabilities for the Indian Ocean region, which stands out globally as an area with the highest predictive skill in the 2-9yr range (Guemas et al. 2013).

The eastern Indian Ocean has sustained considerable changes in sea surface salinity (SSS) in recent decades, with implications for halosteric impacts on sea surface height (Vargas-Hernandez et al. 2014, Llovel and Lee 2015). On interannual time scales, Hu and Sprintall (2016a) found that the halosteric component of the ITF transport contributes 35% of the total ITF variability. Indeed, over the past decade the enhanced rainfall over the Indonesian maritime continent, potentially as a regional manifestation of decadal trends in the Walker Circulation (Du et al. 2015), in conjunction with Indo-Pacific equatorial wind trends, is thought to have contributed to the strengthened ITF

transport (Feng et al. 2015, Hu and Sprintall 2016b) playing a key role in the global ocean freshwater distribution.

To better understand the hydrological cycle over the Indian Ocean region more broadly, observations of precipitation, riverine input (runoff), and evaporation at daily resolution are warranted. Focus areas for this should include the Maritime Continent region and northwest shelf off Australia given the large decadal signal there (Feng et al. 2015, Hu and Sprintall 2016a,b), as well as the Bay of Bengal where high riverine input and rainfall make the bay's surface waters the freshest of any tropical ocean (Mahadevan et al. 2016a). In the Bay of Bengal in particular, uncertainty in the freshwater distribution and mixing pathways for riverine input is high and shallow, salinity-controlled mixed layers significantly affect upper-ocean heat content and SST (Wijsekera et al. 2016).

Since 2010, the Soil Moisture and Ocean Salinity (SMOS) satellite provides SSS measurements consistent with *in situ* observations of the equatorial and southern Indian Ocean from the RAMA array, but exhibits large errors in the Bay of Bengal and Arabian Sea. This is likely due to errors in the SSS retrieval due to land contamination and strong winds (Ratheesh et al. 2013, Sharma et al. 2016), making it difficult to capture the largest SSS gradients in the Bay of Bengal (Mahadevan et al. 2016b). With new satellite missions, such as Soil Moisture Active Passive (SMAP), remotely sensed SSS measurements will hopefully improve in their utility for marginal seas and coastal regions (Sharma et al. 2016).

13.3 Essential ocean variables

To understand how Indian Ocean conditions modulate regional hydroclimate variability across a range of timescales and ultimately improve rainfall predictions for Indian Ocean rim countries, sustained measurements of essential ocean variables (EOVs) are required as follows:

1. Surface variables at the air-sea interface, such as SST, SSS, surface winds, and surface fluxes, are needed at daily timescale across the entire Indo-Pacific region with large-scale coverage (e.g., satellite observations).

2. Direct observations of quantities related to the hydrological cycle (e.g., precipitation, riverine input/runoff, and evaporation) are warranted at daily resolution, especially for the Maritime Continent region, northwest shelf of Australia, and the Bay of Bengal with its large riverine input.

3. Concurrent measurements of surface meteorology, air-sea fluxes of heat, freshwater, and momentum, as well as near-surface ocean temperature, salinity, and velocity at sub-daily timescale from *in situ* observations are needed in key locations identified as particularly influential in modulating regional rainfall, such as the SCTR, Arabian Sea, Bay of Bengal, eastern and western equatorial Indian Ocean, and northwest shelf off Australia.

4. Upper-ocean properties, primarily temperature and salinity, for the top 300m at daily to weekly resolution that relate to thermocline variations are sought with a focus on the SCTR, Arabian Sea, Bay of Bengal, the eastern equatorial upwelling region off Sumatra and Java, the western equatorial Indian Ocean, as well as the northwest shelf off Australia.

13.4 Actionable recommendations

Given the EOVs highlighted above to further our understanding of the Indian Ocean's influence on regional hydroclimate and improve its prediction, the following recommendations for IndOOS are made:

a. Maintain existing satellite observations for relevant variables at the air-sea interface with basin-scale coverage over the Indo-Pacific region. [points 1 and 2 in Section 13.3]

b. Maintain and replace SSS-sensing satellites with improved capabilities over marginal seas and coastal regions (cf. SMAP, Aquarius, SMOS). [point 2 in Section 13.3]

c. Maintain and improve river gauge network to observe runoff and riverine input from Indian Ocean rim countries along the coasts. [point 2 in Section 13.3]

d. Maintain the current RAMA array along the equator and the meridional sections, especially for 90°E into the Bay of Bengal, 55°E and 67°E for the SCTR, and in the eastern Indian Ocean (95°-107°E). [points 1, 3, and 4 in Section 13.3]

e. Complete the equatorial RAMA sites near 55°E in the western Indian Ocean. [points 3 and 4 in Section 13.3]

f. Establish a RAMA surface mooring and flux reference site on the northwest shelf off Australia. [points 3 and 4 in Section 13.3]

14. The regional sea-level variability and change

Han W., J. Vialard, M. McPhaden, M.K. Roxy, M. Feng, T. Shinoda, and T. Lee

14.1 Background

The low-lying coastal areas and island nations of the Indian Ocean are subject to significant stress of sea level change (SLC), including the likely increased incidence and magnitude of extreme high sea level events in a changing climate (Church et al. 2013; Rhein et al. 2013; Kay et al. 2015). These regions are highly vulnerable to SLC, as they harvest one third of the world populations with many developing countries, which have poor disaster management resources and strategies (Figure 14.1; Nicholls and Cazenave 2010). The rapid population growth will worsen the situation in the future. By 2030, the Indian Ocean will harbour 10 countries (India, Bangladesh, Indonesia, Thailand, Pakistan, Myanmar, Tanzania, Malaysia, Somalia, Mozambique) among the top 25 with the largest projected population in low-elevation coastal zones, with a total of 339 million people at risk (Neumann et al. 2015). Consequently, there is a strong societal demand for improved understanding of SLC on regional and local scales (Milne et al. 2009; Church et al. 2013*)*. This understanding is instrumental for reliable predictions of future SLC over the Indian Ocean rim. A reliable prediction could help to inform decision-making, adaptation and response options. Yet, our knowledge on Indian Ocean regional SLC, sea level variability at a wide-range of timescales particularly at decadal and multi-decadal timescales, and their major drivers remains limited, due to the lack of observational records. Here, SLC refers to the secular change associated with greenhouse gas forcing.

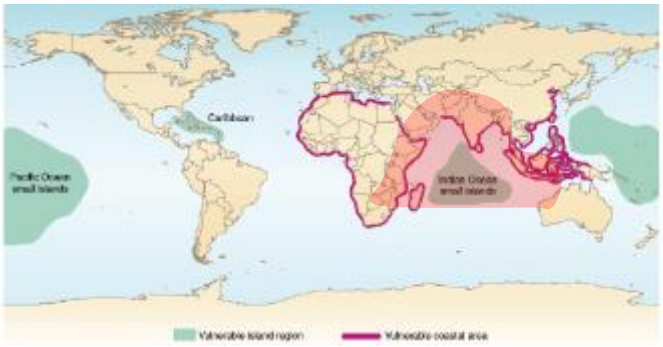

Figure 14.1. Vulnerable regions to coastal flooding caused by future sea level rise, due to dense population, low elevation, strong subsidence rates and/or inadequate adaptive capacity (from Nicholls and Cazenave, 2010). The Indian Ocean region is highlighted.

Tide gauge data are valuable sources for directly detecting multi-decadal and centennial trends and inter-decadal variability of sea level at different regions/locations of the Indian Ocean. A rising trend of sea level at 1~2 mm yr^{-1} has been detected around the Indian coast, using tide gauge records of longer than 40yrs (Unnikrishnan and Shankar 2007); but no statistically significant centennial trend is detected at Saint Paul Island of the south Indian Ocean for the 1874-2009 period based on archaeology records (Testut et al. 2010). A century-long tide gauge record at Mumbai documented significant inter-decadal sea level variability (Shankar and Shetye 1999). Attempt has been made to estimate the regional patterns of sea level trend over the Indian Ocean. It has been shown that sea level rises at all tide gauge locations since the 1960s except for the Zanzibar station, where sea level falls during recent decades (Figure 14.2, black lines). The record length, however, is only 20 yrs (from 1985 to early 2000s) at Zanzibar, which is significantly shorter than the records at all other stations (Han et al. 2010). The sparseness of tide gauge stations, together with the very limited long records, restricts our ability to directly detect the spatial patterns of multi-decadal sea level trend over the entire Indian Ocean. Indeed, there are only a dozen data points over the Indian Ocean rim with record lengths >50yrs and only two >100yrs (Bradshaw et al. 2015).

To compensate for this limitation, reconstructed sea level data were analysed and OGCM experiments were performed using atmospheric reanalyses as forcing fields (e.g., Han et al. 2010). The results showed that the sea level fall at Zanzibar is associated with large-scale sea level

reduction in the southwest tropical Indian Ocean basin (Figure 14.2; e.g., Han et al., 2010; Timmerman et al., 2010; Dunne et al., 2012). This distinct spatial pattern is forced by the changing surface winds associated with changing Indian Ocean Walker and Hadley circulations (Han et al. 2010). While the multi-decadal trend of surface winds might be largely associated with natural variability, AGCM experiments suggested that part of it could be forced by Indian Ocean warming (Han et al. 2010), which was attributed to anthropogenic greenhouse gas forcing (Du and Xie 2008; Dong et al. 2014). What are the spatial patterns and magnitudes of multi-decadal and centennial sea level trends? What is the effect of natural internal climate variability vs that induced by external (both natural and anthropogenic) forcing? These are important issues that have not yet been resolved.

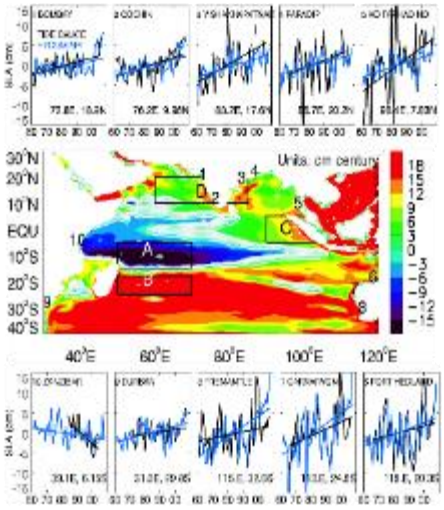

Figure 14.2. Tide gauge observed and OGCM simulated annual mean sea level anomalies (SLA) and their trends during 1961-2008. The 10 tide gauge stations with records longer than 30 years (20 years for Zanzibar) are shown. All trends exceed 95% significance except for stations 6 and 9 tide gauge data. Middle color panel shows trend of HYCOM SLA for 1961-2008. Light blue/green regions are below and the rest above 95% significance. Figure from Han et al. (2010).

Overlying the multi-decadal trend, there is large amplitude variability from intraseasonal to decadal timescales. The advent of satellite altimetry since the early 1990s has revolutionized our ability to detect basin-scale patterns of sea level variations (Lee et al. 2017). On intraseasonal timescales, satellite altimeter data observed strong sea level variability associated with equatorial Kelvin and Rossby waves (e.g., Han 2005; Fu 2007; Iskandar and McPhaden 2011; Nagura and McPhaden 2012), which propagate into the Northern Indian Ocean coastal waveguide (Vialard et al. 2009), and led to the discovery of 90-day basin-resonance in the equatorial Indian Ocean (e.g., Han 2005). On seasonal and interannual timescales, large amplitude sea level variability was observed in various regions of the Indian Ocean associated with the mean seasonal cycle and the Indian Ocean Dipole (IOD) (e.g., Perigaud and Delecluse 1992; Fu and Smith 1996; Shankar et al. 2010; Nagura and McPhaden, 2010; McPhaden and Nagura, 2014). Interannual signals associated with the IOD also propagate into the North Indian Ocean via coastal waveguide, which can affect surface anoxic events and thus marine ecosystems (Parvathi et al. 2017). Decadal reversals of basin-wide sea level trend patterns from 1993-2000 to 2000-2006, and from 1993-2004 to 2004-2014 have also been documented (Lee and McPhaden 2008; Thompson et al. 2016; Srinivasu et al 2017). The sea level differences between the east and west coasts of the tropical south Indian Ocean have been used to infer the changes of the meridional pycnocline transport (the lower limb of the shallow overturning circulations) and the linkages to the Pacific shallow overturning circulation (Lee 2004, Lee and McPhaden 2008, Feng et al. 2010).

Among the many factors that can cause sea level to change regionally (Church et al., 2013; Stammer et al., 2013; Kopp et al., 2015), surface winds - with a large portion being associated with natural internal climate variability (e.g., the MJO, monsoon, ENSO and IOD) - are shown to be the major force for basin-scale sea level variations on all timescales (e.g., Li and Han 2015; reviews by Stammer et al. 2013 and Han et al. 2017). For instance, a distinct spatial pattern of sea level variability on interannual timescale is associated with the IOD (Figure 14.3), which is primarily driven by IOD-related surface winds (e.g., Han and Webster 2002; Rao et al. 2002; McPhaden and

Nagura, 2014). ENSO can affect Indian Ocean sea level through both atmospheric bridge (e.g., surface wind) and oceanic connection via the Indonesian Archipelagos. While ENSO-associated winds can cause large sea level variability in the thermocline ridge region (e.g., Xie et al. 2002), its effect via the ITF is primarily confined to the southeast Indian Ocean, particularly near the west coast of Australia (e.g., Trenary and Han 2012; Feng et al. 2013). Similar conclusions hold for the effects of the Interdecadal Pacific Oscillation (IPO) on decadal sea level variations over the Indian Ocean (e.g., Feng et al., 2004, 2010; Trenary and Han, 2013; Nidheesh et al., 2013; Srinivasu et al. 2017). Bain-wide sea level patterns induced by ENSO and IPO via the integral effect of atmospheric bridge and oceanic connection, however, are not well understood. Recent studies suggested that the ITF influence on decadal sea level variability over the south Indian Ocean has intensified since the early 1990s (Trenary and Han 2013), and most of the "missing heat" of the global warming hiatus since ~2002 has been transported from the Pacific into the Indian Ocean (e.g., Lee et al. 2015; Nieves et al. 2015; Vialard 2015). Modelling studies demonstrated that Indian Ocean warming trend and 10-20yr SST variability during recent decades might have intensified the easterly trades of the Pacific (Luo et al. 2012; Han et al. 2014; Hamlington et al. 2014; Dong and McPhaden 2017), and therefore may have contributed to the intensified ITF influence on the Indian Ocean. Where is the extra heat stored, how is it distributed and how does this "heat" affect the regional sea level variations over the Indian Ocean? These are key science questions remain to be answered. Given that the tropical Indian Ocean has experienced a rapid surface warming during 1950-2015 compared to the global mean SST trend (~1.04°C vs 0.64°C; e.g., Roxy et al. 2014, Cheng et al. 2017), the possible contribution of the "extra heat" to surface warming and to thermosteric sea level variations demands immediate attention.

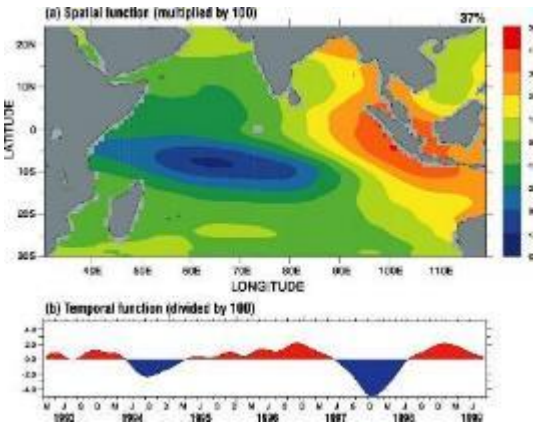

Figure 14.3. The leading Complex EOF of SSH (a) and PC1 (b), based on TOPEX/Poseidon SSH anomaly from 1993-1999. This spatial pattern of SSH anomaly is associated with the IOD (Rao et al. 2002). Figure downloaded from: http://www.jamstec.go.jp/frcgc/research/d1/iod/fig_1.jpg.

Sea level represents an integral effect of surface and subsurface oceanic processes, particularly ocean heat content. Thermosteric sea level is the primary contributor to regional sea level patterns, with the upper 700m thermosteric sea level explaining most of the observed decadal sea level variations (e.g., Fukumori and Wang 2013; Nidheesh et al. 2013; Srinivasu et al. 2017). Halosteric sea level, however, can have significant contributions in some regions (e.g., Shankar and Shetye 1999; Fukumori and Wang 2013; Llovel and Lee, 2015). Thermosteric and halosteric sea level variations tend to compensate each other in most regions of the interior ocean, suggesting the importance of oceanic advection in affecting regional sea level patterns (Stammer et al. 2013). Large ensemble climate model experiments have been done recently using post-CMIP5 models, but the regional SLC patterns since the 1950s vary widely among models (e.g., the 100 member ensemble of the Max-Plank Institute of Meteorology model vs 40 member ensemble of NCAR's CESM1 model; figure not shown). This further suggests our need to fully understand the forcing and processes for sea level variability and change.

In addition to the sea level variations induced by surface and lateral boundary forcing, oceanic internal variability is shown to have a significant contribution to sea level variability on various timescales in some regions of the Indian Ocean (e.g., Li and Han 2015), and it dominates the small-scale (<6º) sea level variance globally (Sérazin et al. 2015).

14.2 EOVs for Indian Ocean sea level variability and change

Even though significant progress has been made toward detecting and understanding Indian Ocean sea level variability and change (see above), our knowledge is still limited particularly on decadal and longer timescales. Direct sea level observations using tide gauge and satellite altimetry are crucial for understanding sea level variability and change. Thus far, continuous satellite records with a quarter degree resolution exist only since the early 1990s, which are still too short for understanding decadal and longer-timescale variability. The importance of wind-driven ocean circulation, the dominance of thermosteric, and the regional contribution of halosteric sea level discussed above stress our needs for sustained observations of current, temperature, salinity as well as surface winds, in order to provide reliable detection and improved understanding of regional sea level variability and change over the Indian Ocean. Spatially and temporally continuous records, however, are extremely lack.

Efforts have been made to generate reliable longer data records for climate studies (e.g., temperature, winds, sea level) by quality control of existing historic datasets, assimilating observations into numerical models (reanalysis products), and applying statistical techniques to reconstruct basin- and global-scale datasets during earlier periods when observations were sparsely distributed (reconstructed data). There is however a non-negligible spread among these products, especially before the satellite era, leading to significant uncertainties on multidecadal trends (e.g., winds, air-sea fluxes). There are also significant differences among reconstructed sea level datasets before the satellite era regarding both global mean SLC and regional multidecadal trends (e.g. Nidheesh et al. 2017). Continuous effort is needed to further improve the quality of existing historical, reanalysis and reconstructed datasets, by advancing our statistical techniques and improving data archaeology to overcome the known limitations. There is also a need to inter-calibrate successive satellite missions with the help of in situ data, in order to yield more homogeneous basin-scale products for the key variables discussed above.

14.3 Actionable recommendations

Based on the EOVs discussed above, the following actionable items are recommended for IndOOS:

a. Maintain the existing tide gauge stations to provide continuous, long-term records; the recently added tide gauge in the thermocline ridge region in 2010 (Bradshaw et al. 2015) is particularly important; add new tide gauges around the thermocline ridge (e.g., at Agaléga, Rodrigues & St Brandon of Mauritius, French “Iles éparses” such as Tromelin, Europa & Juan de Nova);

b. Maintain the Argo network in the entire Indian Ocean to obtain basin-wide estimation of thermosteric and halosteric sea level contributions;

c. Improve deep ocean observations (e.g., deep ocean moorings and deep Argo) to observe temperature and salinity to assess the effect of deep ocean variability on SLC;

d. Maintain the existing RAMA array, particularly the meridional sections at 67°E and 80°E where sea level variability is large over the thermocline ridge region (Figures 14.1 and 14.2), and the zonal sections at the equator, 2°N and 2°S (IOD wind, subsurface thermal and salinity signals, and current) and all moorings in the eastern equatorial Indian Ocean for temperature and current measurement;

e. Maintain the IX01 XBT line to sustain the mass and heat transport estimate of the ITF and sea level variability near the west coast of Australia; Maintain the trans-Indian Ocean hydrographic observations along the 32°S line, including the boundary current regions near the Leeuwin and Agulhas currents;

f. Continue satellite altimetry data (e.g., Jason series), which are essential for providing basin-wide multidecadal records, and satellite missions for measuring vector winds over the ocean surface; the upcoming SWOT mission is important for resolving the small scale sea level variability due to oceanic internal variability; Continue Earth gravity satellite missions such as GRACE and GOCE to better capture the changes of mass distribution in the ocean.

Part II: Operational Drivers

15. Indian Ocean observations for operational subseasonal and seasonal forecasts

Aneesh C. Subramanian, Frederic Vitart, Chidong Zhang, Arun Kumar and Magdalena A. Balmaseda

15.1 Introduction

Intraseasonal (ISV) and seasonal variability are two of the dominant modes of variability in the tropical Indian ocean-atmosphere system (see chapter 5) linking weather systems to long term interannual and decadal climate modes of variability. A majority of the annual rainfall over Southeast Asia is received from the southwest monsoon during June to September. The tropical ISV influences many temporal and spatial phenomena, including, the diurnal cycle of tropical convection (Tian et al. 2006; Oh et al. 2012; Seo et al. 2014), tropical cyclone activity (Bessafi and Wheeler 2006; Kim et al. 2009; Camargo et al., 2009; Vitart 2010;Kim et al. 2014), synoptic disturbances over the monsoon trough (Goswami et al. 2003; Neena and Goswami 2010), Asian and Australian monsoons (Sikka and Gadgil 1980; Hendon and Liebmann 1990; Webster et al. 1998; Goswami 2005), coupled modes such as El Nino Southern Oscillation (ENSO; Lau and Chan 1988; Takayabu et al. 1999; Roundy et al. 2008), the Indian Ocean Dipole (IOD; Saji et al., 1999; Rao and Yamagata 2004; Han et al. 2006) and many other weather-climate phenomena (Zhang 2013). The eastward propagating Madden–Julian Oscillation (MJO) is the most common and energetic mode of ISV in the tropics (Madden and Julian 1972, 1994; Wheeler and Kiladis 1999; Zhang 2005; Lau and Waliser 2011). The MJO represents the planetary scale convectively coupled eastward propagating disturbance of 30–60 day periodicity. In the Indian Ocean region, the monsoon intraseasonal oscillation (MISO) is another manifestation of ISV and refers to a quasi-oscillatory mode that modulates the Asian summer monsoon in the region (Goswami 2005; Waliser et al. 2006a, b). In addition to the eastward propagation, the MISO manifests also as strong northward propagating convective rainbands and influences intraseasonal rainfall over the south Asian monsoon region. The subseasonal to seasonal (S2S) variability of rainfall in the region has profound impacts on the agriculture, economy, water resources and the ecosystem. Recent droughts in 2002, 2004 and 2009 were poorly predicted by both statistical and dynamical seasonal forecast models. The economic impacts on the region due to the lack of forecast skill on subseasonal and seasonal timescales (Gadgil et al. 2005) for the region stresses the need for improved prediction on these timescales for the region.

While the MJO is more active during boreal winter (Madden 1986), the MISO is most active during boreal summer. The MISO manifests as a quasi-oscillatory mode embedded within the seasonal variability of the Asian summer monsoon (Webster et al. 1998; Goswami 2005; Waliser 2006a, b). The MISO typically exhibits a shorter period of two - three weeks compared to a month or two for the boreal winter MJO (Wang et al. 2006). The MISO is seen as a strong northward propagating band of convection and precipitation that strongly influences the weather over the entire south Asian Monsoon domain during this season. Northward propagation is apparent from the equator into the Northern Hemisphere for both precipitation and zonal wind over a period of two weeks, with precipitation leading zonal wind by 5-7 days. Many different mechanisms have been proposed for MISO northward propagation. These include Rossby wave responses to equatorial eastward propagation (Wang and Xie 1997; Kemball-Cook and Wang 2001), barotropic vorticity induced by mean easterly vertical wind shear (Jiang et al. 2004), air–sea interaction with SST, radiation and latent heat fluxes playing a key role in the propagation (Kemball-Cook and Wang 2001; Fu et al. 2003), wind induced moisture-convection feedbacks (Bellon and Sobel 2008a) and others that incorporate various aspects of the interactions between the largescale tropical dynamics and convection (Bellon and Sobel 2008b, Boos and Kuang 2010, Kang et al. 2010). The key ocean mechanisms alluded to in these theories are the upper ocean mixed layer processes that play a role in SST variability and upper ocean heat content variability. These are modulated mainly by

wind induced mixing, latent heat release and freshwater input from precipitation and can act as sources of predictability on the S2S timescales. Hence, observing and modeling these upper ocean processes at daily or subdaily frequencies and improving relevant data assimilation capabilities for reducing uncertainties in representing these processes in the initial conditions can help improve forecasts on S2S timescales.

The processes controlling MISO characteristics like moisture sensitivity and surface-feedbacks are still not well understood and are likely different from those that govern the MJO dynamics (Goswami, 2005 and references therein). Global climate models (GCM) are known to have serious problems simulating the salient features of MISO. Major deficiencies are observed in simulating its spatial structure, northward propagation and scale-selection (Sperber et al. 2001; Kang et al. 2002; Waliser et al. 2003; Sperber and Annamalai 2008; Lin et al. 2008; Sperber et al. 2013; Sabeerali et al. 2013). The northwest–southeast tilted rain band structure is another feature that is often misrepresented in the models (Waliser et al. 2003; Sperber and Annamalai 2008; Sperber et al. 2013; Sabeerali et al. 2013). This is often associated with the models' limitations in simulating the eastward propagation and the associated wave responses (Sperber and Annamalai 2008).

15.2 Modeling, Observation and Prediction

Atmosphere-only models with prescribed SST forcing have been used for monsoon seasonal forecasting for several decades (Charney and Shukla 1981; Shukla 1998). These atmosphere-only models show relatively poor skill in predicting the monsoon as they lack air-sea interaction, which is a major source of predictability for the S2S timescale in the region (Wang et al. 2005; Wu and Kirtman 2005). The fidelity of GCMs in representing the seasonal monsoon variations and MISOs depends on the representation of the air-sea interaction over the Tropical Indian Ocean region (Wang and Schlesinger 1999; Maloney and Hartmann 2001; Lin et al. 2006; Zhang and Song 2009; Zhou et al. 2012). A community effort towards improving MJO simulation in many different global models over the last two decades has helped improve the current generation model physics and their representation of the MJO (Slingo 1996; Benedict and Randall 2007; Waliser et al. 2009; Bechtold et al. 2008; Kim et al. 2011, 2014; Vitart 2014; Jiang et al. 2015). However, The current generation climate and weather forecasting models are still very limited in terms of prediction skill of MISO events, compared to the potential predictability (Lee et al. 2015, Neena et al. 2015). This is likely due to the more complex land-ocean-atmosphere interactions involved with the monsoon prediction problem compare to the eastward propagating MJO over the ocean. Hence, a concerted effort in diagnosing deficiencies in the representation of air-sea interaction processes in the Tropical Indian Ocean region is much needed for a similar improvement in MISO representation and prediction in current generation models.

Recent international field campaigns in the central equatorial Indian Ocean and Bay of Bengal (BoB) have collected unique observations to discern coupled atmosphere-ocean dynamics in the region. The Dynamics of the MJO (DYNAMO) field campaign in 2011-12 (Yoneyama et al. 2013) and the Air-Sea Interactions in the Northern Indian Ocean (ASIRI) in 2013-2017 combined mature and new observational platforms to study multiscale dynamics, thermodynamics and interaction. These field campaigns observed the myriad processes involved in the MJO and MISO propagation through the Indian Ocean. The DYNAMO field campaign and follow-on studies show the importance of ocean-atmosphere interaction in the MJO propagation through the Indian Ocean region (Zhang et al. 2013). Thes DYNAMO and ASIRI field campaign data revealed the rich frontal features, sub-mesoscale variability, shallow mixed layer dynamics with weak mixing, strong wind-forced surface currents, diurnal air-sea interaction, and other dynamic features of the regions, which were less known previously. All these processes lead to determining the modulation of the SST and heat fluxes from the ocean surface into the atmosphere on S2S timescales. The inability of forecast models to capture these cross-component interactions well translates to forecast errors and limits on prediction skill for MISOs, MJO and the seasonal monsoon. Improving the observations of air-sea interactions in the region and the upper ocean processes can help understand how they modulate the boundary layer dynamics in both the ocean and atmosphere

and how this links to MJO and MISO convection. This will further help improve our prediction capabilities for the monsoon, MISO and the MJO on S2S timescales.

The MJO initiation and propagation in observations have most commonly been studied using the Realtime Multivariate MJO (RMM) index of Wheeler and Hendon (2004). A recent study (Zhang and Ling, 2017) compared results derived from the RMM index to those from a new method of tracking precipitation of individual MJO events (Ling et al., 2012). They show that while the starting longitudes for the MJO events are distributed over the entire tropics when using the RMM index (Matthews, 2008), most of them form over the Indian Ocean (Fig. 15.1a) when derived from tracking precipitation signals. The distribution of ending longitudes exhibits two peaks: one over the Maritime Continent (MC) and the other over the central Pacific (Fig. 15.1a). This is direct evidence for the MC barrier effect on the MJO: an MJO event either fails to propagate through the MC and vanishes there or continues to move eastward until it reaches the cold sea surface east of the western Pacific warm pool.

The role of coupled processes in the MJO has also been investigated in the European Centre for Medium-Range Weather Forecasts Extended-Range Forecasting System. A series of subseasonal (extended range) forecasts initialized daily over the Tropical Ocean Global Atmosphere Coupled Ocean Atmosphere Response Experiment (TOGA-COARE) period were performed with sea surface temperatures (SSTs) provided by persistence of initial conditions, observed SSTs and coupling to a full dynamical ocean model with vertical resolution in the upper ocean typical of coupled models (10 m). The subseasonal forecast experiment with the full dynamical ocean model showed improved forecast skill for the MJO compared with the persisted and observed SST experiments, indicating a role for coupled processes in the MJO (Fig. 15.2). Sensitivity experiments in this context have revealed that the improved representation of the diurnal cycle in the upper ocean, which results from the increased vertical resolution in the upper ocean, is a significant factor in improving the forecast skill (Woolnough et al. 2007; Ge et al. 2017). Hence, observing the upper ocean (upper 50 m) at a high temporal and spatial resolution could help improve our understanding of the diurnal cycle and its modulations in the Indian Ocean. This can help improve the process representation of the diurnal cycle in seasonal forecast models either with an improved parameterization (Zeng and Beljaars 2005; Large and Caron 2015) or with data assimilation (Koster et al. 2016; Penny et al. 2017).

Hence, being able to observe and understand the diurnal cycle in the upper ocean and how it couples to the atmospheric boundary layer will require a sustained observing system with moorings or other platforms and would be beneficial for both improving model representations and parameterizations of these processes. The sustained observations can also be assimilated in the forecast models to improve initial conditions for subseasonal forecasts. The sustained moorings would need to have a high vertical resolution measurement (1 m or less) of temperature, salinity and currents in the ocean every hour or three hours minimum over the top 25 - 50 m. If this can be complemented with concurrent surface meteorological measurements of the heat fluxes, surface temperature, humidity and other variables, it will revolutionize our understanding of air-sea interactions in the region. This will help improve our models and hence forecasting capabilities for the monsoon and the MJO in the region.

The impact of biases and errors in SST on subseasonal forecasts for the MISOs has been studied by Abhilash et al. (2014). They show that bias correction in SST has minimal impact in short-to-medium range, but has a substantial influence on prediction skill for MISOs on subseasonal (12–18 days) time ranges. Several encouraging studies have shown that air-sea coupling may extend MISO predictability and suggesting that ocean plays a key role in MISO dynamics and may be a source of predictability for the MISO (Fu et al., 2008 and references there in).

De Boisseson et al (2012) and Wang et al. (2015) showed that the MJO prediction skill is sensitive to the choice of SST analysis products, with state of the art high resolution SST analyses producing different results. Recent work with the ECMWF extended-range and seasonal systems also show that sampling the uncertainty in the ocean initial conditions influence the amplitude of the ensemble spread significantly on seasonal timescales in the Eastern Indian Ocean region (and therefore the potential predictability, Andrejczuk et al. 2016). This is also a key geographical region for

influencing the prediction of the MJO, ENSO and Indian Ocean Dipole, and needs to be investigated further. Hence, observing the Eastern Indian Ocean region as well as the Bay of Bengal with sustained moorings with near surface measurements to complement the Argo array of subsurface ocean measurements in the region will help improve our understanding of forecast model uncertainities in the region. The Argo floats are challenged to sample in the strongly upwelling regions due to strong offshore Ekman transport advecting the Argo floats out of the region. Hence, having another observation platform that can sample the upwelling region in the Eastern Indian Ocean region can help improve our understanding of the region and how it influences S2S forecasts over the South Asian region. There is also an increasing interest on developing coupled data assimilation methods for initialization of extended range forecast and for reanalyses applications. Coupled data assimilation involves the assimilation of both oceanic and atmospheric observations simultaneously into a coupled forecasting system prior to initializing the forecasts. This will require collocated observations across the ocean and atmosphere, and the IndOOS will be instrumental to develop such coupled systems (see details in the final section on recommendations).

Hence, availability of a sustained observation system and process-oriented field observations in the Indian Ocean region targeting timescales from diurnal cycles to longer time periods can help inform and improve coupled prediction systems in improving their upper ocean representation as well as air-sea interaction processes. These observations will also be highly useful for coupled data assimilation to help improve initial conditions for subseasonal and seasonal forecasting over the entire globe. For observations to have an impact in the complex data assimilation systems, the observations must also be quality controlled and preferably processed to reduce representational errors in data assimilation (Penny et al. 2015).

15.3 Essential Ocean Variables (EOV)

The atmospheric forcing associated with the monsoon in the boreal summer months and the MJO in boreal winter months influence the upper ocean processes significantly and lead to strong air-sea interaction which can in turn modulate the monsoons and MJO. Hence, observing the surface heat fluxes, temperature, salinity and upper ocean variability in the tropical Indian Ocean is crucial for improving our understanding as well as forecasting capabilities of the MJO and the monsoon. Air-sea interaction over the Bay of Bengal is dominated by the upper ocean stratification forced by anomalously high fresh water influx into the region. The air-sea coupling in this region influences the development and propagation of MISO significantly. Hence, sustained observations of the freshwater input into Bay of Bengal from the river runoff as well as precipitation is necessary. Similarly surface salinity and temperature in the Arabian Sea influence the monsoon jet propagation as well as moisture transport into the continent and hence, needs to be monitored carefully. The upper ocean diurnal cycle plays a key role in the evolution of both the MJO as well as the MISO events. Hence, observing the diurnal cycle over the equatorial Indian Ocean as well as in the Maritime continent with sustained high frequency measurements can help improve our sampling of this variability. This can help improve our model representations of the upper ocean diurnal cycle through coupled data assimilation methods to ingest these sustained observations into forecast systems.

Variables of interest

Temperature, salinity, velocity in the upper 50 m of the ocean including the surface, 10 m winds, 2m air temperature and humidity, precipitation, shortwave and longwave radiation

Resolutions

Temporal resolution: One hour (minimum 3 hours) to resolve the diurnal cycle

Zonal resolution: 5° in longitude (~1110 km)

Meridional resolution: 1° in latitude (~111 km) near the equator to resolve equatorial wave guide.

15.4 Recommendations

Sustained long-term measurements of the upper ocean temperature, salinity and currents are key to observe and understand air-sea interaction over the Indian Ocean region. They are also very important to assimilate into S2S forecast models to help improve MISO, MJO and seasonal monsoon predictions in the region. Hence, maintaining the current network of IndOOS especially the RAMA array and Argo program is the first priority. Recommendations for the enhancements to the current observing capabilities are described below:

Given the importance of representing the diurnal cycle in forecast models for improving MJO and MISO forecasts, we recommend increasing the vertical resolution in the upper 10 m of RAMA buoy. Suggested depths of temperature and conductivity sensors are: 0.5 m, 1.0 m, 2.0 m, 3 m, 5 m, 7 m, 10 m, and every 5 m below that upto 50 m which can better resolve the shallow diurnal warm layer (upper few meters) and the mixed layer deepening during night time.

The zonal and meridional resolution of the current RAMA buoy network are coarser than that recommended in the previous section on EOVs. Since the resources are limited, it is likely more critical to sample the upper ocean at a higher vertical resolution and supplement the spatial resolution of the moorings with Argo and satellite observations. Here are some specific recommendations for improved observations in key areas to help improve MJO and monsoon predictions. They are listed below:

(1) Adding a new sites of surface buoys in the eastern Indian Ocean with both upper ocean temperature, salinity sensors as well as a meteorological station.

The SST anomalies on interannual timescale varies significantly in this region due to both ENSO as well as the Indian Ocean Dipole. The SST in this strong upwelling region influences both the MJO and MISO propagation through the region. Hence better understanding of air-sea interaction in this region will help to improve MJO and monsoon representation in the forecast models. The importance of this location for other climate and ecosystem variability is discussed in other chapters.

(2) Increase the surface flux buoy sites in western Indian Ocean (equatorial and Arabian Sea) while also maintaining the existing surface mooring sites in the revised RAMA-2.0 design.

The surface fluxes in this region, especially the latent heat flux, determines the strength of vapor transport in the monsoon flow and hence is a key driver for downstream precipitation over the continent. Being able to observe and predict this better on subseasonal timescales can help advance our warning and disaster mitigation for heavy rainfall events over the continent.

(3) Enhance some of the existing RAMA buoy measurements by augmenting the existing upper ocean measurements with concurrent high frequency meteorological measurements for the atmospheric state

This can help improve our understanding of the diurnal cycle in the region and help improve representation and prediction of both the MJO and MISO events in the forecast models.

(4) Increase observations of coastal regions especially near the Maritime Continent region.

Argo floats as well as current RAMA array do not observe the ocean state near the coast of the complex Indonesian Throughflow region. Given that this region is a key connector between two large ocean basins (Pacific and Indian Ocean), it is important to observe and understand the complex ocean-atmosphere-land interactions in the region. This will help reduce current model MJO forecast biases in terms of not propagating MJOs across the Maritime Continent as well as in nature.

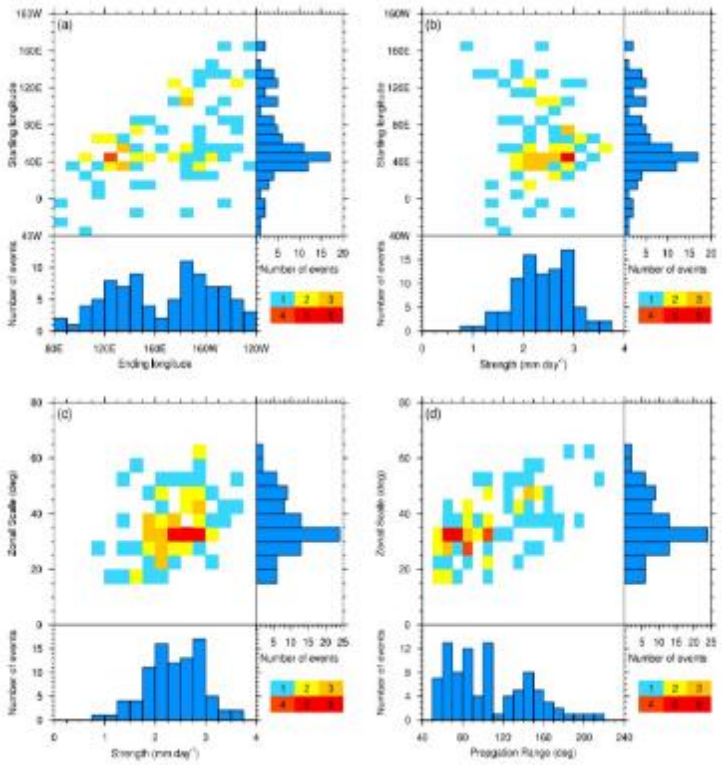

Figure 15.1. Individual and joint number distributions of (a) starting vs ending longitudes, (b) starting longitudes vs mean strength, (c) mean zonal scales vs mean strength, and (d) mean zonal scales vs propagation ranges of tracked MJO events using the TRMM precipitation data. Colors of the joint distributions represent the number of events. Source: Zhang and Ling (2017)

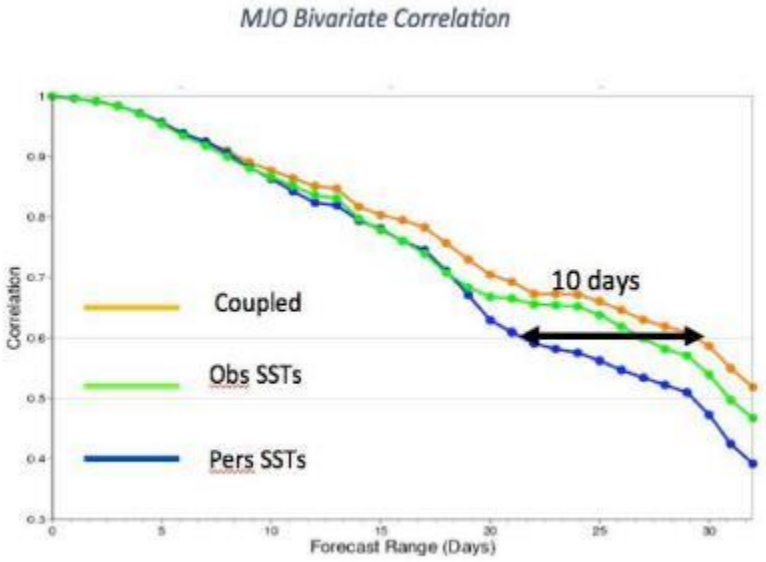

Figure 15.2. Correlation of the observed RMM times series with the ensemble mean forecast time series for a control experiment with observed SST forcing (green line), coupled ocean (orange line) and the persisted SST experiment (blue line).

16. Improvement of surface fluxes

Lisan Yu, Woods Hole Oceanographic Institution, Woods Hole, MA, USA

Michael J. McPhaden, NOAA/Pacific Marine Environmental Laboratory, Seattle, WA

16.1 Progress made in improving air-sea flux climatologies in past 10 years

When designing the RAMA moored array 10 years ago (McPhaden et al. 2009), there was strong consensus on the need for surface moorings that are instrumented with enhanced measurement capabilities for comprehensive air–sea fluxes (i.e., “flux reference site” moorings) and placed at key dynamical regimes. The rationale was plain and clear: better surface heat and moisture flux climatologies are highly desired in a region where surface fluxes are important in determining mixed-layer temperature and salinity variability from diurnal to intraseasonal and longer timescales (e.g. Yaremchuk 2006; Yu et al. 2007). Better surface fluxes are essential for improving numerical weather prediction and climate forecast skills. Better surface fluxes are understanding of the mechanisms responsible for the frontal-scale air-sea interaction over the western boundary currents (Beal et al, SD 07 in this review).

During the RAMA design phase, six surface flux climatologies that were available at that time were examined to provide a first-hand experience of the quality of the surface fluxes and to help develop strategies for air-sea measurements (Yu et al. 2007). The six flux products showed large discrepancies over the Indian Ocean (Fig.16.1). The standard deviation (STD) in the long-term mean net heat flux exceeded 25 Wm^{-2} over almost the entire basin north of 20°S, with the maximum difference of 40 Wm^{-2} occurring in the vicinity of the Somali Current.

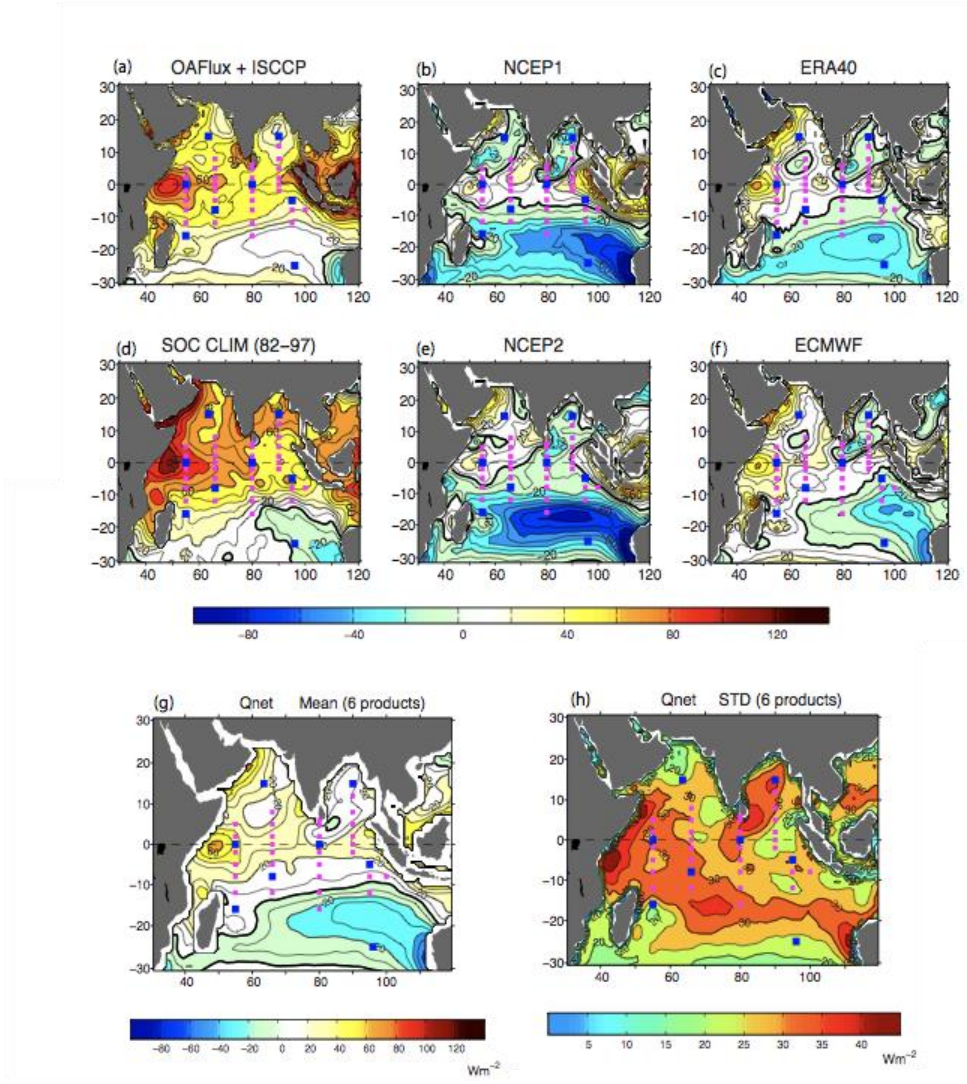

Figure 16.1 Time-mean Qnet from (a) OAFlux+ISCCP, (b) NCEP1, (c) ERA40, (d) SOC, (e) NCEP2, and (f) ECMWF for the period 1988-2000. (g) ensemble mean and (h) STD spread of these 6 Qnet products (adapted from Yu et al. 2007). The designed RAMA buoy locations are superimposed, and those marked by blue squares denote flux reference sites.

The net surface heat flux (Q_{net}) going into the ocean is the sum of a number of heat exchange processes at the air-sea interface. These processes include incoming and reflected solar radiation, outgoing and re-emitted longwave radiation, sensible heat (SH) transfer by conduction and convection, and latent heat (LH) release by evaporation of surface water. In general, these heat flux components are estimated using bulk flux parameterizations with surface meteorological variables obtained from one of the following sources: numerical weather prediction (NWP) reanalysis, ship reports from the Comprehensive Ocean-Atmosphere Data Set (COADS), and satellite retrievals. Different data sources have different biases that result from sample frequency, coverage, and statistical and/or dynamical interpolation frameworks. Different bulk flux algorithms incorporate different physical parameterizations for surface wave spectra, convective gustiness, roughness length, etc. (Brunke et al. 2002). All these differences could lead to significant differences between surface flux products. For instance, the buoy measurements of Weller et al. (1998) taken during the Arabian Sea Experiment in 1994-95 showed a net heat gain of 60.3 Wm^{-2}, while the Q_{net} produced from the National Centers for Environmental Prediction (NCEP) reanalysis

had a net heat loss of – 4.5Wm^{-2} – the mean differences between the two are nearly 65 Wm^{-2}. If biases in data are disregarded, the flux algorithms alone can give rise to differences of 23 Wm^{-2} (or 16% relative to the algorithm-averaged flux) in monthly LH and 0.013 N m^{-2} (or 19% relative to the algorithm-averaged value) in monthly wind stress in regions of high SST (> 27.75°C) (Brunke et al. 2002).

Significant progress has been made in surface flux estimates from satellite analyses and atmospheric reanalyses in the past 10 years due largely to two factors. The ever-advancing satellite technology for retrieving flux-related variables (Josey et al. 2013), such as near-surface air temperature and humidity, most significantly, the advancement in surface radiation products. The CERES instrument onboard the polar-orbiting Aqua satellite and follow-on missions since 2000 have provided the first ever complete coverage of highly accurate energy budget and cloud observations over the Indian basin, from which the surface radiative budget has been computed using an energy balanced and filled (EBAF) approach (Kato et al. 2013). Previous surface radiation products, such as ISCCP and GEWEX SRB, were constructed from geostationary satellites which have a broad gap in coverage over the Indian Ocean (Zhang et al. 2004). This gap has been a major obstacle for estimating basin-scale Qnet spatial and temporal variability and trends in recent decades, coincident with the period that the basin has seen an unprecedented rise in sea surface temperature and heat content (Roxy et al. 2014; Lee et al. 2015). The second factor is successive generations of atmospheric reanalyses that have improved in quality as a result of better physical models, more observations to constrain the models, and better assimilation methods. As a result, there has been a wave of latest versions of global reanalyses from NCEP (Saha et al., 2010), JMA (Kobayashi et al. 2015), NASA (Rienecker et al., 2011), and ECMWF (Dee et al. 2011). Given all these improvements, we would anticipate an improvement in Qnet.

The degree of improvement in Qnet over the past 10 years can be evaluated using 6 of the latest Qnet products (Figs. 16.2a-f) to construct the ensemble mean (Fig.16.2g) and STD between the 6 mean products (Fig. 16.2h) for the period 2001-2010. Compared to the Qnet ensemble mean of 10 years ago (Fig.16.1), the present Qnet shows a similar spatial pattern but with enhanced magnitude in both maximum net heat gain (Qnet >0) and maximum net heat loss (Qnet <0) regimes. The maximum oceanic net heat gain occurs in the western equatorial region off the coast of Somali and is enhanced by about 10 Wm^{-2} in the present estimate. Meanwhile, the maximum net heat loss occurs over the southeastern subtropical basin and is also enhanced by about 10 Wm^{-2}. Compared to the Qnet ensemble spread of 10 years ago (Fig. 16.1h versus Fig.16.2h), the spread in the 6 recent Qnet products is reduced by more than 50%, with the STD difference of 25 Wm^{-2} confined mostly in the equatorial region and the Somali current region.

Reduction in the mean Qnet is most evident in the CERES EBAF and the newly developed satellite-only, high-resolution OAFlux (OAFlux-HR) (Fig. 16.2a). This combined satellite Qnet captures the net heat loss over the subtropical Indian Ocean, which is a major correction to the basin-wide warm bias in OAFlux+ISCCP. The correction is attributed mainly to the better surface radiation products from CERES (Kato et al. 2013) and the use of an improved turbulent bulk flux algorithm (Jim Edson, personal communication, 2017) in the OAFlux-HR computation. A reduction in mean Qnet produced by NOC2.0 (previously SOC) using ICOAD ship reports (Berry and Kent 2009) is also evident (Fig. 16.2d), with the improvement possibly due to increased sampling in the region. The agreement between the four reanalysis Qnet is poor however and they still have large uncertainties. CFSR has an excessive net heat gain (+ 80 Wm^{-2}) in the equatorial region, and MERRA2 has an excessive net heat loss (− 30 Wm^{-2}) in the Bay of Bengal and the eastern equatorial basin (Figs. 16.2c and 16.2f). The differences in these two products account for a large portion of the STD between the products (Fig. 16.1e). Significantly, despite the fact that ERA-interim and OAFlux-HR + CERES are totally independent, with one produced by reanalysis system and the other constructed from satellite retrievals, the two exhibit broad-scale consistency both in spatial pattern and magnitude.

The largest heat loss in the Indian Ocean occurs in mid latitudes along the path of the warm Agulhas Current, the Current Retroreflection, and the Return Current. Except for NOCS2 that lacks of in situ representation in the region, the flux products from the recent satellite-derived

(OAFluxHR+CERES) and latest reanalyses (CFSR, MERRA2, and ERA-interim) are generally doing well in capturing the flux variability associated the meandering pattern of the Agulhas current system. Nevertheless, the STD difference between the 6 mean patterns exceed 25 Wm^{-2} along the path of the current, reflecting largely the differences in products in representing the strength and width of air-sea fluxes on the frontal scales.

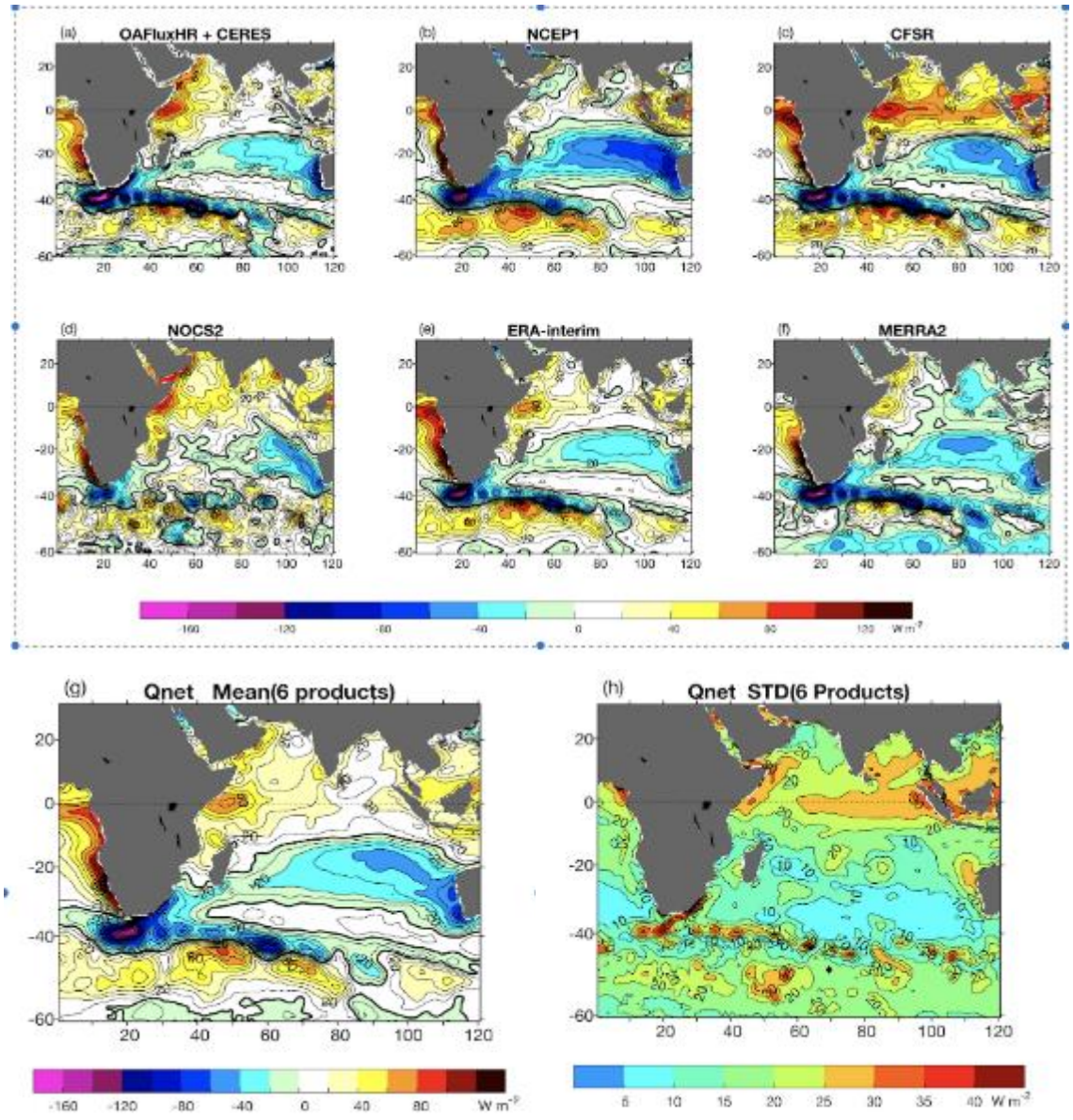

Figure 16.2 Time-mean Qnet from (a) OAFluxHR+CERES, (b) NCEP1, (c) CFSR, (d) NOCS2, (e) ERA-interim, and (f) MERRA2 for the period 2001-2010. (g) ensemble mean and (h) STD spread of these 6 Qnet products.

16.2 Leading source of uncertainty and role of RAMA reference sites

Although there has been significant progress in reducing the uncertainty in surface flux estimates over the past 10 years, the spread in Qnet mean values remains large (~20 Wm^{-2}) over the warm waters of the tropical Indian Ocean north of 10°S (Fig.16.1e). Moreover, the progress is more evident in satellite and ship-based products than in the atmospheric reanalyses. As pointed out by

Yu et al. (2017), reanalysis systems have a total energy balance constraint placed at the top of the atmosphere, not at the surface. Without an energy balance constraint over the ocean surface, the errors in each flux component add up and give rise to large biases in the analyzed mean Qnet. Given the current configuration in the reanalysis systems, it appears that improving model parameterizations of surface flux processes might be the only way forward for improving the mean Qnet from a reanalysis.

Since Qnet is the sum of a number of heat exchange processes at the air-sea interface, it is necessary to identify the leading source of uncertainties in order to guide improvements in reanalysis products. 14 products are compared (9 reanalyses (NCEP1, NCEP2, CFSR, ERA-interim, ERA-20C, MERRA, MERRA-2, JRA55, 20CR), 4 satellite products (ISCCP, SRB, CERES, OAFlux-HR), and 1 ship-based product (NOC)) to gain an understanding of the overall uncertainty in each flux component over the 10 year period 2001-2010. The STD of the means for the 14 products is computed for both surface radiation (net shortwave and longwave (SW+LW)) and turbulent latent and sensible heat fluxes (LH+SH) (Figs.16.3a-b) to show that the uncertainty in SW+LW dominates the uncertainty in Qnet in the tropical Indian Ocean. This uncertainty in SW+LW is not unique to the Indian Ocean – but is a problem common to the reanalysis models over all tropical warm pool waters. Net freshwater flux (evaporation-minus-precipitation) products show a similar STD spread and pattern in the mean precipitation (Yu et al. 2017). This similarity in the uncertainty patterns in SW+LW and precipitation, along with their close connection to tropical warm pool waters, indicates that the long-standing problems of parameterizing tropical convective clouds in reanalysis models impact the surface radiative budget, leading to major errors in the net heat balance at the tropical ocean surface.

The original RAMA array design included 8 full-flux reference sites (Fig.16.1a), although 2 of them in the Arabian Sea and the western equatorial basin have not yet been occupied. Nevertheless, the surface flux measurements that were acquired at the 6 sites since RAMA was implemented in 2006 provide solid benchmark time series to help diagnose the problems in reanalyzed radiation products. At buoy sites, only downward components of shortwave and longwave radiation are measured. Comparing these measurements to reanalysis models (Figs 16.4a-b), the downward shortwave radiation is poorly produced, while the downward longwave radiation is better. The models perform badly when insolation is low (<150 Wm^{-2}), conditions under which the models tend to overestimate solar radiation. Overall, ERA-interim surface radiation appears to be least biased, and CFSR most biased. A similar pattern is obtained using TAO-TRITON buoys for the western Pacific warm pool.

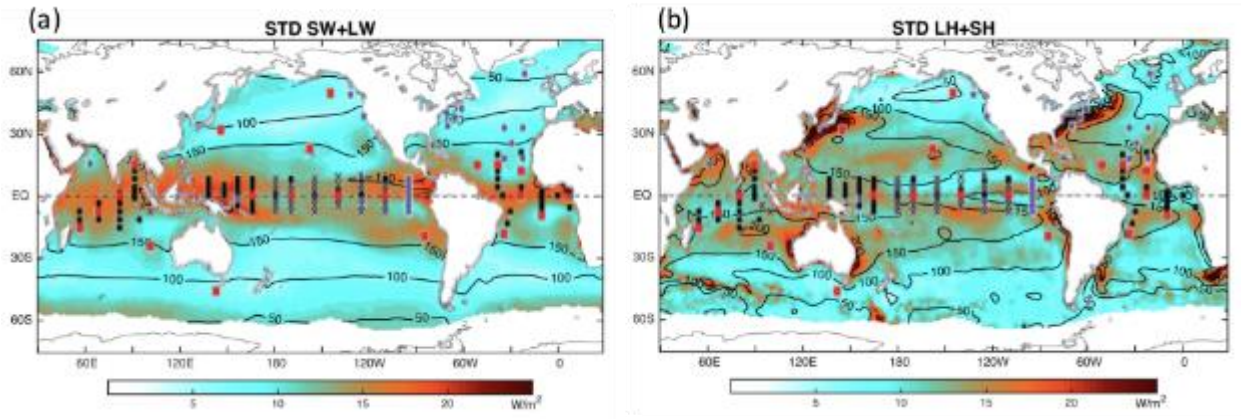

Figure 16.3 STD of the means based on 14 products for (a) SW+LW and (b) LH+SH. Black contours denote the ensemble mean patterns. The location of the global moored surface buoys is superimposed, with red dots indicating flux reference moorings.

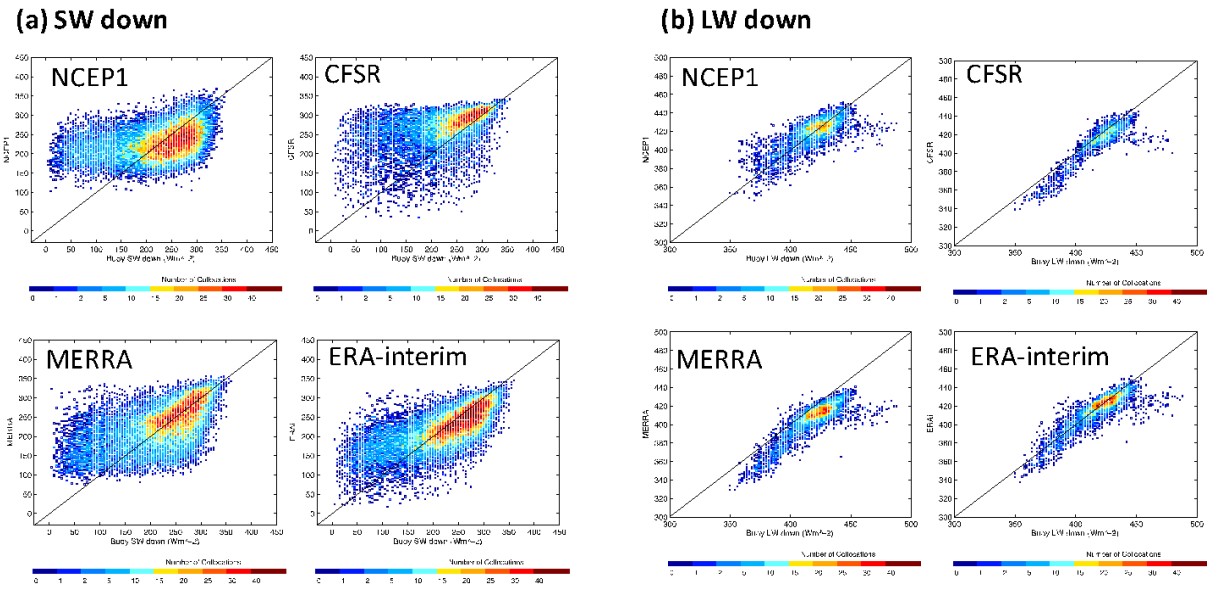

Figure 16.4 Scatter plots of daily-mean buoy versus reanalysis fluxes for (a) SW downward component and (b) LW downward component for four reanalysis products (NCEP1, CFSR, MERRA, and ERA-interim).

16.3 Air-sea flux EOVs for the Indian Ocean

Ocean-surface wind stress are a flux EOV. It has been recommended that turbulent latent and sensible heat fluxes be designated as flux EOVs. Given the lack of the energy and freshwater budget balance constraints at the ocean surface in the reanalysis systems, the improvement of the reanalysis products can best be made through improving model parameterizations of tropical convective clouds, as a first priority. Since improvements to the net heat and freshwater balance in the latest reanalyses is less than anticipated, the use of reanalyses products for flux estimates in the near future is not promising. One exception is the ERA-interim product, as its mean Qnet is more consistent with satellite-based products and buoys than other reanalyses. However, the time series of ERA-interim has spurious trends, induced by the injection of new SST datasets (e.g. Liang and Yu 2016).

Satellite products are promising candidates for gridded quality flux estimates into the future, except none of the surface heat flux components are directly retrieved from remote sensing. Surface radiation is computed from the radiation observed at the top of the atmosphere using an energy balanced and filled approach (Kato et al. 2013). Surface moisture and heat fluxes are computed from bulk flux parameterization using surface meteorological variables (SST, wind, near-surface air temperature and humidity). Retrieving near-surface air temperature and humidity from satellite scanners and sounders remains difficult (Jin et al. 2015) and the uncertainty in bulk flux algorithms is not negligible (Brunke et al. 2002). Thus, we need flux reference sites at the ocean surface to evaluate improvements and new developments for satellite retrieval algorithms and flux products. Long time series from moored buoys in general, both as part of the Global Tropical Moored Buoy Array (McPhaden et al, 2010) and the OceanSites program (Send et al, 2010), are also valuable as inputs to constrain atmospheric analyses and reanalyses.

16.4 Actionable Recommendations

Actionable recommendations on the current IndOOS design are given as follow:

i. Implement unoccupied flux reference sites in Arabian Sea and western Indian Ocean and maintain established flux reference sites in the revised RAMA-2.0 design (see McPhaden et al. white paper).

ii. Enhance a subset of the flux reference sites for direct flux measurements to validate bulk algorithm flux computations.

iii. Engage with the atmospheric reanalysis community to help evaluate and guide the future improvement of tropical convective parameterizations.

iv. Engage with the satellite surface radiation producers to help diagnose and validate surface radiative products

17. Contributions of IndOOS to improving ocean data assimilation

Tony Lee, NASA

17.1 Improving ocean state estimation as a driver for IndOOS

A suite of ocean data assimilation (ODA) systems has been developed in the past couple of decades to characterize ocean variability and understand the related processes, to evaluate observing system impacts, to initialize climate prediction, and to drive biogeochemistry models. One of the important drivers for IndOOS is to improve the ODA products to facilitate the aforementioned applications. Prior to the mid 2000s, ODA systems were primarily constrained by satellite-derived SST and SSH data as well as measurements from the sparse XBT network in the Indian Ocean sector. The lack of in-situ data has limited the evaluation of ODA products in terms of the representation of subsurface ocean structure, especially for currents and salinity, across various spatiotemporal scales.

The development of IndOOS since the mid 2000s, especially for RAMA and Argo, has significantly enhanced the constraint and evaluation ODA products in terms of subsurface ocean. For example, the assimilation of Argo salinity data in NOAA National Center for Environmental Prediction (NCEP) Global Ocean Data Assimilation System (GODAS) has significantly reduced the regional salinity biases in the GODAS product, including the thickness of barrier layer in the Indian Ocean (Huang et al. 2008) (Figure 17.1). Comparison of independent data also suggested associated improvements in zonal currents and SSH in the tropical Indian Ocean. IndOOS in-situ data have also been important to evaluating and improving the subsurface temperature and salinity structure, surface and subsurface currents, and SSH in the ODA system of the Indian National Centre for Ocean Information Services (INCOIS), which is enhanced from NCEP's GODAS system in collaboration with NCEP (Rahaman et al 2016).

In the past decade, there has been significant progress in the development and enhancement of ODA systems for operational oceanography, initialization of seasonal-to-interannual prediction, and analysis of seasonal-to-decadal variability of ocean circulation (cf. reviews articles by Dombrowsky et al. 2009, Lee et al. 2009, and Fujii et al. 2015). Much of the IndOOS observations from in-situ and satellite platforms provide backbone observational constraints of these system (https://www.godae-oceanview.org/science/ocean-forecasting-systems/assimilation-characteristics/). IndOOS data are not only fundamental to the evaluation and improvement of individual ODA systems, but essential to the assessment of the consistency and fidelity of various ODA systems. In particular, IndOOS is an integral element of the global ocean observing system that is used in various intercomparison and evaluation of a suite of ODA systems under the Ocean ReAnalysis Intercomparison Project (ORA-IP) (Balmaseda et al. 2015). As an extension of the ORA-IP effort, a set of multi-decadal ODA products have been collected and put on a common grid to facilitate the intercomparison under a NASA-sponsored project Collaborative REAnalysis Technical Environment (CREATE) (https://esgf.nccs.nasa.gov/projects/create-ip/data_description#OceanRe). Comparison of these products shows that there is a generally better consistency among these products since the mid 2000s (i.e., since the development of Argo and RAMA) than the previous decades (see example in Figure 17.2).

17.2 Future observational needs

Despite the encouraging improvements brought by IndOOS observations, there remain significant discrepancies between ODA products and observations as well as among different ODA products. These arise from limitations in forward ocean models (including errors in model physics and forcing) as well as in data assimilation. Improving ocean models, surface forcing (for momentum, heat, and freshwater fluxes), and data assimilation is a longer-term effort than the relatively short development time of IndOOS. For testing the impacts of ODA on initializing seasonal-to-interannual prediction, the observational records need to cover many realizations of interannual events such

as IOD. Moreover, observational records for the Indian Ocean, especially from the Argo and RAMA arrays, are too short to evaluate ODA products on multi-decadal time scales. Therefore, sustaining measurements from IndOOS is imperative for future improvements of ODA systems.

Enhancement of IndOOS is also necessary. For example, the roles of the deep ocean below 2000 m (the maximum profiling depth of the current Argo array) may become important at the longer time scales. Deep-ocean (> 2000 m) structure and changes in ODA products are not well constrained, thereby prompting for the enhancement by deep Argo. Other areas where IndOOS need to be enhanced include the coverage of coastal regions that are not sampled or not well sampled by Argo and RAMA. Continuity and enhancement of satellite measurements as addressed in Chapter IR 1 are also important to improving ODA products. Examples include (1) the continuity and enhancement of temporal sampling of wind stress measurements from satellites to capture the diurnal cycle, and (2) the continuity, enhancement of spatial resolution, and improvement of data quality for satellite SSS, which is especially important for the Indian Ocean due to the very dynamic variability of SSS across various spatiotemporal scales.

The observations of the Indonesian throughflow (ITF) is of particular importance to the Indian Ocean. There is no current observing system that can monitor the ITF adequately. The data from the IX1 XBT line allows estimate of the geostrophic transport of the ITF relative to 750 m (e.g. Wijffels et al. 2008). Effect of salinity on the geostrophic transport was inferred from only a climatological temperature-salinity relation as opposed to be based on direct measurement of salinity. Moreover, transport deeper than 750 m is not accounted for. ODA products have significant discrepancies in representing the ITF (e.g., Lee et al. 2010). This has ramifications to the representation of the state of the Indian Ocean as well as heat and freshwater exchanges between the Pacific and Indian Oceans. Development of a sustained observing system for the ITF is thus an important aspect that needs to be considered between IndOOS and the Tropical Pacific Observing System (TPOS).

Most ODA systems do not assimilate surface meteorology measurements from IndOOS. Efforts of coupled ocean-atmosphere data assimilation are emerging (e.g., Saha et al. 2010, Penny et al. 2017). Measurements of the coupled ocean-atmosphere boundary layers can provide effective constraints on such coupled assimilation systems. Therefore, enhancement of these measurements will be more important for the future generation of coupled assimilation systems.

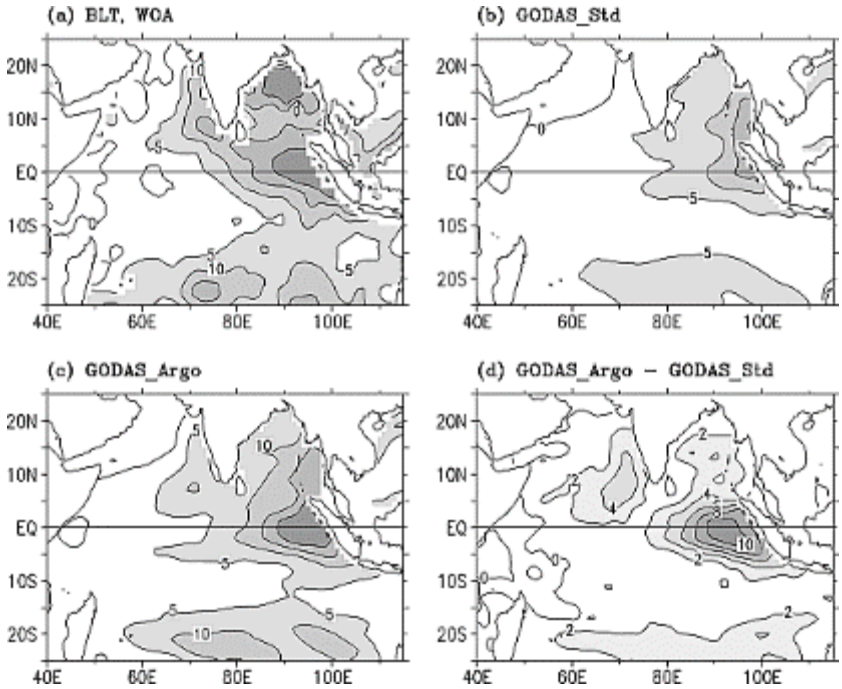

Figure 17.1. Barrier-layer thickness inferred from observations from the World Ocean Atlas (WOA) data (a), GODAS standard assimilation without using Argo data (b), GODAS assimilation with Argo data (c), and the difference between (c) and (b) (d). After Huang et al. 2008).

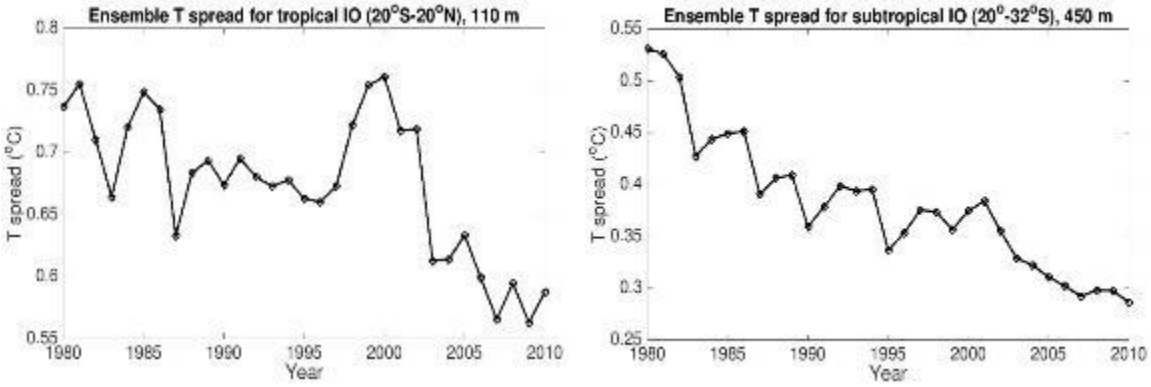

Figure 17.2. Ensemble spread of subsurface temperature near the thermocline in the tropical (a) and subtropical Indian Ocean (b) among eight multi-decadal ocean state estimation products. The consistency (as indicated by smaller spread) is significantly better since the mid 2000s after the development of the Argo and RAMA arrays.

Part III: IndOOS Component Review

18. Past, present & future satellites in support of IndOOS

Tony Lee, NASA

18.1 Past and current contributions of satellites to Indian Ocean research

Satellites have been an integral component of the IndOOS. Oceanographic satellite missions have been providing measurements for a suite of oceanographic variables such as sea surface temperature (SST) and height (SSH), significant wave height (SWH), ocean mass, variables related to ocean color (e.g., chlorophyll concentration), and in the past several years, sea surface salinity (SSS). In addition, satellites also provide measurements of surface meteorology variables such as ocean surface wind speed and wind stress, precipitation, outgoing longwave radiation (OLR), and surface radiation. Combinations of satellite measurements also provide estimates of ocean surface currents and surface turbulent heat fluxes (cf. Chapter OD 2 for further discussion of surface fluxes). Even before the major elements of the in-situ component of IndOOS were developed in the 2000s, ocean observing satellites have been providing routine measurements of some oceanic variables. Examples include SST from Advanced Very High Resolution Radiometers (AVHRRs) since the early 1981 and SSH anomalies from TOPEX/Poseidon (1992-2006).

Satellites present advantages in observing the Indian Ocean in many aspects. They have overall more uniform spatiotemporal sampling than *in-situ* systems to capture oceanographic features. The extensive spatial sampling of satellite observations enables the calculation of spatial derivative fields that are important for the study of ocean and atmospheric circulation and air-sea interaction. Such derivative fields include SST and SSS gradients, surface geostrophic currents (from horizontal gradients of SSH), and the ocean surface wind stress curl and divergence. Satellite data help capture spatiotemporal variations at scales not resolved or inadequately captured by in-situ data. Even though some satellite measurements of the ocean adjacent to land are contaminated by land signals, satellites in general provide more useful measurements in coastal oceans and marginal seas than those obtained from in-situ platforms. The more extensive (often global) coverage of satellites facilitates studies of large-scale teleconnections and impacts over and beyond the Indian Ocean.

Satellite observations are complementary to in-situ observations in the Indian Ocean (e.g., from RAMA moorings, Argo array, XBT, and shipboard CTD). Satellite altimetry data (and in some cases together with gravimetry data) in combination with Argo observations since the mid 2000s have enabled a comprehensive study of sea level and the relative contributions of thermosteric, halosteric, and mass contributions, including those for the Indian Ocean (e.g., Fukumori and Wang 2013, Llovel and Lee 2015). Satellites and mooring data together have greatly facilitated the studies of upper-ocean processes such as mixed-layer heat balance (e.g., Foltz et al. 2010) and the dynamics of equatorial Indian Ocean currents (e.g., Nagura and McPhaden 2012).

On the other hand, in-situ data help interpret surface observations from satellites by providing information about vertical structure below the sea surface (e.g., Llovel and Lee 2015). In-situ data also provide independent measurements that are critical to the calibration and validation of many satellite measurements (e.g., Ebuchi et al. 2012, Lee 2016). High-frequency measurements of some in-situ data (e.g., mooring measurements) help de-alias signals that are not adequately sampled by satellites such as diurnal variability (e.g., Gille et al. 2003). Sustained in-situ measurements are critical to the inter-calibration of an observed variable from different satellite missions (e.g., Wentz et al. 2017).

Satellite observations have provided fundamental contributions to Indian Ocean research. A comprehensive review of the huge body of related literature is not possible within this manuscript. The following simply provides a brief summary on various time scales. On intraseasonal time scales, various satellite observations (e.g., SSH, winds, surface currents, SST, SSS, and ocean color) have been used to study the nature of intraseasonal variations of the Indian Ocean in relation

to Kelvin and Rossby waves, basin mode (resonance), wind-thermocline-SST coupling, the response to MJO, and effects of mesoscale eddies (e.g., Han et al. 2001, Han 2005, Fu 2007, Zhou and Murtugudde 2010, Nagura and McPhaden 2012, Grunseich et al. 2013, Gaube et a. 2013, Suresh et al. 2013; Girish Kumar et al. 2013, Guan et al. 2014). In particular, microwave measurements from satellites, not affected by clouds, allow studies of sea surface properties such as SST and SSS under convective regions. On seasonal time scales, satellite data have been used to understand the dynamics of seasonal SSH in the Indian Ocean, in particular, the roles of Rossby waves driven by winds and radiated from the eastern boundary (e.g., Fu and Smith 1996, Eigenheer and Quadfasel 2000, Yang et al. 2001, Wang et al. 2001, Brandt 2002), and the different signatures of annual Rossby waves from SSH and SSS (Menezes et al. 2014). On interannual time scales, satellite data revealed the variations associated with Indian Ocean Zonal/Dipole Mode (IOZDM) and the basin-scale warming in the Indian Ocean associated with the 1997-98 El Nino (e.g., Yu and Reinecker 1999, Webster et al. 1999), the interpretation of IOZDM in terms of Recharge Oscillator theory (McPhaden and Nagura 2014), and the relationships of the IOZDM with variations in the southern tropical Indian Ocean (Rao et al. 2002, Han and Webster 2002, Xie et al. 2002, Rao and Behera 2005). On decadal time scales, satellite observations illustrated the relationships of SSH changes with local and remote forcings, the extent of regional association with decadal variability of the Pacific sector, and the inference of changes of the shallow meridional overturning circulations (e.g., Lee 2004, Lee and McPhaden 2008, Llovel and Lee 2015, Wang et al. 2015, Srinivasu et al., 2017).

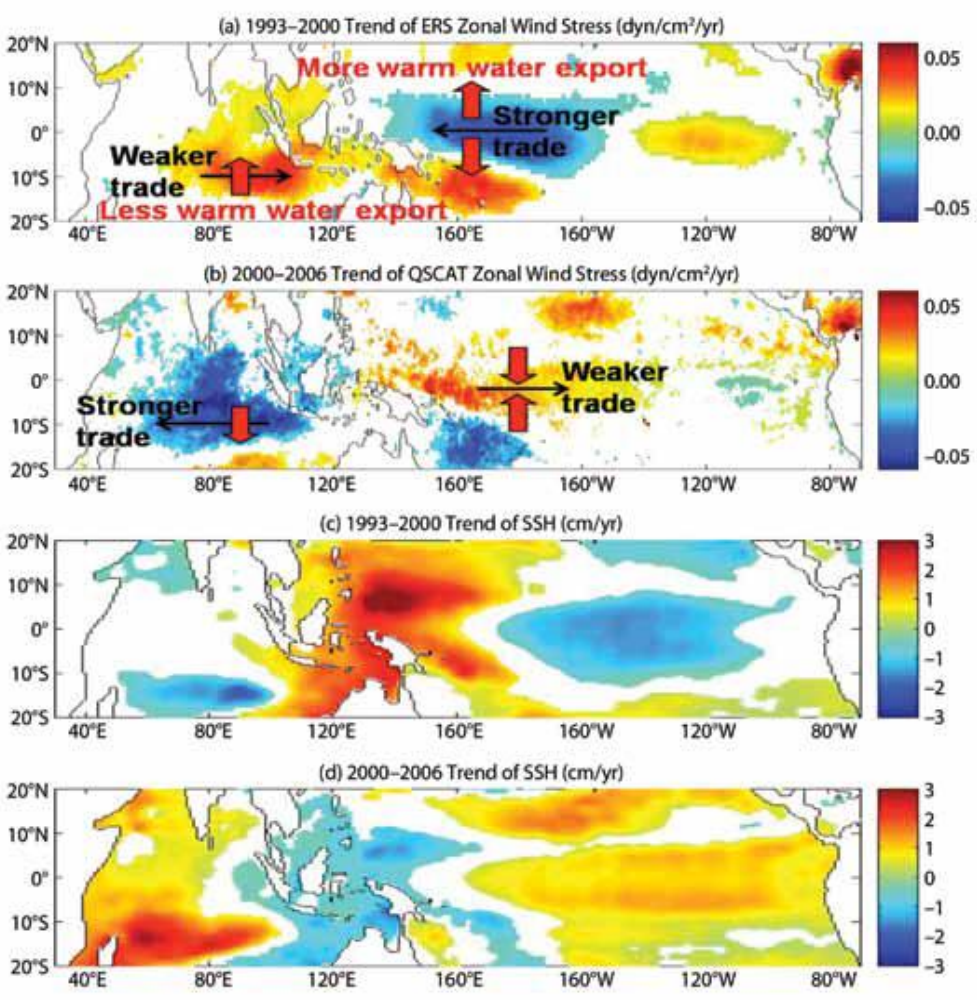

Figure 18.1 Trends of zonal wind stress during 1993-2000 estimated from ERS scatteromer data (a) and those during 2000-2006 estimated from QuikScat scatterometer data. SSH trends for the

1993-2000 (a) and 2000-2006 (b) periods estimated from altimeter data. These observations were also used to infer changes in the upper and lower branches of the shallow overturning circulations in the Pacific and Indian Oceans and their linkages as described in Indo-Pacific linkage subsection. After Lee et al. (2010). Adapted from Lee and McPhaden (2008).

18.2 Enhancement of satellite observing capability for the future IndOOS

Despite the significant contributions of satellite observations to Indian Ocean research in the past few decades, there are several areas where improvements are required in order to further advance our knowledge of ocean dynamics and air-sea interaction in the Indian Ocean sector as well as biogeochemical impacts. Of particular importance is the enhancement for spatiotemporal sampling. The need to enhance spatiotemporal sampling is particularly important for the Bay of Bengal where mesoscale and sub-mesoscale variability is abundant, which is believed to be important to the horizontal dispersal of freshwater as well as vertical mixing of heat and nutrients (e.g., Ramachandran et al. 2017). The Surface Water Ocean Topography (SWOT) satellite, scheduled to be launched in 2021, is expected to provide critical observational resources to study these sub-mesoscale processes. This will complement other Ka-band SAR altimeter missions that have capability to monitor sub-mesocale SSH (e.g., CryoSat-2, Altika, Sentinel-3, and Jason-CS/Sentinel-6). The BoB is also associated with narrow coastal freshwater plumes caused by river discharge and ocean dynamics that have significant implications to biogeochemistry and cyclone genesis. The currently ~40-km resolution of the satellite SSS from SMOS and SMAP (Reul et al. 2013, Fore et al. 2016) is marginal to study these features. Future enhancement of the spatial resolution of satellite SSS and improvement of accuracy are necessary to enhance the capability to monitor these plumes, the interaction between the Bay of Bengal and the Arabian Sea, and effects on biogeochemistry and cyclone genesis.

Enhancement of the temporal sampling of satellite-derived wind and wind stress measurements is important for the Indian Ocean, especially in the equatorial Indian Ocean and near the Maritime Continent where diurnal variability is strong. Currently, there are only two continuity series of satellite scatterometers: the MetOp series by the European Space Agency (ESA) and EUMETSAT and the Oceansat series by the Indian Space Research Organization (ISRO). Two scatterometers only have an approximately 60% coverage of the ocean at the 6-hourly interval, the de-correlation time scale of the diurnal cycle. Wind measurements from additional scatterometers and passive microwave radiometers can improve the sampling of diurnal variability to minimize the aliasing of diurnal variations into lower frequencies. In addition to wind and wind stress, continuity and enhancement of other surface meteorology variables such as OLR, surface radiation, and precipitation are important to further advancement of IndOOS research.

In addition to the need for enhancing spatiotemporal sampling, the continuity of satellite observations of Essential Ocean Variables (EOVs) is essential for the future IndOOS. SSH measurements from nadir altimetry missions are reasonably ensured to 2030 and beyond. There are also operational commitment for IR SST and various missions planned for ocean color measurements in the foreseeable future. However, the equatorial Indian Ocean and southern subtropical Indian Ocean are associated with strong atmospheric convection (e.g., associated with MJO and the Southern Indian Ocean convergence zone). Passive microwave (PMW) SST retrievals are not influenced by clouds like IR SST. The continuity PMW SST, which is not currently ensured, is important for the Indian Ocean. The continuity of satellite missions for SSS is also an issue. The Indian Ocean has the most dynamic variability of SSS among major oceans in the world. In-situ measurements have limited coverage in coastal regions (that are key to the linkage with terrestrial water cycle) and generally sparse sampling in the open ocean. Sustaining satellite SSS measurements is thus necessary to further the understanding of the dynamics of the Indian Ocean and its linkages with climate variability and regional terrestrial water cycle. Remote sensing technologies for direct measurements of ocean surface currents are also being developed, which may further enhance IndOOS research in the future.

19. Argo Profiling floats in the Indian Ocean

M. Ravichandran[1], T V S Udaya Bhaskar[2], and Nick. J. Hardman-Mountford[3]
[1]*National centre for Antarctic and Ocean Research (NCAOR), Goa, India*
[2]*Indian National Centre for Ocean Information Services (INCOIS), Hyderabad, India*
[3]*CSIRO Oceans and Atmosphere, Indian Ocean Marine Research Centre, Crawley, Western Australia, Australia*

Abstract

Argo is a global array of profiling floats to measure temperature and salinity of the upper 2000 m of the Ocean, once in 10 days. This document provides the present status of Argo floats and its typical applications, both operational and scientific, in the Indian Ocean. Also presented is an update on future directions of Argo in the Indian Ocean, such as the implementation of a Deep Argo array to map the heat and mass below 2000 m, enhancement of floats with biogeochemical and bio-optical sensors to understand biogeochemical processes (contributing to plans for Global Biogeochemical Argo) and enhancing the number of floats in the equatorial Indian Ocean to fully capture the intraseasonal to interannual variability. Recommendations are made on the need for observing system (OSE) and observing system simulation experiments (OSSE) to define requirements for the optimum number of floats and other *in-situ* observational components in the Indian Ocean.

19.1 Introduction

Ocean and climate have a symbiotic connection through the complex processes of heat and mass transfer that are still not well understood. The international oceanographic community recognized the imperative for enhancing ocean predictability and the requirement for well-designed and sustained operational ocean observations to enable this. Under a unique, internationally coordinated effort, it was envisaged to establish a global array of about 3000 floats to map the heat and mass of the global ocean. Hence, the Argo programme was realized. The Argo programme is an element of the *in-situ* observing system and an important component of the Global Ocean Observing System (GOOS), designed to continuously measure temperature and salinity of the upper 2000 m of the ice-free ocean once every 10 days (Riser et al, 2016). Temperature and salinity are both essential ocean variables (EOV) and essential climate variables (ECV) of GOOS and the Global Climate Observing System (GCOS). Once deployed, Argo floats descend to a parking depth of 1000 m, drift at that depth for nearly 9 days and then descend again to a profiling depth of 2000 m. From 2000 m, the float acquires temperature and salinity data while ascending, at predetermined depths (pressures) up to the ocean surface. Once it reaches the surface, it transmits the data to a ground station via satellite for real-time availability. Both ARGOS and Iridium satellites are used for communication, however, Iridium provides much higher data transmission capability than ARGOS, allowing greater vertical sampling resolution and two-way communication. Argo data are made available by the National Argo Data Assembly Centers to the global community on the global telecommunication system (GTS) to enable its use for operational forecasts, within 24 hours of collection. Fully quality-controlled data sets are also made available by the Regional Argo Data Centers to the Global Community within 6 months. The regional Argo Data Center for the Indian Ocean is maintained at INCOIS (http://www.incois.gov.in/argo/ARDCenter.jsp), making available a range of derived Argo products, such as objectively analyzed data for the Indian Ocean, present status of floats, yearly float deployments and profiles, age of floats, etc. The Global Data Centers archive the global data sets at http://www.coriolis.eu.org/Observing-the-Ocean/ARGO or http://www.usgodae.org/argo/argo.html. Many operational centers (http://www.argo.ucsd.edu/Use_by_Operational.html) use Argo data to provide real time ocean analysis and also forecasting the state of ocean for the different regions and Global Ocean.

19.2 Present status of Argo floats in the Indian Ocean

To meet the Global Argo design requirement of one float per 3° x 3°deg, the Indian ocean requires 450 floats north of 40° S. Presently, 576 active floats are providing temperature and salinity data from the surface to 2000 m (Fig. 19.1). Over and above, 48 floats are Biogeochemical-Argo floats, which provide dissolved oxygen (DO), chlorophyll fluorescence, backscattering of light by particles (as a measure of particle distributions) light attenuation and in some cases nitrate concentration and pH, as well as the standard measurements of temperature and salinity. Deployment of Argo floats with Oxygen alone sensor started in 2008 and with chlorophyll fluorescence, backscattering and other started since 2012. Although the target number of core Argo floats (floats with only CTD) has been achieved in the Indian ocean, there are gaps, especially in the central Indian ocean, northern Bay of Bengal (BoB), Andaman Sea, etc, while other regions are over-sampled with respect to the Global Argo design requirement, such as Arabian Sea, central BoB, etc. Most of the floats in the BoB provide 5 days temporal resolution (to capture the intra seasonal variations), whereas standard Argo floats are deployed with 10 days temporal resolution.

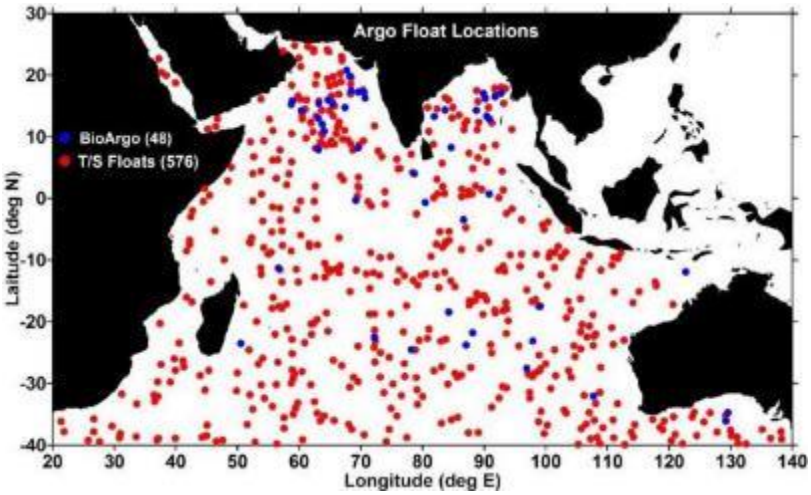

Figure 19.1. Present status of Argo profiling floats in the Indian Ocean. Red color dots indicate core Argo, provides temperature and salinity, and blue color indicate locations of Bio-Argo.

The growth of Argo array in the Indian ocean is shown in Fig. 19.2. Since 2008, full coverage has been achieved for the Indian ocean with more than 450 floats and more than 600 floats sustained for the past 8 years. Australia, China, France, Germany, India, Japan, Korea, U.K, and U.S has contributed to the growth of Argo both in terms of ship time for deployments and instruments. Though availability of ship time for the Arabian was a problem earlier due to piracy issue, now there more ship is operating in that area and hence there is no problem in deploying floats in the North Indian Ocean. However, there are less opportunity to deploy floats in the Southern Indian ocean. Argo Information Center and Regional Argo data center are coordinating the ships of opportunity to deploy floats in the Indian Ocean. Also, RAMA cruises provide opportunities for Argo deployments, which could be mentioned as a synergetic interaction in the implementation of these two IndOOS programs.

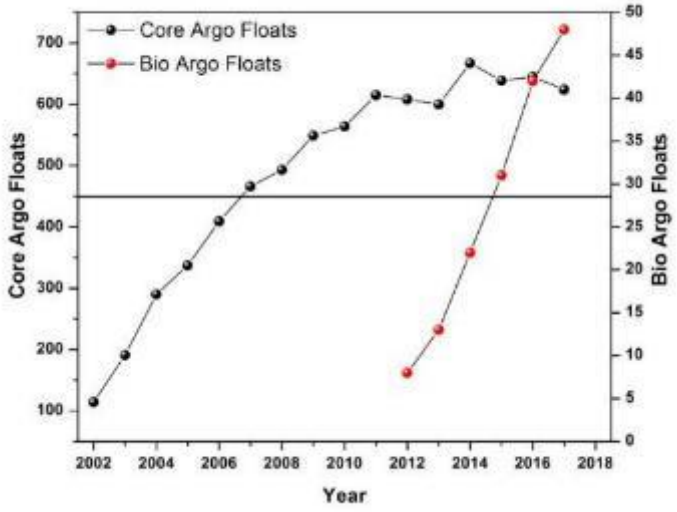

Figure 19.2: Growth of active Argo profiling floats in the Indian Ocean. Horizontal line indicates the 450 floats mark indicating full coverage of core Argo floats in the Indian Ocean.(note different axes for core and bioArgo floats)

19.3 Argo applications

Though Argo float deployments commenced in 1999, the build-up of an Argo array in the Indian Ocean began in 2001. Data from these floats, together with satellite remote sensing and other *in-situ* observations, are enhancing the understanding of the ocean circulation pattern and its influence on the global climate variability. Argo has revealed the local balances of evaporation minus precipitation in the salinity structure of the upper ocean (Durack et. al 2012, Helm et. al 2010, Hosoda et. al 2009), as well as longer term changes in temperature/salinity characteristics of subsurface water masses brought about by climate change (Zhang et. al 2008, Downes et. al 2009). Furthermore, these data sets are contributing to improving prediction skill for seasonal climate variability. Presently, many operational centers are assimilating these data for seasonal prediction of the monsoon, El Niño, Indian Ocean Dipole (IOD), etc.

Although these observations are envisaged for studying seasonal to climate time scale phenomena, many new insights have been gained, utilizing these data by many investigators. Detailed publication lists are available at http://www.argo.ucsd.edu/Bibliography.html. Assimilation of subsurface temperature and salinity profiles from Argo in the Indian Ocean has been initiated to understand the impact of Argo floats in simulating temperature and salinity (Oke and Schiller, 2007, Agarwal et. al 2008, Schiller et al 2008, Oke et al 2008, Krishnamurti etal, 2007, Huang et.al, 2008, Siva Reddy et al, 2017). The assimilation of Argo data has revealed that the subsurface ocean temperatures carry signatures on the passage of the intraseasonal waves (Krishnamurti et.al, 2007) and the inclusion of subsurface Argo data can be useful for prediction of the intraseasonal waves in the atmosphere/oceans. On the technology front, Riser et. al, (2008) demonstrated float-based three hourly measurements of wind speed and rainfall in the Bay of Bengal and Ravichandran et al (2012) demonstrated the importance and usefulness of Bio-Argo deployed in the Arabian Sea.

Yet, Argo floats cannot satisfy all the requirements of a comprehensive ocean observing system, although this technology is a major step forward to enable the first regular sampling of the global ocean on broad spatial scales, thus making possible a comprehensive observing system. Considering the mature technology of profiling floats, the bio-geochemical and bio-optical community has begun to benefit from the increase in observational capacities by integrating key bio-optical, bio-geochemical and ecosystem sensors such as chlorophyll-a, dissolved oxygen,

optical back scattering or attenuation coefficients - proxies of particulate organic Carbon - colored dissolved organic matter, pH, nitrate, etc., enabling the emergence of Biogeochemical-Argo (BGC- or Bio-Argo) floats.

19.4 Future directions

The core Argo has been implemented and sustained in the Indian Ocean since 2008 and it is imperative to have more observations in the Indian Ocean, in terms of spatial, vertical, temporal resolution of data and also incorporating biogeochemical sensors in the Argo floats to capture many missing ecosystem and climate links. These can be achieved by deploying deep ocean Argo floats, Bio-Argo floats, and twice the number of floats in the equatorial Indian Ocean.

19.4.1 Deep Ocean Argo

The Argo array provides temperature and salinity of the upper ocean upto 2000 m, which is half of the total ocean volume. The need for deep ocean observations has been recognized since the upper ocean warming has shown uncertainties in the Ocean's role in the Earth's energy budget and transient climate sensitivity. Also, the information below 2000 m significantly contributes to both heat content and sea level (Zilberman et. al 2017). Deep Argo floats profile down to 4000/6000 m, providing temperature and salinity information to understand the deep ocean thermohaline changes and its circulation, which enables the closure of global budgets of heat content, freshwater, and steric sea level.

Many countries have already deployed Deep Argo floats in the global ocean, as a pilot study to demonstrate the technical capability of floats and scientific value of the data. In the western Indian Ocean, 2 Deep NINJA floats were deployed by JAMSTEC, Japan in early 2016. These floats profile down to 4000 m with 10-30 days cycles. In the South Australian Basin, 8 Deep SOLO floats and 1 Deep APEX float were deployed in October 2016 by Scripps Institution of Oceanography. Deep SOLO floats are presently cycling to or near the ocean bottom every 10 days. The Deep APEX float is cycling every 5 days down to 5200 m. JAMSTEC plans to deploy 1 more Deep NINJA float in the eastern Indian Ocean in November 2017, and 2 Deep Apex with dissolved oxygen in the South Australian Basin in December 2017. More efforts are required to deploy deep Argo in the Indian Ocean to observe the thermohaline changes below 2000 m. The global Argo design is to have one deep Argo float per 5° lat x 5° long, and hence the Indian Ocean requires at least 250 floats north of 40° S. However, in the coming years, it is important to deploy at least one float in each key region of the Arabian Sea, BoB, eastern equatorial Indian Ocean, western equatorial Indian ocean, themocline ridge region and at least four floats in the southern Indian Ocean.

19.4.2 Enhancement of Bio-Argo

Bio-Argo or Biogeochemical Argo is the extension of the Argo array by augmenting additional biogeochemical sensors such as dissolved oxygen – to understand marine photosynthesis and respiration, and exchange with atmosphere; chlorophyll fluorescence –a proxy of phytoplankton biomass; nitrate – for understanding new production, and particulate backscattering – as a proxy for particulate carbon. Additionally, pH, CDOM, PAR, irradiance and transmissometry are important for many biogeochemical studies, mainly to address six major scientific questions related to carbon uptake, OMZs and nitrate cycling, acidification, the biological carbon pump, and phytoplankton communities (see http://Biogeochemical-argo.org). Despite limited data from Bio-Argo floats deployed in the Indian Ocean, some insightful studies have been published: e.g. on oxycline depth in the Arabian Sea OMZ (Prakash et al. 2012), chlorophyll distributions in eddies (Dufois et al. 2017) and chlorophyll variability in the southeastern Arabian Sea (Ravichandran et al 2012). A Global Biogeochemical Argo group has been established and initial designs indicate a need for 1000 floats globally. To meet this global design, the Indian Ocean requires at least 200 Biogeochemical floats. Presently, the Australia-India joint Indian Ocean Bio-Argo project brings

together Indian Ocean researchers interested in Biogeochemical Argo observations. Most of the active floats (48) are mainly integrated with sensors to measure oxygen, chlorophyll and particle backscattering at 700 nm. It is imperative to increase the number of Bio-Argo floats to answer the above six critical scientific challenges in the Indian Ocean, especially in the North Indian Ocean and it is important to augment the array with other biogeochemical sensors. The specifications of the floats and its sensor is available at https://soccom.princeton.edu/content/float-specifications.

19.4.3 Enhancement of Equatorial floats

A successful Argo pilot deployment was carried out following the decline of TAO in 2013. 41 faster cycling (7 days) floats were deployed by US Argo along the Pacific equator in early 2014. These are providing an unprecedented view of intraseasonal (kelvin wave) propagation.

Using a decade long observations of temperature and salinity profiles, a new mapping of the upper ocean in the equatorial Pacific, double the spatial sampling, is reported by Gasparin et al (2015). Following Roemmich and Gilson's procedures, which were formulated for describing monthly large scale anomalies globally, Gasparin et al (2015) constructed anomaly fields at 5 day intervals utilizing improvements in the optimal interpolation that include more accurate representation of zonal and meridional scales and the noise-to-signal ratio, and by including the time domain. Argo is able to represent around 70-80% of the variance at intraseasonal time scales and more than 90% of the variance for the seasonal to long term variability in the Pacific Ocean (Gasparin et al, 2015).

From the above study, it is clear that even in the Indian Ocean it is essential to deploy double the number of floats within a few degrees of the equator (10° S to 10° N), with the objective of improving the resolution of intraseasonal to internannual variability – critical for observation of IOD, Monsoon, MJO, etc. It is worth mentioning here that Iridium floats need to be deployed in these regions, since these floats have a shorter surface time compared to ARGOS, and hence these floats will not drift away from equator.

19.5 Conclusion

Deployment of Argo profiling floats in the Indian Ocean was initiated in the year 2001 and matured in the year 2008. The array is sustained from 2008 until now. The data from these floats are utilized both for operational use (e.g. seasonal forecast) as well as to improve our understanding of oceanography and climate variability in the Indian Ocean sector. The use of this data has also revealed some new insights in the Indian Ocean which were not possible earlier due to lack of sufficient data mapping. About 576 core Argo floats and 48 Bio-Argo floats are active in the Indian Ocean. The spatial requirement of Argo floats was designed two decades ago and it is important to re-think now. Also, important to measure additional parameters (Oxygen, chlorophyll, pH, nitrate, light attenuation, etc.) to better understand biogeochemical processes, enhancement of floats in the equatorial Indian Ocean to fully capture the intraseaonal to interannual variabilities, and to map the heat and salt trapped below 2000 m. Accordingly, it is recommended to deploy more biogeochemical floats, double the number of floats in the equatorial Indian ocean and deployment of deep Argo in the Indian Ocean. It is important to conduct Observing System Experiment (OSE) and Observing system simulation experiment (OSSE) to evaluate the relative importance of existing observational components and future observational requirements, both spatial and temporal resolutions, similar to Schiller et al (2004) and Vecchi and Harrison (2007).

20. RAMA-2.0

M. J. McPhaden[1], M. Ravichandran[2], K. Ando[3], W. Yu[4], E. Schulz[5]

[1]NOAA/Pacific Marine Environmental Laboratory (PMEL), Seattle, WA
[2]Indian National Center for Ocean Information Service (INCOIS), Hyderabad, India
[3]Japan Agency for Marine-Earth Science and Technology (JAMSTEC), Yokosuka, Japan
[4]State Oceanic Administration (SOA)/First Institute of Oceanography (FIO), Qingdao, China
[5]Bureau of Meteorology, Melbourne, Australia

Abstract

We briefly summarize scientific progress enabled by RAMA—The Research Moored Array for African-Asian-Australian Monsoon Analysis and Prediction—as well as the current status of its implementation and the challenges involved in sustaining it. We also propose adjustments to the design of RAMA based on lessons learned over the past decade. These adjustments will result in a more robust and cost-effective array design for meeting the scientific objectives of CLIVAR and GOOS. Finally, a protocol is described for establishing new sites in the array to address scientific questions that have arisen since the array was originally designed.

20.1 Introduction

RAMA was first established 13 years ago in 2004 as the moored buoy component of the Indian Ocean Observing System (IndOOS; Masumoto et al, 2010). It is the Indian Ocean complement to the TAO/TRITON moored buoy array in the Pacific and the PIRATA moored buoy array in the Atlantic Ocean, which together comprise the Global Tropical Moored Buoy Array Program (McPhaden et al, 2010). There are four type of moorings in RAMA (Figure 20.1), namely standard ATLAS or ATLAS-equivalent surface moorings, more heavily instrumented surface moorings for comprehensive air-sea flux determination (Flux Reference Sites), Acoustic Doppler current profiler (ADCP) sites for direct measurement of velocity in the upper ocean, and three Deep Ocean sites along the equator equipped with current meters at selected depths down to 4000 m. All the surface moorings transmit data in real-time to shore for use in weather, ocean and climate forecasting.

Moorings have the advantage that they provide high-resolution time series in real-time of key oceanographic and surface meteorological variables for studies of ocean-atmosphere interactions and ocean dynamics. They are especially valuable in the tropics where there is a broad spectrum of energetic variations in both the ocean and the atmosphere across a wide range of time scales and where the ocean response to atmospheric forcing is very rapid. Moored arrays are thus a vital element in a balanced network of satellite and in situ platforms required to deliver essential ocean variables (EOVs) and essential climate variables (ECVs) as part of the Global Ocean Observing System (GOOS) and the Global Climate Observing System (GCOS).

RAMA has successfully enabled a number of scientific advances since inception and is a valuable source of data for ocean, weather and climate forecasting. New multi-national partnerships have been formed between institutions within and outside the Indian Ocean rim region to both build RAMA and to promote joint research and capacity building efforts. An open RAMA data policy and easy access to RAMA data (https://www.pmel.noaa.gov/gtmba/) has facilitated collaborations across national boundaries on key scientific questions concerning the Indian Ocean's role in climate. Some of these collaborations have been interdisciplinary in nature, involving studies of biogeochemistry and biophysical interactions unique to the Indian Ocean basin. An extensive and growing bibliography of RAMA-related refereed journal publications, with authorship spanning many nations, attests to the array's success (http://www.pmel.noaa.gov/tao/rama/ramapubs.html). As one measure of success, the original RAMA publication (McPhaden et al, 2009) has been cited 229 times through the end of October 2017. This document recommends evolving the RAMA array design based on lessons learned since its inception to make the array more robust, cost-effective, and operationally efficiency.

20.2 Current Implementation Challenges

The current RAMA design (Figure 20.1) consists of 46 moorings intended to sample key oceanographic and climate regimes around the basin. These regimes, and the need for sustained moored measurements in them, are described in McPhaden et al (2009). At present the array is 78% complete, thanks to the efforts of many institutions in countries committed to advancing Indian Ocean science. India, Indonesia, Japan, China, the United States, Australia, the 13 African nations that comprise the Agulhas and Somali Current Large Marine Ecosystem (ASCLME) program and the 8 Asian countries that comprise the Bay of Bengal Large Marine Ecosystem (BOBLME) program have all participated.

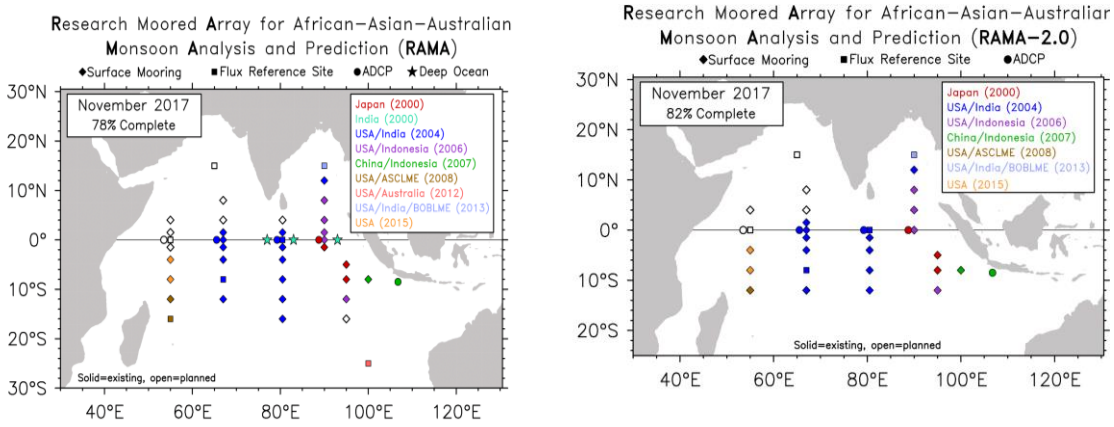

Figure 20.1 (left). Current status of RAMA. Sponsoring nations/programs are color coded by site in the legend, with the first year of engagement shown in parentheses. (right) Proposed configuration for RAMA-2.0.

There are a variety of challenges to fully implementing RAMA that need to be addressed. Piracy is a major reason why the array is not yet 100% complete after 13 years. Piracy has kept ships from freely working in the Arabian Sea for several years, preventing the establishment of sites in this key region. Fortunately, through naval interventions of many nations and the introduction of best practices for ship operations, piracy is now non-existent in the region. As an indictor of progress, in December 2015 Lloyds of London significantly reduced the so-called piracy "high risk area," where insurance premiums for merchant vessels were substantially higher (http://www.hellenicshippingnews.com/indian-oceans-piracy-risk-area-reduced-in-a-boost-for-shipping-firms/). Also, in early 2018, the NOAA Ship *Ron Brown* will venture into the Arabian Sea, occupying three sites there for the first time.

Another significant challenge to completing and sustaining the array is ship time. Surface moorings have a design lifetime of one year and require regular servicing from specialized vessels capable of deep sea mooring operations. Securing adequate ship time has been an ongoing challenge in RAMA. On average over 2014-16 for example, only 94 sea days per year were available to service U.S. cooperative sites maintained with PMEL equipment, well short of the estimated 145 sea days that were needed. Several sites have not been serviced in the past 3-4 years because of this lack of ship time as detailed in an earlier and more extended version of this document (McPhaden et al, 2016). Among these sites are two flux reference sites at 25°S, 100°E and 16°S, 55°E (Table 1).

A third significant challenge is fishing vandalism, which plagues all surface mooring programs in the tropics. Some RAMA sites, though regularly maintained, are characterized by very poor data return because of this problem. At such sites, mooring equipment is either heavily damaged or completely lost because of fishing interference. The most extreme example of this situation is the

mooring at 1.5°N, 80.5°E where data return for the past 12 years has been only ~50% and less than half of the 11 moorings deployed there have been recovered. This is the worst performing site maintained with PMEL equipment in the array. The site is relatively close to land, which is a major factor in the prevalence of fishing damage experienced by surface moorings. Vandalism has also increased at 1.5°N, 90°E and 1.5°S, 95°E possibly due to changes in fishing practices. In particular, there are indications that purse seine fishing has increased in the eastern Indian Ocean, for which gear conflict leads to more severe mooring damage than in the case of long line fishing.

The site at 4°N, 80.5°E is in the Sri Lankan EEZ and has never been occupied. Its Achilles heel is proximity to land and the likelihood of debilitating fishing vandalism. Arguably we might have anticipated this situation in the design phase of RAMA. However, the severity of now well documented damage over the past decade from fishing vandalism further south at 1.5°N, 80.5°E convinces us that this site in the Sri Lankan EEZ is not viable.

Some mooring sites have been terminated because of programmatic changes. For instance, maintenance of the deep sea mooring at 0°, 93°E by India's National Institute of Oceanography (NIO) ended in late 2014. There is no longer a mooring at this location and no future deployments are planned there. Final recoveries of the NIO equatorial deep ocean moorings at 77°E and 83°E were made in November/December 2016 and there is no plan to replace them.

Finally, budgetary issues are also a concern that must be addressed in RAMA. For example, PMEL's annual operating budgets have been flat for many years, which translates into decreased funding because of inflation. At the same time, PMEL is transitioning to a newer mooring system called T-Flex that will replace legacy ATLAS systems. T-Flex is more capable and will provide much higher data throughput in real-time, which will reduce the impact of mooring losses on the availability of high-resolution data (i.e., data sampled at 10 minute to hourly intervals). But it is also a costlier mooring system because it uses commercially available off-the-shelf (COTS) components almost exclusively.

20.3 A Sustainable Mooring Array

Given budget pressures, ship time limitations, heavy equipment losses at sites prone to fishing vandalism, and the reality that some sites have already been decommissioned in RAMA, we propose a modified array design that still meets most of the scientific objective described in McPhaden et al (2009), but with fewer moorings. This modified RAMA design (Figure 20.1), optimized for long-term viability and sustainability, contains 30 rather than 46 sites. Even with fewer moorings, key regions such as the equatorial waveguide, the Seychelles-Chagos Thermocline Ridge (SCTR), Bayof Bengal, Arabian Sea, and the eastern and western poles of the Indian Ocean Dipole are still well sampled. This modified array design, embedded in the full multi-platform IndOOS observing system, will allow us to concentrate efforts on maintaining sites that have produced good data, are logistically accessible, and still meet most of the original objectives of RAMA. The table below lists the mooring sites scheduled for decommissioning and the primary reason for it. In addition to these reasons, there are budgetary constraints as well that are an aggregate factor as well.

Mooring Site	Reason
1.5°N, 90°E	Vandalism
1.5°S, 90°E	Vandalism
16°S, 95°E	Ship Time
25°S, 100°E	Ship Time

4°N, 80.5°E	Vandalism
1.5°N, 80.5°E	Vandalism
16°S, 80.5°E	Ship Time
0°, 77°E	Program Termination
0°, 83°E	Program Termination
0°, 93°E	Program Termination
1.5°N, 55°E	Ship Time
1.5°S, 55°E	Ship Time
16°S, 55°E	Ship Time

Table 1. List of RAMA sites to be decommissioned and the primary reason for this action.

With fewer moorings in RAMA-2.0 overall, the total ship time requirement will be considerably lower than would be needed for the original RAMA design. With fewer mooring sites to occupy, we will also be able to accelerate the transition from the PMEL's legacy ATLAS system to the new more capable T-Flex mooring system. Considering all existing mooring sites in RAMA-2.0, we estimate the total ship time requirement to be about 160 days per year.

20.4 Potential New Sites

In addition to winnowing out RAMA sites that are either unsustainable or have already been decommissioned, we recognize there may be compelling reason to add sites based in new scientific insights that have been gained since the original design. One example of a possible addition that has been mentioned in discussions over the past few years is a Flux Reference site in the Timor Sea (14°S, 115°E). The Timor Sea exhibits the largest instraseasonal SST variability associated with the MJO in the tropical Indian Ocean. Air-sea interactions in this region affect tropical storm formation and rainfall variations across southern and eastern Australia. Improved description and understanding of air-sea interaction in this region would lead to a better understanding and ability to predict intraseasonal variations of the MJO and their remote impacts. The Timor Sea is a heavily fished region however, so feasibility of maintaining a surface mooring in the region needs to be demonstrated.

There are other examples of new sites that could be considered for inclusion in RAMA, so to accommodate evolving scientific priorities we propose a protocol for expansions that was devised by the Tropical Moored Buoy Implementation Panel (TIP), an Action Group of the Data Buoy Cooperation Panel, and that has been adopted successfully by PIRATA (Bourles et al, 2008). Parties interested in establishing a new site or sites formulate a proposal defining the scientific objectives, how they are consistent with the mission of array, how the sites would be funded, and how they would be maintained logistically (specifically with regard to ship time). These proposals are submitted to the CLIVAR/GOOS Indian Ocean Regional Panel (IORP) for review and approval. Approved expansions are given a three-year pilot phase to demonstrate feasibility, namely that the site can be continuously maintained, not suffer grievously from fishing vandalism, produce good data, and stimulate new scientific progress. At the end of the three years, the parties submit a report to the the IORP describing outcomes in relation to objectives. If deemed successful by the IORP, the expansion becomes a permanent part of the array. This proposal driven process ensures a scientifically sound approach to expansions and a committed constituency who will find the resources to establish and maintain new sites.

20.5 Conclusion

RAMA was established in 2004 through partnerships involving several nations with a commitment to advancing Indian Ocean science in support of monsoon research and forecasting. It has proven to be a highly successful venture in sustained ocean observing that has enabled many new scientific discoveries as well as contributing to capacity building in the region. However, after 13 years, the array is not yet complete and we have learned some practical lessons since 2004 that need to be incorporated into a redesign to make RAMA more cost-effective and sustainable, while still preserving its core functions and its value to the oceanographic and climate science communities. The proposed array configuration, dubbed RAMA-2.0, takes these lessons into account.

This document has focused primarily on the geographical dimensions of the RAMA network design. However, we recognize that moorings can be enhanced with wide variety of additional sensors for specialized studies. In particular, it is possible to add more temperature/salinity vertical resolution in the surface mixed layer, additional current meters, or other sensors for focused air-sea interaction studies at selected locations. It would also be valuable to introduce biogeochemical measurements into RAMA-2.0 as a contribution to the Second International Indian Ocean Expedition (IIOE-2) in collaboration with the Sustained Indian Ocean Biogeochemistry and Ecosystem Research (SIBER) program (Hood et al, 2015). This document can serve as a basis for discussions on how to move forward on a robust and sustainable integrated Indian Ocean observing system that addresses ocean, weather, climate, biogeochemistry, and ecosystem research imperatives for the next decade.

21. Surface Drifter Observations in the Indian Ocean

Rick Lumpkin[a1] and Luca Centurioni[b]

[a] NOAA/Atlantic Oceanographic and Meteorological Laboratory, Miami, FL, USA

[b] Scripps Institution of Oceanography, La Jolla, CA, USA

21.1 Overview

A satellite tracked Surface Velocity Program (SVP) drifter (hereafter "drifter") of NOAA's Global Drifter Program (GDP) is a Lagrangian instrument drogued to follow currents at a depth of 15m. The product between the cross-sectional area of the drogue and the drag coefficient is at least 40 times than that of the tether and surface float, in order to guarantee an accuracy of the 15 m depth mixed-layer currents better than 1 cm s^{-1} per 10 m s^{-1} wind (Niiler et al., 1995, 1987). There are many other drifter designs that have been exploited for various regional studies and operational purposes (for a recent review, see Lumpkin et al., 2016).

Drifters observe several key EOVs, principally surface currents and SST. Approximately half of the drifters additionally measure surface barometric pressure because of the large positive impact of the data in numerical weather prediction and for other applications including inverse barometer effect correction of satellite altimetry product and computation of several climate indexes (Centurioni et al., 2016). Less than 1% of the drifters measure upper ocean temperature (to a depth of 150m), surface wind velocity, SSS, and/or surface waves.

21.2 History

Overviews of the purpose and history of the GDP are given by Niiler (2001), Lumpkin and Pazos (2007), and Maximenko et al. (2014). Large-scale deployments of GDP drifters in the Indian Ocean (25ºE—125ºE, 30ºN—32ºS, excluding the region northeast of Indonesia and Malaysia) started in 1995. Fig. 21.1 shows a time series of the number of drifters in the Indian Ocean since that time, and also of the fraction of 5º×5º bins occupied by at least one drifter (the Global Ocean Observing System requirements for in-situ surface temperature and velocity measurements call for observations at 5º×5º resolution; Needler et al., 1999). Since 1996, around 60—80% of region is sampled; this has increased to 80—95% in the last three years thanks to several research initiatives sponsored by the US Office of Naval Research and partnerships associated with the basin-scale moored buoy array known as the Research Moored Array for African–Asian–Australian Monsoon Analysis and Prediction (RAMA) partnerships.

[1] Corresponding author e-mail: Rick.Lumpkin@noaa.gov

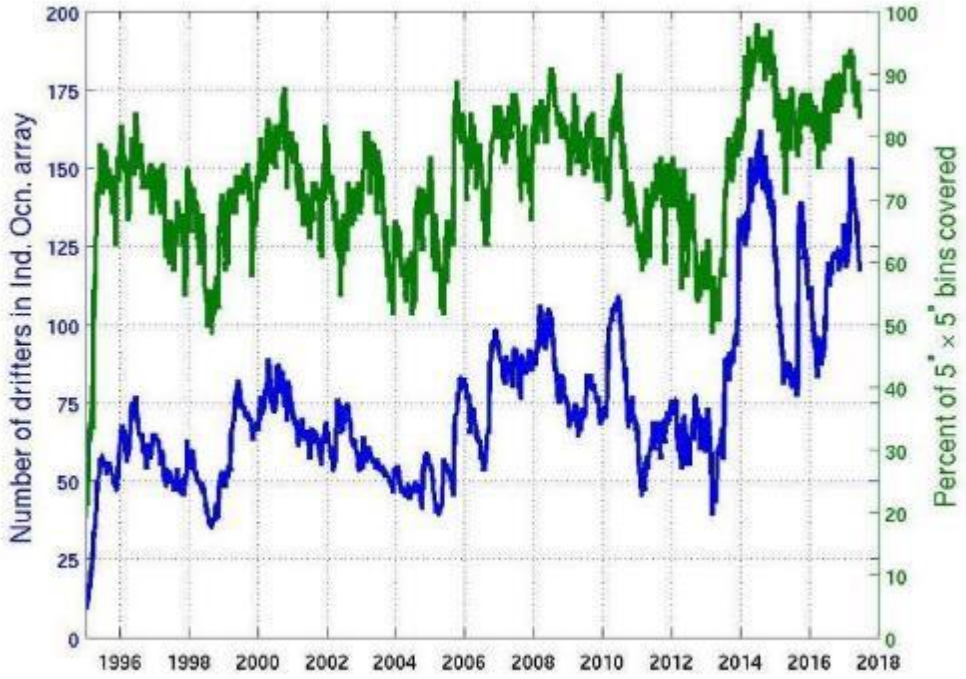

Fig. 21.1: number of GDP drifters in the Indian Ocean (blue) and percent of 5º×5º bins sampled by the drifters (green).

Of recent scientific interest was the deployment of 36 high-temporal-resolution (5 min) salinity drifters designed by the Lagrangian Drifter Laboratory (LDL) at the Scripps Institution of Oceanography (SIO) in the Bay of Bengal in September 2015, as a part of the ONR Air-Sea Interactions Regional Initiative (ASIRI) field campaign (Hormann et al., 2016). These drifters revealed salinity patches with anomalies of >1.5 psu in a field with spatial scales of <5 km and temporal scales of only a few hours (Hormann et al., 2016).

21.3 Current status

Fig. 21.2 shows the density of GDP observations in the historical database, in drifter days per square degree. As of this writing, over 90% of the 5º×5º bins are sampled by drifters. Historically undersampled regions include the eastern equatorial region, the central and northern Somali Current and Great Whirl, and the region between Australia and Indonesia. In order to achieve 100% coverage, deployment opportunities must be sustained in these regions. The Somali Current and Great Whirl are persistently under-sampled because drifters passing westward in the South Equatorial Current (SEC) north of Madagascar tend to run aground at the Mozambique/East Africa Coastal Current (EACC)-Somali Current bifurcation (i.e., the coasts of Mozambique and Tanzania). The Andaman Sea is also poorly sampled but drifters are likely to run aground rapidly in this shallow water region; other platforms are more appropriate to collect observations there.

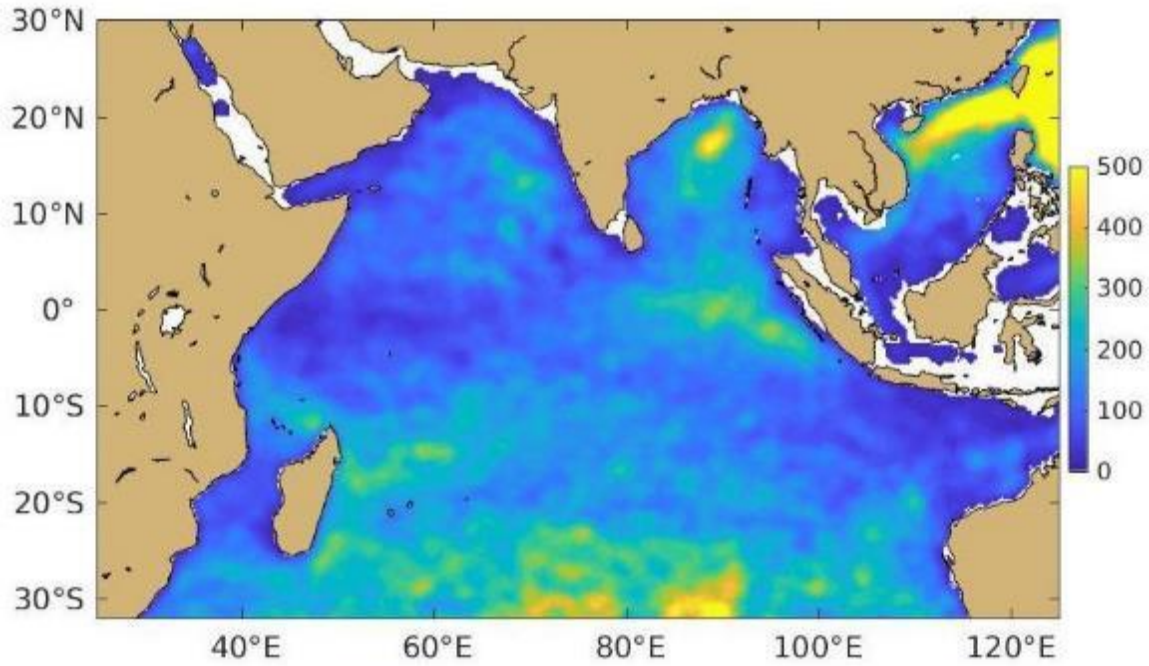

Fig. 21.2: density of drifter observations (drifter days per square degree) in the Indian Ocean, in the quality-controlled GDP database (observations through 30 June 2017).

A number of active partnerships are used to deploy drifters in the Indian Ocean. The Australian Bureau of Meteorology arranges the deployment of nearly 40 drifters equipped with barometers per year in the equatorial and South Indian Ocean. GO-SHIP lines such as I05, I06S and I07N are used in years that they are occupied. Through collaboration with NOAA/PMEL, drifters are deployed during RAMA mooring cruises originating from Indonesia, India, Korea, and other RAMA partners.. Because this cruise happens only one time per year, there is a strong desire to increase deployment efforts and increase collaboration with Indonesia. Through collaborations with the Kenyan Meteorological Agency, the US Naval Oceanographic Office, and the Royal Australian Navy, over 50 GDP NOAA and ONR funded drifters are currently being deployed each year in the western and northern Arabian Sea.

21.4 Data policy compliance

Drifter data are made available in near-real time and through ftp and web application services by the LDL, Collecte Localisation Satellites (CLS), and MeteoFrance on the Global Telecommunications System for operational purposes, and in delayed mode (approximately three months, after quality control and interpolation) at the GDP web page (www.aoml.noaa.gov/phod/dac) and (with an additional six months' delay) at the data archive at Canada's Marine Environmental Data Service (MEDS). Work is underway to archive the delayed mode data at NOAA's National Center for Environmental Information (NCEI) (real-time data is already archived there) and assign them a digital object identifier. The drifter data management plan is described in the OceanObs'09 Community White Paper "Data Management System for Drifting Buoys" (Keely et al., 2009).

21.5 GDP-Specific Recommendations for the IndOOS:

1. Deploy drifters in persistently undersampled regions such as the Somali Current, Great Whirl, and the region between Australia and Indonesia west of the Timor Sea.
2. Sustain the array via international partnerships coordinated through the Data Buoy Cooperation Panel.
3. Evaluate the GOOS/GCOS sampling requirements in light of the scales of motion in the basin. E.g., 5º×5º bins are very coarse compared to features such as the Wyrtki Jet, Somali Jet, and East India Coastal Current.
4. Evaluate the value of barometric pressure observations in this region for numerical weather forecasting efforts, in order to evaluate if 100% of the drifters should collect these observations.

22. XBT network

Ming Feng, CSIRO Ocean and Atmosphere, Perth, Western Australia, Australia

Janet Sprintall, Scripps Institution of Oceanography, La Jolla, California, USA

Rebecca Cowley, CSIRO Ocean and Atmosphere, Hobart, Tasmania, Australia

22.1 Background

The eXpendable BathyThermograph (XBT) network consists of transects across all ocean basins where XBTs are used to collect temperature observations of the upper 1 km of the ocean. The XBTs are deployed from research vessels and ships of opportunity program (SOOP). XBT lines combined with Argo floats are effective in cutting the upper ocean into regions where the net transport in or out of the region, and along with the estimates of the interior heat and freshwater storage and the surface fluxes, provide a method for understanding the role of ocean dynamics in climate variations (International CLIVAR Project Office, 2006). XBT transect data are important for model testing, ENSO prediction, tropical ocean variability and prediction, and heat content and climate change estimates (Smith et al, 2001). The repeat XBT transects also are effective for monitoring changes in specific ocean structures that affect Indian Ocean climate, such as the upwelling zones of Java, Somalia, the Lakshadweep Dome and the thermocline ridge near 10°S.

The XBT network in the Indian Ocean was originally established as individual research projects under TOGA (1985-1994) and WOCE (1990-1997). The network has been largely operated by national agencies from Australia, India, and the US. After the introduction of Argo, the XBT observations shifted from so called "broad-scale sampling" to "line sampling", and so became more focused on monitoring changes of the narrow boundary currents and ocean fronts, mesoscale variability, as well as maintaining across-basin transects to monitor and study meridional heat transport. There are two modes of XBT line sampling. XBTs can be deployed in High Resolution (HR) mode and so transects are carried out at least 4 times per year along near-exactly repeating transects, with XBTs typically deployed every 20 to 30 km to obtain high spatial resolution in one single realization to resolve the spatial structure of mesoscale eddies, fronts and currents. XBTs can also be deployed in Frequently Repeated (FR) mode sampling, with ~12 transects carried out per year and XBT deployments every 100 to 150 km so as to obtain reasonably high spatial resolution in consecutive realizations in regions where temporal variability is strong. An implementation plan for the XBT operations in the Indian Ocean was recommended (International CLIVAR Project Office, 2006) and more recently these transects were prioritized as part of the 2017 JCOMM SOT-9 panel. The main Indian Ocean transects are shown in Figure 22.1: FR transect IX01 line monitors the Indonesian Throughflow (ITF) and the Java/Sumatra upwelling zone and began sampling in 1983; FR IX22 samples through the Banda Sea Indonesia to the Northwest Australian shelf and began sampling in 1987; FR IX12 samples the thermocline ridge in the central Indian Ocean and the Arabian Sea boundary currents and began in 1983; FR IX14 crosses the Bay of Bengal; and HR IX15/IX21 together closes the southern limit of the subtropical Indian Ocean and began in 1994 (Table 22.1). Hence many of these XBT transects have been in operation for over 30 years.

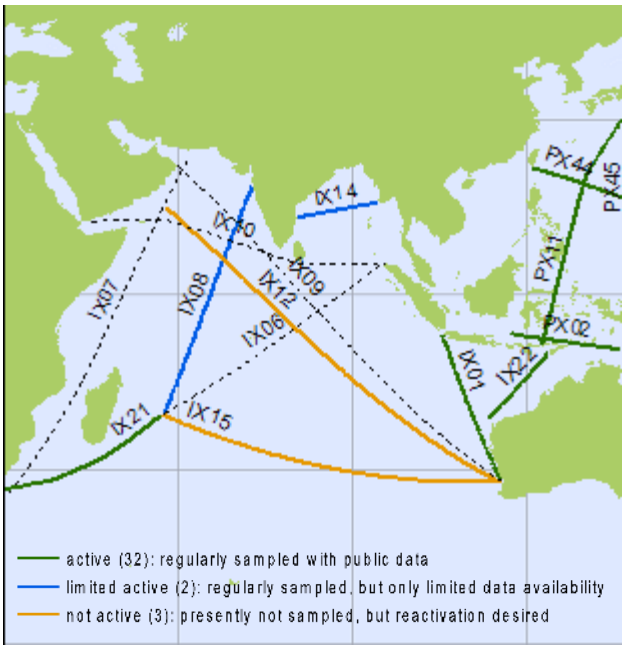

Figure 22.1: Implemented XBT lines in the Indian Ocean. Numbers in brackets refer to global totals.

Table 22.1. Summary of status and sampling strategy for XBT transects shown in Figure 1. FR: frequently repeated; HD: high density; LD: low density.

Line	**Status**	**Data years**	**Number of transects per year**	**Operator**
IX01	*Active*	*1983-present*	*FR and HD, >12*	*Australia*
IX06	*Ceased*	*Infrequent*	*-*	*USA*
IX07	*Ceased*	*Infrequent*	*-*	*France*
IX08	*Data unavailable*	*Unknown*	*-*	*India*
IX09	*Ceased*	*1990-1998*	*LD*	*-*
IX10	*Ceased*	*1990-1998*	*LD*	*-*
IX12	*Inactive*	*1986-2015*	*FR and HD, Up to 20*	*Australia*
IX14	*Data unavailable*	*Unknown*	*-*	*India*
IX15	*Inactive*	*1994-2013*	*HD, 4*	*USA*
IX21	*Active*	*1994-present*	*HD, 4*	*USA*
PX11/IX22	*Active*	*1986-present*	*FR, Up to 20*	*Australia*

As of 2017, transects IX01, IX08, IX14, IX21, and IX22 remain in operation. The vessels that sampled along IX12 went offline in 2015, but the XBT community is actively seeking a replacement vessel to continue this important time series. Transect IX15 is not currently operable due to a lack of shipping traffic along this route.

All XBT profile data from IX01, IX22, IX12, IX21 and IX15 are publicly available through NCEI (https://www.nodc.noaa.gov), as well as in transect mode from IMOS and SIO (imos.org.au;

http://www-hrx.ucsd.edu). Transect data along IX14 and IX08 are maintained by India and data along these transects is presently not publicly available.

22.2 What have we learnt from XBT observations in the Indian Ocean?

The XBT observations provided >50 % of the subsurface thermal structure and variations prior to the arrival of the Argo data stream in ~2003. As such, they played a crucial role in closing the global heat budget under the influence of anthropogenic global warming (e.g. Domingues et al., 2008). They have also played a significant role in improving our understanding the Indian Ocean response and feedback to the climate change hiatus period in the recent decades (Drijfhout et al., 2014; Dong and McPhaden 2016), as well as decadal variations in the Indian Ocean (Han et al., 2014).

The XBT network is at present the main element of the global observing system to provide systematically repeating observations to resolve the narrow swift boundary currents, including those boundary currents in the Indian Ocean as well as the Indonesian throughflow. XBTs from IX01 and IX22 in the Indonesian Seas provide the only real-time profiling data in an area where Argo float observations are sparse, particularly in the coastal wave-guides. These XBT data, which are transmitted in real-time, are fed into ocean and seasonal weather and climate forecasting models. The IX01 and IX22 XBT data have been used to quantify the Indonesian throughflow volume and heat transport (Meyer et al., 1995; Sprintall et al., 2002; Wijffels et al., 2008), and their interannual and decadal variability (Meyer 1996; Wijffels and Meyers 2004; Liu et al., 2015). The IX01 and IX12 XBT data have also been used to quantify the upwelling characteristics off Java-Sumatra and their interannual variations associated with the Indian Ocean Dipole (Feng and Meyers 2003), geostrophic transport (Donguy and Meyers, 1995), as well as large scale Rossby wave propagation in the tropical/subtropical Indian Ocean, influenced by the planetary waves transmitted from the Pacific (Masumoto and Meyers 1998; Feng and Meyers 2003). More recently, the IX12 data have been used to examine changes in the Arabian Sea boundary current system as part of the U.S. ONR NASCar project. The IX21/IX15 data are being used to examine the long-term variability in the Agulhas Current. All the XBT data have been assimilated into numerical models and reanalysis products (e.g. EN4) to better capture the dynamics of these interannual and decadal processes in the Indian Ocean (e.g. Good et al., 2013; Zhuang et al., 2013). The IX01 XBT data has been used to identify the strengthening trend of the ITF up to 1 Sv per decade during the 30-year period of 1984-2013 (Liu et al., 2015), which could be important in the heat transfer from the Pacific into the Indian Ocean over the last decade (Lee et al. 2015, Nieves et al. 2016; Vialard, 2015).

In deriving volume and heat transport across the XBT lines, dynamic height and geostrophic velocities are derived by assuming a tight T-S relationship obtained through a look-up table of salinity climatology. Interannual and decadal variations of upper ocean salinity have been found to influence the geostrophic calculations along the IX1 section (Liu et al., 2015), thus, it is still important to monitor upper ocean salinity variability along IX1 that measures the ITF as it exits into the Indian Ocean, to be able to more accurately capture the across-section fluxes.

22.3 EOVs

As noted above, XBTs measure the EOV of temperature in the upper 1 km of the ocean. Although the function of the XBT network for broad scale upper ocean heat storage monitoring has been largely replaced by the Argo program, the XBTs still provide the only sustained observation tool for repeat surveying of upper ocean temperature in the marginal seas, within the ocean boundary currents and in Argo data void regions. The repeated XBT lines across the outflow of the ITF and the Agulhas Current system are the only long term observations of the major ocean fluxes that are crucial for the Indian Ocean basin scale heat and freshwater balances. Thus, it is still the utmost importance to maintain XBT transect sampling of the Indian Ocean boundary currents (IX21, IX12, IX14, IX08), as well as the XBT lines that transect the Indonesian seas (IX01, IX22). Salinity measurements along the IX1 section is also a crucial EOV for accurate flux estimations.

22.4 Actionable recommendations

Based on the suggested Essential Ocean Variables listed above, as well as in line with the XBT community recommendations made as part of the 2017 JCOMM SOT panel, actionable recommendations for the current IndOOS design follow:

a. *Maintain the Frequently Repeated IX01 and IX22 XBT lines: permits monitoring geostrophic mass and heat transport of the ITF into the Indian Ocean;*

b. *Maintain thermosalinograph measurement along the IX01 line (e.g. Phillips et al., 2005);*

c. *Enhance Argo deployment density along IX01 XBT line to better resolve salinity variability related to the ITF;*

d. *Maintain the High Resolution IX21 XBT line to monitor the long term changes of the Agulhas Current system.*

e. *Reactivate the Frequently Repeated IX12 XBT line to detect long term changes in the tropical thermocline ridge as well as the boundary current system in the Arabian Sea*

f. *Maintain the Frequently Repeated IX08 and IX14 (Bay of Bengal) XBT lines which are important for model testing, ENSO, Indian Ocean Dipole, and Asian monsoon associated tropical ocean variability and prediction, and heat content and climate change estimates (Smith et al, 2001). Further, encourage the public release of XBT data along these two transects that are maintained by India.*

g. *The implementation of automatic XBT launchers in the Indian Ocean, such as AXIS – the Automated eXpendable Instrument System (Frantantoni et al., 2017) that is operational in the Atlantic XBT program and the SIO Autolauncher that is operational on US maintained lines in the Pacific and Indian (IX21) Oceans, needs to be more fully explored to alleviate crew intervention on the SOOP vessels (Andres et al., this report).*

h. *The installation of ADCP velocity measuring instruments on ships that participate in the XBT network should be encouraged where possible. Combined with simultaneous velocity measurements from hull-mounted ADCPs, this could provide a powerful way to monitor the upper ocean heat transport across key transects, such as the ITF, the Agulhas Current, and across the southern Indian Ocean (Beal, this report).*

23. Tide gauges in the Indian Ocean

A.S. Unnikrishnan[1], Andrew Matthews[2], Médéric Gravelle[3], Laurent Testut[4], Thorkild Aarup[5] and Philip L. Woodworth[2], B. Ajay Kumar[6]

[1]CSIR-National Institute of Oceanography, Goa, India, [2]National Oceanography Centre, Liverpool, U.K., [3]LIENS, La Rochelle, France, [4]LEGOS, Toulouse, France,[5]GLOSS/IOC, UNESCO, Paris, France, [6]ESSO-INCOIS, Hyderabad, India

23.1 Introduction

Tide-gauge measurements provide data for routine tidal predictions in ports as well as reporting of extreme events such as storm surges and tsunamis. Along with satellite altimeter measurements, tide gauges give data that can be used for estimating sea-level rise trends. This is particularly important for impact assessment in low-lying coastline of south Asia as well as islands such as Maldives in the Indian Ocean.

Current status of the network

Figure 23.1 shows a map of active tide gauge stations in the Indian Ocean either supplying quality controlled monthly mean sea level data to the Permanent Service for Mean Sea Level (PSMSL, http://www.psmsl.org) or real-time data to the Intergovernmental Oceanographic Commission's Sea Level Station Monitoring Facility (http://www.ioc-sealevelmonitoring.org), operated by the Flanders Marine Institute (VLIZ, Belgium). The stations shown as 'PSMSL only' include historical records, possibly without complete datum control (non-Revised Local Reference (RLR) stations). However, many of these are of short duration. Real-time stations have increased in number since the 2004 tsunami. In Figure 23.1, the stations that have both real-time and PSMSL data are shown in red. There are 20 stations that have datum-controlled records (RLR) longer than 40 years that can be used for estimating long-term changes (shown in blue). However, most of them are in the northern hemisphere. It may be noted that only two stations, namely, Mumbai (along the west coast of India) and Fremantle (west coast of Australia) have more than 100 years of data. In Figure 23.2, the network of Global Navigation Satellite System (GNSS) stations co-located with tide gauges in the Indian Ocean is shown; GNSS is needed for monitoring changes in the level of the land on which the gauges are located.

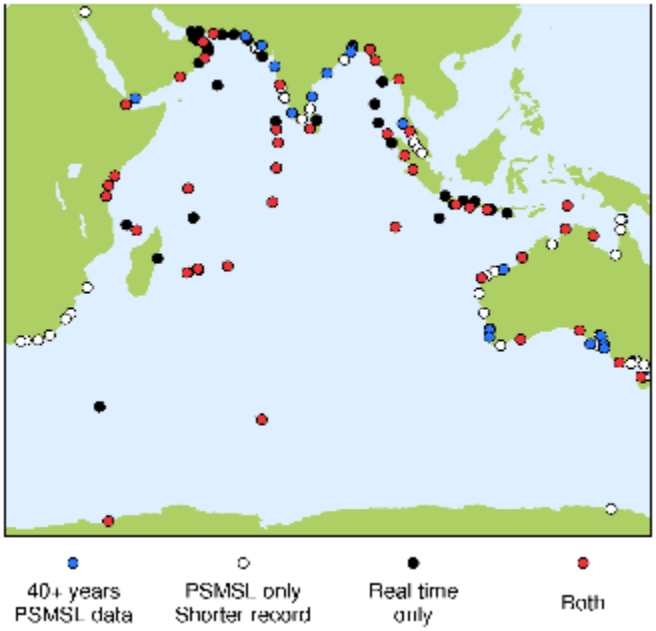

Figure 23.1 Distribution of active tide gauge stations in the Indian Ocean. PSMSL stations are considered active if data is available for 2011 or later. Real-time stations are considered active if they have supplied data in 2017.

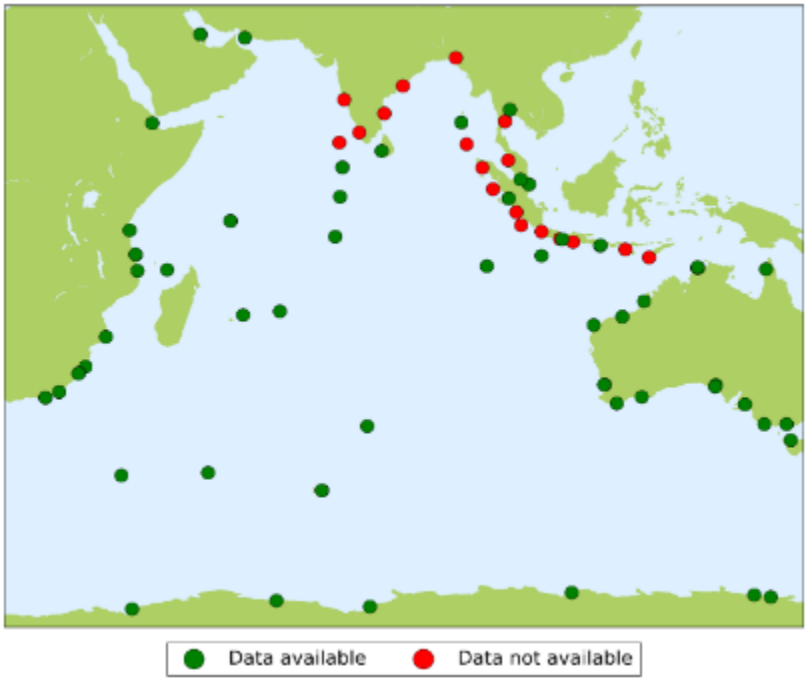

Figure 23.2 Current status of the GNSS network co-located with tide gauges in the Indian Ocean. Data since 2016 are considered.

High-frequency data:

The tide-gauge network in the Indian Ocean has been extended since the commencement of the Indian Ocean Tsunami Warning and Mitigation System (IOTWMS) following the 2004 Indian Ocean tsunami. This was achieved by upgrading some stations and with installations of some new stations. There are now more than 100 tide gauges in the Indian Ocean (GLOSS and non-GLOSS) that provide sea level data in real time (not quality controlled) via the IOC Sea Level Station Monitoring Facility (http://www.ioc-sealevelmonitoring.org). Higher-frequency, quality-controlled data (hourly values and similar) are available from the University of Hawaii Sea Level Center (http://uhslc.soest.hawaii.edu/).

23.2 Recommendations

The spatial coverage of the tide- gauge network in the Indian Ocean is not as good as in the Atlantic and Pacific. Due to the inadequacies in spatial data coverage, particularly in the southern Indian Ocean, questions to do with long-term trends and variability at decadal and longer time scales are less well addressed.

Since the 2004 tsunami, the network in the Indian Ocean was strengthened. However, many of these stations fall in the north Indian Ocean. For studies leading to understanding of various oceanographic processes, for example, the contribution of Indonesian throughflow waters to the variability in the southern Indian Ocean, there is a need for more observations than those that are presently available. . There is a particular need for strengthening the network at island stations.

Specific Recommendations of Essential Ocean Variables

- The tide-gauge network needs to be improved in many regions, such as the coast of Thailand western equatorial Indian Ocean, the coast of Africa and the Southern Ocean sector. The network in island stations is highly useful in comparing with satellite altimeter data and in the combined 'reconstructions' of long-term regional sea level change. Inconsistency across different sea-level reconstruction products in determining decadal variability has been shown by Nidheesh et al. (2017).
- The existing networks in the Southern Ocean and Antarctica, particularly difficult to maintain, must be consolidated and sustained on a long term basis by their countries (namely Australia, France, Japan, Russia, South Africa and UK).
- The core tide gauge network for GLOSS and for tsunami monitoring (IOC, 2015) should be sustained. The CLIVAR linkage and support in this respect is beneficial. Tide gauge hardware with real time transmission has declined in price, and one can expect the network may be more readily densified over coming years.

There is a corresponding requirement for GNSS equipment to be co-located at GLOSS core network tide gauge stations (IOC, 2012). Figure 23.2 shows where GNSS data are available near to tide gauges as stored in the SONEL (Service d'Observation du Niveau des Eaux Littorales) database (http://www.sonel.org); it can be seen that the Indian Ocean is particularly deficient in this respect. King (2014) has highlighted several sites as priorities for GNSS stations near to Indian Ocean tide gauges. There is a particular need for long-term datum control within the tide gauge network and for ties between the tide gauges and GNSS equipment (Woodworth et al., 2017).

- 'Data archaeology' and archival of historical sea level data not already in data banks needs to take place in several countries through the digitization of old records.
- Lastly, there is a need for some level of network linkage activities (advocacy, technical assistance/training) among national operators of tide gauge and GNSS stations in order to sustain the network.

24. New Technologies for In Situ IndOOS Measurements

M. Andres, Woods Hole Oceanographic Institution, Woods Hole, MA, USA.
C.M. Lee, Applied Physics Laboratory, University of Washington, Seattle, Washington, USA.
E.L. Shroyer, Oregon State University, Corvallis, Oregon, USA.
L. Centurioni, Scripps Institution of Oceanography, La Jolla, CA, USA.

Observational strategies that cleverly leverage technology are required to achieve the goal of the Indian Ocean Observing System (IndOOS) to "provide sustained high-quality oceanographic and marine meteorological measurements to support knowledge based decision-making through improved scientific understanding, weather and climate forecasts, and environmental assessments for the benefit of society". Autonomous platforms provide access to regions of the spatial and temporal sampling spectrum that have previously been unachievable. Integrated systems that employ complementary platforms, exploiting each for their particular strengths, will be required to resolve the broad range of spatial and temporal scales inherent to the dynamics of the Indian Ocean. A sampling of technologies and approaches follows below.

24.1 Giving New Life to an Old Technology

Targeted subsurface temperature observations from expendable bathythermographs (XBTs) have been important for documenting changes in ocean heat content and will likely continue to play an important role in the IndOOS (e.g., Cheng et al., 2016 and Feng et al., this report) particularly when combined with the growing Indian Ocean Argo array. One way to make repeated XBT lines a sustainable part of an observing system is through the use of volunteer observing ships (VOS) with automatic launchers that require no rider on the ship and little intervention from the ship's crew, while providing an Iridium satellite link to enable remote data retrieval and mission setup. One such system, AXIS – the Automated eXpendable Instrument System (Fratantoni et al., 2017), has been part of an Atlantic Meridional Overturning Circulation (AMOC) observing system since 2011. VOSs can also be equipped with hull-mounted acoustic Doppler current profilers (ADCPs); this provides a powerful way to obtain repeated measures of upper-ocean heat transport (Rossby et al., 2017). If suitable commercial partners and vessels can be found, the 10,000 km long southern boundary of the Indian Ocean (e.g. between Cape Town and Melbourne) would be a particularly suitable repeat-line for of an AXIS system (or other auto launcher) in combination with a hull-mounted ADCP.

24.2 Boundary Current Observations with CPIESs and Underwater Gliders

Current and pressure-sensor-equipped inverted echo sounders (CPIESs) can be used to obtain long-duration, high temporal resolution time series of western boundary current transport and velocity structure. Process studies with CPIESs include investigations of (1) the coupling between the upper ocean and deep ocean, (2) interactions between eddies and western boundary currents and (3) the role of topography in shaping the flow. CPIESs have been deployed as 'transport lines'—e.g., as part of the ACT time series, OKTV Line, PN Line and ASUKA Line (Beal and Elipot, 2016; Andres et al., 2015), in 'dynamics arrays'—e.g., KESS, CDRAKE, SYNOP, SK-II and FLEAT (Donohue et al., 2010; 2016) and in various 'niche' applications such as the study of non-linear internal waves in the South China Sea (Li et al., 2009).

CPIESs are deployed on the seafloor in a rigid anchor stand for typical durations ranging from about one to five years. Each CPIES measures the round-trip surface-to-bottom acoustic travel time (typically from 24 pings per hour to obtain an hourly measure); near-bottom pressure and temperature; and the horizontal currents 50 m above the seabed. In many regions, an empirical lookup table can be used to convert the CPIESs' acoustic travel times to full-water column profiles of temperature, salinity and density. From these profiles, the velocity shear between pairs of CPIESs can be estimated using the thermal wind relationship. This shear is referenced using the

CPIESs' time-varying pressure records that have been 'leveled' with the time-mean currents. (Leveling is the technique of referencing all pressure measurements onto a common geopotential surface.) The result is time series of absolute geostrophic velocity profiles from the surface to the bottom and the corresponding absolute geostrophic transports. Several technological advances are under development to enhance the capabilities of CPIESs. These include (1) the capability for remote retrievals of data batches (via a popup data shuttle which rises to the surface at a prescribed time and links to the satellite Iridium network) and (2) incorporation of a Doppler current profiler instead of the current sensor (DCPS-PIES).

Gliders have seen widespread success for science (Rudnick, 2016 provides a review) and operational missions, and could contribute to IndOOS. Underwater gliders are small (50-kg mass, 2-m length), buoyancy driven vehicles that have been optimized for extended endurance. Gliders propel themselves by changing buoyancy, such that they sink or rise through the water column, and adjusting attitude to use lift provided by hull and wings to project vertical motion into the horizontal. This allows the vehicles to navigate from point to point while profile vertically through the water column. At the surface between dives, gliders geolocate using GPS, and upload data and download new commands via Iridium satellite modem. Gliders carry flexible payloads that can include sensors for temperature, conductivity (for salinity), velocity profiles, dissolved oxygen, chlorophyll and CDOM fluorescence, optical backscatter, temperature and shear microstructure, nitrate, spectral irradiance, PAR, nitrate, zooplankton and marine mammals.

Gliders are well-suited for quantifying boundary current variability within the IndOOS. Gliders move slowly (20 km/day) to provide finely-spaced profiles, with the capability to maintain continuous sampling for periods typically lasting roughly half a year. They can thus resolve scales of a few kilometers and weeks over sections of hundreds of kilometers length, while maintaining sampling over seasons to years – scales that are well-matched to resolving variability in Indian Ocean boundary flows. (While trans-basin glider missions have been achieved–see the Challenger Program, https://challenger.marine.rutgers.edu/2-uncategorised/33-indian-ocean-perth-to-sri-lanka–this type of endurance is not yet routine.) Geostrophic transports can be reliably calculated from density sections using the thermal wind relationship (e.g. Lien et al., 2014), referenced to the depth-average current calculated as the difference between observed and modeled glider displacement over a dive (Eriksen et al., 2001; Rudnick and Cole, 2011), or direct transports can be measured using glider-mounted ADCPs (Todd et al., 2017). Gliders have been successfully used for sustained, multi-year quantification of eastern (California Current; Todd et al., 2011; Zaba and Rudnick, 2016) and western (Kuroshio Current; Lien et al., 2014) boundary currents. Similar approaches, using logistics local to target regions in the Indian Ocean, could be applied to sustain measurements for the IndOOS.

Recent use of moorings and CPIESs in tandem with gliders has proven invaluable for leveraging each platform's capabilities. Gliders can resolve water mass changes that CPIESs or moorings alone could not detect (Andres et al., 2017). The combination of fixed (moorings and CPIESs) and mobile (gliders) platforms resolves a broader range of scales than could be achieved by one of these platforms alone, allowing investigations of the interactions between scales. In the Indian Ocean, integrated glider/CPIESs arrays could contribute significantly to studies of surface boundary currents and their undercurrents (e.g., the Agulhas, the Somali Current, and Leeuwin Current) and the currents along the equator, to establish both the mean and the time varying transports and velocity structures. They could be used to investigate the flows' interactions with topography at the many dramatic ridges in the Indian Ocean and the interactions of mesoscale eddies with these ridges and the western boundary currents. In addition, CPIESs are well suited to study the thermocline movement (and the bottom pressure signals) at the Seychelles-Chagos Thermocline Ridge.

24.3 Moored Profilers for High-Current Regimes

In some cases it is desirable to resolve subtle changes in water properties at a fixed location (like within a boundary current) or to resolve transport variability in density space rather than depth space. Moored profilers, which can sample temperature, salinity and velocity at high vertical

resolution as they ride up and down a mooring line are particularly suitable for such studies and have been used as part of the AMOC observing system in a 10-year study of the Deep Western Boundary Current south of Cape Cod on Line W (Toole et. al., 2017). Two important enhancements to the basic moored profiler technology are underway at the Woods Hole Oceanographic Institution (WHOI) and these enhancements, which build on the success of moored profilers at Line W, are important innovations for long-endurance observing systems. The first is an Articulated Profiler, which minimizes drag (and hence increases endurance by minimizing the instrument's power requirement) by aligning the profiler body with the relative 3-D flow. The sensors will be mounted at the leading end of the body so that sampling is in undisturbed water (leading to less noisy measurements). The second development leverages hydrodynamic lift from the incident ocean currents. A LAMP (Lift-Assisted Moored Profiler) will provide better reliability in strong currents, where the present traction drive wheel sometimes stalls. This will make moored profiler measurements of strong current like the Agulhas feasible.

24.4 Capitalizing on Expendable Platforms

The operational contribution of the Global Drifter Program to IndOOS in terms of mixed layer (15-m depth) ocean currents, in-situ SST and sea-level pressure (SLP) data is discussed by Lumpkin and Centurioni (this report). Emerging technologies have the potential to further the impact of surface observations from Lagrangian drifters. Low-cost, expendable, undrogued drifters equipped with SST and GPS sensors capable of measuring the directional spectra of surface gravity waves have been developed by the Lagrangian Drifter Laboratory (LDL) at the Scripps Institution of Oceanography (Centurioni et. al. 2017). The Directional Wave Spectra (DWS) drifter samples the vertical, zonal and meridional velocity components of the GPS antenna for approximately 17 min at 2 Hz. The drifter controller, also developed by the LDL, computes the power spectral density, co-spectra and quadrature-spectra parameters with the Fourier transforms of the correlation functions of each pair of the velocity time-series, and the first 5 independent Fourier coefficients (a_0, a_1, a_2, b_1, b_2) of the wave spectra at a minimum interval of 30 min. These are relayed to the LDL data server in real-time through the Iridium satellite system. Commands sent over two-way Iridium communication can modify the mission for power consumption and telemetry cost savings while the DWS drifter mission is underway. All of the transmitted wave data, as well DWS drifter status are accessible in real time on a dedicated website as wells as through the Global Telecommunication System of the World Weather Watch. The first open ocean array of 22 DWS drifters deployed in the tropical North Pacific Ocean was deployed in winter 2016.

Surface Lagrangian drifters equipped with salinity sensors were deployed in the Bay of Bengal in 2015 as part of the Office of Naval Research (ONR) funded program ASIRI (Hormann et al, 2016) but their cost prevents basin-wide, sustained implementation. New low-cost sensors are currently being tested for long-term stability and may offer viable solution for the calibration and validation of satellite salinity observations.

Expendable Lagrangian drifters equipped with sonic anemometers and configurable for air or ship deployment also exist and could represent a valuable addition to the IndOOS and the global array. Such drifters, termed Minimets (see for example http://gdp.ucsd.edu/ldl_drifter/index.html) have been used for over a decade to measure sea-level wind within hurricanes and typhoons. Other promising unmanned platforms that are being used in an experimental mode to obtain momentum and flux measurements, as well other sea surface and meteorological observations, include the Saildrone and the Wave Glider. An inexpensive (and hence expendable) freely-drifting spar buoy instrument system (X-Spar) that could provide cost-effective, distributed measurements of meteorological variables is under development at WHOI. It will return near-surface meteorological and oceanographic observations for periods of a year or longer. Since data are recovered remotely via Iridium satellite link, it will be particularly suitable to use in regions where regular shipboard mooring servicing is not feasible.

24.5 Augmenting the Capabilities of Existing Assets

Integration of new sensors on existing IndOOS platforms, such as Argo and the RAMA array, offers added value and targets specific science focuses. For example, the shallow stratification in the Bay of Bengal necessitates clean near-surface measurements of both temperature and salinity. Modifications to the standard Argo capabilities by including a secondary, unpumped conductivity-temperature sensor allows for near-surface sampling without loss in quality of deep measurements by the primary sensor (Anderson and Riser 2014). Furthermore, addition of optical and chemical sensors to Argo floats provides the potential to greatly enhance our understanding of the biogeochemistry and biophysical connections in this historically undersampled region (Ravichandran, this report). Supported through ONR's DYNAMO program (Moum et al., 2013) and continuing with the ASIRI and MISO-BOB initiatives (Wijesekera et al., 2016), turbulent mixing sensors (-pods) have been added to the Equatorial and Bay of Bengal RAMA moorings along the Equatorial Indian Ocean and within the Bay of Bengal along 90E (e.g., Warner et al., 2016). -pods provide a direct measurement of temperature, velocity, and temperature variance dissipation at each deployment location (Moum and Nash 2009). These sensors have allowed for evaluation of multi-year time series of turbulent mixing, and the role of subsurface fluxes in modulation of the upper ocean structure (e.g., Moum et al., 2013, Warner at al., 2016). -pods are also being integrated on the SOLO II floats with the long-term goal of including this capability within the Argo program (Shroyer et al., 2016). -SOLO floats were first tested in the Bay of Bengal in 2015, yielding both upper ocean turbulent flux information as well as a clean in situ measurement of temperature within a few centimeters of the ocean's surface.

24.6 Concluding Remarks

Future efforts to sustain and improve the capabilities of the IndOOS should look to novel approaches that integrate complementary combinations of platforms. Key components of the observing system where recent technological advancements and synergies between platforms could be leveraged include the following:

- Monitoring boundary current strength, velocity structure and water masses with arrays comprising CPIES, gliders and articulated moored profilers or LAMPs in regions like the Somali, Leewin and Agulhas Currents.

- Investigating the remote Indian Ocean interior with autonomous or expendable platforms that incorporate traditional and new sensor technologies including DWS drifters (with SST and GPS sensors), -SOLO floats X-Spar floats, Saildrones, Wave gliders, and Minimets.

- Continued integration of -pods mounted on RAMA moorings through the Bay of Bengal and across the Equatorial array to examine seasonal transitions within the Equatorial wave guide and the accompanying atmospheric and oceanic variability.

- Doubling of traditional XBT sampling on some key lines like IX01, that monitors exchanges between the Pacific and Indian Oceans.

- Outfitting commercial vessels with hull-mounted ADCPs and XBT auto launchers to provide a measure of the heat flux across key lines like the southern boundary of the Indian Ocean between Cape Town and Melbourne.

Continued advancements in the technology and analysis techniques will be critical to achieving the IndOOS goals.

25. The Global Ocean Ship-Based Hydrographic Investigations Progrmam (GO-SHIP)

Bernadette M. Sloyan[1,3] and Rik Wanninkhof[2,3]

[1] CSIRO, Ocean and Atmosphere, Hobart Australia 7001

[2] NOAA Atlantic Oceanographic and Meteorological Laboratory Miami USA

[3] Co-Chair GO-SHIP

25.1 Introduction

GO-SHIP is the systematic and global survey of select hydrographic sections, carried out by an international consortium countries and laboratories (Figure 25.1). These span all of the major ocean basins and the full-depth water column with measurements of the climate accuracy, attainable only with research ships at present and for the foreseeable future.

Global hydrographic surveys have been carried out approximately every decade since the 1950s through research programs such as IGY, IIOE, GEOSECS, WOCE / JGOFS, and CLIVAR. In 2009 the Global Ocean Ship-based Hydrographic Program (GO-SHIP, http://www.go-ship.org) was established as part of the Global Climate Observing System (GCOS) as a component of the Global Ocean Observing System (GOOS) to provide international coordination and scientific oversight of the decadal global ocean survey. The international hydrographic surveys of the 1960s, 1990s (WOCE) and 2000s (CLIVAR Repeat Hydrography and GO-SHIP) were successful in answering many first- order questions about large-scale ocean circulation and carbon inventories. Their results also raised many new questions concerning ocean variability and trends, circulation, and biogeochemical controls on carbon and tracer inventories, distributions, and long-term secular trends associated with climate change and ocean acidification. These observations showed that the full-depth ocean exhibits significant interannual variability on top of the expected smooth decadal trend as part of patterns of global change, complicating efforts to detect and attribute human influences on the ocean.

GO-SHIP will continue to build the time-series of full-depth repeat ocean measurements capable of resolving decadal and longer time scale changes in the circulation and property storage (including heat, freshwater, oxygen and carbon) of the global oceans.

25.2 GO-SHIP Objectives

The GO-SHIP principal scientific objectives are:

(1) Understanding and documenting the large-scale ocean water property distributions, their changes, and drivers of those changes, and

(2) Addressing questions of the large physical, biogeochemical and biological changes anticipated for the future ocean. This includes increasing dissolved inorganic carbon, warming, acidification, and increased stratification due to atmospheric CO2 increases and associated changes in the Earth's radiation balance.

The observations will aid understanding of interaction of anthropogenic perturbations with natural cycles of water and sea-ice and with changes in circulation and ventilation processes.

In addition, to the scientific objective, GO-SHIP provides the high-quality reference observations to other components of ocean observing system that use autonomous observing platforms (e.g. Argo, BCG-Argo) for delayed mode quality control procedures of these programs. GO-SHIP also support the testing new ocean observing technologies and sensors.

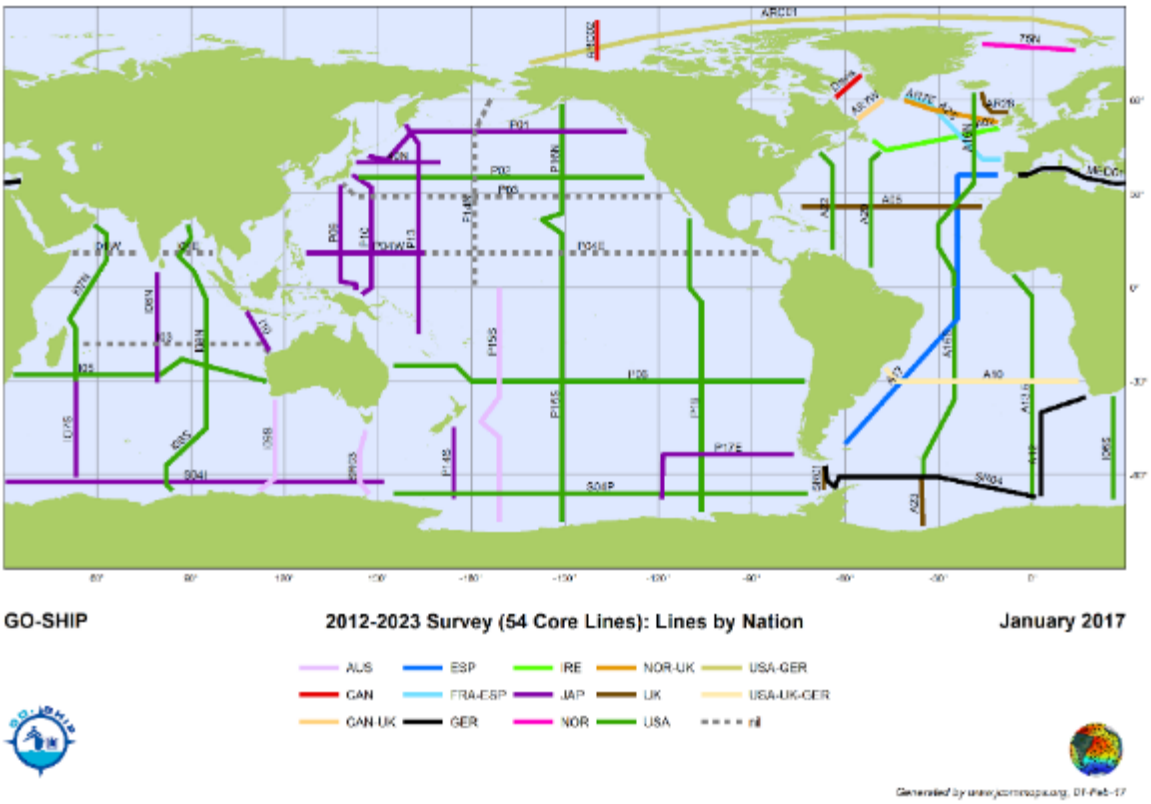

Figure 25.1. Hydrographic sections that comprise GO-SHIP. Countries undertaking sections of the 2012-2023 global survey are shown. Section without national support are shown are gray dashed lines.

A globally coordinated sustained hydrography program is built on 5 basic components:

(1) Joint Planning: Nations come together for joint planning exercises for each basin to agree on implementation to avoid gaps and duplications. Nations agree to adhere to GO-SHIP sampling resolution, measurement of core variables, and data release policy.

(2) Implementation: Nations commit to implement sections according to agreements and timeframes. International collaborations are established where necessary to ensure that the full suite of measurements are made on all cruises.

(3) Data Assembly and Quality Control: National programs and/or individual scientists submit their data following data release timeframes to the appropriate data assembly centers. The Data Assembly Centers assemble, check, and disseminate data to the scientific community. Accuracy requirements are verified and problems signaled. The Global DAC serves as a clearinghouse for all hydrographic data variables, and provides global coordination for monitoring data flow.

(4) Data Product Development and Joint Scientific Syntheses: As the basin and global surveys are completed, scientific synthesis groups are brought together to develop data products and establish collaborations for global, interdisciplinary science projects, including collaborations with other parts of the observing system.

(5) Network Evaluation and System Design Feedback: Based on the science, implementation and data flow evaluations, the observing network is reviewed and redesigned as necessary in collaboration with other components of the observing system.

25.3 GO-SHIP: Indian Ocean

GO-SHIP has a number of sections in the Indian Ocean that are part of the global decadal survey. A number of these sections have national commitments for occupation, however the section in the northern Indian Ocean - I01E and I01W- have no confirmed commitments (Figure 25.2). These sections have not been occupied since approximately 1998. The I03 sections was last completed in 2003. While this section remains on the GO-SHIP survey plan, a study on the value of retaining two mid-latitude sections - I03 and I05- in the Indian Ocean is warranted.

Collaboration between GO-SHIP and the CLIVAR Indian Ocean panel provides a unique opportunity for (1) leveraging national support to complete the Indian Ocean survey; (2) increasing high quality observation of a suite of ocean measurements and; (3) building a sustained observational program for ship-based observations of the Indian Ocean.

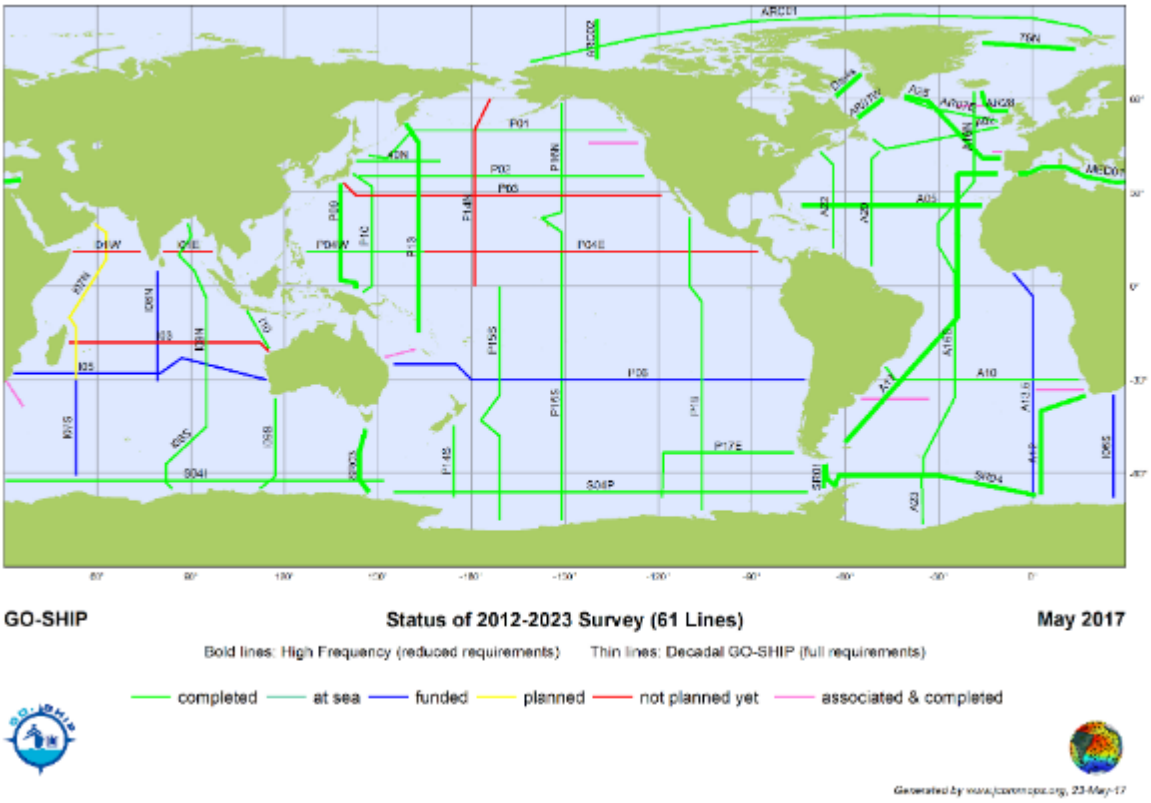

Figure 25.2.

25.4 GO-SHIP Variables and Data Time Line Policy

The GO-SHIP measurement suite is largely adopted from the U.S. GO-SHIP guidelines and endorsed by all international participating nations. They are divided into three levels in order of priority: Level 1, Level 2 and Level 3. These data provide approximately decadal resolution of the changes in inventories and transport of heat, freshwater, carbon, oxygen, nutrients and transient tracers, covering the ocean basins from coast to coast and full depth (sea surface to ocean floor).

Level 1 core measurements are mandatory on all cruises, and include standard hydrographic and tracer profiling, and velocity profiling. The rationale for classifying a measurement as Level 1 is

based on data required to directly quantify change in ocean carbon inventory, estimate anthropogenic CO2 empirically, characterize large-scale water mass ventilation rates, constrain horizontal heat, freshwater, carbon, nitrogen, and oxygen transports and/or net divergence, and provide an ongoing basis for model evaluation.

Level 2 measurements are highly desirable on a subset of cruises. They may be collected on coarser station spacing and are closely coordinated with the core effort.

Level 3 ancillary measurements are done according to opportunity and space available. They should not significantly interfere with Level 1 or 2 efforts, and may be regional or specific to an individual cruise. They include new technologies and measurement techniques.

Measurement standards for all Level 1 and 2 measurements should adhere to or be higher than those set by the GO-SHIP repeat hydrography manual (Hood et al. 2010b), which update standards laid out originally in the WOCE manuals (http://cchdo.ucsd.edu/policy). These measurement standards are routinely reviewed and updated. Certified reference materials are used for all measurements where such standards are available.

Table1 GO-SHIP Measurement and Data Release Schedules. Notes (1) Data available daily during the cruise. (2) Data released to the relevant data management structure within 5 weeks of the cruise; (2P) in preliminary form. (3) Data released within 6 months of shore-based analysis. (4) Data released within 15 months of sample collection.

Level 1: (*All data are to be released in final form 6 months after the cruise except where noted*) Inorganic carbon system parameters: Dissolved inorganic carbon (DIC); Total Alkalinity (TAlk); pH (two of three) (2P); CTD pressure, temperature, conductivity (salinity) (1,2); CTD oxygen (sensor) (2P); Bottle salinity (2); Nutrients by standard auto analyzer (NO3/NO2, PO4, SiO3) (2); Dissolved oxygen (2P); Chlorofluorocarbons (CFC-11, CFC-12) and SF6 (2P); Surface underway parameters (T, S, pCO2) (1); ADCP shipboard (2P); ADCP lowered (2P); Underway navigation and bathymetry (2); Meteorological data (1).
Level 2: (*All data are to be released in final form 6 months after the cruise except where noted*) Examples include discrete pCO2 (2); N2O (2); 14C (3); CCl4 (2); ∂13C of DIC (3); Dissolved organic carbon; dissolved organic nitrogen; 3H/3He (4); Fe/trace metals; CTD Transmissometer; Surface underway measurements (nutrients, O2, Chl, pH, DIC, TAlk, skin temperature).
Level 3: (*All data are to be released in final form within 2 years of analysis*) Examples include, but are not limited to, microstructure/turbulence; chlorophyll; Primary production; HPLC pigments; Experimental continuous analyzers; ∂15N; NO3; 32Si; ∂18O of H2O; NH4; Low level nutrients; Total organic phosphorus; Upper ocean optical; isotopes of O2; N2, Ar, O2; Methyl halides; DMS.

25.5 Data policies

The GO-SHIP data policy is stringent and geared toward rapid, open dissemination, with a clear structure for all data to undergo quality control and to be sent to and available from recognized data centers. The policy includes:

1) All Level 1 and 2 observations, cruise reports, and metadata are made public in preliminary form through a specified data center soon after collection ("early release"), with final calibrated data provided six months after the cruise, with the exception of those data requiring on-shore analyses (see Table 1).

2) All data collected as part of the program are submitted to a designated data management structure for quality control and dissemination for synthesis.

25.6 Conclusion

GO-SHIP builds on previous global-scale hydrography efforts. The program evolves based on the findings of the previous work and emerging science requirements and technological developments. A future development will include addition of further biogeochemistry and biology measurements to enable GO-SHIP to determine trends and variability in marine biogeochemistry and ecosystems. These objectives will be incorporated into the sustained primary objectives of GO-SHIP.

GO-SHIP will continue to provide and expand its capacity to provide a mechanism for testing and validating new autonomous sensors and serve as a reference/calibration dataset for other observing system. As biogeochemical and biological sensors are added to these autonomous platforms, the GO-SHIP data will be invaluable for validating and calibrating these new sensors. In addition, the global hydrographic survey will continue to provide a means to access remote ocean areas for the deployment of all autonomous observing platforms.

25.7 ACTIONS

- GO-SHIP and CLIVAR INDIAN Ocean panel to work constructively to increase national participation in the GO-SHIP program, with focus on increase Indian Ocean rim country activity in GO-SHIP.
- Promote a strong collaboration between GO-SHIP and IndOOS to enable optimum use of GO-SHIP research vessels and support of other component of the Indian Ocean Observing system, where feasible.

124 25.8 ADDITIONAL FIGURES

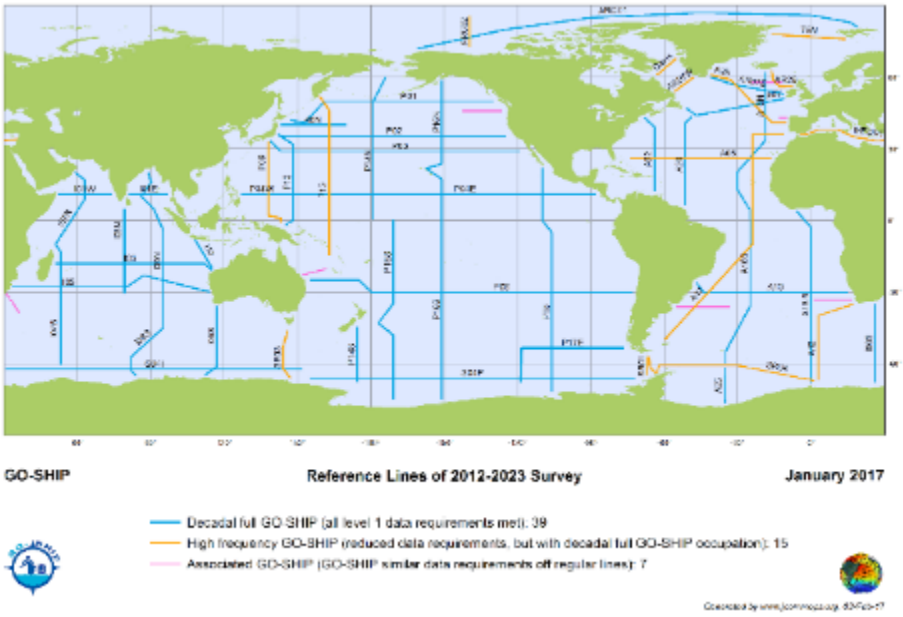

Figure 25.3 Reference Lines of 212-2023 Survey

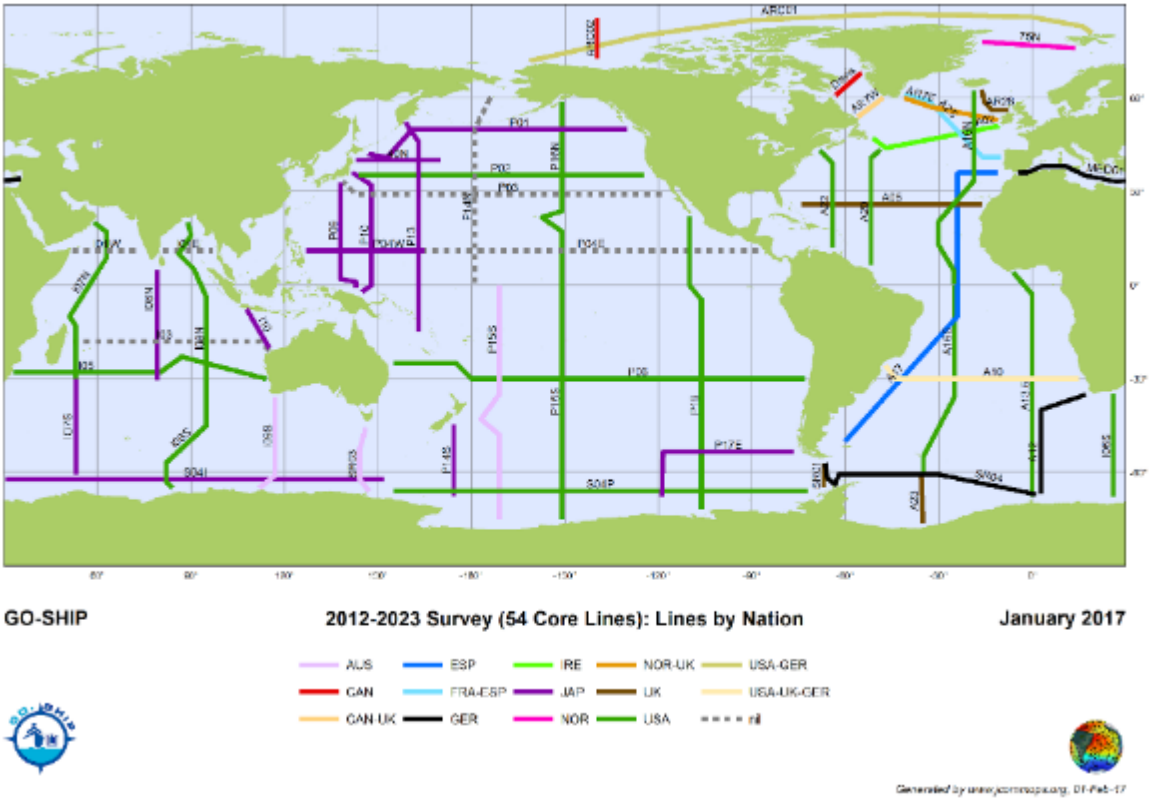

Figure 25.4 2012-2-23 Survey (54 Core Lines): Lines by Nation

Reference

Chapter 1

Anderson, J.E., and S. C. Riser, 2017: Near-surface variability of temperature and salinity in the near-tropical ocean: Observations from profiling floats.

Annamalai, H., P. Liu, P and S.P. Xie., 2005: Southwest Indian Ocean SST variability: Its local effect and remote influence on Asian Monsoons. J. Climate, 18, 4150–4167.

Annamalai, H., B. Taguchi, K.R. Sperber, J.P. McCreary, M. Ravichandran, A. Cherchi, G. Martin and A. Moise., 2015: Persistence of systematic errors in the Asian-Australian monsoon precipitation in climate models: a way forward: CLIVAR Exchanges, Special Issue on Monsoons: Advancing understanding ofmonsoon variability and improving prediction, Vol 66, 19-23 pp.

Annamalai, H., B. Taguchi, J. P McCreary, M. Nagura and T. Miyama, 2017: Systematic errors in south Asian monsoon simulation: Importance of Equatorial Indian Ocean processes. J. Climate, 30 (19), 8159-8178, doi:10.1175/JCLI-D-16-0573.1.

Dai A. et al. 2009: Changes in Continental Freshwater Discharge from 1948 to 2004, J. Climate, 22, 2773-2792.

Del Sole, T., and J. Shukla., 2002: Linear prediction of Indian monsoon rainfall. J. Climate, 15, 3645-3658.

Durand, F et al. 2004: Impact of temperature inversions on SST evolution in the South-Eastern Arabian Sea during the pre-summer monsoon season, Geo. Phys. Lett., 31, L01305, doi:10.1029/2003GL018906

Graham, N. E., and T. P. Barnett, 1987: Sea surface temperature, surface wind divergence, and convection over the tropical oceans. Science, 238, 657–659.

Han, W., J.P. McCreary, D.L.T. Anderson, and A.J. Mariano., 1999: Dynamics of the eastern surface jets in the equatorial Indian Ocean. J. Phys. Oceanogr., 29, 2191–2209.

Howden, S.D., and R. Murtugudde, 2001: Effects of river inputs into the Bay of Bengal. J. Geophys. Res., 106(C9), 19825-19843. doi:10.1029/2000JC000656

Joseph, P. V., Warm pool over the Indian Ocean and monsoon onset., 1990: Trop. Ocean–Atmos. Newslett., Winter, 1–5.

Krishnamurti, T. N., Ardanuy, P., Ramanathan, Y. and Pasch, R., 1981: On the onset vortex of the summer monsoons. Mon. Weather Rev., 109, 344–363.70.

Levine, R. C., Turner, A. G., Marathayil, D. and Martin, G. M., 2013. The role of northern Arabian Sea surface temperature biases in CMIP5 model simulations and future projections of Indian summer monsoon rainfall. Climate Dynamics, 41, 155-172.

Lindstorm, E.J., et al. 2017: Autonomous multi-platform observations during the Salinity Processes in the Upper-ocean Regional Study. Oceanography, 30(2):38-48, https://doi.org/10.5670/oceanog.2017.218

Lukas R., and E.J. Lindstorm 1991: The mixed layer of the western equatorial Pacific Ocean. J. Geophys. Res., 96, 3343-3357, doi:10.1029/90JC01951

Mahadevan, A., G. Spiro Jaeger, M. Freilich, M. Omand, E.L. Shroyer, and D. Sengupta. 2016. Freshwater in the Bay of Bengal: Its fate and role in air-sea heat exchange. Oceanography 29(2):72–81, http://dx.doi.org/10.5670/oceanog.2016.40.

Masson, S., C. Menkes, P. Delecluse, and J.-P. Boulanger, 2003: Impacts of salinity on the eastern Indian Ocean during the termination of the fall Wyrtki Jet. J. Geophys. Res., 108, 3067 (doi:10.1029/2001JC000833)

Masson, S., et al. 2005: Impact of barrier layer on winter-spring variability of the southeastern Arabian Sea. Geo. Phys. Lett., 32, L07703, doi:10.1029/2004GL021980.

Martin, G. M., S.F. Milton, C.A. Senior, M.E. Brooks, S. Ineson, T. Reichler, and J. Kim., 2010: Analysis and reduction of systematic errors through a seamless approach to modeling weather and climate. J. Climate, 23, 5933–5957.

McPhaden, M.J., Y. Wang and M. Ravichandran, 2015: Volume transports of the Wyrtki jets and their relationship to the Indian Ocean Dipole. J. Geophys. Res. Oceans, 120, doi:10.1002/2015JC010901.

Nagura M., et al., 2013: Longitudinal biases in the Seychelles Dome simulated by 35 ocean-atmosphere coupled general circulation models, J. Geophys. Res. Oceans, 118, doi:10.1029/2012JC008352.

Nagura, M., T. Terao and M. Hashizume., 2015: The role of temperature inversions in the generation of seasonal and interannual SST Variability in the far northern Bay of Bengal. J. Climate, 28, 3671-3693.

Nagura, M., J.P. McCreary and H. Annamalai, 2017: Origins of coupled-model biases in the Arabian-Sea climatological state. J. Climate (in press)

Neema, C. P., Hareeshkumar, P. V. and Babu, C.A., 2012. Characteristics of Arabian Sea mini warm pool and Indian summer monsoon. Climate Dynamics, 38, 2073-2087.

Nyadjro, E. S., Subrahmanyam, B., Murty, V. S. N. and Shriver, J. F., 2012. The role of salinity on the dynamics of the Arabian Sea mini warm pool. Journal of Geophysical Research: Oceans, 117(C9).

Rao, R.R., and R. Sivakumar, 2000: Seasonal variability of near-surface thermal structure and heat budget of the mixed layer of the tropical Indian Ocean from a new global ocean temperature climatology. J. Geo. Phys. Res., 105, 985-1015.

Rainville, L., J.I Gobat and G.B Shilling, 2017: Multi-month dissipation estimates using microstructure from autonomous underwater gliders. Oceanography 30(2): 49-5, https://doi.org/10.5670/oceanog.2017.219

Raymond, D. J., 2000: Thermodynamic control of tropical rainfall, Quart. J. Roy. Meteor. Soc., 126, 889-898.

Reverdin, G.,1987: The upper equatorial Indian Ocean: The climatological seasonal cycle. J. Phys. Oceanogr., 17, 903-927.

Sandeep S., and R.S. Ajayamohan., 2014: Origin of cold bias over the Arabian Sea in climate models. Sci. Rep., 4, 6403.

Schott, F.A., S.-P. Xie, and J.P. McCreary Jr., 2009: Indian Ocean circulation and climate variability. Rev. Geophys., 47, RG1002, doi:10.1029/2007RG000245.

Schott, F., and J.P. McCreary., 2001: The monsoon circulation of the Indian Ocean. Prog. Oceanogr., 51, 1–123.

Sengupta D, M. Ravichandran. (2001): Oscillations of Bay of Bengal sea surface temperature during the 1998 summer monsoon. Geo. phys. Res. Lett. 28, 2033–2036.

Seo, H., S.P. Xie, R. Murtugudde, M. Jochum and A.J. Miller, 2009: Seasonal effects of Indian Ocean freshwater forcing in a regional coupled model. J. Climate, 22, 6577-6596.

Shenoi, S.S.C., D. Shankar and S.R. Shetye., 2002: Differences in heat budgets of the near surface Arabian Sea and Bay of Bengal: Implications for the summer monsoon. J. Geo. Phy., 107, NO. C6, 3052, 10.1029/2000JC000679.

Shukla, J., and M. Fennessy 1994: Simulations and predictability of monsoons, in Proceedings of the International Conference on Monsoon variability and predictability, Tech. Rep. WCRP , 567-575, World Climate Research Programme, Geneva, Switzerland.

Sijikumar, S. and Rajeev, K., 2012. Role of the Arabian Sea warm pool on the precipitation characteristics during the monsoon onset period. Journal of Climate, 25, 1890-1899.

Slingo, J., Spencer, H., Hoskins, B., Berrisford, P. and Black, E. (2005) The meteorology of the Western Indian Ocean, and the influence of the east African highlands. Philosophical Transactions of the Royal Society A: Mathematical, Physical and Engineering Sciences, 363 (1826). pp. 25-42. ISSN 1364-503X doi: 10.1098/rsta.2004.1473

Sperber, K.R. et al., 2013: The Asian monsoon: an intercomparison of CMIP3vs CMIP5 simulations of the late 20th century. Clim. Dyn. 41 (9-10), 2711-2744, doi:10.1007/s00382-012-1607-6.

Stephens, G.L., S.V. Heever and L. Pakula., 2008: Radiative–Convective Feedbacks in Idealized States of Radiative–Convective Equilibrium. J. Atmos. Sci., 65, 3989, 3916.

Turner, A. G., H. Annamalai., 2012: Climate change and the South Asian summer monsoon. Nature Climate Change, 2, 587–595, doi:10.1038/nclimate1495.

Thadathil, P., et al. 2007: Observed seasonal variability of barrier layer in the Bay of Bengal, J. Geo. Phy. VOL. 112, C02009, doi:10.1029/2006JC003651

Thadathil, P., et al. 2016: Surface layer temperature inversion in the Bay of Bengal: Main characteristics and related mechanisms. J. Geo. Phys. Res., 121: 5682-5696. doi:10.1002/2016JC011674.

Vilard et al. 2009: CIRENE: Air-Sea Interactions in the Seychelles-Chagos Theromocline Ridge Region. Bull. Amer. Met. Soc., 46-61 pp.

Vinaychandran, P.V., D. Shankar, J. Kurian, F. Durand and S.S.C. Shenoi, 2002: Arabian Sea mini warm pool and monsoon onset vortex. Current Science, 93, 203-214.

Wijesekera, et al., 2016: ASIRI: An Ocean-Atmosphere Initiative for Bay of Bengal. Bull. Amer. Met. Society, 1859-1884 pp.

Wyrtki, K., 1973: An equatorial jet in the Indian Ocean. Science, 181, 262-264.

Xie, S.P., H. Annamalai, F. Schott and J.P. McCreary., 2002: Structure and Mechanisms of South Indian Ocean Climate Variability. J. Climate, 15, 864-878.

Yokoi, T., T. Tozuka, and T. Yamagata (2009), Seasonal variations of the Seychelles Dome simulated in the CMIP3 models, J. Climate, 39, 449–457.

Zhao et al. 2017: The GFDL Global Atmosphere and Land ModelAM4.0/LM4.0: Documentation and Simulations with Prescribed SSTs – Part I: Simulation Characteristics (submitted to JAMES)

Chapter 2

Allison, E.H. et al., 2009. Vulnerability of national economies to the impacts of climate change on fisheries. Fish and Fisheries, 10: 173-196: 10.1111/j.1467-2979.2008.00310.x.

Bange, H.W., 2009. Nitrous oxide in the Indian Ocean. In: J.D. Wiggert, R.R. Hood, S.W.A. Naqvi, K.H. Brink and S.L. Smith (Editors), Indian Ocean Biogeochemical Processes and Ecological Variability. Geophysical Monograph. American Geophysical Union, Washington, D. C., pp. 205-216.

Bange, H.W. et al., 2001. Nitrous oxide emissions from the Arabian Sea: A synthesis. Atmos. Chem. Phys., 1: 61-71.

Bange, H.W., Wajih, S., Naqvi, A. , Codispoti, L.A., 2005. The nitrogen cycle in the Arabian Sea. Prog. Ocean., 65: 145-158.

Barange, M. et al., 2014. Impacts of climate change on marine ecosystem production in societies dependent on fisheries. Nature Climate Change, 4: 211-216: 10.1038/nclimate2119.

Bopp, L., Resplandy, L., Untersee, A., Mezo, P.L., Kageyama, M., 2017. Ocean (de)oxygenation from the Last Glacial Maximum to the twenty-first century: insights from Earth System models. Phil. Trans. R. Soc. A 375, 20160323. doi:10.1098/rsta.2016.0323.

Bopp, L., Resplandy, L., Orr, J.C., Doney, S.C., Dunne, J.P., Gehlen, M., Halloran, P., Heinze, C., Ilyina, T., Séférian, R., Tjiputra, J., Vichi, M., 2013. Multiple stressors of ocean ecosystems in the 21st century: projections with CMIP5 models. Biogeosciences 10, 6225–6245. doi:10.5194/bg-10-6225-2013.

Codispoti, L.A. et al., 2001. The oceanic fixed nitrogen and nitrous oxide budgets: Moving targets as we enter the anthropocene? Sci. Mar., 65: 85-105.

Currie, J.C. et al., 2013. Indian Ocean Dipole and El Nino/Southern Oscillation impacts on regional chlorophyll anomalies in the Indian Ocean. Biogeosci., 10: 6677-6698: 10.5194/bg-10-6677-2013.

Doney, S.C. et al., 2012. Climate change impacts on marine ecosystems. Ann. Rev. Mar. Sci., 4: null: doi:10.1146/annurev-marine-041911-111611.

Ekau, W., Auel, H., Portner, H.O. , Gilbert, D., 2010. Impacts of hypoxia on the structure and processes in pelagic communities (zooplankton, macro-invertebrates and fish). Biogeosci., 7: 1669-1699: 10.5194/bg-7-1669-2010.

Eppley, R.W., 1972. Temperature and phytoplankton growth in the sea. Fish. Bull., 70: 1063-1085.

Gomes, H.D. et al., 2014. Massive outbreaks of Noctiluca scintillans blooms in the Arabian Sea due to spread of hypoxia. Nature Communications, 5: 10.1038/ncomms5862.

Gruber, N., 2011. Warming up, turning sour, losing breath: ocean biogeochemistry under global change. Philosophical Transactions of the Royal Society a-Mathematical Physical and Engineering Sciences, 369: 1980-1996: 10.1098/rsta.2011.0003.

Hood, R.R., Beckley, L.E. , Wiggert, J.D., 2017. Biogeochemical and ecological impacts of boundary currents in the Indian Ocean. Prog. Ocean., 156: 290-325: http://dx.doi.org/10.1016/j.pocean.2017.04.011.

Lachkar, Z., Smith, S., Levy, M. , Pauluis, O., 2016. Eddies reduce denitrification and compress habitats in the Arabian Sea. Geophys. Res. Lett., 43: 9148-9156: 10.1002/2016gl069876.

Mahowald, N.M. et al., 2006. Change in atmospheric mineral aerosols in response to climate: Last glacial period, pre-industrial, modern and doubled-carbon dioxide climates. J. Geophys. Res., 111: doi:10.1029/2005JD006653.

McCreary, J.P. et al., 2013. Dynamics of the Indian-Ocean oxygen minimum zones. Prog. Ocean., 112: 15-37: 10.1016/j.pocean.2013.03.002.

Menard, F., Marsac, F., Bellier, E. , Cazelles, B., 2007. Climatic oscillations and tuna catch rates in the Indian Ocean: a wavelet approach to time series analysis. Fish. Oceanogr., 16: 95-104.

Morrison, J.M. et al., 1999. The oxygen minimum zone in the Arabian Sea during 1995. Deep-Sea Res. II, 46: 1903-1931.

Naqvi, S.W.A. et al., 2010. Marine hypoxia/anoxia as a source of CH4 and N2O. Biogeosci., 7: 2159-2190: 10.5194/bg-7-2159-2010.

Naqvi, S.W.A. et al., 1998. Severe fish mortality associated with "red tide" observed in the sea of Cochin. Curr. Sci., 75: 543-544.

Paulmier, A. , Ruiz-Pino, D., 2009. Oxygen minimum zones (OMZs) in the modern ocean. Prog. Ocean., 80: 113-128: 10.1016/j.pocean.2008.08.001.

Rabalais, N.N. et al., 2010. Dynamics and distribution of natural and human-caused hypoxia. Biogeosci., 7: 585-619.

Ram, A. et al., 2014. Nutrients, hypoxia and Mass Fishkill events in Tapi Estuary, India. Estuar. Coast. Shelf Sci., 148: 48-58: 10.1016/j.ecss.2014.06.013.

Resplandy, L. et al., 2012. Controlling factors of the oxygen balance in the Arabian Sea's OMZ. Biogeosci., 9: 5095-5109: 10.5194/bg-9-5095-2012.

Resplandy, L. et al., 2011. Contribution of mesoscale processes to nutrient budgets in the Arabian Sea. J. Geophys. Res., 116: 10.1029/2011jc007006.

Rixen, T., Baum, A., Gaye, B. , Nagel, B., 2014. Seasonal and interannual variations in the nitrogen cycle in the Arabian Sea. Biogeosci., 11: 5733-5747: 10.5194/bg-11-5733-2014.

Saji, N.H., Goswami, B.N., Vinayachandran, P.N. , Yamagata, T., 1999. A dipole mode in the tropical Indian Ocean. Nature, 401: 360-363.

Seitzinger, S.P. et al., 2010. Global river nutrient export: A scenario analysis of past and future trends. Global Biogeochem. Cycles, 24: 10.1029/2009gb003587.

Stramma, L., Schmidtko, S., Levin, L.A. , Johnson, G.C., 2010. Ocean oxygen minima expansions and their biological impacts. Deep-Sea Res. I, 57: 587-595: 10.1016/j.dsr.2010.01.005.

Vaquer-Sunyer, R. , Duarte, C.M., 2008. Thresholds of hypoxia for marine biodiversity. Proc. Natl. Acad. of Sci., 105: 15452-15457: 10.1073/pnas.0803833105.

Webster, P.J., Moore, A.M., Loschnigg, J.P. , Leben, R.R., 1999. Coupled ocean-temperature dynamics in the Indian Ocean during 1997-98. Nature, 401: 356-360.

Wiggert, J.D., Vialard, J., Behrenfeld, M., 2009. Basinwide modification of dynamical and biogeochemical processes by the positive phase of the Indian Ocean Dipole during the SeaWiFS era. In: J.D. Wiggert, R.R. Hood, S.W.A. Naqvi, K.H. Brink and S.L. Smith (Editors), Indian Ocean Biogeochemical Processes and Ecological Variability. Geophysical Monograph Series. American Geophysical Union, Washington, D. C., pp. 350.

Wishner, K.F. et al., 2008. Vertical zonation and distributions of calanoid copepods through the lower oxycline of the Arabian Sea oxygen minimum zone. Prog. Ocean., 78: 163-191: 10.1016/j.pocean.2008.03.001.

Chapter 3

Bakun, A., 1990, Global climate change and intensification of coastal ocean upwelling. Science, 247(4939), 198-201.

Chen G., W. Han, Y. Li and D. Wang, 2016, Interannual Variability of Equatorial Eastern Indian Ocean Upwelling: Local versus Remote Forcing. *J. Geophys. Res.*, doi: 10.1175/JPO-D-15-0117.1.

Currie, J. C., M. Lengaigne, J. Vialard, D. M. Kaplan, O. Aumont, S. W. A. Naqvi, and O. Maury, 2013, Indian Ocean Dipole and El Niño/Southern Oscillation impacts on regional chlorophyll anomalies in the Indian Ocean. *Biogeosciences*, 10, 6677–6698, doi:10.5194/bg-10-6677-2013.

deCastro, M., M. C. Sousa, F. Santos, J. M. Dias, and M. Gómez-Gesteira, 2016, *Sci. Rep.*, 6, 30137, doi:10.1038/srep30137.

FAO, 2004, The State of the World Fisheries and Aquaculture. In Food and Agriculture Organization of the United Nations. Rome, Italy.

Foltz, G. R., J. Vialard, P. Kumar, and M. J. McPhaden, 2010, Seasonal mixed layer heat balance of the southwestern tropical Indian Ocean. J. Climate, 23, 947-965.

Ghofar, A., 2005, Marine fisheries management plan in Indonesia a case study of the Bali Strait fishery, Indonesian Journal of Marine Sciences, 10, 177-84.

Gopalakrishna, V. V., R. R. Rao, K. Nisha, M. S. Girishkumar, T. Pankajakshan, M. Ravichandran, Z. Johnson, K. Girish, N. Aneeshkumar, M. Srinath, and S. Rajesh, 2008, Observed anomalous upwelling in the Lakshadweep Sea during the summer monsoon season of 2005. *J. Geophys. Res.,* doi:10.1029/2007JC004240.

Hermes, J.C. and C.J.C. Reason, 2009, The sensitivity of the Seychelles-Chagos thermocline ridge to large-scale wind anomalies. *ICES Journal of Marine Science* 66:7, 1455-1466.

Hood, R.R., H.W. Bange, L. Beal, L.E. Beckley, P. Burkill, G.L. Cowie, N. D'Adamo, G. Ganssen, H. Hendon, J. Hermes, M. Honda, M. McPhaden, M. Roberts, S. Singh, E. Urban, and W. Yu. 2015. Science Plan of the Second International Indian Ocean Expedition (IIOE-2): A Basin-Wide Research Program. *Scientific Committee on Oceanic Research*, Newark, Delaware, USA.

Hood, R. R., L. E. B. Beckley, and J. D. Wiggert. 2017, Biogeochemical and ecological impacts of boundary currents in the Indian Ocean, Progress in Oceanography, 156, 290-325.

Iskandar, I., W. Mardiansyah, Y. Masumoto, and T. Yamagata, 2005, Intraseasonal Kelvin Waves along the Southern Coast of Sumatra and Java. *J. Geophys. Res.,* 110, C04013, 10.1029/2004JC002508.

Izumo, T., C. de Boyer Montégut, J. J. Luo, S. K. Behera, S. Masson, and T. Yamagata, 2008, The role of the western Arabian Sea upwelling in Indian monsoon rainfall variability. *J. Clim.*, 21, 5603–5623.

Kaplan, D. M., E. Chassot, J. M. Amande, S. Dueri, H. Demarcq, L. Dagorn, and A. Fonteneau, 2014, Spatial management of Indian Ocean tropical tuna fisheries: potential and perspectives, ICES J. Mar. Sci., 71(7), 1728-1749, doi:10.1093/icesjms/fst233.

Lee, T., 2004, Decadal weakening of the shallow overturning circulation in the South Indian Ocean. *Geophys. Res. Lettr.*, 31, L18305, doi:10.1029/2004GL020884.

Menard, F., F. Marsac, E. Bellier, and B. Cazelles, 2007, Climatic oscillations and tuna catch rates in the Indian Ocean: a wavelet approach to time series analysis, *Fish. Oceanogr.*, 16(1), 95-104.

Praveen, V., R. S. Ajayamohan, V. Valsala, S. Sandeep, 2016. Intensification of upwelling along Oman coast in a warming scenario. Geophysical Research Letters, 43(14), 7581-7589.

Resplandy, L., Levy, M., Madec, G., Pous, S., Aumont, O., Kumar, D., 2011, Contribution of mesoscale processes to nutrient budgets in the Arabian Sea. *J. Geophys. Res.*, 116, C11007.

Rossi V., M. Feng, C. Pattiaratchi, M. Roughan and A. M. Waite, 2013, On the factors influencing the development of the sporadic upwelling in the Leeuwin Current system. *J. Geophys. Res.*, DOI: doi:10.1002/jgrc.20242.

Saji N. H., B. N. Goswami, P. N. Vinayachandran, and T. Yamagata, 1999, A dipole mode in the tropical Indian Ocean, *Nature*, 401, 360-363.

Sartimbul, A., H. Nakata, E. Rohadi, B. Yusuf, and H. P. Kadarisman, 2010, Variations in chlorophyll-a concentration and the impact on Sardinella lemuru catches in Bali Strait, Indonesia, Progress in Oceanography, 87, 168-74.

Vialard, J., J. P. Duvel, M. J. McPhaden, P. Bouruet-Aubertot, B. Ward, E. Key, D. Bourras, R. Weller, P. Minnett, A. Weill, C. Cassou, L. Eymard, T. Fristedt, C. Basdevant, Y. Dandonneau, O. Duteil, T. Izumo, C. de Boyer Montégut, S. Masson, F. Marsac, C. Menkes, and S. Kennan, 2009, Cirene: Air Sea Interactions in the Seychelles-Chagos thermocline ridge region, Bull. Am. Met. Soc., 90, 45-61.

Vialard, J., A. Jayakumar, C. Gnanaseelan, M. Lengaigne, D. Sengupta, B.N. Goswami, 2012: Processes of 30-90 day sea surface temperature variability in the Northern Indian Ocean during boreal summer, *Clim. Dynamics*, 38, 1901-1916.

Vic C., X. Capet, G. Roullet and X. Carton, 2017, Western boundary upwelling dynamics off Oman. *Ocean Dyn.*, DOI: 10.1007/s10236-017-1044-5.

Vinayachandran, P. N., and T. Yamagata, 1998, Monsoon response of the sea around Sri Lanka: Ge neration of thermal domes and anticyclonic vortices, *J. Phys. Oceanogr.*, 28, 1946 – 1960.

Wiggert, J.D., Murtugudde, R.G., Christian, J.R., 2006, Annual ecosystem variability in the tropical Indian Ocean: results of a coupled bio-physical ocean general circulation model. *Deep-Sea Res. II*, 53, 644–676.

Wiggert, J. D., J. Vialard, and M. J. Behrenfeld, 2009, Basinwide modification of dynamical and biogeochemical processes by the positive phase of the Indian Ocean Dipole during the SeaWiFS era, in: Indian Ocean Biogeochemical Processes and Ecological Vari- ability, vol. 185, edited by: J. D. Wiggert, R. R. Hood, S. Wajih, A. Naqvi, K. H. Brink, and S. L. Smith, p. 350.

Xie, S.-P., H. Annamalai, F.A. Schott, and J.P. McCreary, 2002, Structure and mechanisms of South Indian Ocean climate variability. *J. Climate*, 15, 864-878.

Yokoi, T., T. Tozuka, and T. Yamagata, 2008, Seasonal Variation of the Seychelles Dome. *J. Climate*, 21, 3740-3754, doi: 10.1175/2008JCLI1957.1

Yu W., R. Hood, N. D'Adamo, M. McPhaden, R. Adi, R. Tisiana, D. Kuswardani, M. Feng, G. Ivey, T. Lee, G. Meyers, I. Ueki, M. Landry, R. Ji, C. Davis, W. Pranowo, L. Beckley and Y. Masumoto, 2016, The EIOURI Science Plan, available at http://www.iioe-2.incois.gov.in/IIOE-2/pdfviewer.jsp?docname=EIOURI_Science_Plan.pdf

Chapter 4

Antony, C., Testut, L., & Unnikrishnan, A. S. (2014). Observing storm surges in the Bay of Bengal from satellite altimetry. *Estuarine, Coastal and Shelf Science*, *151*, 131-140.

Astier, N., Plu, M., & Claud, C. (2015). Associations between tropical cyclone activity in the Southwest Indian Ocean and El Niño Southern Oscillation. *Atmospheric Science Letters*, *16*(4), 506-511.

Balaguru K, P Chang, R Saravanan, LR Leung, Z Xu, M Li and J-S Hsieh (2012), Ocean barrier layers' effect on tropical cyclone intensification, *PNAS,* 109, *36,* 14343–14347, doi:10.1073/pnas.1201364109.

Balaguru K, S Taraphdar, LR Leung and GR Foltz (2014), Increase in the intensity of postmonsoon Bay of Bengal tropical cyclones, *Geophys. Res. Lett.*, 41, 3594–3601, doi:10.1002/2014GL060197.

Bessafi, M., and Wheeler, M. C. (2006). Modulation of south Indian Ocean tropical cyclones by the Madden–Julian oscillation and convectively coupled equatorial waves. *Monthly Weather Review*, *134*(2), 638-656.

Cione JJ and EW Uhlhorn (2003), Sea surface temperature variability in hurricanes: Implications with respect to intensity change. *Mon. Wea. Rev., 131*, 1783–1796.

DeMaria M, CR Sampson, JA Knaff, KD Musgrave (2014), Is tropical cyclone intensity guidance improving? *Bull. Amer. Meteor. Soc*., 95, 387-398.

DeMaria, M., Mainelli, M., Shay, L. K., Knaff, J. A., & Kaplan, J. (2005). Further improvements to the statistical hurricane intensity prediction scheme (SHIPS). Weather and Forecasting, 20(4), 531-543.

Du, Y., Xie, S.-P., Huang, G. & Hu, K. M. Role of Air-Sea Interaction in the Long Persistence of El Nino-Induced North Indian Ocean Warming. J. Clim. 22, 2023–2038 (2009).

Duvel, J. P., Basdevant, C., Bellenger, H., Reverdin, G., Vialard, J., & Vargas, A. (2009). The Aeroclipper: A new device to explore convective systems and cyclones. *Bulletin of the American Meteorological Society*, *90*(1), 63-71.

Elsner, J. B., J. P. Kossin, and T. H. Jagger (2008). The increasing intensity of the strongest tropical cyclones. *Nature*, 455, 92–95.

Felton, C. S., Subrahmanyam, B., & Murty, V. S. N. (2013). ENSO-modulated cyclogenesis over the Bay of Bengal. *Journal of Climate*, *26*(24), 9806-9818.

Feng, M., McPhaden, M. J., Xie, S., & Hafner, J. La Niña forces unprecedented Leeuwin Current warming in 2011. Scientific Reports 3, 1277; DOI:10.1038/srep01277 (2013).

Feng, M., H. H. Hendon, S.-P. Xie, A. G. Marshall, A. Schiller, Y. Kosaka, N. Caputi, and A. Pearce (2015), Decadal increase in Ningaloo Niño since the late 1990s, Geophys. Res. Lett., 42, 104-112, doi:10.1002/2014GL062509.

Hobday et al., A hierarchical approach to defining marine heatwaves. Prog. Oceanogr., doi:10.1016/j.pocean.2015.12.014.

Karim, M.F., Mimura, N., 2008. Impacts of climate change and sea level rise on cyclonic storm surge floods in Bangladesh. Glob. Environ. Change 18, 490–500.

Kataoka T., T. Tozuka, S. Behera, and T. Yamagata, 2014: On the Ningaloo Niño/Niña, Clim. Dyn., 43, 1463-1482

Knapp KR, MC Kruk, DH Levinson, HJ Diamond and CJ Neumann (2010) The International Best Track Archive for Climate Stewardship (IBTrACS): Unifying Tropical Cyclone Data. Bull Amer Meteor Soc 91(3):363-376. doi:10.1175/2009BAMS2755.1.

Knutson TR, Sirutis JJ, Zhao M, et al (2015) Global Projections of Intense Tropical Cyclone Activity for the Late Twenty-First Century from Dynamical Downscaling of CMIP5/RCP4.5 Scenarios. http://dxdoiorg/101175/JCLI-D-15-01291 28:7203–7224. doi: 10.1175/JCLI-D-15-0129.1

Kossin, J. P., T. L. Olander, and K. R. Knapp (2013). Trend analysis with a new global record of tropical cyclone intensity. *J. Climate*, **26**, 9960–9976

Kuleshov, Y., Qi, L., Fawcett, R., & Jones, D. (2008). On tropical cyclone activity in the Southern Hemisphere: trends and the ENSO connection. Geophysical Research Letters, 35(14).

Lin II, CH Chen, IF Pun, WT Liu and CC Wu (2009), Warm ocean anomaly, air sea fluxes, and the rapid intensification of tropical cyclone Nargis (2008), *Geophys. Res. Lett.*, 36, L03817, doi:10.1029/ 2008GL035815.

Malan, N., Reason, C. J. C., & Loveday, B. R. (2013). Variability in tropical cyclone heat potential over the Southwest Indian Ocean. *Journal of Geophysical Research: Oceans*, *118*(12), 6734-6746.

Marshall, A.G., H.H. Hendon, M. Feng, and A Schiller, 2015: Initiation and amplification of the Ningaloo Niño, Clim. Dyn., doi:10.1007/s00382-015-2477-5

Murakami H., Mizuta R., Shindo E. (2011): Future changes in tropical cyclone activity projected by multi-physics and multi-SST ensemble experiments using the 60-km-mesh MRI-AGCM. Clim. Dyn. 39:2569–2584.

Needham, H. F., B. D. Keim, and D. Sathiaraj (2015), A review of tropical cyclone-generated storm surge: Global data sources, obervations, and impacts, Rev. Geophys., 53, 545-591, doi:10.1002/2014RG0004

Neetu, S., Lengaigne, M., Vincent, E. M., Vialard, J., Madec, G., Samson, G., ... & Durand, F. (2012). Influence of upper-ocean stratification on tropical cyclone-induced surface cooling in the Bay of Bengal. *Journal of Geophysical Research: Oceans*, *117*(C12).

Paul, B. K. (2009), Why relatively fewer people died? The case of Bangladesh's Cyclone Sidr, Nat. Hazards, 50, 289–304.

Pearce, A. F. & Feng, M. The rise and fall of the "marine heat wave" off Western Australia during the summer of 2010/2011. J. Mar. Syst. 111–112, 139–156 (2013).

Price, J. F. (1981). Upper ocean response to a hurricane. Journal of Physical Oceanography, 11(2), 153-175.

Ramsay, H. A., S. J. Camargo, and D. Kim (2012), Cluster analysis of tropical cyclone tracks in the Southern Hemisphere. *Climate Dyn.*, **39**, 897–917, doi:10.1007/s00382-011-1225-8.

Ramsay, H. A., M. B. Richman, and L. M. Leslie (2017), The modulating influence of Indian Ocean sea surface temperatures on Australian region seasonal tropical cyclone counts. *J. Climate*, 30, 4843-4856.

Rajeevan M., Srinivasan J., Niranjan Kumar, Gnanaseelan C. and Ali M.M. (2013): On the epochal variation of intensity of tropical cyclones in the Arabian Sea. Atmospheric Science Letters vol. 14, issue 4; 249-255.

Singh OP (2007): Long-term trends in the frequency of severe cyclones of Bay of Bengal, observations and simulations. Mausam 58, 59-66.

Tozuka, T., Yokoi, T., & Yamagata, T. (2010). A modeling study of interannual variations of the Seychelles Dome. *Journal of Geophysical Research: Oceans*, *115*(C4).

Vialard, J., Duvel, J. P., Mcphaden, M. J., Bouruet-Aubertot, P., Ward, B., Key, E., ... & Cassou, C. (2009). Cirene: air–sea interactions in the Seychelles–Chagos thermocline ridge region. *Bulletin of the American Meteorological Society*, *90*(1), 45-61.

Vialard J, Drushka K, Bellenger H, et al (2012) Understanding Madden-Julian-Induced sea surface temperature variations in the North Western Australian Basin. Clim Dyn 41:3203–3218. doi: 10.1007/s00382-012-1541-7

Vincent, E. M., M. Lengaigne, G. Madec, J. Vialard, G. Samson, N. C. Jourdain, C. E. Menkes, and S. Jullien (2012a), Processes setting the characteristics of sea surface cooling induced by tropical cyclones, J. Geophys. Res., 117, C02020, doi:10.1029/2011JC007396.

Vincent, E. M., M. Lengaigne, J. Vialard, G. Madec, N. C. Jourdain, and S. Masson (2012b), Assessing the oceanic control on the amplitude of sea surface cooling induced by tropical cyclones, J. Geophys. Res., 117, C05023, doi:10.1029/2011JC007705.

Webster PJ (2008) Myanmar's deadly "daffodil." *Nat. Geosci.*, 1, 488–490.

Vincent EM, Emanuel KA, Lengaigne M, et al (2014) Influence of upper ocean stratification interannual variability on tropical cyclones. Journal of Advances in Modeling Earth Systems n/a–n/a. doi: 10.1002/2014MS000327

Wernberg, T. et al. An extreme climatic event alters marine ecosystem structure in a global biodiversity hotspot. Nat. Clim. Chang. 3, 78–82 (2013).

Wernberg T et al. 2016 Climate-driven regime shift of a temperate marine ecosystem. Science 353, 169–172

Xie, SP, Annamalai H, Schott FA, McCreary JP. 2002. Structure and mechanisms of South Indian Ocean climate variability. Journal of Climate. 15:864-878.

Yuan JP and J Cao (2013), North Indian Ocean tropical cyclone activities influenced by the Indian Ocean Dipole mode, Science China Earth Sciences, 56, 855–865.

Zhang, N., M. Feng, H. Hendon, A. Hobday, J. Zinke (2017), Opposite polarities of ENSO drive distinct patterns of coral bleaching potentials in the southeast Indian Ocean, Scientific Reports, 7, 2443.doi: 10.1038/s41598-017-02688-y

Zinke J, Rountrey A, Feng M, et al (2014) Corals record long-term Leeuwin current variability including Ningaloo Niño/Niña since 1795.

Chapter 5

Achuthavarier, D., and V. Krishnamurthy, 2011: Role of Indian and Pacific SST in Indian summer monsoon intraseasonal variability, J. Clim., 24(12), 2915–2930.

Ajayamohan RS, Rao SA, Yamagata T. 2008: Influence of Indian Ocean Dipole on poleward propagation of boreal summer intraseasonal oscillations. Journal of Climate 21: 5437–5454.

Annamalai, H., and M. J. Slingo, 2001: Active/break cycles: diagnosis of the intraseasonal variability of the Asian Summer Monsoon, Clim. Dyn., 18(1), 85–102.

Bellon, G., A.H. Sobel and J. Vialard, 2008: Ocean-atmosphere coupling in the monsoon intraseasonal oscillation: a simple model study, Journal of Climate, 21, 5254-5270.

DeMott, C. A., N. P. Klingaman, and S. J. Woolnough 2015: Atmosphere-ocean coupled processes in the Madden-Julian oscillation, *Rev. Geophys.,* 53, 1099–1154, doi:10.1002/2014RG000478.

Duvel, J. P., R. Roca, and J. Vialard, 2004: Ocean mixed layer temperature variations induced by intraseasonal convective perturbations over the Indian Ocean, *J. Atmos. Sci.*, *61*, 1004–1022.

Duvel J.P., and J. Vialard, 2007: Indo-Pacific sea surface temperature perturbations associated with intraseasonal oscillations of tropical convection. *J. Clim.* 20, 3056–3082.

Drushka, K., J. Sprintall, and S. T. Gille, 2012: In situ observations of Madden-Julian oscillation mixed layer dynamics in the Indian and western Pacific Oceans, *J. Clim.*, *25*, 2306–2328

Fu, X., W. Wang, J.-Y. Lee, B. Wang, K. Kikuchi, J. Xu, J. Li, and S. Weaver, 2015: Distinctive Roles of Air-Sea Coupling on Different MJO Events: A New Perspective Revealed from the DYNAMO/CINDY Field Campaign. *Mon. Wea. Rev*., 143 (3), 794-812.

Goswami, B. N., and R. S. Ajaya Mohan (2001), Intraseasonal oscillations and interannual variability of the Indian summer monsoon, J. Clim., 14(6), 1180–1198.

Halkides, D. J., D. E. Waliser, T. Lee, D. Menemenlis, and B. Guan 2015: Quantifying the processing controlling intraseasonal mixed-layer temperature variability in the tropical Indian Ocean, *J. Geophys. Res. Oceans*, *120*, 692–715, doi:10.1002/2014JC010139.

Han, W., D. Yuan, W. T. Liu and D. J. Halkides, 2007: Intraseasonal variability of the Indian Ocean sea surface temperature during boreal winter: Madden – Julian Oscillation verus submonthly forcing and processes, *J. Geophys. Res.,* 112, C04001, doi:10.1029/2006JC003791.

Han, W., T. Shinoda, L-L. Fu, and J. McCreary, 2006: Impact of atmospheric intraseasonal oscillations on the Indian Ocean dipole. J. Phys. Oceanogr., 36, 670-690.

Hendon, H.H., and B. Liebmann, 1990: A composite study of onset of the Australian monsoon. J. Atmos. Sci., 47, 2227-2240.

Hermes, J. and C. J. C. Reason, 2008: Annual cycle of the South Indian Ocean (Seychelles-Chagos) thermocline ridge in a regional ocean model. J. Geophys. Res., 113:C04035. doi:10.1029/2007JC004363.

439 Hoyos, C. D., and P. J. Webster (2007), The role of intraseasonal variability in the nature of Asian
440 monsoon precipitation, J. Clim., 20(17), 4402–4424.

441 Inness, P. M., and J. M. Slingo, 2006: The interaction of the Madden-Julian Oscillation with the
442 Maritime Continent in a GCM, *Q. J. R. Meteorol. Soc.*, 132 (618),1645-1667.

443 Jayakumar A, J. Vialard, M. Lengaigne, C. Gnanaseelan, J.P. McCreary, B. Praveen Kumar, 2011:
444 Processes controlling the surface temperature signature of the Madden-Julian Oscillation in the
445 thermocline ridge of the Indian Ocean. *Clim. Dyn*. 37:2217–2234.

446 Jongaramrungruang S, H. Seo H, and C. C. Ummenhofer, 2017: Intraseasonal rainfall variability in
447 the Indian Ocean during the summer monsoon: coupling with the ocean and modulation by the
448 Indian Ocean Dipole. Atmospheric Science Letters, 18, 88-95.

449 Karmakar, N., A. Chakraborty, and R. S. Nanjundiah, 2015: Decreasing intensity of monsoon low-
450 frequency intraseasonal variability over India, Environ. Res. Lett. 10 054018

451 Kemball-Cook, S., and B. Wang (2001), Equatorial waves and air–sea interaction in the boreal
452 summer intraseasonal oscillation, J. Clim., 14(13), 2923–2942.

453 Kemball-Cook, S., B. Wang, and X. Fu, 2002: Simulation of the ISO in the ECHAM4 model: The
454 impact of coupling with an ocean model, *J. Atmos. Sci.*, *59*, 1433–1453.

455 Kessler, W. S., and R. Kleeman, 2000: Rectification of the Madden-Julian oscillation into the ENSO
456 cycle. J. Climate, 13, 3560-3475.

457 Kessler, W. S., M. J. McPhaden, and K. M. Weickmann, 1995: Forcing of intraseasonal Kelvin
458 waves in the equatorial Pacific Ocean. J. Phys. Oceanogr., 23, 608-625.

459 Kim, H.-M., C. D. Hoyos, P. J. Webster, and I.-S. Kang, 2008: Sensitivity of MJO simulation and
460 predictability to sea surface temperature variability, *J. Clim.*, *21*, 5304–5317.

461 Krishnamurti, T. N., D. K. Oosterhof, and A. V. Metha, 1988: Air-sea interaction on the timescale of
462 30–50 days, *J. Atmos. Sci.*, *45*, 1304–1322.

463 Krishnamurti, T. N., and D. Subrahmanyam, 1982: The 30-50 day mode at 850 mb during MONEX,
464 *J. Atmos. Sci.*, *39*(9), 2088-2095.

465 Lau, K. M., and S. Yang, 1996: Seasonal variation, abrupt transition, and intraseasonal variability
466 associated with the Asian summer mon- soon in the GLA GCM, J. Clim., 9(5), 965–985.

467 Li, Y., W. Han, T. Shinoda, C. Wang, M. Ravichandran, and J.-W. Wang, 2014: Revisiting the
468 Wintertime Intraseasonal SST Variability in the Tropical South Indian Ocean: Impact of the Ocean
469 Interannual Variation, *J. Phys. Oceanogr.*, *44*(7), 1886-1907.

470 Li, Y., W. Han, T. Shinoda, C. Wang, R.-C. Lien, J. N. Moum, and J.-W. Wang, 2013: Effects of the
471 diurnal cycle in solar radiation on the tropical Indian Ocean mixed layer variability during wintertime
472 Madden-Julian oscillation, *J. Geophys. Res. Oceans*, *118*, 4945–4964, doi:10.1002/jgrc.20395.

473 Li, Y., W. Han, W. Wang, M. Ravichandran, and T. Shinoda (2017), Bay of Bengal salinity
474 stratification and Indian summer monsoon intrasea-

475 sonal oscillation: 1. Intraseasonal variability and causes, J. Geophys. Res. Oceans.

476 Li, Y., Han, W., Wang, W., Ravichandran, M., T. Shinoda, T. Lee, T.,. 2017a: Bay of Bengal Salinity
477 Stratification and Indian Summer Monsoon Intraseasonal Oscillation: 1. Intraseasonal variability
478 and causes. *J. Geophys. Res.-Oceans*, DOI: 10.1002/2017JC012692

479 Li, Y., Han, W., Wang, W., Ravichandran, M., Lee, T., Shinoda, T. 2017b: Bay of Bengal Salinity
480 Stratification and Indian Summer Monsoon Intraseasonal Oscillation: 2. Impact on SST and
481 convection. *J. Geophys. Res.-Oceans*, DOI: 10.1002/2017JC012692.

482 Liebmann, B., H. H. Hendon, and J. D. Glick, 1994: The relationship between tropical cyclones of
483 the eastern Pacific and Indian Oceans and the Madden-Julian oscillation. J. Meteor. Soc. Japan,
484 72, 401-411.

Madden, R. A., and P. R. Julian, 1972: Description of global-scale circulation cells in the tropics with a 40-50 day period. *J. Atmos. Sci.*, 29, 1109-1123.

Maloney, E. D., and D. L. Hartmann, 2000: Modulation of eastern North Pacific hurricanes by the Madden–Julian oscillation, *J. Clim.*, *13*, 1451 – 1460.

Maloney, E. D., and D. L. Hartmann, 2000: Modulation of hurricane activity in the Gulf of Mexico by the Madden-Julian Oscillation, Science, 287, 2002–2004, doi:10.1126/science.287.5460.2002.

Marshall, A.G., and H.H. Hendon. 2014: Impacts of the MJO in the Indian Ocean and on the Western Australian coast*., Clim. Dyn*. 42: 579. doi:10.1007/s00382-012-1643-2.

McPhaden, M. J., 1999: Genesis and evolution of the 1997–98 El Niño. Science, 283, 950–954.

McPhaden, M. J., 2002: Mixed layer temperature balance on intraseasonal timescales in the equatorial Pacific Ocean, *J. Climate*, *15*, 2632 – 2647.

McCreary J.P. Jr, Kundu P.K., Molinari R.L. 1993: A numerical investigation of dynamics, thermodynamics and mixed-layer processes in the Indian Ocean. Prog Oceanogr 31:181–244

Moum, J. N., and Coauthors, 2013: Air–sea interactions from westerly wind bursts during the November 2011 MJO in the Indian Ocean. *Bull. Amer. Meteor. Soc*., 95, 1185–1199.

Neale, R. and J. Slingo, 2003: The Maritime Continent and its role in the global climate: A GCM Study. *J. Climate,* 16, 834-848.

Napitu, A.M., A.L. Gordon, and K. Pujiana, 2015: Intraseasonal Sea Surface Temperature Variability across the Indonesian Seas. J. Climate, 28, 8710-8727.

Rajendran, K., and A. Kitoh, 2006: Modulation of tropical intraseasonal oscillations by ocean–atmosphere coupling, J. Clim., 19(3), 366–391.

Rao, R. R., and R. Sivakumar (2003), Seasonal variability of sea surface salinity and salt budget of the mixed layer of the north Indian Ocean, J. Geophys. Res., 108(C1), 3009, doi:10.1029/2001JC000907.

Roxy M, and Y. Tanimoto, 2007: Role of SST over the Indian Ocean in Influencing the Intraseasonal Variability of the Indian Summer Monsoon. J Meteorol Soc Jpn 85(3):349–358.

Sabeerali, C., 2014: Modulation of monsoon intraseasonal oscillations in the recent warming period. JGR-Atmospheres 119 (9):5185-5203.

Sengupta, D., B. N. Goswami, and R. Senan (2001), Coherent intraseasonal oscillations of ocean and atmosphere during the Asian summer monsoon, Geophys. Res. Lett., 28(21), 4127–4130.

Sengupta, D., G. N. Bharath Raj, M. Ravichandran, J. Sree Lekha, and F. Papa (2016), Near-surface salinity and stratification in the north Bay of Bengal from moored observations, Geophys. Res. Lett., 43, 4448–4456, doi:10.1002/2016GL068339.

Seo, H., A. C. Subramanian, A. J. Miller, and N. R. Cavanaugh, 2014: Coupled impacts of the diurnal cycle of sea surface temperature on the Madden-Julian Oscillation. *J. Climate*, 27, 8422-8443.

Seo, K.-H., J.-K. E. Schemm, W. Wang, and A. Kumar (2007), The boreal summer intraseasonal oscillation simulated in the NCEP climate fore- cast system: The effect of sea surface temperature, Mon. Weather Rev., 135(5), 1807–1827.

Shinoda, T., 2005: Impact of diurnal cycle of solar radiation on intraseasonal SST variability in the western equatorial Pacific. *J. Climate*, 18, 2628-2636.

Shinoda, T., and W. Han, 2005: Influence of Indian Ocean dipole on atmospheric subseasonal variability. J. Climate, 18, 3891-3909.

Shinoda, T., and H. H. Hendon (1998), Mixed layer modeling of intraseasonal variability in the tropical western Pacific and Indian Oceans, *J. Climate*, *11*, 2668–2685.

Shinoda, T., H. H. Hendon and J. Glick, 1998: Intraseasonal variability of surface fluxes and sea surface temperature in the tropical western Pacific and Indian Oceans. *J. Climate*, **11**, 1685-1702.

Sobel, A. H., Maloney, E. D., Bellon, G., and Frierson, D. M., 2008: The role of surface heat fluxes in tropical intraseasonal oscillations. *Nature Geoscience*, *1*(10), 653-657.

Sperber, K. R., 2004: Madden-Julian variability in NCAR CAM2.0 and CCSM2.0, *Clim. Dyn.*, *23*, 259–278.

Vecchi, G. A., and D. E. Harrison (2002), Monsoon breaks and subseasonal sea surface temperature variability in the Bay of Bengal, J. Clim., 15(12), 1485–1493.

Vialard, J., G. R. Foltz, M. J. McPhaden, J.-P. Duvel, and C. de Boyer Montégut, 2008: Strong Indian Ocean sea surface temperature signals associated with the Madden-Julian oscillation in late 2007 and early 2008, *Geophys. Res. Lett.*, *35*, L19608, doi:10.1029/2008GL035238.

Vialard, J., A. Jayakumar, C. Gnanaseelan, M. Lengaigne, D. Sengupta, B.N. Goswami, 2012: Processes of 30-90 day sea surface temperature variability in the Northern Indian Ocean during boreal summer, Clim. Dynamics, 38, 1901-1916.

Vialard, J., K. Drushka, H. Bellenger, M. Lengaigne, S. Pous and J-P. Duvel, 2013: Understanding Madden-Julian-induced sea surface temperature variations in the North Western Australian Basin, Clim. Dyn., 41, 3203-3218.

Vinayachandran, P. N., V. S. N. Murty, and V. Ramesh Babu (2002), Observations of barrier layer formation in the Bay of Bengal during summer monsoon, J. Geophys. Res., 107(C12), 8018, doi:10.1029/2001JC000831.

Vinayachandran, P. N., and N. H. Saji, 2008: Mechanisms of South Indian Ocean intraseasonal cooling, *Geophys. Res. Lett.*, *35*, L23607, doi:10.1029/2008GL035733.

Waliser, D. E., R. Murtugudde, and L. E. Lucas, 2003: Indo-Pacific Ocean response to atmospheric intraseasonal variability: 1. Austral summer and the Madden-Julian Oscillation, J. Geophys. Res., 108(C5), 3160, doi:10.1029/2002JC001620.

Waliser, D. E., R. Murtugudde, and L. E. Lucas (2004), Indo-Pacific Ocean response to atmospheric intraseasonal variability: 2. Boreal summer and the intraseasonal oscillation, J. Geophys. Res, 109, C03030, doi:10.1029/2003JC002002.

Wang, W., M. Chen, and A. Kumar (2009), Impacts of ocean surface on the northward propagation of the boreal summer intraseasonal oscillation in the NCEP climate forecast system, J. Clim., 22(24), 6561–6576.

Webster, P. J., and R. Lukas, 1992: TOGA COARE: Coupled Ocean–Atmosphere Response Experiment. Bull. Amer. Meteor. Soc.,73, 1377–1416.

Webster, P. J., V. Magaa, T. Palmer, J. Shukla, R. Tomas, M. U. Yanai, and T. Yasunari, 1998: Monsoons: Processes, predictability, and the prospects for prediction, J. Geophys. Res., 103(C7), 14,451–14,510.

Webster, P. J., et al. (2002), The JASMINE pilot study, Bull. Am. Meteorol. Soc., 83, 1603–1630.

Weickmann, K. M., G. R. Lussky, and J. E. Kutzbach, 1985: Intraseasonal (30-60 day) fluctuations of outgoing longwave radiation and 250mb streamfunction during northern winter. Mon. Wea. Rev., 113, 941-961.

Weller, R.A., and Coauthors, 2016: Air-sea interaction in the Bay of Bengal. Oceanography 29(2):28–37.

Weller, R. A., and S. P. Anderson, 1996: Surface meteorology and air–sea fluxes in the western equatorial Pacific warm pool during the TOGA Coupled Ocean Atmosphere Response Experiment. J. Climate, 9, 1959–1990.

Wheeler, M. C., and H. H. Hendon, 2004: An all-season real-time multivariate MJO index: Development and index for monitoring and prediction, *Mon. Weather Rev.*, *132*, 1917–1932.

Woolnough, S. J., F. Vitart, and M. A. Balmaseda, 2007: The role of the ocean in the Madden-Julian oscillation: Implications for MJO prediction, *Q. J. R. Meteorol. Soc.*, *133*, 117–128.

Xie, S-P., H. Annamalai, F. A. Schott, and J. P. McCreary, 2002: Structure and mechanisms of south Indian Ocean climate variability. J. Climate, 15, 864–878.

Yasunari, T., 1979: Cloudiness fluctuations associated with the Northern Hemisphere summer monsoon, *J. Meteorol. Soc. Jpn*, *57*, 227–242.

Yasunari, T., 1980: A quasi-stationary appearance of 30 to 40 day period in the cloudiness fluctuations during the summer monsoon over India, J. Meteorol. Soc. Jpn., 58, 225–229

Yoneyama, K., C. Zhang, C.N. Long, 2013: Tracking pulses of the Madden-Julian oscillation. Bull. Amer. Meteorol. Soc. , 94, 1871–1891.

Zhang, C., M. Dong, S. Gualdi, H. H. Hendon, E. D. Maloney, A. Marshall, K. R. Sperber, and W. Wang, 2006: Simulations of the Madden-Julian oscillation in four pairs of coupled and uncoupled global models, *Clim. Dyn.*, *27*, 573–592.

Chapter 6

Behera, S. K., and T. Yamagata, 2001: Subtropical SST dipole events in the southern Indian Ocean. *Geophys. Res. Lett.*, **28,** 327–330.

Cai, W., A. Santoso, G. Wang, E. Weller, L. Wu, K. Ashok, Y. Masumoto, and T. Yamagata, 2014: Increased frequency of the Indian Ocean Dipole events due to greenhouse warming. *Nature*, **510,** 254–258.

Depczynski, M. et al., 2013: Bleaching, coral mortality and subsequent survivorship on a West Australian fringing reef. *Coral Reefs*, **32,** 233–238.

Doi, T., S. K. Behera, and T. Yamagata, 2013: Predictability of Ningaloo Niño/Niña. *Sci. Rep.*, **3,** 2892, doi:10.1038/srep02892.

Doi, T., S. K. Behera, and T. Yamagata, 2016: Improved seasonal prediction using the SINTEX-F2 coupled model. *J. Adv. Modeling Earth Sys.*, **8,** 1847–1867.

Doi, T., A. Storto, S. K. Behera, A. Navarra, and T. Yamagata, 2017: Improved prediction of the Indian Ocean Dipole Mode by use of subsurface ocean observations. *J. Clim.*, **30,** 7953–7970.

Du, Y., S.-P. Xie, Y.-L. Yang, X.-T. Zheng, L. Liu, and G. Huang, 2013: Indian Ocean variability in the CMIP5 multimodel ensemble: The basin mode. *J. Clim.*, **26,** 7240–7266.

Feng, M., M. J. McPhaden, S.-P. Xie, and J. Hafner, 2013: La Niña forces unprecedented Leeuwin Current warming in 2011. *Sci. Rep.*, **3,** 1277, doi:10.1038/srep01277.

Feng, M., H. H. Hendon, S.-P. Xie, A. G. Marshall, A. Schiller, Y. Kosaka, N. Caputi, and A. Pearce, 2015a: Decadal increase in Ningaloo Niño since the late 1990s. *Geophys. Res. Lett.*, **42,** 104–112.

Feng, M., A. Marshall, and H. H. Hendon, 2015b: A review of progress in understanding the Ningaloo Niño. *CLIVAR Exchanges No. 68*, 4–6.

Feng, M., J. Benthuysen, N. Zhang, and D. Slawinski, 2015c: Freshening anomalies in the Indonesian throughflow and impacts on the Leeuwin Current during 2010–2011. *Geophys. Res. Lett.*, **42,** 8555–8562.

Halkides, D. J., and T. Lee, 2009: Mechanisms controlling seasonal-to-interannual mixed layer temperature variability in the southeastern tropical Indian Ocean. *J. Geophys. Res.*, **114,** C02012, doi:10.1029/2008JC004949.

618 Horii, T., H. Hase, I. Ueki, and Y. Masumoto, 2008: Oceanic precondition and evolution of the 2006
619 Indian Ocean Dipole. *Geophys. Res. Lett*., **35,** L03607, doi:10.1029/2007GL032464.

620 Kataoka, T., T. Tozuka, and T. Yamagata, 2012: The Indian Ocean subtropical dipole mode
621 simulated in the CMIP3 models. *Clim. Dyn.*, **39,** 1385–1399.

622 Kataoka, T., T. Tozuka, S. K. Behera, and T. Yamagata, 2014: On the Ningaloo Niño/Niña. *Clim.*
623 *Dyn.*, **43,** 1463–1482.

624 Kataoka, T., T. Tozuka, and T. Yamagata, 2017: Generation and decay mechanisms of Ningaloo
625 Niño/Niña. *J. Geophys. Res. Oceans*, doi: 10.1002/2017JC012966.

626 Kido, S., T. Kataoka, and T. Tozuka, 2016: Ningaloo Niño simulated in the CMIP5 models. *Clim.*
627 *Dyn.*, **47,** 1469–1484.

628 Kido, S., and T. Tozuka, 2017: Salinity variability associated with the positive Indian Ocean Dipole
629 and its impact on the upper ocean temperature. *J. Clim.*, **30,** 7885-7907.

630 Klein, S. A., B. J. Soden, and N. C. Lau, 1999: Remote sea surface temperature variations during
631 ENSO: evidence for a tropical atmospheric bridge. *J. Clim.*, **12,** 917–932.

632 Liu, H., Y. Tang, D. Chen, and T. Lian, 2017: Predictability of the Indian Ocean Dipole in the coupled
633 models. *Clim. Dyn.*, **48,** 2005–2024.

634 Liu, L. S.-P. Xie, X.-T. Zheng, T. Li, Y. Du, G. Huang, and W. Yu, 2014: Indian Ocean variability in
635 the CMIP5 multi-model ensemble: the zonal dipole mode. *Clim. Dyn.*, **43,** 1715–1730.

636 Luo, J.-J., S. Masson, S. Behera, and T. Yamagata, 2007: Experimental forecasts of the Indian
637 Ocean Dipole using a coupled OAGCM. *J. Clim.*, **20,** 2178–2190.

638 Luo, J.-J., S. Behera, Y. Masumoto, H. Sakuma, and T. Yamagata, 2008: Successful prediction of
639 the consecutive IOD in 2006 and 2007. *Geophys. Res. Lett.*, **35,** L14S02,
640 doi:10.1029/2007GL032793.

641 Luo, J.-J., and Coauthors, 2016: Current status of intraseasonal-seasonal-to-interannual prediction
642 of the Indo-Pacific climate, in Indo-Pacific Climate Variability and Predictability, chap. 3, pp. 63–
643 107, World Sci. Publ. Co.

644 Marshall, A. G., and H. H. Hendon, 2014: Impacts of the MJO in the Indian Ocean and on the
645 Western Australian coast. *Clim. Dyn.*, **42,** 579-595.

646 Marshall, A. G., H. H. Hendon, M. Feng, and A. Schiller, 2015: Initiation and amplification of the
647 Ningaloo Niño. *Clim. Dyn.*, **45,** 2367–2385.

648 McPhaden, M. J., and M. Nagura, 2014: Indian Ocean Dipole interpreted in terms of recharge
649 oscillator theory. *Clim. Dyn*., **42,** 1569–1586.

650 McPhaden, M.J., Y. Wang, and M. Ravichandran, 2015: Volume transports of the Wyrtki Jets and
651 their Relationship to the Indian Ocean Dipole. *J. Geophys. Res*., **120,** 5302-5317,
652 doi:10.1002/2015JC010901.

653 Morioka, Y., T. Tozuka, and T. Yamagata, 2010: Climate variability in the southern Indian Ocean
654 as revealed by self-organizing maps. *Clim. Dyn.*, **35,** 1075–1088.

655 Nagura, M., and M. J. McPhaden, 2010: Dynamics of zonal current variations associated with the
656 Indian Ocean Dipole. *J. Geophys. Res*., **115,** C11026, doi:10.1029/2010JC006423.

657 Qiu, Y., W. Cai, L. Li, and X. Guo, 2012: Argo profiles variability of barrier layer in the tropical Indian
658 Ocean and its relationship with the Indian Ocean Dipole. *Geophys. Res. Lett.*, **39,** L08605,
659 doi:10.1029/2012GL051441.

660 Rao, S. A., and T. Yamagata, 2004: Abrupt termination of Indian Ocean dipole events in response
661 to intraseasonal disturbances. *Geophys. Res. Lett.*, **31,** L19306, doi:10.1029/2004GL020842.

662 Rayner, N. A., D. E. Parker, E. B. Horton, C. K. Folland, L. V. Alexander, D. P. Rowell, E. C. Kent,
663 and A. Kaplan, 2003: Global analyses of sea surface temperature, sea ice, and night marine air
664 temperature since the late nineteenth century. *J. Geophys. Res.*, **108,** 4407,
665 10.1029/2002JD002670.

666 Reason, C. J. C., 2001: Subtropical Indian Ocean dipole events and southern African rainfall.
667 *Geophys. Res. Lett.*, **28,** 2225–2227.

668 Reverdin, G., D. L. Cadet, and D. Gutzler, 1986: Interannual displacements of convection and
669 surface circulation over the equatorial Indian Ocean. *Quart. J. Roy. Meteorol. Soc.*, **112,** 43–67.

670 Saji, N. H., B. N. Goswami, P. N. Vinayachandran, and T. Yamagata, 1999: A dipole mode in the
671 tropical Indian Ocean. *Nature*, **401,** 360–363.

672 Saji, N. H., and T. Yamagata, 2003: Possible impacts of Indian Ocean Dipole events on global
673 climate. *Clim. Res.*, **25,** 151–169.

674 Saji, N. H., S.-P., Xie, and T. Yamagata, 2006: Tropical Indian Ocean variability in the IPCC
675 twentieth-century climate simulations. *J. Clim.*, **19,** 4397–4417.

676 Tanizaki, C., T. Tozuka, T. Doi, and T. Yamagata, 2017: Relative importance of the processes
677 contributing to the development of SST anomalies in the eastern pole of the Indian Ocean Dipole
678 and its implication for predictability. *Clim. Dyn.*, doi:10.1007/s00382-016-3382-2.

679 Tozuka, T., T. Kataoka, and T. Yamagata, 2014: Locally and remotely forced atmospheric
680 circulation anomalies of Ningaloo Niño/Niña. *Clim. Dyn.*, **43,** 2197–2205.

681 Wajsowicz, R. C., 2005: Potential predictability of tropical Indian Ocean SST anomalies. *Geophys.*
682 *Res. Lett.*, **32,** L24702, doi: 10.1029/2005GL024169.

683 Webster, P. J., A. M. Moore, J. P. Loschnigg, and R. R. Leben, 1999: Coupled ocean–atmosphere
684 dynamics in the Indian Ocean during 1997-98. *Nature*, **401,** 356–360.

685 Wernberg T., D. A. Smale, F. Tuya, M. S. Thomsen, T. J. Langlois, T. de Bettignies, S. Bennett, C.
686 S. Rousseaux, 2013: An extreme climatic event alters marine ecosystem structure in a global
687 diversity hotspot. *Nat. Clim. Change*, **3,** 78–82.

688 Wernberg, T. and Coauthors, 2016: Climate-driven regime shift of a temperate marine ecosystem.
689 *Science*, **353,** 169–172.

690 Xie, S.-P., K. Hu, J. Hafner, H. Tokinaga, Y. Du, G. Huang, and T. Sampe, 2009: Indian Ocean
691 capacitor effect on Indo–Western Pacific climate during the summer following El Niño. *J. Clim.*, **22,**
692 730–747.

693 Yamagata, T., S. K. Behera, J.-J. Luo, S. Masson, M. R. Jury, S. A. Rao, 2004: Coupled ocean-
694 atmosphere variability in the tropical Indian Ocean. In Earth's climate: The ocean-atmosphere
695 interaction. *Geophys. Monogr. Ser.*, **147,** 189–211.

696 Yang, J., Q. Liu, S.-P. Xie, Z. Liu, and L. Wu, 2007: Impact of the Indian Ocean SST basin mode
697 on the Asian summer monsoon. *Geophys. Res. Lett.*, **34,** L02708, doi:10.1029/2006GL028571.

698 Yang, Y., S.-P. Xie, L. Wu, Y. Kosaka, N.-C. Lau, and G. A. Vecchi, 2015: Seasonality and
699 predictability of the Indian Ocean Dipole mode: ENSO forcing and internal variability. *J. Clim.*, **28,**
700 8021–8036.

701 Yu, L., and M. Rienecker, 1999: Mechanisms for the Indian Ocean warming during the 1997–98 El
702 Niño. *Geophys. Res. Lett.*, **26,** 735–738.

703 Yuan, C., T. Tozuka, J.-J. Luo, and T. Yamagata, 2014: Predictability of the subtropical dipole
704 modes in a coupled ocean–atmosphere model. *Clim. Dyn.*, **42,** 1291–1308.

705 Zhang, Y., Y. Du, S. Zheng, Y. Yang, and X. Cheng, 2013: Impact of Indian Ocean dipole on the
706 salinity budget in the equatorial Indian Ocean. *J. Geophys. Res. Oceans*, **118,** 4911–4923.

Zheng, X. T., S.-P. Xie, G. A. Vecchi, Q. Liu, and J. Hafner, 2010: Indian Ocean Dipole response to global warming: Analysis of ocean–atmospheric feedbacks in a coupled model. *J. Clim.*, **23,** 1240–1253.

Chapter 7

Alory, G., Wijffels, S., and Meyers, G. (2007). Observed temperature trends in the Indian Ocean over 1960–1999 and associated mechanisms. Geophysical Research Letters, 34(2).

Bindoff, N. L., and McDougall, T. J. (2000). Decadal changes along an Indian Ocean section at 32 S and their interpretation. Journal of Physical Oceanography, 30(6), 1207-1222.

Bryden, H. L., and Beal, L. M. (2001). Role of the Agulhas Current in Indian Ocean circulation and associated heat and freshwater fluxes. Deep Sea Research Part I, 48(8), 1821-1845.

Cai, W., Cowan, T., Dix, M., Rotstayn, L., Ribbe, J., Shi, G., and Wijffels, S. (2007). Anthropogenic aerosol forcing and the structure of temperature trends in the southern Indian Ocean. Geophysical Research Letters, 34(14).

Cheng L., K. Trenberth, J. Fasullo, T. Boyer, J. Abraham, J. Zhu, (2017) Improved estimates of ocean heat content from 1960 to 2015, Science Advances, 3, e1601545.

Desbruyeres, D., E. L. McDonagh, B. A. King, and V. Thierry (2017). Global and full-depth ocean temperature trends during the early 21st century from Argo and repeat hydrography. J. Climate, 30(6), 1985-1997, 10.1175/JCLI-D-16-0396.1

Feng, M., C. Böning, A. Biastoch, E. Behrens, E. Weller, and Y. Masumoto (2011), The reversal of the multi-decadal trends of the equatorial Pacific easterly winds, and the Indonesian Throughflow and Leeuwin Current transports, Geophys. Res. Lett., 38, L11604, doi:10.1029/2011GL047291.

Feng, M., Zhang, X., Sloyan, B., and Chamberlain, M. (2017). Contribution of the deep ocean to the centennial changes of the Indonesian Throughflow. Geophysical Research Letters, 44(6), 2859-2867.

Funk, C., Dettinger, M. D., Michaelsen, J. C., Verdin, J. P., Brown, M. E., Barlow, M., and Hoell, A. (2008). Warming of the Indian Ocean threatens eastern and southern African food security but could be mitigated by agricultural development. Proceedings of the national academy of sciences, 105(32), 11081-11086.

Ganachaud, A. and C. Wunsch, 2000: Improved estimates of global ocean circulation, heat transport and mixing from hydrographic data. Nature, 408 (6811), 453–457.

Han, W., Meehl, G. A., Rajagopalan, B., Fasullo, J. T., Hu, A., and Lin, J. (2010). Patterns of Indian Ocean sea-level change in a warming climate.

Han, W., J. Vialard, M. J. McPhaden, T. Lee, Y. Masumoto, M. Feng, and W. P. de Ruijter, 2014: Indian ocean decadal variability: A review. Bulletin of the American Meteorological Society, 95(11), 1679-1703.

Hernández-Guerra, A., and Talley, L. D. (2016). Meridional overturning transports at 30 S in the Indian and Pacific Oceans in 2002–2003 and 2009. Progress in Oceanography, 146, 89-120.

Johns, W. E., Baringer, M. O., Beal, L. M., Cunningham, S. A., Kanzow, T., Bryden, H. L., ... and Curry, R. (2011). Continuous, array-based estimates of Atlantic Ocean heat transport at 26.5 N. J. Climate, 24(10), 2429-2449.

Kanzow, T., Cunningham, S. A., Johns, W. E., Hirschi, J. J., Marotzke, J., Baringer, M. O., ... and Collins, J. (2010). Seasonal variability of the Atlantic meridional overturning circulation at 26.5 N. J. Climate, 23(21), 5678-5698.

Katsumata, K., and Masuda, S. (2013). Variability in Southern Hemisphere Ocean Circulation from the 1980s to the 2000s. Journal of Physical Oceanography, 43(9), 1981-2007.

Lee, S.-K., W. Park, M. O. Baringer, A. Gordon, B. Huber and Y. Liu (2015), Pacific origin of the abrupt increase in Indian Ocean heat content during the warming hiatus, Nature Geosci., 8, 445-450.

Lumpkin, R. and K. Speer, 2007: Global ocean meridional overturning. J. Phys. Oceanogr., 37 (10), 2550–2562.

McDonagh, E. L., Bryden, H. L., King, B. A., Sanders, R. J., Cunningham, S. A., and Marsh, R. (2005). Decadal changes in the South Indian Ocean thermocline. Journal of Climate, 18(10), 1575-1590.

McDonagh, E. L., H. L. Bryden, B. A. King, and R. J. Sanders, 2008: The circulation of the Indian Ocean at 32 S. Progress in Oceanography, 79 (1), 20–36.

Macdonald, A. M. (1998). The global ocean circulation: a hydrographic estimate and regional analysis. Progress in Oceanography, 41(3), 281-382.

Purkey, S. G., and Johnson, G. C. (2010). Warming of global abyssal and deep Southern Ocean waters between the 1990s and 2000s: Contributions to global heat and sea level rise budgets. J. Climate, 23(23), 6336-6351.

Robbins, P. E. and J. M. Toole, 1997: The dissolved silica budget as a constraint on the meridional overturning circulation of the indian ocean. Deep Sea Res. Part I, 44 (5), 879–906.

Roberts, C. D., Palmer, M. D., Allan, R. P., Desbruyeres, D. G., Hyder, P., Liu, C., and Smith, D. (2017). Surface flux and ocean heat transport convergence contributions to seasonal and interannual variations of ocean heat content. J. Geophys. Res.: Oceans, 122(1), 726-744.

Roxy et al. 2016: A reduction in marine primary productivity driven by rapid warming over the tropical Indian Ocean. Geophys. Res. Lett., 43, 826-833

Smith, R. L., A. Huyer, J. S. Godfrey, and J. Church, 1991: The Leeuwin Current off western Australia, 1986–1987. J. Phys. Oceanogr., 21, 323–345.

Sprintall, J., and A. Révelard (2014), The Indonesian Throughflow response to Indo-Pacific climate variability. J. Geophys. Res., 119, 1161-1175, doi:10.1002/2013JC009533.

Sprintall, J., Gordon, A. L., Koch-Larrouy, A., Lee, T., Potemra, J. T., Pujiana, K., and Wijffels, S. E. (2014). The Indonesian seas and their role in the coupled ocean-climate system. Nature Geoscience, 7(7), 487-492.

Talley, L. D. (2008). Freshwater transport estimates and the global overturning circulation: Shallow, deep and throughflow components. Progress in Oceanography, 78(4), 257-303.

Talley, L. D., 2013: Closure of the global overturning circulation through the Indian, Pacific and Southern Oceans: Schematics and transports. Oceanography, 26 (1), 80–97.

Watson, P. J. (2011). Is there evidence yet of acceleration in mean sea level rise around mainland Australia?. Journal of Coastal Research, 27(2), 368-377.

Wijffels, S. E., Meyers, G., and Godfrey, J. S. (2008). A 20-yr average of the Indonesian Throughflow: Regional currents and the interbasin exchange. Journal of Physical Oceanography, 38(9), 1965-1978.

Wu, L., Cai, W., Zhang, L., Nakamura, H., Timmermann, A., Joyce, T., ... and Chang, P. (2012). Enhanced warming over the global subtropical western boundary currents. Nature Climate Change, 2(3), 161.

Yang, H., Lohmann, G., Wei, W., Dima, M., Ionita, M., and Liu, J. (2016). Intensification and poleward shift of subtropical western boundary currents in a warming climate. Journal of Geophysical Research: Oceans, 121(7), 4928-4945.

Chapter 8

Bakker, D. C. E., and et al. 2014. 'An update to the Surface Ocean CO2 Atlas (SOCAT version 2)', *Earth Systems Science Data*, 6: 69-90.

Bates, N. R., A. C. Pequignet, and C. L. Sabine. 2006. 'Ocean carbon cycling in the Indian Ocean: I. Spatio-temporal variability of inorganic carbon and air-sea CO_2 gas exchange', *Global Biogeochemical Cycles*, 20: GB3020.

Bednarsek, N., G. A. Tarling, D. C. E. Bakker, S. Fielding, E. M. Jones, H. J. Venables, P. Ward, A. Kuzirian, B. Leze, R. A. Feely, and E. J. Murphy. 2012. 'Extensive dissolution of live pteropods in the Southern Ocean', *Nature Geoscience*, 5: 881-85.

de Moel, H., G. M. Ganssen, F. J. C. Peeters, S. J. A. Jung, D. Kroon, G. J. A. Brummer, and R. E. Zeebe. 2009. 'Planktonic foraminiferal shell thinniing in the Arabian Sea due to anthropogenic ocean acidification?', *Biogeosciences*, 6: 1917-25.

Doney, S. C. 2010. 'The growing human footprint on coastal and open-ocean biogeochemistry', *Science*, 328: 1512-16.

Feely, R. A., S. C. Doney, and S. R. Cooley. 2009. 'Ocean acidification: Present conditions and future changes in a high-CO_2 world', *Oceanography*, 22: 36-47.

Gattuso, J.-P., and L. Hansson. 2011. *Ocean Acidification* (Oxford University Press: Oxford, UK).

Graham, N. A. J., S. K. Wilson, S. Jennings, N. V. C. Polunin, J. Robinson, J. P. Bijoux, and T. M. Daw. 2007. 'Lag effects in the impacts of mass coral bleaching on coral reef fish, fisheries, and ecosystems', *Conservation Biology*, 21: 1291-300.

Hoegh-Guldberg, O., P. J. Mumby, A. J. Hooten, R. S. Steneck, P. Greenfield, E. Gomez, C. D. Harvell, P. F. Sale, A. J. Edwards, K. Caldeira, N. Knowlton, C. M. Eakin, R. Iglesias-Prieto, N. Muthiga, R. H. Bradbury, A. Dubi, and M. E. Hatziolos. 2007. 'Coral reefs under rapid climate change and oceand acidification', *Science*, 318: 1737-42.

Hood, R. R. , V. J. Coles, A. J. Sutton, and M. J McPhaden. 2017. 'Physical forcing of air-sea carbon flux in the Bay of Bengal', *Geophysical Research Letters*, in preparation.

Hutchins, D. A., F.-X. Fu, Y. Zhang, M. E. Warner, Y. Feng, K. Portune, P. W. Bernhardt, and M. R. Mulholland. 2007. 'CO_2 control of Trichodesmium N_2 fixation, photosynthesis, growth rates, and elemental ratios: Implications for past, present, and future ocean biogeography', *Limnology and Oceanography*, 52: 1293-304.

IPCC. 2007. The Physical Science Basis. Contribution of Working Group I to the Fourth Assessment Report of the Intergovernmental Panel on Climate Change, S. Solomon et al., Eds. (Cambridge Univ. Press, Cambridge, UK, and New York, 2007).

McClanahan, T. R., M. Ateweberhan, N. A. J. Graham, S. K. Wilson, C. R. Sebastian, M. M. M. Guillaume, and J. H. Bruggemann. 2007. 'Western Indian Ocean coral communities: bleaching responses and susceptibility to extinction', *Marine Ecology Progress Series*, 337: 1-13.

Moore, J. A. Y., L. M. Bellchambers, M. R. Depczynski, R. D. Evans, S. N. Evans, S. N. Field, K. J. Friedman, J. P. Gilmour, T. H. Holmes, R. Middlebrook, B. T. Radford, T. Ridgway, G. Shedrawi, H. Taylor, D. P. Thomson, and S. K. Wilson. 2012. Unprecedented mass bleaching and loss of coral across 12º of latitude in Western Australia in 2010-11. *PLoS ONE*, 7(12): e51087. doi:10.1317/journal.pone.0051807.

Pierrot, Denis, Craig Neill, Kevin Sullivan, Robert Castle, Rik Wanninkhof, Heike Lüger, Truls Johannessen, Are Olsen, Richard A. Feely, and Catherine E. Cosca. 2009. 'Recommendations for autonomous underway pCO2 measuring systems and data-reduction routines', *Deep Sea Research Part II: Topical Studies in Oceanography*, 56: 512-22.

Piketh, S. J. , P. D. Tyson, and W. Steffen. 2000. 'Aeolian transport from southern Africa and iron fertilization of marine biota in the South Indian Ocean', *South African Journal of Science*, 96: 244-46.

Rashid, T., S. Hoque, and F. Akter. 2013. 'Ocean acidification in the Bay of Bengal', *Scientific Reports*, 2: 699.

Sarma, V. V. S. S., A. Lenton, R. M. Law, N. Metzl, P. K. Patra, S. Doney, I. D. Lima, E. Dlugokencky, M. Ramonet, and V. Valsala. 2013. 'Sea-air CO2 fluxes in the Indian Ocean between 1990 and 2009', *Biogeosciences*, 10: 7035-52.

Sutton, A. J., C. L. Sabine, S. Maenner-Jones, N. Lawrence-Slavas, C. Meinig, R. A. Feely, J. T. Mathis, S. Musielewicz, R. Bott, P. D. McLain, H. J. Fought, and A. Kozyr. 2014. 'A high-frequency atmospheric and seawater pCO2 data set from 14 open-ocean sites using a moored autonomous system', *Earth System Science Data*, 6: 353-66.

Takahashi, T., and et al. 2009. 'Climatological mean and decadal change in surface ocean pCO2, and net sea-air CO2 flux over the global ocean', *Deep-Sea Rearch, part II*, 56: 554-77.

Takahashi, T., S.C. Sutherland, D. Chipman, J. G. Goddard, C. Ho, T. Newberger, C. Sweeney, and D. R. Munro. 2014. 'Climatological distributions of pH, pCO2, total CO2, alkalinity, and CaCO3 saturationh in the global surface ocean, and temporal changes at selected locations', *Marine Chemistry*, 164: 95-125.

Takahashi, T., S.C. Sutherland, C. Sweeney, A. Poisson, N. Metzl, B. Tilbrook, N. Bates, R. Wanninkhof, R.A. Feely, C. Sabine, J. Olafsson, and Y. Nojiri. 2002. 'Global sea-air CO_2 flux based on climatological surface ocean pCO_2, and seasonal biological and temperature effects', *Deep-Sea Research Part II*, 49: 1601-23.

Valsala, V., S. Maksyutov, and R. Murtugudde. 2012. 'A window for carbon uptake in the southern subtropical Indian Ocean', *Geophysical Research Letters*, 39: L17605.

Wiggert, J. D., R. G. Murtugudde, and J. R. Christian. 2006. 'Annual ecosystem variability in the tropical Indian Ocean: Results of a coupled bio-physical ocean general circulation model', *Deep-Sea Research, Part II*, 53: 644-76.

Chapter 9

Alford, M. H., M. C. Gregg, and M. Ilyas (1999), Diapycnal mixing in the Banda Sea: Results of the first microstructure measurements in the Indonesian Throughflow, *Geophys.Res. Lett.*, 26, 2741–2744.

Beal, Lisa M., and Shane Elipot. "Broadening not strengthening of the Agulhas Current since the early 1990s." *Nature* 540.7634 (2016): 570-573.

Beal, Lisa M., et al. "Capturing the transport variability of a western boundary jet: Results from the Agulhas Current Time-Series Experiment (ACT)." *Journal of Physical Oceanography* 45.5 (2015): 1302-1324.

Beal, Lisa M., et al. "The response of the surface circulation of the Arabian Sea to monsoonal forcing." *Journal of Physical Oceanography* 43.9 (2013): 2008-2022.

Beal, Lisa M., and Teresa K. Chereskin. "The volume transport of the Somali Current during the 1995 southwest monsoon." *Deep Sea Research Part II: Topical Studies in Oceanography* 50.12 (2003): 2077-2089.

Benthuysen, J., Furue, R., McCreary, J., Bindoff, N. and Phillips, H., 2014: Dynamics of the Leeuwin Current: Part 2. Impacts of mixing, friction, and advection on a buoyancy-driven eastern boundary current over a shelf. *Dynamics of Atmospheres and Oceans.* Vol. 65, pp 39-63.

885 Cai, W., Borlace, S., Lengaigne, M., Van Rensch, P., Collins, M., Vecchi, G., Timmermann, A.,
886 Santoso, A., McPhaden, M.J. and Wu, L., 2014. Increasing frequency of extreme El Niño events
887 due to greenhouse warming. Nature climate change, 4(2): 111-116.

888 Cai, W., Wang, G., Santoso, A., McPhaden, M.J., Wu, L., Jin, F.-F., Timmermann, A., Collins, M.,
889 Vecchi, G. and Lengaigne, M., 2015. Increased frequency of extreme La Niña events under
890 greenhouse warming. Nature Climate Change, 5(2): 132-137.

891 Deckker, P., 2016: The Indo-Pacific warm pool: critical to world oceanography and world climate,
892 *Geosci. Lett.,* 3:20, DOI 10.1186/s40562-016-0054-3.

893 Domingues, C., M. Maltrud, S. Wijffels, J. Church, and M. Tomczak, 2007: Simulated Lagrangian
894 pathways between the Leeuwin Current System and the upper-ocean circulation of the southeast
895 Indian Ocean. Deep-Sea Res. II, 54, 797–817, doi:10.1016/j.dsr2.2006.10.003.

896 Elipot, Shane, and Lisa M. Beal. "Characteristics, energetics, and origins of Agulhas Current
897 meanders and their limited influence on ring shedding." *Journal of Physical Oceanography* 45.9
898 (2015): 2294-2314.

899 Feng, M., G. Meyers, A. Pearce, S. Wijffels, 2003: Annual and Interannual Variations of the
900 Leeuwin Current at 32°S. *Journal of Geophysical Research*, **108**(11), 3355.

901 Feng, M., C. Boning, A. Biastoch, E. Behrens, E. Weller, and Y. Masumoto (2011), The reversal of
902 the multi-decadal trends of the equatorial Pacific easterly winds, and the Indonesian Throughflow
903 and Leeuwin Current transports. *Geophys. Res. Lett*., **38**, L11604, doi:10.1029/2011GL047291.

904 Feng, M., McPhaden, M. J., Xie, S., & Hafner, J. *La Niña* forces unprecedented Leeuwin Current
905 warming in 2011. *Scientific Reports* **3**, 1277; DOI:10.1038/srep01277 (2013).

906 Feng, M., X. Zhang, B. Sloyan, and M. Chamberlain (2017), Contribution of the deep ocean to the
907 centennial changes of the Indonesian Throughflow, Geophys. Res. Lett., 44,
908 doi:10.1002/2017GL072577.

909 Ffield, A., and A. L. Gordon,1996: Tidal mixing signatures in the Indonesian seas, *J. Phys.*
910 *Oceanogr*., 26, 1924–1937.

911 Furue, R., McCreary, J.P., Benthuysen, J., Phillips, H. and Bindoff, N., 2013: Dynamics of the
912 Leeuwin Current: Part 1. Coastal flows in an inviscid, variable-density, layer model. *Dynamics of*
913 *Atmospheres and Oceans.* Vol. 63, pp 24-59.

914 Furue, R., K. Guerreiro, H.E. Phillips, J. P. McCreary and N. Bindoff, 2017: On the Leeuwin Current
915 System and its linkage to zonal flows in the South Indian Ocean as inferred from a gridded
916 hydrography. *J. Phys. Oceanogr.* Vol 47, pp. 583-602. DOI: 10.1175/JPO-D-16-0170.1

917 Gordon, A. L., J. Sprintall, H. M.Van Aken, R. D. Susanto, S. Wijffels, R. Molcard, A. L. Ffield, W.
918 Pranowo, and S. Wirasantosa, 2010: The Indonesian Throughflow during 2004-2006 as observed
919 by the INSTANT program. *Dyn. Atmos. Oceans*, 50 115-128,
920 doi:10.1016/j.dynatmoce.2009.12.002

921 Han, W., Vialard, J., McPhaden, M. J., Lee, T., Masumoto, Y., Feng, M., & De Ruijter, W. P. (2014).
922 Indian Ocean decadal variability: A review. *Bulletin of the American Meteorological Society*, *95*(11),
923 1679-1703.

924 Hatayama, T., 2004: Transformation of the Indonesian throughflow water by vertical mixing and its
925 relation to tidally generated internal waves, *J. Oceanography*, 60 (3), 569–585.

926 International CLIVAR project office, 2006: Understanding The Role Of The Indian Ocean In The
927 Climate System — Implementation Plan For Sustained Observations. January. International
928 CLIVAR Project Office, CLIVAR Publication Series No.100. (not peer reviewed).

929 Koch-Larrouy, A., G. Madec, P. Bouruet-Aubertot, T. Gerkema, L. Bessi`eres, and R. Molcard ,
930 2007: On the transformation of PacificWater into Indonesian ThroughflowWater by internal tidal
931 mixing, *Geophys. Res. Lett.*, 34, L04,604, doi:10.1029/2006GL028405.

Koch-Larrouy, A., M. Lengaigne, P. Terray, G. Madec, and S. Masson, 2010: Tidal mixing in the Indonesian Seas and its effect on the tropical climate system, *Clim. Dyn*., 34, 891–904, doi:10.1007/s00382-009-0642-4

Koch-Larrouy, A., A. Atmadipoera, P. van Beek, G. Madec, J. Aucan, F. Lyard, J. Grelet, and M. Souhaut, 2015: Estimates of tidal mixing in the Indonesian archipelago from multidisciplinary INDOMIX in-situ data, *Deep-Sea Res*., 106, 136–153.

Lee, S-K, W. Park, M. O. Baringer, A L. Gordon, B. Huber and Y.Liu, 2015: Pacific origin of the abrupt increase in Indian Ocean heat content during the warming hiatus, *Nature Geoscience*, doi:10.1038/ngeo2438.

Liang, X, Spall, M and Wunsch, C. 2017. Global ocean vertical velocity from a dynamically consistent ocean state estimate. *Journal of Geophysical Research: Oceans, 122.* doi:10.1002/2017JC012985.

Liu, Q, M. Feng, D. Wang, S.Wijffels (2015), Interannual variability of the Indonesian Throughflow transport: a revisit based on 30-year expendable bathythermograph data, J. Geophys. Res., 120, 8270-8282, doi:10.1002/2015JC011351.

McCreary, J. P., S. R. Shetye, and P. K. Kundu, 1986: Thermohaline forcing of eastern boundary currents: With application to the circulation off the west coast of Australia. J. Mar. Res., 44, 71–92, doi:10.1357/002224086788460184.

Menezes, V. V., H. E. Phillips, A. Schiller, C. Domingues, N. L. Bindoff, 2013: Salinity dominance on the Indian Ocean Eastern Gyral Current. *Geophysical Research Letters.* Vol. 40, 1–6, doi:10.1002/2013GL057887.

Menezes, V. V., H. E. Phillips, A. Schiller, N. L. Bindoff, C. M. Domingues, and M. L. Vianna (2014), South Indian Countercurrent and associated fronts, *J. Geophys. Res. Oceans*, **119**, 6763–6791,

Meyers, G., R. J. Bailey, and A. P. Worby (1995), Geostrophic transport of Indonesian Throughflow, Deep Sea Res. Part I, 42(7), 1163–1174.

Meyers, G. (1996), Variation of Indonesian throughflow and the El Nino– Southern Oscillation, J. Geophys. Res., 101(C5), 12,255–12,263.

Nagai, T., and T. Hibiya, 2015: Internal tides and associated vertical mixing in the Indonesian Archipelago, *J. Geophys. Res*., 120, 3373–3390, doi:10.1002/2014JC010592.

Nauw, J. J., et al. "Observations of the southern East Madagascar Current and undercurrent and countercurrent system." *Journal of Geophysical Research: Oceans* 113.C8 (2008).

Palastanga, V., P. J. van Leeuwen, M. W. Schouten, and W. P. M. de Ruijter (2007), Flow structure and variability in the subtropical Indian Ocean: Instability of the South Indian Ocean Countercurrent, J. Geophys. Res., 112, C01001, doi:10.1029/2005JC003395.

Potemra, J. T., 2005: Indonesian throughflow transport variability estimated from satellite altimetry, *Oceanogr.*, 18, 94–103.

Ray, R. and R. D. Susanto, 2016: Tidal mixing signatures in the Indonesian seas from high-resolution sea-surface temperature, *Geophys. Res. Lett.*, 43, doi:10.1002/2016GL069485

Ridderinkhof, H., et al. "Seasonal and interannual variability in the Mozambique Channel from moored current observations." *Journal of Geophysical Research: Oceans* 115.C6 (2010).

Ridderinkhof, W., et al. "Dipoles of the South East Madagascar Current." *Geophysical Research Letters* 40.3 (2013): 558-562.

Schott, F., and J. P. McCreary (2001), The monsoon circulation of the Indian Ocean, *Prog. Oceanogr.*, **51**, 1–123.

977 Schott, F. A., S.-P. Xie, and J. P. McCreary, 2009: Indian Ocean circulation and climate variability.
978 Rev. Geophys., 47, RG1002, doi:10.1029/2007RG000245.

979 Sen Gupta, A., S. McGregor, E. van Sebille, A. Ganachaud, J. Brown, and A.
980 Santoso (2016), Future changes to the Indonesian Throughflow and Pacific circulation: The
981 differing role of wind and deep circulation changes, *Geophys. Res. Lett.*, **43**, 1669–1678,

982 Siedler, G., M. Rouault, and J. Lutjeharms (2006), Structure and origin of the subtropical South
983 Indian Ocean Countercurrent, Geophys. Res. Lett., 33, L24609, doi:10.1029/2006GL027399.

984 Smith, R. L., A. Huyer, J. S. Godfrey, and J. A. Church, 1991: The Leeuwin Current off Western
985 Australia, 1986–1987. J. Phys. Oceanogr., 21, 323–345, doi:10.1175/1520-0485(1991)021,0323:
986 TLCOWA.2.0.CO;2.

987 Sprintall, J., S. E. Wijffels, R. Molcard, and I. Jaya, 2009: Direct estimates of the Indonesian
988 throughflow entering the Indian Ocean: 2004-2006, *J. Geophys. Res.*, 114, C07001,
989 doi:10.1029/2008JC005257.

990 Sprintall, J., A. L. Gordon, A. Koch-Larrouy, T. Lee, J. T. Potemra, K. Pujiana, and S. Wijffels ,
991 2014: The Indonesian Seas and their role in the coupled ocean-climate system, *Nature Geosci.*, 7,
992 487–492.

993 Sprintall, J., and A. Revelard, 2014: The Indonesian throughflow response to Indo-Pacific climate
994 variability, *J. Geophys. Res. Oceans*, 119, 1161–1175, doi:10.1002/2013JC009533.

995 Susanto, R. D. , A. L. Gordon Q. Zheng, 2001 : Upwelling along the coasts of Java and Sumatra
996 and its relation to ENSO, *Geophys. Res. Lett.*, 28, 8, 1599-1602, DOI: 10.1029/2000GL011844.

997 Susanto, R. D., and J. Marra, 2005: The effect on 1997/98 El Nino on chlorophyll-a concentration
998 along the southern coasts of Java and Sumatra, *Oceanography*, 18, 4, 124-127,
999 DOI:10.5670/oceanog.2005.13

1000 Susanto, R.D., A.L. Gordon and J. Sprintall, 2007: Observations and Proxies of the Surface Layer
1001 Throughflow in Lombok Strait, *J. Geophys. Res.-Oceans*, Vol. 112, No. C3, C03S92,
1002 10.1029/2006JC003790.

1003 Susanto, R D; Fang, G; Soesilo, I; Zheng, Q; Qiao, F; Wei, Z; Sulistyo, B., 2010: New Surveys of
1004 a Branch of the Indonesian Throughflow, *EOS Trans. AGU*, 91 (30), doi:10.1029/2010EO300002

1005 Susanto, R. D, Z. Wei, T.R. Adi, B. Fan, S. Li, and G. Fang, 2013: Karimata throughflow from
1006 December 2007 to November 2008, *Acta Oceanol. Sin.*, 32,5,p1-6, DOI: 10.1007/s13131-013-
1007 0307-3.

1008 Susanto, R. D, Y.T. Song, 2015: Indonesian throughflow proxy from satellite altimeters and
1009 gravimeters, *J. Geophys. Res. Oceans*, 120, doi:10.1002/2014JC010382

1010 Susanto, R. D., Z. Wei, T. R. Adi, Q. Zheng, G. Fang, F. Bin, A. Supangat, T. Agustiadi, S. Li, M.
1011 Trenggono, and Agus Setiawan, 2016: Oceanography Surrounding Krakatau Volcano in the Sunda
1012 Strait, Indonesia, *Oceanography*, 29, 2, 228-237, http://dx.doi.org/10.5670/ oceanog.2016.31.

1013 Talley, L. D., Pickard, G. L., Emery, W. J., Swift, J. H, 2011: Descriptive Physical Oceanography:
1014 an introduction. Sixth edition, Academic Press.

1015 Thompson, R. O. R. Y., 1984: Observations of the Leeuwin Current off Western Australia. J. Phys.
1016 Oceanogr., 14, 623–628, doi:10.1175/1520-0485

1017 Wainwright, L., G. Meyers, S. Wijffels, and L. Pigot (2008), Change in the Indonesian Throughflow
1018 with the climatic shift of 1976/77, Geophys. Res. Lett., 35, L03604, doi:10.1029/2007GL031911.

1019 Wei, Z. X., Fang, G. H., Susanto, R. D., Adi, T. R., Fan, B., Setiawan, A., Li, S. J., Wang, Y. G.,
1020 and Gao, X. M., 2016: Tidal elevation, current and energy flux in the area between the South China
1021 Sea and Java Sea, *Ocean Sci.*, 12, 2831-2861, doi:10.5194/osd-12-2831-2015.

Wijffels, S. E., G. Meyers, and J. S. Godfrey, 2008: A 20-yr average of the Indonesian Throughflow: Regional currents and the interbasin exchange. J. Phys. Oceanogr., 38, 1965–1978, doi:10.1175/2008JPO3987.1.

Woo, L. M., and C. B. Pattiaratchi, 2008: Hydrography and water masses off the western Australian coast. Deep-Sea Res. I, 55, 1090–1104, doi:10.1016/j.dsr.2008.05.005.

Zhuang, W., M. Feng, Y. Du, A. Schiller, and D. Wang (2013): Low-frequency sea level variability in the southern Indian Ocean and its impacts on the oceanic meridional transports, J. Geophys. Res. Oceans, 118, 1302-1315.

Chapter 10

Alexander, M. (2010). Extratropical Air-Sea Interaction, Sea Surface Temperature Variability, and the Pacific Decadal Oscillation. *Climate Dynamics: Why Does Climate Vary?*, 123-148.

Alory G, Wijffels S, Meyers G (2007) Observed temperature trends in the Indian Ocean over 1960–1999 and associated mechanisms. Geophysical Research Letters 34 (2).

Annamalai, H., Murtugudde, R., Potemra, J., Xie, S. P., Liu, P., & Wang, B. (2003). Coupled dynamics over the Indian Ocean: Spring initiation of the zonal mode. *Deep Sea Research Part II: Topical Studies in Oceanography*, **50,** 2305-2330.

Behera, S. K., & Yamagata, T. (2001). Subtropical SST dipole events in the southern Indian Ocean. *Geophysical Research Letters*, **28,** 327-330.

Dong, L., Zhou, T., Dai, A., Song, F., Wu, B., & Chen, X. (2016). The footprint of the inter-decadal Pacific oscillation in Indian Ocean sea surface temperatures. *Scientific reports*, **6.**

Dong, L. and M.J. McPhaden (2016); Interhemispheric SST gradient trends in the Indian Ocean prior to and during the recent global warming hiatus. J. Climate, 29, 9077-9095.

Dong, L. and M.J. McPhaden (2017). Why has the relationship between Indian and Pacific Ocean decadal variability changed in recent decades? J. Climate, 30, 1971-1983.

Feng, M., Meyers, G., Pearce, A., & Wijffels, S. (2003). Annual and interannual variations of the Leeuwin Current at 32 S. *Journal of Geophysical Research: Oceans*, **108.**

Feng, M., Y. Li, and G. Meyers (2004), Multidecadal variations of Fremantle sea level: Footprint of climate variability in the tropical Pacific, *Geophys. Res. Lett.,* **31,** L16302, doi:10.1029/2004GL019947.

Feng M, McPhaden MJ, Xie S, Hafner J (2013) La Niña forces unprecedented Leeuwin Current warming in 2011. *Sci Rep,* **3,** doi:10.1038/srep01277

Feng, M., H. H. Hendon, S.-P. Xie, A. G. Marshall, A. Schiller, Y. Kosaka, N. Caputi, and A. Pearce (2015), Decadal increase in Ningaloo Niño since the late 1990s, *Geophys. Res. Lett.,* **42,** doi:10.1002/2014GL062509.

Gordon, A. L., Sprintall, J., Van Aken, H. M., Susanto, D., Wijffels, S., Molcard, R., ... & Wirasantosa, S. (2010). The Indonesian throughflow during 2004–2006 as observed by the INSTANT program. *Dynamics of Atmospheres and Oceans*, **50,** 115-128.

Han, W., Vialard, J., McPhaden, M. J., Lee, T., Masumoto, Y., Feng, M., & De Ruijter, W. P. (2014a). Indian Ocean decadal variability: A review. *Bulletin of the American Meteorological Society*, **95,** 1679-1703.

Han, W., Meehl, G. A., Hu, A., Alexander, M. A., Yamagata, T., Yuan, D., ... & Quan, X. W. (2014b). Intensification of decadal and multi-decadal sea level variability in the western tropical Pacific during recent decades. *Climate dynamics*, **43,** 1357-1379.

Klein, S. A., B. J. Soden, and N.-C. Lau, 1999: Remote sea surface temperature variations during ENSO: Evidence for a tropical atmospheric bridge. *J. Clim.,* **12,** 917–932.

Kosaka, Y., and S.-P. Xie, 2013: Recent global-warming hiatus tied to equatorial Pacific surface cooling. *Nature,* **501,** 403–407, doi:10.1038/nature12534.

Lau KM, Weng HY (1999) Interannual, decadal-interdecadal, and global warming signals in sea surface temperature during 1955-97. Journal of Climate 12 (5):1257-1267

Lee, T., and M. J. McPhaden (2008), Decadal phase change in large-scale sea level and winds in the Indo-Pacific region at the end of the 20th century, *Geophys. Res. Lett.,* **35,** doi:10.1029/2007GL032419.

Lee, S.-K., W. Park, M. O. Baringer, A. L. Gordon, B. Huber, and Y. Liu, 2015: Pacific origin of the abrupt increase in Indian Ocean heat content during the warming hiatus. *Nat. Geosci.,* **8,** 445–449, doi:10.1038/ngeo2438.

Liu, Z. (2012). Dynamics of interdecadal climate variability: a historical perspective. *Journal of Climate*, **25,** 1963-1995.

Liu, W., Xie, S. P., & Lu, J. (2016). Tracking ocean heat uptake during the surface warming hiatus. *Nature communications*, **7.**

Nidheesh, A.G., M. Lengaigne, J. Vialard, T. Izumo, A.S. Unnikrishnan, B. Meyssignac, B. Hamlington and C. de Boyer Montégut, 2017: Robustness of observationally-derived decadal sea-level variability in the Indo-Pacific region, *Geophys. Res. Lett.,* **in revision.**

Nidheesh, A.G., M. Lengaigne, J. Vialard, A.S. Unnikrishnan and H. Dayan, 2013: Decadal and long-term sea level variability in the tropical Indo-Pacific Ocean, *Clim. Dyn.,* **41,** 381-402.

Nieves, V., J. K. Willis, and W. C. Patzert, 2015: Recent hiatus caused by decadal shift in Indo-Pacific heating. *Science,* **349,** 532–535, doi:10.1126/science.aaa4521.

Roxy MK, Ritika K, Terray P, Masson S (2014) The curious case of Indian Ocean warming. Journal of Climate 27 (22):8501-8509. doi:10.1175/JCLI-D-14-00471.1.

Schott, F. A., Dengler, M., & Schoenefeldt, R. (2002). The shallow overturning circulation of the Indian Ocean. *Progress in Oceanography,* **53,** 57-103.

Srinivasu, U., M. Ravichandran, W. Han,S. Sivareddy, H. Rahman, Y. Li, and S. Nayak, 2017: Causes for the reversal of North Indian Ocean decadal sea level trend in recent two decades. *Clim. Dyn.,* DOI: 10.1007/s00382-017-3551-y .

Thompson, P. R., C. G. Piecuch,, M. A. Merrifield, J. P. McCreary, and E. Firing (2016), Forcing of recent decadal variability in the Equatorial and North Indian Ocean, *J. Geophys. Res. Oceans,* **121,** 6762–6778, doi:10.1002/2016JC012132.

Tozuka, T., Luo, J. J., Masson, S., & Yamagata, T. (2007). Decadal modulations of the Indian Ocean dipole in the SINTEX-F1 coupled GCM. *Journal of climate*, **20,** 2881-2894.

Ummenhofer, C. C., Biastoch, A., & Böning, C. W. (2017). Multidecadal Indian Ocean variability linked to the Pacific and implications for preconditioning Indian Ocean dipole events. *Journal of Climate,* **30,** 1739-1751.

Vialard, J., 2015: Hiatus heat in the Indian Ocean, *Nature Geoscience,* doi:10.1038/ngeo2442.

Xie, S. P., Hu, K., Hafner, J., Tokinaga, H., Du, Y., Huang, G., & Sampe, T. (2009). Indian Ocean capacitor effect on Indo–western Pacific climate during the summer following El Niño. *Journal of Climate*, **22,** 730-747.

Yu, W., B. Xiang, L. Liu, and N. Liu (2005), Understanding the origins of interannual thermocline variations in the tropical Indian Ocean, *Geophys. Res. Lett.,* **32,** doi:10.1029/2005GL024327.

Zinke, J., Hoell, A., Lough, J. M., Feng, M., Kuret, A. J., Clarke, H., ... & McCulloch, M. T. (2015). Coral record of southeast Indian Ocean marine heatwaves with intensified Western Pacific temperature gradient. *Nature communications*, **6.**

Chapter 11

Alory G, Wijffels S, Meyers G (2007) Observed temperature trends in the Indian Ocean over 1960–1999 and associated mechanisms. Geophysical Research Letters 34 (2)

Barnett TP, Pierce DW, AchutaRao KM, Gleckler PJ, Santer BD, Gregory JM, Washington WM (2005) Penetration of human-induced warming into the world's oceans. Science 309 (5732):284-287

Cheng L, Zheng F, Zhu J (2015) Distinctive ocean interior changes during the recent warming slowdown. Scientific reports 5, 14346; doi: 10.1038/srep14346.

Cheng L., K. Trenberth, J. Fasullo, T. Boyer, J. Abraham, J. Zhu, (2017) Improved estimates of ocean heat content from 1960 to 2015, Science Advances, 3, e1601545.

Dong, L., and T. Zhou, 2014a: The Indian Ocean Sea Surface Temperature Warming Simulated by CMIP5 Models during the 20th Century: Competing Forcing Roles of GHGs and Anthropogenic Aerosols, Journal of Climate, 27, 3348-3362

Dong L, Zhou T, Wu B (2014b) Indian Ocean warming during 1958–2004 simulated by a climate system model and its mechanism. Climate Dynamics 42 (1-2):203-217

Dong Lu, Tianjun Zhou, Aiguo Dai, Fengfei Song, Bo Wu, Xiaolong Chen, 2016: The Footprint of the Inter-decadal Pacific Oscillation in Indian Ocean Sea Surface Temperatures, Scientific Reports,6:21251, DOI:10.1038/srep21251.

Du Y, Xie SP (2008) Role of atmospheric adjustments in the tropical Indian Ocean warming during the 20th century in climate models. Geophysical Research Letters 35 (8)

Durack PJ, Wijffels SE (2010) Fifty-year trends in global ocean salinities and their relationship to broad-scale warming. Journal of Climate 23 (16):4342-4362.

Durack, P. J., Gleckler, P. J., Landerer, F. W., & Taylor, K. E. (2014). Quantifying underestimates of long-term upper-ocean warming. Nature Climate Change, 4(11), 999-1005.

Durack, P. J., Wijffels, S. E., & Gleckler, P. J. (2014). Long-term sea-level change revisited: the role of salinity. Environmental Research Letters, 9(11), 114017.

Durack, P. J., Lee, T., Vinogradova, N. T., & Stammer, D. (2016). Keeping the lights on for global ocean salinity observation. Nature Climate Change, 6(3), 228-231.

Gasparin F, Roemmich D, Gilson J, Cornuelle B (2015) Assessment of the upper-ocean observing system in the equatorial Pacific: The role of Argo in resolving intraseasonal to interannual variability. Journal of Atmospheric and Oceanic Technology 32 (9):1668-1688.

Gille, S. T. (2008). Decadal-scale temperature trends in the Southern Hemisphere ocean. Journal of Climate, 21(18), 4749-4765.

Giannini A., R. Saravanan, and P. Chang, 2003: Oceanic forcing of Sahel rainfall on interannual to interdecadal time scales. Science, 302, 1027-1030.

Gleckler, P. J., Santer, B. D., Domingues, C. M., Pierce, D. W., Barnett, T. P., Church, J. A., ... & Caldwell, P. M. (2012). Human-induced global ocean warming on multidecadal timescales. Nature Climate Change, 2(7), 524-529.

Gnanaseelan C, Roxy MK, Deshpande A (2017) Variability and Trends of Sea Surface Temperature and Circulation in the Indian Ocean. In: Rajeevan MN, Nayak S (eds) Observed Climate Variability and Change over the Indian Region. Springer Singapore, Singapore, pp 165-179. doi:10.1007/978-981-10-2531-0_10.

1154 Hamlington, B. D., Strassburg, M. W., Leben, R. R., Han, W., Nerem, R. S., & Kim, K. Y. (2014).
1155 Uncovering an anthropogenic sea-level rise signal in the Pacific Ocean. Nature Climate Change,
1156 4(9), 782-785.

1157 Han W, Meehl GA, Rajagopalan B, Fasullo JT, Hu A, Lin J, Large WG, Wang J-w, Quan X-W,
1158 Trenary LL (2010) Patterns of Indian Ocean sea-level change in a warming climate. Nature
1159 Geoscience 3 (8):546-550.

1160 Han, W., Meehl, G. A., Hu, A., Alexander, M. A., Yamagata, T., Yuan, D., ... & Quan, X. W. (2014).
1161 Intensification of decadal and multi-decadal sea level variability in the western tropical Pacific
1162 during recent decades. Climate dynamics, 43(5-6), 1357-1379.

1163 Hoerling, M., J.W. Hurrell, T. Xu, G. Bates, A. Phillips, 2004: Twentieth century north Atlantic
1164 climate change. Part II: understanding the effect of Indian Ocean warming. Clim. Dyn., 23, 391-
1165 405.

1166 Hoerling, Martin, Jon Eischeid, Judith Perlwitz, Xiaowei Quan, Tao Zhang, Philip Pegion, 2012: On
1167 the Increased Frequency of Mediterranean Drought. J. Climate, 25, 2146–2161.

1168 Hosoda, S., Suga, T., Shikama, N., & Mizuno, K. (2009). Global surface layer salinity change
1169 detected by Argo and its implication for hydrological cycle intensification. Journal of Oceanography,
1170 65(4), 579-586.

1171 Ihara C, Kushnir Y, Cane MA (2008) Warming trend of the Indian Ocean SST and Indian Ocean
1172 dipole from 1880 to 2004. Journal of Climate 21 (10):2035-2046. doi:Doi 10.1175/2007jcli1945.1

1173 IPCC (2013) IPCC WGI Fifth Assessment Report, Chapter 3 - Observations: Ocean.

1174 IPCC (2013) IPCC WGI Fifth Assessment Report, Chapter 13 Sea Level Change.

1175 Kay S. and coauthors, 2015: Modelling the increased frequency of extreme sea levels in the
1176 Ganges-Brahmaputra-Meghna delta due to sea level rise and other effects of climate change.
1177 Environ Sci Process Impacts., 17, 1311-22.

1178 Knutson TR, Delworth TL, Dixon KW, Held IM, Lu J, Ramaswamy V, Schwarzkopf MD, Stenchikov
1179 G, Stouffer RJ (2006) Assessment of twentieth-century regional surface temperature trends using
1180 the GFDL CM2 coupled models. Journal of Climate 19 (9):1624-1651

1181 Lau KM, Weng HY (1999) Interannual, decadal-interdecadal, and global warming signals in sea
1182 surface temperature during 1955-97. Journal of Climate 12 (5):1257-1267.

1183 Lee S-K, Park W, Baringer MO, Gordon AL, Huber B, Liu Y (2015) Pacific origin of the abrupt
1184 increase in Indian Ocean heat content during the warming hiatus. Nature Geosci 8 (6):445-449.
1185 doi:10.1038/ngeo2438.

1186 Levitus S, Antonov JI, Boyer TP, Baranova OK, Garcia HE, Locarnini RA, Mishonov AV, Reagan
1187 J, Seidov D, Yarosh ES (2012) World ocean heat content and thermosteric sea level change (0–
1188 2000 m), 1955–2010. Geophysical Research Letters 39 (10).

1189 Li, G., Xie, S. P., & Du, Y. (2016). A robust but spurious pattern of climate change in model
1190 projections over the tropical Indian Ocean. Journal of Climate, 29(15), 5589-5608.

1191 Liu, W., Lu, J., & Xie, S. P. (2015). Understanding the Indian Ocean response to double CO2.
1192 Ocean Dynamics, 65(7), 1037-1046.

1193 Luo, J. J., Sasaki, W., & Masumoto, Y. (2012). Indian Ocean warming modulates Pacific climate
1194 change. Proceedings of the National Academy of Sciences, 109(46), 18701-18706.

1195 Luo, Y., Lu, J., Liu, F., & Wan, X. (2016). The positive Indian Ocean Dipole–like response in the
1196 tropical Indian Ocean to global warming. Advances in Atmospheric Sciences, 33(4), 476-488.

1197 Nidheesh A, Lengaigne M, Vialard J, Unnikrishnan A, Dayan H (2013) Decadal and long-term sea
1198 level variability in the tropical Indo-Pacific Ocean. Climate dynamics 41 (2):381-402

1199 Pierce DW, Barnett TP, AchutaRao KM, Gleckler PJ, Gregory JM, Washington WM (2006)
1200 Anthropogenic warming of the oceans: observations and model results. Journal of Climate 19
1201 (10):1873-1900.

1202 Rahul, S., & Gnanaseelan, C. (2016). Can large scale surface circulation changes modulate the
1203 sea surface warming pattern in the Tropical Indian Ocean?. Climate dynamics, 46(11-12), 3617-
1204 3632.

1205 Rao SA, Dhakate AR, Saha SK, Mahapatra S, Chaudhari HS, Pokhrel S, Sahu SK (2012) Why is
1206 Indian Ocean warming consistently? Climatic change 110 (3-4):709-719

1207 Roxy MK, Ritika K, Terray P, Masson S (2014) The curious case of Indian Ocean warming. Journal
1208 of Climate 27 (22):8501-8509. doi:10.1175/JCLI-D-14-00471.1

1209 Roxy MK, Ritika K, Terray P, Murtugudde R, Ashok K, Goswami BN (2015) Drying of Indian
1210 subcontinent by rapid Indian Ocean warming and a weakening land-sea thermal gradient. Nature
1211 Communications 6:7423. doi:10.1038/ncomms8423.

1212 Roxy, M. K., Modi, A., Murtugudde, R., Valsala, V., Panickal, S., Prasanna Kumar, S., ... & Lévy,
1213 M. (2016). A reduction in marine primary productivity driven by rapid warming over the tropical
1214 Indian Ocean. Geophysical Research Letters, 43(2), 826-833.

1215 Saha A, Ghosh S, Sahana A, Rao E (2014) Failure of CMIP5 climate models in simulating post-
1216 1950 decreasing trend of Indian monsoon. Geophysical Research Letters 41 (20):7323–7330.

1217 Sallée, J. B., Speer, K., Rintoul, S., & Wijffels, S. (2010). Southern Ocean thermocline ventilation.
1218 Journal of Physical Oceanography, 40(3), 509-529.

1219 Schuckmann Kv, Traon P-YL (2011) How well can we derive Global Ocean Indicators from Argo
1220 data? Ocean Science 7 (6):783-791.

1221 Skliris, N., Marsh, R., Josey, S. A., Good, S. A., Liu, C., & Allan, R. P. (2014). Salinity changes in
1222 the World Ocean since 1950 in relation to changing surface freshwater fluxes. Climate dynamics,
1223 43(3-4), 709-736.

1224 Srinivasu U, Ravichandran M, Han W, Sivareddy S, Rahman H, Li Y, Nayak S (2017) Causes for
1225 the reversal of North Indian Ocean decadal sea level trend in recent two decades. Climate
1226 Dynamics:1-18.

1227 Stott, P. A., Sutton, R. T., & Smith, D. M. (2008). Detection and attribution of Atlantic salinity
1228 changes. Geophysical Research Letters, 35(21).

1229 Stramma, L., Schmidtko, S., Levin, L. A., & Johnson, G. C. (2010). Ocean oxygen minima
1230 expansions and their biological impacts. Deep Sea Research Part I: Oceanographic Research
1231 Papers, 57(4), 587-595.

1232 Terray, L., Corre, L., Cravatte, S., Delcroix, T., Reverdin, G., & Ribes, A. (2012). Near-surface
1233 salinity as nature's rain gauge to detect human influence on the tropical water cycle. Journal of
1234 Climate, 25(3), 958-977.

1235 Trenberth K, K., J. Fasullo, K. v. Schuckmann, L. Cheng (2016), Insights into Earth's energy
1236 imbalance from multiple sources. Journal of Climate, 29, 7495-7505.

1237 Unnikrishnan A, Nidheesh A, Lengaigne M (2015) Sea-level-rise trends off the Indian coasts during
1238 the last two decades.

1239 Wang G., Cheng L., Abraham, J., Li, C., (2017) Consensuses and discrepancies of basin-scale
1240 ocean heat content changes in different ocean analyses. Climate Dynamic, doi: 10.1007/s00382-
1241 017-3751-5.

1242 Yao, S. L., Huang, G., Wu, R. G., Qu, X., & Chen, D. (2016). Inhomogeneous warming of the
1243 Tropical Indian Ocean in the CMIP5 model simulations during 1900–2005 and associated
1244 mechanisms. Climate dynamics, 46(1-2), 619-636.

Chapter 12

Barber, R. T., J. Marra, R. R. Bidigare, L. A. Codispoti, D. Halpern, Z. Johnson, R. Latasa, R. Goericke, and S. L. Smith (2001), Primary productivity and its regulation in the Arabian Sea during 1995, Deep Sea Research II, 48, 1127-1172, doi: 1110.1016/S0967-0645(1100)00134-X.

Behrenfeld, M. J., and P. G. Falkowski (1997), Photosynthetic rates derived from satellite-based chlorophyll concentration, Limnol. and Oceanogr., 42(1), 1-20.

Biogeochemical-Argo Planning Group. 2016. The scientific rationale, design and Implementation Plan for a Biogeochemical-Argo float array. Edited by Ken Johnson and Hervé Claustre. doi:10.13155/46601.

Currie, J. C., M. Lengaigne, J. Vialard, D. M. Kaplan, O. Aumont, S. W. A. Naqvi, and O. Maury (2013), Indian Ocean Dipole and El Niño/Southern Oscillation impacts on regional chlorophyll anomalies in the Indian Ocean, Biogeosciences, 10(10), 6677-6698, doi:10.5194/bg-10-6677-2013.

Dufois, F., N. J. Hardman-Mountford, M. Fernandes, B. Wojtasiewicz, D. Shenoy, D. Slawinski, M. Gauns, J. Greenwood, and R. Toresen (2017), Observational insights into chlorophyll distributions of subtropical South Indian Ocean eddies, Geophys. Res. Lett., 44(7), 3255-3264, doi:10.1002/2016gl072371.

Gaube, P., D. B. Chelton, P. G. Strutton, and M. J. Behrenfeld (2013), Satellite observations of chlorophyll, phytoplankton biomass, and Ekman pumping in nonlinear mesoscale eddies, Journal of Geophysical Research: Oceans, 118(12), 6349-6370, doi:10.1002/2013JC009027.

Hood, R. R., L. E. Beckley, and J. D. Wiggert (2017), Biogeochemical and ecological impacts of boundary currents in the Indian Ocean, Progress in Oceanography, 156, 290.325.

Keerthi, M.G. et al. (2016), Physical control of the interannual variations of the winter chlorophyll bloom in the northern Arabian Sea. Biogeosciences Discuss., https://doi.org/10.5194/bg-2016-153.

Lee, P.-F., I.-C. Chen, and W.-N. Tzeng (2005), Spatial and temporal distibution patterns of Bigeye Tuna (*Thunnus obesus*) in the Indian Ocean, Zoological Studies, 44(2), 260-270.

McCreary, J. P., R. Murtugudde, J. Vialard, P. N. Vinayachandran, J. D. Wiggert, R. R. Hood, D. Shankar, and S. Shetye (2009), Biophysical Processes in the Indian Ocean, in Indian Ocean Biogeochemical Processes and Ecological Variability, edited, pp. 9-32, American Geophysical Union, doi:10.1029/2008GM000768.

Roxy, M. K., K. Ritika, P. Terray, and S. Masson (2014), The curious case of Indian Ocean warming, J. Climate, 27(22), 8501-8509.

Roxy, M. K., A. Modi, R. Murtugudde, V. Valsala, S. Panickal, S. Prasanna Kumar, M. Ravichandran, M. Vichi, and M. Lévy (2016), A reduction in marine primary productivity driven by rapid warming over the tropical Indian Ocean, Geophys. Res. Lett., 43, 826–833, doi:810.1002/2015GL066979.

Srokosz, M. A., J. Robinson, H. McGrain, E. E. Popova, and A. Yool (2015), Could the Madagascar bloom be fertilized by Madagascan iron?, Journal of Geophysical Research: Oceans, 120(8), 5790-5803, doi:10.1002/2015JC011075.

Strutton, P. G., V. J. Coles, R. R. Hood, R. J. Matear, M. J. McPhaden, and H. E. Phillips (2015), Biogeochemical variability in the central equatorial Indian Ocean during the monsoon transition, Biogeosciences, 12(8), 2367-2382, doi:10.5194/bg-12-2367-2015.

Takahashi, T., et al. (2009), Climatological mean and decadal change in surface ocean pCO2, and net sea–air CO2 flux over the global oceans., Deep Sea Research Part II: Topical Studies in Oceanography, 56(8-10), 554-577.

Vinayachandran, P. N. (2009), Impact of Physical Processes on Chlorophyll Distribution in the Bay of Bengal, in Indian Ocean Biogeochemical Processes and Ecological Variability, edited, pp. 71-86, American Geophysical Union, doi:10.1029/2008GM000705.

Wiggert, J.D., J. Vialard, and M.J. Behrenfeld (2009), Basin-wide modification of dynamical and biogeochemical processes by the Indian Ocean Dipole. In: Indian Ocean Biogeochemical Processes and Ecological Variability, J.D.Wiggert, R.R. Hood, S.W.A. Naqvi, S.L. Smith, and K.H. Brink (ed.), American Geophysical Union, Washington, D. C, pp 385-408.

Yaremchuk, M., Z. Yu, and J. McCreary (2005), River discharge into the Bay of Bengal in an inverse ocean model, Geophys. Res. Lett., 32(16), doi:10.1029/2005GL023750.

Zeitzschel, B. (1973) The biology of the Indian Ocean. Springer-Verlag, Berlin.

Chapter 13

Abram, N. J., M. K. Gagan, M. T. McCulloch, J. Chappell, W. S. Hantoro, 2003. Coral reef death during the 1997 Indian Ocean Dipole linked to Indonesian wildfires. *Science*, 301, 952–955.

Ajayamohan, R.S., S. A. Rao, T. Yamagata, 2008. Influence of Indian Ocean Dipole on poleward propagation of boreal summer intraseasonal oscillations. *Journal of Climate*, 21, 5437–5454.

Aldrian, E., 2008: Dominant factors of Jakarta's three largest floods. *Jurnal Hidrosfir Indones.*, 3, 105–112

Annamalai, H., and K. R. Sperber, 2005. Regional heat sources and the active and break phases of boreal summer intraseasonal (30–50 day) variability. *Journal of Atmospheric Sciences*, 62, 2726–2748.

Annamalai, H., P. Liu, and S.-P. Xie, 2005a. Southwest Indian Ocean SST variability: Its local effect and remote influence on Asian monsoons. Journal of Climate, 18, 4150–4167.

Annamalai, H., J. Potemra, R. Murtugudde, J. P. McCreary, 2005b. Effect of preconditioning on the extreme climate events in the tropical Indian Ocean. *Journal of Climate*, 18, 3450–3469.

Ashok, K., Z. Guan, T. Yamagata, 2001. Impact of the Indian Ocean dipole on the relationship between the Indian monsoon rainfall and ENSO. *Geophysical Research Letters*, 28, 4499–4502.

Ashok, K., Z. Guan, T. Yamagata, 2003. Influence of the Indian Ocean Dipole on the Australian winter rainfall. *Geophysical Research Letters*, 30, doi:10.1029/2003GL017926.

Ashok, K., Z. Guan, N. H. Saji, T. Yamagata, 2004. Individual and combined influences of the ENSO and Indian Ocean Dipole on the Indian summer monsoon. *Journal of Climate*, 17, 3141–3155.

Behera, S. K., R. Krishnan, T. Yamagata, 1999. Unusual ocean-atmosphere conditions in the tropical Indian Ocean during 1994. *Geophysical Research Letters*, 26, 3001–3004.

Behera, S. K., and T. Yamagata, 2001. Subtropical SST dipole events in the southern Indian Ocean. *Geophysical Research Letters*, 28, 327-330.

Birkett, C., R. Murtugudde, R. Allan, 1999. Indian Ocean climate event brings floods to East Africa's lakes and the Sudd Marsh. *Geophysical Research Letters*, 26 (8), 1031-1034.

Black, E., J. Slingo, K. R. Sperber, 2003. An observational study of the relationship between excessively strong short rains in coastal East Africa and Indian Ocean SST. *Monthly Weather Review*, 131, 74–94.

Cai, W., T. Cowan, M. Raupach, 2009a. Positive Indian Ocean Dipole events precondition southeast Australia bushfires. *Geophysical Research Letters*, 36 (L19710), doi:10.1029/2009GL039902.

1333 Cai, W., T. Cowan, A. Sullivan, 2009b. Recent unprecedented skewness towards positive Indian
1334 Ocean Dipole occurrences and their impact on Australian rainfall. *Geophysical Research Letters*,
1335 doi:10.1029/2009GL037604.

1336 Cai, W., A. Pan, D. Roemmich, T. Cowan, X. Guo, 2009c. Argo profiles a rare occurrence of three
1337 consecutive positive Indian Ocean Dipole events, 2006–2008. *Geophysical Research Letters*, 36
1338 (L08701), doi:10.1029/2008GL037038.

1339 Cai, W., A. Santoso, G. Wang, E. Weller, L. Wu, K. Ashok, Y. Masumoto, T. Yamagata, 2014.
1340 Increased frequency of extreme Indian Ocean Dipole events due to greenhouse warming. *Nature*,
1341 510, 254-258.

1342 D'Arrigo, R. and R. Wilson, 2008. El Nino and Indian Ocean influences on Indonesian drought:
1343 implications for forecasting rainfall and crop productivity. *International Journal of Climatology*, 28,
1344 611–616.

1345 D'Arrigo, R., N. Abram, C. Ummenhofer, J. Palmer, M. Mudelsee, 2011. Reconstructed streamflow
1346 for Citarum River, Java, Indonesia: linkages to tropical climate dynamics. *Climate Dynamics*, 36,
1347 451–462.

1348 Du, Y., Y. Zhang, M. Feng, T. Wang, N. Zhang, S. Wijffels, 2015. Decadal trends of the upper
1349 ocean salinity in the tropical Indo-Pacific since mid-1990s. *Scientific Reports*, 5,
1350 doi:10.1038/srep16050.

1351 Feng, M., H. H. Hendon, S.-P. Xie, A. G. Marshall, A. Schiller, Y. Kosaka, N. Caputi, and A. Pearce,
1352 2015. Decadal increase in Ningaloo Niño since the late 1990s. *Geophysical Research Letters*, 42,
1353 104–112.

1354 Gadgil, S., P. N. Vinayachandran, P. A. Francis, S. Gadgil, 2004. Extremes of the Indian summer
1355 monsoon rainfall, ENSO and equatorial Indian Ocean oscillation. *Geophysical Research Letters*,
1356 31, L12213.

1357 Guemas, V., S. Corti, J. Garcia-Serrano, F. J. Doblas-Reyes, M. Balmaseda, L. Magnusson, 2013.
1358 The Indian Ocean: The region of highest skill worldwide in decadal climate prediction. *Journal of*
1359 *Climate*, 26, 726–739.

1360 Hendon, H. H., 2003. Indonesian rainfall variability: Impacts of ENSO and local air–sea interaction.
1361 *Journal of Climate*, 16, 1775–1790.

1362 Hu, S. and J. Sprintall, 2016a. Interannual variability in the Indonesian Throughflow: the salinity
1363 effect. *Journal of Geophysical Research*, 21, 2596–2615.

1364 Hu, S. and J. Sprintall, 2016b. Observed strengthening of interbasin exchange via the Indonesian
1365 Seas due to rainfall intensification. *Geophysical Research Letters*, 44,1448–1456.

1366 Jongaramrungruang, S., H. Seo, C. C. Ummenhofer, 2017. Intraseasonal rainfall variability in the
1367 Indian Ocean during the summer monsoon: coupling with the ocean and modulation by the Indian
1368 Ocean Dipole. *Atmospheric Science Letters*, 18, 88-95.

1369 Katsumata, M., P. E. Ciesielski, R. H. Johnson, 2011. Evaluation of budget analyses during
1370 MISMO. *Journal of Applied Meteorology and Climatology*, 50, 241-254.

1371 Krishnamurthy, L. and V. Krishnamurthy, 2016. Decadal and interannual variability of the Indian
1372 Ocean SST. *Climate Dynamics*, 46, 57–70.

1373 L'Heureux, M. L., S. Lee, B. Lyon. 2013. Recent multidecadal strengthening of the Walker
1374 circulation across the tropical Pacific. *Nature Climate Change*, 3, 571–576.

1375 Liebmann, B., M. P. Hoerling, C. Funk, I. Bladé, R. M. Dole, D. Allured, X. Quan, P. Pegion, and J.
1376 K. Eischeid, 2014. Understanding recent eastern Horn of Africa rainfall variability and change.
1377 *Journal of Climate*, 27, 8630–8645.

1378 Llovel, W. and T. Lee, 2015. Importance and origin of halosteric contribution to sea level change in
1379 the southeast Indian Ocean during 2005–2013. *Geophysical Research Letters*, 42, 1148–1157.

Mahadevan, A., T. Paluszkiewicz, M. Ravichandran, D. Sengupta, A. Tandon, 2016a. Introduction to the special issue on the Bay of Bengal: From monsoons to mixing. *Oceanography*, 29, 14–17.

Mahadevan, A., G. Spiro Jaeger, M. Freilich, M. Omand, E. L. Shroyer, D. Sengupta, 2016b. Freshwater in the Bay of Bengal: Its fate and role in air-sea heat exchange. *Oceanography*, 29, 72–81.

Manatsa, D., B. Chipindu, S. K. Behera, 2012. Shifts in IOD and their impacts on association with East African rainfall. *Theoretical and Applied Climatology*, 110, 115-128.

Manatsa, D. and S. K. Behera, 2013. On the epochal strengthening in the relationship between rainfall of East Africa and IOD. *Journal of Climate*, 26, 5655-5673.

Nicholson, S. E., 2015. Long-term variability of the East African "short rains" and its links to large-scale factors. *International Journal of Climatology*, doi:10.1002/joc.4259.

Ratheesh, S., R. Sharma, S. Basu, 2014. An EnOI assimilation of satellite data in an Indian Ocean circulation model. *IEEE Transactions on Geoscience Remote Sensing*, 52, 4106–4111.

Reason, C. J. C., 2001. Subtropical Indian Ocean SST dipole events and southern African rainfall. *Geophysical Research Letters*, 28, 2225-2227.

Reason, C. J. C., 2002. Sensitivity of the southern African circulation to dipole sea-surface temperature patterns in the south Indian Ocean. *International Journal of Climatology*, 22, 377–393.

Saji, N. H., B. N. Goswami, P. N. Vinaychandran, T. Yamagata, 1999. A dipole mode in the tropical Indian Ocean. *Nature*, 401, 360-363.

Saji, N. H., and T. Yamagata, 2003. Possible impacts of Indian Ocean Dipole mode events on global climate. *Climate Research*, 25, 151-169.

Schott, F. A., S.-P. Xie, J. McCreary, J. P., 2009. Indian Ocean variability and climate variability. *Reviews of Geophysics*, 47 (RG1002), doi:10.1029/2007RG000245.

Sharma, R., N. Agarwal, A. Chakraborty, S. Mallick, J. Buckley, V. Shesu, A. Tandon, 2016. Large-scale air-sea coupling processes in the Bay of Bengal using space-borne observations. *Oceanography*, 29, 192–201.

Tangang, F. T., L. Juneng, E. Salimun, P. N. Vinayachandran, Y. K. Seng, C. J. C. Reason, S. K. Behera, T. Yasunari, 2008. On the roles of the northeast cold surge, the Borneo vortex, the Madden- Julian oscillation, and the Indian Ocean dipole during the extreme 2006/2007 flood in southern peninsular Malaysia. *Geophysical Research Letters*, 35, L14S07, doi:10.1029/2008GL033429.

Ummenhofer, C. C., A. Sen Gupta, M. J. Pook, M. H. England, 2008. Anomalous rainfall over southwest Western Australia forced by Indian Ocean sea surface temperatures. *Journal of Climate*, 21, 5113-5134.

Ummenhofer, C. C., M. H. England, G. A. Meyers, P. C. McIntosh, M. J. Pook, J. S. Risbey, A. Sen Gupta, A. S. Taschetto, 2009a. What causes Southeast Australia's worst droughts? *Geophysical Research Letters*, 36 (L04706), doi:10.1029/2008GL036801.

Ummenhofer, C. C., A. Sen Gupta, M. H. England, C. J. C. Reason, 2009b. Contributions of Indian Ocean sea surface temperatures to enhanced East African rainfall. *Journal of Climate*, 22, 993–1013.

Ummenhofer, C. C., A. Sen Gupta, A. S. Taschetto, M. H. England, 2009c. Modulation of Australian precipitation by meridional gradients in east Indian Ocean sea surface temperature. *Journal of Climate*, 22, 5597–5610.

Ummenhofer, C. C., A. Sen Gupta, M. H. England, 2009d. Effect of tropical and subtropical Indian Ocean dipoles in driving precipitation around Indian Ocean rim countries. 9th International Conference for Southern Hemisphere Meteorology and Oceanography, Feb. 9-13, 2009, Melbourne, Australia.

Ummenhofer, C. C., A. Sen Gupta, Y. Li, A. S. Taschetto, M. H. England, 2011a. Multi-decadal modulation of the El Niño-Indian monsoon relationship by Indian Ocean variability. *Environmental Research Letters*, 6 (034006), doi:10.1088/1748–9326/6/3/034006.

Ummenhofer, C. C., A. Sen Gupta, P. R. Briggs, M. H. England, P. C. McIntosh, G. A. Meyers, M. J. Pook, M. R. Raupach, J. S. Risbey, 2011b. Indian and Pacific Ocean influences on Southeast Australian drought and soil moisture. *Journal of Climate*, 24, 1313–1336.

Ummenhofer, C. C., A. Biastoch, C. W. Böning, 2017a. Multi-decadal Indian Ocean variability linked to the Pacific and implications for preconditioning Indian Ocean Dipole events. *Journal of Climate*, 30, 1739-1751.

Ummenhofer, C. C., M. Kulüke, J. E. Tierney, 2017b. Extremes in East African hydroclimate and links to Indo-Pacific variability on interannual to decadal timescales. *Climate Dynamics*, doi:10.1007/s00382-017-3786-7.

Vargas-Hernandez, J. M., S. Wijffels, G. Meyers, N. J. Holbrook, 2014. Evaluating SODA for IndoPacific Ocean decadal climate variability studies. *Journal of Geophysical Research - Oceans*, 119, 7854–7868.

Vecchi, G. A., and D. E. Harrison, 2004. Interannual Indian rainfall variability and Indian Ocean sea surface temperature anomalies. In *Earth Climate: The Ocean-Atmosphere Interaction*, C. Wang, S.-P. Xie, and J.A. Carton (eds.), American Geophysical Union, Geophysical Monograph 147, Washington D.C., 247–260

Vecchi, G. A. and B. J. Soden, 2007. Global warming and the weakening of the tropical circulation. *Journal of Climate*, 20, 4316–4340.

Vialard, J., G. R. Foltz, M. J. McPhaden, J. P. Duvel, C. de Boyer Montégut, 2008. Strong Indian Ocean sea surface temperature signals associated with the Madden-Julian Oscillation in late 2007 and early 2008, *Geophysical Research Letters*, 35, L19608, doi:10.1029/2008GL035238.

Vialard, J. et al., 2009. Cirene: Air Sea Interactions in the Seychelles-Chagos thermocline ridge region. *Bulletin of the American Meteorological Society*, 90, 45-61.

Webster, P. J., A. M. Moore, J. P. Loschnigg, R. R. Leben, 1999. Coupled ocean-atmosphere dynamics in the Indian Ocean during 1997–98. *Nature*, 401, 356–360.

Wijesekera, H. W. et al., 2016. ASIRI: an ocean–atmosphere initiative for Bay of Bengal. *Bulletin of the American Meteorological Society*, 97, 1859-1884.

Williams, A. P. and C. Funk, 2011. A westward extension of the warm pool leads to a westward extension of the Walker circulation, drying eastern Africa. *Climate Dynamics*, 37, 2417-2435.

Zhang, C. 2005. Madden-Julian Oscillation. *Reviews of Geophysics*, 43, RG2003, doi:10.1029/2004RG000158.

Zhang, C. 2013. Madden-Julian Oscillation: Bridging weather and climate. *Bulletin of the American Meteorological Society*, doi:10.1175/BAMS-D-12-00026.1.

Zhou, L., R. Murtugudde, D. Chen, Y. Tang, 2017. A central Indian Ocean mode and heavy precipitation during the Indian summer monsoon. *Journal of Climate*, 30, 2055-2067.

Chapter 14

Bradshaw E., L. Rickards, and T. Aarup, 2015: Sea level data archaeology and the Global Sea Level Observing System (GLOSS). *GeoResJ,* **6**, 9–16.

Cheng L., K. Trenberth, J. Fasullo, T. Boyer, J. Abraham, J. Zhu, 2017: Improved estimates of ocean heat content from 1960 to 2015, *Science Advances*, **3**, e1601545.

1470 Church, J.A., and coauthors, 2013: Sea Level Change. In: *Climate Change 2013: The Physical*
1471 *Science Basis. Contribution of Working Group I to the Fifth Assessment Report of the*
1472 *Intergovernmental Panel on Climate Change [Stocker, T.F. et al. (eds.)]. Cambridge University*
1473 *Press, Cambridge, United Kingdom and New York, NY, USA*.

1474 Dong, L., T. Zhou, and X. Chen, 2014: Changes of Pacific decadal variability in the twentieth
1475 century driven by internal variability, greenhouse gases, and aerosols, *Geophys. Res. Lett., 41*,
1476 8570–8577.

1477 Dong, L. & McPhaden, M. J., 2017: Why Has the Relationship between Indian and Pacific Ocean
1478 Decadal Variability Changed in Recent Decades? *J. Climate* **30,** 1971–1983.

1479 Du, Y., and S.P. Xie (2008), Role of atmospheric adjustments in the TIO warming during the 20th
1480 century in climate models, *Geophys. Res. Lett.,* **35**, L08712.

1481 Dunne, R.P., S.M. Barbosa, P.L. Woodworth, 2012: Contemporary sea level in the Chagos
1482 Archipelago, central Indian Ocean, *Global and Planetary Change*, **82–83**, 25-37.

1483 Feng, M., Y. Li, and G. Meyers, 2004: Multidecadal variations of Fremantle sea level: Footprint of
1484 climate variability in the tropical Pacific. *Geophys. Res. Lett*., **31**, L16302.

1485 Feng, M., M.J. McPhaden, and T. Lee, 2010: Decadal variability of the Pacific subtropical cells and
1486 their influence on the southeast Indian Ocean. *Geophys. Res. Lett*., **37**, L09606,
1487 doi:10.1029/2010GL042796.

1488 Feng, M., M. J. McPhaden, S.-P. Xie, and J. Hafner, 2013: La Niña forces unprecedented Leeuwin
1489 Current warming in 2011, *Sci. Rep*., **3**, 1277, doi:10.1038/srep01277.

1490 Fukumori, I., and O. Wang, 2013: Origins of heat and freshwater anomalies underlying regional
1491 decadal sea level trends, *Geophys. Res. Lett.,* **40**, 563–567, doi:10.1002/grl.50164.

1492 Fu, L., and R. Smith, 1996: Global ocean circulation from satellite altimetry and high-resolution
1493 computer simulation. *Bull. Amer. Meteor. Soc*., **77**, 2625–2636.

1494 Fu, L.-L., 2007: Intraseasonal variability of the equatorial Indian Ocean observed from sea surface
1495 height, wind, and tempera- ture data. *J. Phys. Oceanogr*., **37**, 188–202.

1496 Hamlington, B.D., M.W. Strassburg, R. Leben, W. Han, R.S. Nerem, and K.Y. Kim (2014),
1497 Uncovering the Anthropogenic Warming-Induced Sea Level Rise Signal in the Pacific Ocean, *Nat.*
1498 *Climate Change,* **4**, 782-785.

1499 Han, W. and P.J. Webster, 2002: Forcing Mechanisms of Sea-Level Interannual Variability in the
1500 Bay of Bengal. *J. Phys. Oceanogr*., **32**, 216-239.

1501 Han, W., 2005: Origins and dynamics of the 90-day and 30–60-day variations in the equatorial
1502 Indian Ocean. *J. Phys. Oceanogr*., **35**, 708–728.

1503 Han, W., G.A. Meehl, B. Rajagopalan, J. Fasullo, A. Hu, J. Lin, W. Large, J. Wang, X. Quan, L.
1504 Trenary, A. Wallcraft, T. Shinoda, and S. Yeager, 2010: Patterns of Indian Ocean Sea Level
1505 Change in a Warming Climate, *Nature Geoscience,* **3**, 546-550.

1506 Han, W., G.A. Meehl, A. Hu, M. Alexander, T. Yamagata, D. Yuan, M. Ishii, P. Pegion, J. Zheng,
1507 B. Hamlington, X.-W. Quan, and R. Leben, 2014: Intensification of decadal and multi-decadal sea
1508 level variability in the western tropical Pacific during recent decades, *Clim. Dyn.,* **43**, 1357-1379.

1509 Han, W., G. Meehl, D. Stammer, A. Hu, B. Hamlington, J. Kenigson, H. Palanisamy, and P.
1510 Thompson, 2017: Spatial Patterns of Sea Level Variability Associated With Natural Internal Climate
1511 Modes. *Surveys in Geophysics*, **38**, 217-250.

1512 Kay S. and coauthors, 2015: Modelling the increased frequency of extreme sea levels in the
1513 Ganges-Brahmaputra-Meghna delta due to sea level rise and other effects of climate change.
1514 *Environ Sci Process Impacts*., **17**, 1311-22.

1515 Kopp, R.E., C.C. Hay, C.M. Little, and J.X. Mitrovica (2015), Geographic Variability of Sea-Level
1516 Change, *Curr. Clim. Change. Rep.,* **1**, 192-204.

1517 Iskandar, I., and M. J. McPhaden, 2011: Dynamics of wind-forced intraseasonal zonal current
1518 variations in the equatorial Indian Ocean, *J. Geophys. Res.,* **116***,* C06019.

1519 Lee, S.-K., Wonsun Park, Molly O. Baringer, Arnold L. Gordon, Bruce Huber & Y. Liu, 2015: Pacific
1520 origin of the abrupt increase in Indian Ocean heat content during the warming hiatus. *Nature*
1521 *Geosci.,* **8**, 445–449.

1522 Lee, T**.**, 2004: Decadal weakening of the shallow overturning circulation in the South Indian Ocean.
1523 *Geophys. Res. Lett.*, 31, L18305, doi:10.1029/2004GL020884.

1524 Lee, T., and M.J. McPhaden, 2008: Decadal phase change in large-scale sea level and winds in
1525 the Indo-Pacific region at the end of the 20th century, *Geophys. Res. Lett.,* **35**, L01605.

1526 Lee, T., J.T. Farrar, T. Durland, S. Arnault, B. Meyssignac, and W. Han, 2017: Monitoring and
1527 interpreting the tropical oceans by satellite altimetry. Chapter 7 in satellite altimetry textbook
1528 "Satellite Altimetry Over Ocean and Land Surfaces", Editors D. Stammer and A. Cazenave, CRC
1529 Press, Taylor and Francis Group, in press.

1530 Li, Y., and W. Han, 2015: Decadal Sea level Variatoins in the Indian Ocean Investigated with
1531 HYCOM: Roles of Climate Modes, Ocean Internal Variability and Stochastic Wind Forcing, *J. Clim*.,
1532 **28**, 9143-9165.

1533 Llovel, W., and T. Lee, 2015: Importance and origin of halosteric contribution to sea level change
1534 in the southeast Indian Ocean during 2005–2013, *Geophys. Res. Lett.*, **42**, 1148–1157.

1535 Luo, J.J., W. Sasaki, and Y. Masumoto, 2012: Indian Ocean warming modulates Pacific climate
1536 change, *Proceedings of the National Academy of Sciences,* **109**, 18701-18706.

1537 McPhaden, M. J. and M. Nagura, 2014: Indian Ocean Dipole interpreted in terms of Recharge
1538 Oscillator theory. *Clim. Dyn., 42*, 1569-1586. doi 10.1007/s00382-013-1765-1.

1539 Milne, G.A., W.R. Gehrels, C.W. Hughes, and M.E. Tamisiea, 2009: Identifying the causes of sea-
1540 level change, *Nature Geosci.,* **2**, 471–478.

1541 Nagura, M., and M. J. McPhaden, 2010: Wyrtki Jet dynamics: Seasonal variability. *J. Geophys.*
1542 *Res., 115,* C07009, doi:10.1029/2009JC005922.

1543 Nagura, M., and M. J. McPhaden, 2012: The dynamics of wind-driven intraseasonal variability in
1544 the equatorial Indian Ocean. *J. Geophys. Res.,* **115***,* C07009.

1545 Neumann B, Vafeidis AT, Zimmermann J, Nicholls RJ, 2015: Future Coastal Population Growth
1546 and Exposure to Sea-Level Rise and Coastal Flooding - A Global Assessment. *PLoS ONE,*
1547 **10(3)**:e0118571. doi:10.1371/journal.pone.0118571

1548 Nicholls RJ, and A. Cazenave, 2010: Sea-Level Rise and Its Impact on Coastal Zones. *Science*,
1549 **328**, 1517–1520. doi: 10.1126/science.1185782

1550 Nieves, V., Josh K. Willis, William C. Patzert, 2015: Recent hiatus caused by decadal shift in Indo-
1551 Pacific heating, *Science*, **349**, 532-535.

1552 Nidheesh, A. G., M. Lengaigne, J. Vialard, A. S. Unnikrishnan, and H. Dayan, 2013: Decadal and
1553 long-term sea level variability in the tropical Indo-Pacific Ocean. *Climate Dyn*., **41**, 381–402.

1554 Nidheesh, A. G., M. Lengaigne, J. Vialard, T. Izumo, A. S. Unnikrishnan, B. Meyssignac, B.
1555 Hamlington, and C. de Boyer Montegut, 2017: Robustness of observationally-derived decadal sea-
1556 level variability in the Indo-Pacific region. *Geophys. Res. Lett.,* submitted.

1557 Parvathi, V., I. Suresh, M. Lengaigne, C. Ethé, J. Vialard, M. Lévy, S. Neetu, O. Aumont, L.
1558 Resplandy, H. Naik and S.W.A. Naqvi, 2017: Positive Indian Ocean Dipole events prevent anoxia
1559 along the west coast of India, Biogeosciences, 14, 1541-1559.

Perigaud, C., and P. Delecluse, 1992: Annual sea level variations in the southern tropical Indian Ocean from Geosat and shallowwater simulations. J. Geophys. Res., **97**, 20,169–20,178.

Rao, S. A., S. K. Behera, Y. Masumoto, and T. Yamagata, 2002: Interannual variability in the subsurface tropical Indian Ocean, *Deep-Sea Res. II*, **49***,* 1549–1572.

Roxy MK, Ritika K, Terray P, Masson S, 2014: The curious case of Indian Ocean warming. *J. Climate,* **27**, 8501-8509.

Rhein, M., S.R. Rintoul, and coauthors, 2013: Chapter 3: Observations: In: Stocker T. et al. (eds) *Climate Change 2013: The Physical Science Basis, contribution of working group I to the fifth assessment report of the intergovernmental panel on climate change*.

Sérazin, G., T. Penduff, S. Grégorio, B. Barnier, J.-M. Molines, and L. Terray, 2015: Intrinsic variability of sea level from Global Ocean simulations: Spatiotemporal scales, *J. Clim.,* **28***, 4279–4292.*

Shankar, D. and S.R. Shetye, 1999: Are interdecadal sea level 1120 changes along the Indian coast influenced by variability of monsoon rainfall? *J. Geophys. Res*., **104**, 26031-26042.

Shankar, D., S.G. Aparna, J.P. McCreary, I. Suresh, S. Neetu, F. Durand, S.S.C. Shenoi, M.A. Al Saafani, 2010: Minima of interannual sea-level variability in the Indian Ocean, Prog. In Oceanogr., **84**, 225–241.

Srinivasu, U., M. Ravichandran, W. Han,S. Sivareddy, H. Rahman, Y. Li, and S. Nayak, 2017: Causes for the reversal of North Indian Ocean decadal sea level trend in recent two decades. Clim. Dyn., DOI: 10.1007/s00382-017-3551-y .

Stammer, D., A. Cazenave, R. M. Ponte, and M. E. Tamisiea (2013), Causes for contemporary regional sea level changes, *Annual Review of Marine Science,* **5**, 21–46.

Testut L., B.M. Miguez, G. Wöppelmann, P. Tiphaneau, N. Pouvreau, and M. Karpytchev, 2010: Sea level at Saint Paul Island, southern Indian Ocean, from 1874 to the present. *J. Geophys. Res*., **115**, C12028.

Thompson, P. R., Piecuch, C. G., Merrifield, M. A., McCreary, J. P. and Firing, E., 2016: Forcing of recent decadal variability in the Equatorial and North Indian Ocean. *J. Geophys. Res. Oceans,* **121**, 6762–6778.

Timmermann, A., S. McGregor, and F.F. Jin (2010), Wind effects on past and future regional sea level trends in the southern Indo-Pacific, *J. Clim.,* **23**, 4429–4437.

Trenary L. and W. Han, 2012: Intraseasonal-to-interannual variability of South Indian Ocean sea level and thermocline: Remote versus local forcing. *J. Phys. Oceanogr*., **42**, 602-627.

Trenary L., and W. Han, 2013: Local and remote forcing of decadal sea level and thermocline depth variability in the south Indian Ocean. JGR-Oceans, **118**, 381-398.

Unnikrishnan, A. S., and D. Shankar, 2007: Are sea-level-rise trends along the coasts of the north Indian Ocean consistent with global estimates? *Global and Planet. Change,* **57**, 301-307.

Vialard, J., S. S. C. Shenoi, J. P. McCreary, D. Shankar, F. Durand, V. Fernando, and S. R. Shetye, 2009: Intraseasonal response of the northern Indian Ocean coastal waveguide to the Madden-Julian oscillation, Geophys. Res. Lett., 36, L14606, doi:10.1029/2009GL038450.

Vialard, J., 2015: Hiatus heat in the Indian Ocean, *Nature Geoscience,* doi:10.1038/ngeo2442.

Xie, S.-P., H. Annamalai, F. A. Schott, and J. P. McCreary, 2002: Structure and mechanisms of south Indian Ocean climate variability. *J. Clim.*, **15**, 864–878.

Chapter 15

Abhilash S, Sahai AK, Pattanaik S, Goswami BN, Kumar A (2014) Extended range prediction of active-break spells of Indian summer monsoon rainfall using an ensemble prediction system in NCEP climate forecast system. Int J Climatol 34:98–113

Andrejczuk, M., Cooper, F.C., Juricke, S., Palmer, T.N., Weisheimer, A. and Zanna, L., 2016. Oceanic stochastic parameterizations in a seasonal forecast system. Monthly Weather Review, 144(5), pp.1867-1875.

Annamalai H, Slingo JM (2001) Active/break cycles: diagnosis of the intraseasonal variability of the Asian summer monsoon. Clim Dyn 18:85–102

Annamalai H, Sperber KR (2005) Regional heat sources and the active and break phases of boreal summer intraseasonal (30– 50 day) variability. J Atmos Sci 62:2726–2748

Bellon G, Sobel A (2008a) Poleward-propagating intraseasonal mon- soon disturbances in an intermediate-complexity axisymmetric model. J Atmos Sci 65:470–489

Bellon G, Sobel A (2008b) Instability of the axisymmetric monsoon ow and intraseasonal oscillation. J Geophys Res 113:D07109. doi:10.1029/2007JD008968

Bessafi M, Wheeler MC (2006) Modulation of south Indian ocean tropical cyclones by the Madden–Julian oscillation and convec- tively coupled equatorial waves. Mon Weather Rev 134:638–656

Boos WR, Kuang Z (2010) Mechanisms of poleward propagating, intraseasonal convective anomalies in cloud system-resolving models. J Atmos Sci 67:3673–3691

Camargo, S. J., M. C. Wheeler, and A. H. Sobel (2009) Diagnosis of the MJO modulation of tropical cyclogenesis using an empirical index, J. Atmos. Sci., doi:10.1175/2009JAS3101.1.

Charney, J. G., and J. Shukla, 1981: Predictability of monsoons. Monsoon Dynamics, J. Lighthill and R. P. Pearce, Eds., Cambridge University Press, 99–108.

de Boisséson, E., Balmaseda, M. A., Vitart, F., and Mogensen, K.: Impact of the sea surface temperature forcing on hindcasts of Madden-Julian Oscillation events using the ECMWF model, Ocean Sci., 8, 1071-1084, https://doi.org/10.5194/os-8-1071-2012, 2012.

Fu X, Wang B, Li T, McCreary JP (2003) Coupling between north- ward-propagating, intraseasonal oscillations and sea surface tem- perature in the Indian Ocean. J Atmos Sci 60:1733–1753

Gadgil S, Rajeevan M, Nanjundiah R (2005) Monsoon prediction: why yet another failure? Curr Sci 88:1389–1400

Ge, X., W. Wang, A. Kumar and Y. Zhang, 2017: Importance of the vertical resolution in simulating SST diurnal and intraseasonal variability in an ocean general circulation model. *J. Climate*, **30**, 3963-3978.

Goswami BN, Ajaya Mohan RS, Xavier PK, Sengupta D (2003) Clus- tering of synoptic activity by Indian summer monsoon intrasea- sonal oscillations. Geophys Res Lett 30(8):1431

Goswami, B.N., 2005. South Asian monsoon. In *Intraseasonal variability in the atmosphere-ocean climate system* (pp. 19-61). Springer Berlin Heidelberg.

Goswami BN (2011) South Asian Summer Monsoon. In: Lau WKM, Waliser DE (eds) Intraseasonal variability of the atmosphere– ocean climate system, 2nd edn. Springer, Heidelberg

Han, W., Shinoda, T., Fu, L.L. and McCreary, J.P., 2006. Impact of atmospheric intraseasonal oscillations on the Indian Ocean dipole during the 1990s. Journal of physical oceanography, 36(4), pp.670-690.

Hendon HH, Liebmann B (1990) The intraseasonal (30–50 day) oscillation of the Australian summer monsoon. J Atmos Sci 47:2909–2924

Kemball-Cook S, Wang B (2001) Equatorial waves and air–sea inter- action in the boreal summer intraseasonal oscillation. J Clim 14:2923–2942

Kim, D., Sperber, K., Stern, W., Waliser, D., Kang, I.S., Maloney, E., Wang, W., Weickmann, K., Benedict, J., Khairoutdinov, M. and Lee, M.I., 2009. Application of MJO simulation diagnostics to climate models. Journal of Climate, 22(23), pp.6413-6436.

Kim, D. M., M. I. Lee, H. M. Kim, S. D. Shubert and J. Yoo, 2014: The Modulation of Tropical Storm Activity in the Western North Pacific by the MJO in GEOS-5 AGCM Experiments, *Atm. Sci. Lett,* 15 (4), 335-341

Klingaman, N.P., Jiang, X., Xavier, P.K., Petch, J., Waliser, D. and Woolnough, S.J., 2015. Vertical structure and physical processes of the Madden-Julian oscillation: Synthesis and summary. Journal of Geophysical Research: Atmospheres, 120(10), pp.4671-4689.

Koster, R.D., Akella, S., Todling, R. and Suarez, M., 2016. Estimation of the Ocean Skin Temperature using the NASA GEOS Atmospheric Data Assimilation System.

Lau KM, Chan PH (1988) Intraseasonal and interannual variations of tropical convection: a possible link between the 40–50 day oscillation and ENSO? J Atmos Sci 45:506–521

Lau KM, Waliser DE (2011) Intraseasonal variability of the atmos- phere-ocean climate system, 2nd edn. Springer, Heidelberg, p 613

Lee, S.S., Wang, B., Waliser, D.E., Neena, J.M. and Lee, J.Y., 2015. Predictability and prediction skill of the boreal summer intraseasonal oscillation in the Intraseasonal Variability Hindcast Experiment. Climate Dynamics, 45(7-8), pp.2123-2135.

Madden RA, Julian PR (1972) Description of global-scale circulation cells in tropics with a 40-50 day period. J Atmos Sci 29:1109–1123

Madden RA, Julian PR (1994) Observations of the 40-50-day tropical oscillation: a review. Mon Weather Rev 122:814–837

Neena JM, Goswami BN (2010) Extension of potential predictability of Indian summer monsoon dry and wet spells in recent decades. Q J R Meteorol Soc 136:583–592

Neena, J.M., Waliser, D. and Jiang, X., 2016. Model performance metrics and process diagnostics for boreal summer intraseasonal variability. Climate Dynamics, pp.1-23.

Oh J.H., Kim KY, Lim GH (2012) Impact of MJO on the diurnal cycle of rainfall over the western Maritime Continent in the austral summer. Clim Dyn 38:1167–1180

Penny, S.G., Akella, S., Buehner, M., Chevallier, M., Counillon, F., Draper, C., Frolov, S., Fujii, Y., Karspeck, A., Kumar, A., Laloyaux, P., Mahfouf, J-F., Martin, M., Peña, M., de Rosnay, P., Subramanian A., Tardif, R., Wu, X 2017. Coupled Data Assimilation for Integrated Earth System Analysis and Prediction: Goals, Challenges, and Recommendations. WMO Tech. Rep.

Penny, S.G., Behringer, D.W., Carton, J.A. and Kalnay, E., 2015. A hybrid global ocean data assimilation system at NCEP. Monthly Weather Review, 143(11), pp.4660-4677.

Rao, S.A. and Yamagata, T., 2004. Abrupt termination of Indian Ocean dipole events in response to intraseasonal disturbances. Geophysical research letters, 31(19), doi:10.1029/2004GL020842.

Robertson, A.W., A. Kumar, M. Peña, and F. Vitart, 2015: Improving and promoting subseasonal to seasonal prediction. Bull. Amer. Meteor. Soc., 96, ES49–ES53. doi: http://dx.doi.org/10.1175/BAMS-D-14-00139.1

Roundy, P.E., 2008. Analysis of convectively coupled Kelvin waves in the Indian Ocean MJO. *Journal of the Atmospheric Sciences*, *65*(4), pp.1342-1359.

Saji, N.H., Goswami, B.N., Vinayachandran, P.N. and Yamagata, T., 1999. A dipole mode in the tropical Indian Ocean. Nature, 401(6751), pp.360-363.

Seo, H., A. C. Subramanian, A. J. Miller, and N. R. Cavanaugh, 2014: Coupled impacts of the diurnal cycle of sea surface temperature on the Madden-Julian Oscillation. Journal of Climate*, 27, 8422–8443*.

Shukla, J., 1998: Predictability in the midst of chaos: A scientific basis for climate forecasting. Science, 282, 728–731.

Sikka DR, Gadgil S (1980) On the maximum cloud zone and the ITCZ over Indian longitudes during the southwest monsoon. Mon Weather Rev 108:1840–1853

Sperber KR, Annamalai H (2008) Coupled model simulations of boreal summer intraseasonal (30–50 day) variability, Part I: systematic errors and caution on use of metrics. Clim Dyn 31:345–372

Sperber KR et al (2000) Predictability and the relationship between subseasonal and interannual variability during the Asian summer monsoon. Q J Roy Meteorol Soc 126:2545–2574

Sperber KR et al (2001) Dynamical seasonal predictability of the Asian summer monsoon. Mon Weather Rev 129:2226–2248 Sperber KR, Annamali H, Kang I-S, Kitoh A, Moise A, Turner A,

Suhas, E., Neena, J.M. and Goswami, B.N., 2013. An Indian monsoon intraseasonal oscillations (MISO) index for real time monitoring and forecast verification. Climate dynamics, 40(11-12), pp.2605-2616.

Takayabu YN, Iguchi T, Kachi M, Shibata A, Kanzawa H (1999) Abrupt termination of the 1997–1998 El Nino in response to a Madden–Julian oscillation. Nature 402:279–282

Tian B, Waliser DE, Fetzer EJ (2006) Modulation of the diurnal cycle of tropical deep convective clouds by the MJO. Geophys. Res. Lett. 33:L20704

Vitart, F. (2009) Impact of the Madden Julian Oscillation on tropical storms and risk of landfall in the ECMWF forecast system. Geophys. Res. Lett., 36, L15802, doi:10.1029/2009GL039089

Vitart,F. (2014): Evolution of ECMWF sub-seasonal forecast skill scores. Quart. J. Roy. Meteor. Soc, 140, 1889-1899.

Vitart, F., Ardilouze, C., Bonet, A., Brookshaw, A., Chen, M., Codorean, C., Déqué, M., Ferranti, L., Fucile, E., Fuentes, M. and Hendon, H., 2016. The sub-seasonal to seasonal prediction (S2S) project database. Bulletin of the American Meteorological Society, (2016), Early online release, doi: *http://dx.doi.org/10.1175/BAMS-D-16-0017.1*.

Wang, B., Q. H. Ding, X. H. Fu, I. S. Kang, K. Jin, J. Shukla, and F. Doblas-Reyes, 2005: Fundamental challenge in simulation and prediction of summer monsoon rainfall. Geophys. Res. Lett., 32, L15711, doi: 10.1029/2005GL022734.

Wang, W., A. Kumar, J.X. Fu, and M. Hung, 2015: What is the Role of the Sea Surface Temperature Uncertainty in the Prediction of Tropical Convection Associated with the MJO?. *Mon. Wea. Rev.,* **143**, 3156–3175, https://doi.org/10.1175/MWR-D-14-00385.1

Waliser DE (2006) Intraseasonal variations. In: Wang B (ed) The Asian monsoon. Springer, Heidelberg, p 787

Webster PJ, Magana VO, Palmer TN, Shukla J, Tomas RA, Yanai M, Yasunari T (1998) Monsoons: processes, predictability, and the prospects for prediction. J Geophys Res 103:14451–14510

Wheeler, M. and Kiladis, G.N., 1999. Convectively coupled equatorial waves: Analysis of clouds and temperature in the wavenumber–frequency domain. *Journal of the Atmospheric Sciences*, *56*(3), pp.374-399.

Woolnough, S. J., Vitart, F. and Balmaseda, M. A. (2007), The role of the ocean in the Madden–Julian Oscillation: Implications for MJO prediction. Q.J.R. Meteorol. Soc., 133: 117–128. doi:10.1002/qj.4

Wu, R. G., and B. P. Kirtman, 2005: Roles of Indian and Pacific Ocean air–sea coupling in tropical atmospheric variability. Climate Dyn., 25, 155–170.

1737 Yoneyama, K., C. Zhang, and C.N. Long, 2013: Tracking pulses of the Madden-Julian Oscillation.
1738 Bull. Amer. Met. Soc., 94, 1871-1891.

1739 Zhang CD (2005) The Madden-Julian oscillation. Rev Geophys. doi: 10.1029/2004RG000158

1740 Zhang, C., 2013: Madden-Julian Oscillation: Bridging Weather and Climate. Bull. Amer. Met. Soc.,
1741 94, 1849–1870.

1742 Zhang, C. and Ling, J., 2017. Barrier Effect of the Indo-Pacific Maritime Continent on the MJO:
1743 Perspectives from Tracking MJO Precipitation. *Journal of Climate*, *30*(9), pp.3439-3459.

1744 Chapter 16

1745 Berry, D. I., and E. C. Kent, 2009: A new air-sea interaction gridded dataset from ICOADS with
1746 uncertainty estimates. Bull. Ameri. Meteorol. Soc., 90 (5)., 645-656.10.1175/2008BAMS2639.1.

1747 Brunke, M. A., X. Zeng, and S. Anderson, 2002: Uncertainties in sea surface turbulent flux
1748 algorithms and data sets. J. Geophys. Res., 102, doi: 10.1029/2001JC000992.

1749 Dee, D. P., and Coauthors, 2011: The ERA-Interim reanalysis: Configuration and performance of
1750 the data assimilation system. Quart. J. Roy. Meteor. Soc., 137, 553–597, doi:10.1002/qj.828.

1751 Jin, X., L. Yu, D. L. Jackson, and G. A. Wick, 2015. An Improved Near-Surface Specific Humidity
1752 and Air Temperature Climatology for the SSM/I Satellite Period. *J. Atmos. Oceanic Technol.*, **32**,
1753 412–433, doi: http://dx.doi.org/10.1175/JTECH-D-14-00080.1.

1754 Josey, S.A., S. Gulev, and L. Yu, 2013. Exchanges through the ocean surface. In, Siedler, G.,
1755 Griffies, S., Gould, J. and Church, J. (eds.) *Ocean Circulation and Climate: A 21st Century*
1756 *Perspective. 2nd Ed.* Oxford, GB, Academic Press, 115-140. (International Geophysics, 103).

1757 Kato, S., N. G. Loeb; F. G. Rose, D. R. Doelling, D. A. Rutan, T. E. Caldwell, L. Yu, R. A. Weller,
1758 2013: Surface irradiances consistent with CERES-derived top-of-atmosphere shortwave and
1759 longwave irradiances. *J. Climate*, **26**, 2719–2740, doi: http://dx.doi.org/10.1175/JCLI-D-12-
1760 00436.1.

1761 Kobayashi, S., and co-authors, 2015: The JRA-55 Reanalysis: General specifications and basic
1762 characteristics. J. Meteor. Soc. Japan, 93, 5-48, doi:10.2151/jmsj.2015-001.

1763 Lee, S.-K., W. Park, M. O. Baringer, A. L. Gordon, B. Huber and Y. Liu, 2015: Pacific origin of the
1764 abrupt increase in Indian Ocean heat content during the warming hiatus. *Nature Geosci.*, 8, 445-
1765 449, doi:10.1038/ngeo2438.

1766 Liang, X., and L. Yu, 2016. Variations of the global net air-sea heat flux during the “hiatus” period
1767 (2001-2010). *J. Climate*. 29, 3647–3660, doi: 10.1175/JCLI-D-15-0626.1.

1768 McPhaden, M. J., G. Meyers, K. Ando, Y. Masumoto, V. S. N. Murty, M. Ravichandran, F.
1769 Syamsudin, J. Vialard, L. Yu, and W. Yu, 2009. RAMA: The research moored array for African-
1770 Asian-Australian monsoon analysis and prediction. *Bulletin of the American Meteorological*
1771 *Society*, 90, 459-480, DOI:10.1175/2008BAMS2608.1.

1772 McPhaden, Michael J., K. Ando, B. Bourles, et al., 2010: The global tropical moored buoy array."
1773 *Proceedings of OceanObs* 9 (2010), 668-682.

1774 Rienecker M. M., and co-authors, 2011: MERRA—NASA's Modern-Era Retrospective Analysis for
1775 Research and Applications. *J. Climate*, DOI: 10.1175/JCLI-D-11-00015.1.

1776 Roxy, M.K., K. Ritika, P. Terray, and S. Masson, 2014: The Curious Case of Indian Ocean
1777 Warming. J. Climate, 27, 8501–8509, https://doi.org/10.1175/JCLI-D-14-00471.1

1778 Saha S, and co-authors, 2010: The NCEP Climate Forecast System Reanalysis. Bull. Amer.
1779 Meteorol. Soc. 91: 1015–1057.

1780 Send U, Weller RA, Wallace D, Chavez F, Lampitt RL, Dickey T,Honda M, Nittis K, Lukas R,
1781 McPhaden M, Feely R. 2010. OceanSITES. In: Hall J, Harrison DE, Stammer D, editors.

Proceedings of OceanObs'09: Sustained ocean observations and information for society (Vol. 2). Venice, Italy: ESA Publication WPP-306; pp. 21–25. doi:10.5270/OceanObs09.cwp.79.

Weller, R. A., M. F. Baumgartner, S. A. Josey, A. S. Fischer, and J. Kindle, 1998: Atmospheric forcing in the Arabian Sea during 1994– 1995: Observations and comparisons with climatology and models. Deep-Sea Res., 45, 1961–1999.

Yu, L., X. Jin, and R.A. Weller, 2007: Annual, Seasonal, and Interannual Variability of Air–Sea Heat Fluxes in the Indian Ocean. J. Climate, 20, 3190–3209, https://doi.org/10.1175/JCLI4163.1

Yu, L., X. Jin, S.A. Josey, T. Lee, A. Kumar, C. Wen, and Y. Xue, 2017: The Global Ocean Water Cycle in Atmospheric Reanalysis, Satellite, and Ocean Salinity. J. Climate, 30, 3829–3852, https://doi.org/10.1175/JCLI-D-16-0479.1

Zhang, Y.-C., W.B. Rossow, A.A. Lacis, V. Oinas, and M.I. Mishchenko, 2004: Calculation of radiative fluxes from the surface to top of atmosphere based on ISCCP and other global data sets: Refinements of the radiative transfer model and the input data. J. Geophys. Res., 109, D19105, doi:10.1029/2003JD004457.

Chapter 17

Balmaseda, M.A., F. Hernandez, and A. Storto, et al., (2015). The ocean reanalysis Intercomparison project (ORA-IP). J. Oper. Oceanogr., 8, 80-97, DOI:10.1080/1755876X.2015.1022329.

Dombrowsky, E., L. Bertino, and G.B. Brassington, et al. (2009). GODAE systems in operation. *Oceanography* 22(3):80–95, http://dx.doi.org/10.5670/oceanog.2009.68.

Fujii, Y., et al., 2015: Evaluation of the tropical Pacific observing system from the ocean data assimilation perspective. Q. J. Rol. Meteorol. Soc., DOI: 10.1002/qj.2579. Oct. 2015.

Huang, B., Y. Xue, and D. W. Behringer (2008). Impacts of Argo salinity in NCEP Global Ocean Data Assimilation System: The tropical Indian Ocean, J. Geophys. Res., 113, C08002, doi:10.1029/2007JC004388.

Lee, T., T. Awaji, M.A. Balmaseda, E. Greiner, and D. Stammer (2009). Ocean state estimation for climate research. *Oceanography* 22(3):160–167, http://dx.doi.org/10.5670/oceanog.2009.74.

Lee, T., T. Awaji, M. Balmaseda, et al. (2010). Consistency and fidelity of Indonesian-throughflow total volume transport estimated by 14 ocean data assimilation products. Dyn. Atmos. Oceans. doi:10.1016/j.dynatmoce.2009.12.004.

Penny et al, 2017 (Penny, S.G. and T.M. Hamill, 2017: Coupled Data Assimilation for Integrated Earth System Analysis and Prediction. Bull. Amer. Meteor. Soc., 98, ES169–ES172, https://doi.org/10.1175/BAMS-D-17-0036.1)

Rahaman, H., D. W. Behringer, S. G. Penny, *and* M. Ravichandran *(*2016*),* Impact of an upgraded model in the NCEP Global Ocean Data Assimilation System: The tropical Indian Ocean, J. Geophys. Res. Oceans, 121, 8039–8062, *doi:10.1002/2016JC012056.*

Saha, S., S. Moorthi, and H.-L. Pan et al. (2010). The NCEP Climate Forecast System Reanalysis. Bull. Amer. Meterol. Soc., https://doi.org/10.1175/2010BAMS3001.1.

Wijffels, S., G. Meyers, and J. S. Godfrey (2008). A 20-Yr Average of the Indonesian Throughflow: Regional Currents and the Interbasin Exchange. J. Phys. Oceanogr., https://doi.org/10.1175/2008JPO3987.1.

Chapter 18

Brandt, P., M. Dengler, and A. Rubino, et al. (2003). Intraseasonal variability in the southwestern Arabian Sea and its relation to the seasonal circulation, Deep Sea Res., Part II, 50, 2129–2141.

1822 Ebuchi, N., H.C. Graber, and M.J. Caruso (2012). Evaluation of Wind Vectors Observed by
1823 QuikSCAT/SeaWinds Using Ocean Buoy Data. J. Atmos Ocean Tech.
1824 https://doi.org/10.1175/1520-0426(2002)019<2049:EOWVOB>2.0.CO;2.

1825 Eigenheer, A., & Quadfasel, D. (2000). Seasonal variability of the Bay of Bengal circulation inferred
1826 from TOPEX/POSEIDON altimetry. *Journal of Geophysical Research*, 105, 3243–3252.

1827 Foltz, G., J. Vialard, and B.P. Kumar, et al. (2010). Seasonal Mixed Layer Heat Balance of the
1828 Southwestern Tropical Indian Ocean. J. Clim. https://doi.org/10.1175/2009JCLI3268.1.

1829 Fore, A.G., S.H. Yueh, and W. Tang, et al. (2016). Combined Active/Passive Retrievals of Ocean
1830 Vector Wind and Sea Surface Salinity with SMAP. IEEE Trans. Geoscience and Remote Sensing.
1831 54,12, doi:10.1109/TGRS.2016.2601486.

1832 Fu, L. (2007). Intraseasonal Variability of the Equatorial Indian Ocean Observed from Sea Surface
1833 Height, Wind, and Temperature Data. J. Phys. Oceanogr., 37, 188-202. DOI: 10.1175/JPO3006.1.

1834 Fu, L., and R. Smith (1996). Global ocean circulation from satellite altimetry and high-resolution
1835 computer simulation. Bull. Amer. Meteor. Soc., 77, 2625–2636.

1836 Fukumori, I., and O. Wang (2013), Origins of heat and freshwater anomalies underlying regional
1837 decadal sea level trends, Geophys. Res. Lett., 40, 563–567, doi:10.1002/grl.50164.

1838 Gaube, P., D. B. Chelton, and P. G. Strutton, et al. (2013). Satellite Observations of Chlorophyll,
1839 Phytoplankton Biomass and Ekman Pumping in Nonlinear Mesoscale Eddies. J. Geophys. Res.,
1840 doi:10.1002/2013JC009027.

1841 Gille, ST, S.G.L. Smith, and M. Lee (2003). Measuring the sea breeze from QuikSCAT
1842 scatterometry. Geophys. Res. Lett.. 30. DOI:.10.1029/2002gl016230.

1843 Girish kumar, M. S., M. Ravichandran, and W. Han (2013). Observed intraseasonal thermocline
1844 variability in the Bay of Bengal. JGR-Oceans, 118, 3336-3349, DOI: 10.1002/jgrc.20245.

1845 Grunseich, G., B. Subrahmanyam, and B. Wang (2013), The Madden-Julian oscillation detected in
1846 Aquarius salinity observations, *Geophys. Res. Lett.*, *40*, 5461–5466, doi:10.1002/2013GL058173.

1847 Guan, B, T. Lee, and D. Waliser, et al. (2014). Aquarius Surface Salinity and the Madden-Julian
1848 Oscillation: the Role of Salinity in Surface Layer Density and Potential Energy. Geophys. Res. Lett.,
1849 41, doi:10.1002/2014GL059704.

1850 Han, W., D.M. Lawrence, and P.J. Webster (2001). Dynamical response of equatorial Indian Ocean
1851 to intraseasonal winds: zonal flow. Geophys. Res. Lett., 28, 4215-4218. DOI:
1852 10.1029/2001GL013701.

1853 Han, W., and P.J. Webster (2002), Forcing Mechanisms of Sea-Level Interannual Variability in the
1854 Bay of Bengal, J. Phys. Oceanogr., 32, 216-239.

1855 Han, W. (2005). Origins and dynamics of the 90-day and 30–60-day variations in the equatorial
1856 Indian Ocean. J. Phys. Oceanogr., 35, 708–728. https://doi.org/10.1175/JPO2725.1.

1857 Lee, T. (2004). Decadal weakening of the shallow overturning circulation in the South Indian Ocean.
1858 *Geophys. Res. Lett.*, 31, L18305, doi:10.1029/2004GL020884.

1859 Lee, T., and M. J. McPhaden (2008). Decadal phase change in large-scale sea level and winds in
1860 the Indo-Pacific region at the end of the 20th century. *Geophys. Res. Lett.*, 35, L01605,
1861 doi:10.1029/2007GL032419.

1862 Lee, T (2016). Consistency of Aquarius sea surface salinity with Argo products on various spatial
1863 and temporal scales. Geophys. Res. Lett., 43, 10.1002/2016GL068822.

1864 Llovel, W., and T. Lee (2015). Importance and origin of halosteric contribution to sea level change
1865 in the southeast Indian Ocean during 2005-2013. 42, 1148-1157, Geophys. Res. Lett.,
1866 DOI: 10.1002/2014GL062611.

McPhaden, M. J. and M. Nagura (2014). Indian Ocean Dipole interpreted in terms of Recharge Oscillator theory. *Clim. Dyn., 42*, 1569–1586. doi 10.1007/s00382-013-1765-1.

Menezes, V. V., M. L. Vianna, and H. E. Phillips (2014), Aquarius sea surface salinity in the South Indian Ocean: Revealing annual-period planetary waves, J. Geophys. Res. Oceans, 119, 3883–3908, doi:10.1002/2014JC009935.

Nagura, M., and M. J. McPhaden (2012). The dynamics of wind-driven intraseasonal variability in the equatorial Indian Ocean, J. Geophys. Res., 117, C02001, doi:10.1029/2011JC007405.

Ramachandran, S., A. Tandon, and J. MacKinnon, et al. (2017). Submesoscale processes at shallow salinity fronts: Observations from the Bay of Bengal during the winter Monsoon, Submitted to *J. Phys. Oceanogr.*

Rao, S. A., S. K. Behera, Y. Masumoto, and T. Yamagata (2002), Interannual variability in the subsurface tropical Indian Ocean, Deep-Sea Res. II, 49, 1549–1572.

Rao, S. A., and S. K. Behera (2005). Subsurface influence on SST in the tropical Indian Ocean: Structure and interannual variability. Dyn. Atmos. Oceans, 39, 103–139.

Reul, N., S. Fournier, and J. Boutin, et al. (2013). Sea surface salinity observations from space with the SMOS satellite: A new means to monitor the marine branch of the water cycle, Surv. Geophys., 681–722.

Srinivasu, U., M. Ravichandran, and W. Han (2017). Causes for decadal reversal of North Indian Ocean sea level in recent two decades, Clim. Dyn., doi:10.1007/s00382-017-3551-y.

Suresh I., J. Vialard, and M. Lengaigne, et al. (2013). Origins of wind-driven intraseasonal sealevel variations in the North Indian Ocean coastal waveguide. Geophys. Res. Lett., 40, 5740-5744, doi:10.1002/2013GL058312.

Wang, L.-P., C.J. Koblinksky, S. Howden (2001). Annual Rossby waves in the Southern Indian Ocean: why does it appear to break down in the middle ocean? J. Phys. Oceanogr., 31, 54-74.

Wang T.Y., Y. Dy, W. Zhuang, and J.B. Wang (2015). Connection of sea level variability between the tropical western Pacific and the southern Indian Ocean during recent two decades. Science China-Earth Sci., 58, 8,1387-1396. DOI: 10.1007/s11430-014-5048-4.

Webster, P. J., A. M. Moore, and J. P. Loschnigg, et al. (1999). Coupled oceanic–atmospheric dynamics in the Indian Ocean during 1997–98. Nature, 401, 356–360.

Wentz, F.J., L. Ricciardulli, and E. Rodriquez (2017). Evaluating and Extending the Ocean Wind Climate Data Record. *IEEE J. Selected Topics in Applied Earth Observations and Remote Sensing*, 10, 5, pp. 2165-2185. doi: 10.1109/JSTARS.2016.2643641.

Xie, S.-P., H. Annamalai, and F. A. Schott, et al. (2002). Structure and mechanisms of south Indian Ocean climate variability. J. Climate, 15, 864–878.

Yang, J., L. Yu, and C. Koblinksky et al. (2001). Dynamics of the seasonalvariations in the Indian Ocean from TOPEX/POSEIDON sea surface height and an ocean model. Geophys. Res. Lett., 25, 11, 1915-1918. DOI: 10.1029/98GL01401.

Yu, L., and M.M. Rienecker (1999). Mechanisms for the Indian Ocean warming during the 1997-98 El Niño. Geophys. Res. Lett., 26, 735-738, 10.1029/1999GL900072.

Zhou, L., and R. Murtugudde (2010). Influences of Madden-Julian oscillations on the eastern Indian Ocean and the maritime continent. Dyn. Atmos. Oceans, 50, 257–274.

Chapter 19

Agarwal, N., Sharma, R., Basu, S., and Agarwal, V. K., 2008. Assimilation of sub-surface temperature profiles from Argo floats in the Indian Ocean in an Ocean General Circulation Model. *Current Science*, **95,** 495-501.

Gasparin, F., Roemmich, D., Gilson, J., and Cornuelle, B., 2015. Assessment of the Upper-Ocean Observing System in the Equatorial Pacific: The Role of Argo in Resolving Intraseasonal to Interannual Variability. *Journal of Atmospheric and Oceanic Technology*, **32,**1668-1688.

Huang, B., Xue, Y., and Behringer, D. W., 2008. Impacts of argo salinity in NCEP global ocean data assimilation system: The tropical Indian ocean. *Journal of Geophysical Research: Oceans*, **113**.

Krishnamurti, T. N., Chakraborty, A., Krishnamurti, R., Dewar, W. K., and Clayson, C. A., 2007. Passage of intraseasonal waves in the subsurface oceans. *Geophysical Research Letters*, **34,** 5.

Oke, P. R. and Schiller, A., 2007. Impact of Argo, SST, and altimeter data on an eddy-resolving ocean reanalysis. *Geophysical Research Letters*, **34**.

Oke, P. R., Brassington, G. B., Griffin, D. A., and Schiller, A., 2008. The Bluelink ocean data assimilation system (BODAS). *Ocean Modelling*, **21,** 46-70.

Prakash, S., Nair, T. M. B., Bhaskar, T. V. S. U., Prakash, P., and Gilbert, D., 2012. Oxycline variability in the central Arabian Sea: An Argo-oxygen study. *Journal of Sea Research*, **71,** 1-8.

Ravichandran, M., Girishkumar, M. S., and Riser, S., 2012. Observed variability of chlorophyll-a using Argo profiling floats in the southeastern Arabian Sea. *Deep Sea Research Part I: Oceanographic Research Papers*, **65,** 15-25.

Riser, S. C., Nystuen, J., and Rogers, A., 2008. Monsoon effects in the Bay of Bengal inferred from profiling float-based measurements of wind speed and rainfall. *Limnology and Oceanography*, **53,** 2080-2093.

Riser, S. C., Freeland, H. J., Roemmich, D., Wijffels, S., Troisi, A., Belbeoch, M., Gilbert, D., Xu, J., Pouliquen, S., Thresher, A., Le Traon, P.-Y., Maze, G., Klein, B., Ravichandran, M., Grant, F., Poulain, P.-M., Suga, T., Lim, B., Sterl, A., Sutton, P., Mork, K.-A., Velez-Belchi, P. J., Ansorge, I., King, B., Turton, J., Baringer, M., and S. R. Jayne, 2016: Fifteen years of ocean observations with the global Argo array. *Nature Clim. Change*, **6,** 145-153.

Schiller, A., Oke, P. R., Brassington, G., Entel, M., Fiedler, R., Griffin, D. A., and Mansbridge, J. V., 2008. Eddy-resolving ocean circulation in the Asian-Australian region inferred from an ocean reanalysis effort. *Progress in Oceanography*, **76,** 334-365.

Schiller, A., Wijffels, S. E., and Meyers, G. A., 2004. Design requirements for an Argo float array in the Indian Ocean inferred from observing system simulation experiments. *Journal of Atmospheric and Oceanic Technology*, **21,** 1598-1620.

Sivareddy, S., Arya Paul, Travis Sluka, Ravichandran M., and Eugenia Kalnay, 2017. The pre Argo ocean reanalyses may be seriously affected by the spatial coverage of moored buoys, Scientific Reports 7, 46685, doi:10.1038/srep46685

Vecchi G.A., and Harrison, M., 2007. An Indian Ocean Observing System Simulation Experiment, Journal of Climate, 20, 3300-3319.

Hosoda, S., Suga, T., Shikama, N., and Mizuno, K., 2009 Global Surface Layer Salinity Change Detected by Argo and Its Implication for Hydrological Cycle Intensification. *Journal of Oceanography*, **65,** 579-586, http://dx.doi.org/10.1007/s10872-009-0049-1

Durack, P. J., Wijffels, S. E., and Matear, R. J., 2012. Ocean Salinities Reveal Strong Global Water Cycle Intensification During 1950 to 2000. *Science*, **336,** 455-458, http://dx.doi.org/10.1126/science.1212222

Helm, K. P., Bindoff, N. L., and Church, J. A., 2010. Changes in the global hydrological-cycle inferred from ocean salinity. *Geophysical Research Letters*, **37,** L18701, http://dx.doi.org/10.1029/2010GL044222

Downes, S. M., Bindoff, N. L., and Rintoul, S. R., 2009. Impacts of Climate Change on the Subduction of Mode and Intermediate Water Masses in the Southern Ocean. *Journal of Climate*, **22,** 3289-3302, http://dx.doi.org/10.1175/2008JCLI2653.1

Zhang, Y. H., Yu, X. L., and Wang, F., 2008. Origins and pathways of the subsurface and intermediate water masses of the Indonesian Throughflow derived from historical and Argo data. *Acta Oceanologica Sinica*, **27,** 17-25

Zilberman, N. V., 2017: Deep Argo: Sampling the Total Ocean Volume in State of the Climate in 2016. *Bull. Am. Meteorol. Soc.*, **98,** S73-S74, https://doi.org/10.1175/2017BAMSStateoftheClimate.1

Chapter 20

Bourlès, B., R. Lumpkin, M.J. McPhaden, F. Hernandez, P. Nobre, E. Campos, L. Yu, S. Planton, A. Busalacchi, A.D. Moura, J. Servain, and J. Trotte, 2008: The PIRATA Program: History, Accomplishments, and Future Directions. *Bull. Amer. Meteor. Soc., 89*, 1111-1125.

Hood, R. R., H. W. Bange, L. Beal, L. E. Beckley, P. Burkill, G. L. Cowie, N. D'Adamo, G. Ganssen, H. Hendon, J. Hermes, M. Honda, M. J. McPhaden, M. Roberts, S. Singh, E. Urban, and W. Yu, 2015: Second International Indian Ocean Expedition (IIOE-2): A Basin-Wide Research Program. Scientific Committee on Oceanic Research, Newark, Delaware, USA.

Masumoto, Y., W. Yu, G. Meyers, N. D'Adamo, L. Beal, W.P.M. de Ruijter, M. Dyoulgerov, J. Hermes, T. Lee, J.R.E. Lutjeharms, J.P. McCreary, Jr., M.J. McPhaden, V.S.N. Murty, D. Obura, C.B. Pattiaratchi, M. Ravichandran, C. Reason, F. Syamsudin, G. Vecchi, J. Vialard, and L. Yu (2010): Observing systems in the Indian Ocean. In *Proceedings of the "OceanObs'09: Sustained Ocean Observations and Information for Society" Conference (Vol. 2)*, Venice, Italy, 21–25 September 2009, Hall, J., D.E. Harrison, and D. Stammer, Eds., ESA Publication WPP-306.

McPhaden, M.J., G. Meyers, K. Ando, Y. Masumoto, V.S.N. Murty, M. Ravichandran, F. Syamsudin, J. Vialard, L. Yu, and W. Yu, 2009: RAMA: The Research Moored Array for African-Asian-Australian Monsoon Analysis and Prediction. *Bull. Am. Meteorol. Soc., 90,* 459-480.

McPhaden, M.J., K. Ando, B. Bourlès, H.P. Freitag, R. Lumpkin, Y. Masumoto, V.S.N. Murty, P. Nobre, M. Ravichandran, J. Vialard, D. Vousden, and W. Yu, 2010: The global tropical moored buoy array. In Proceedings of the *"OceanObs'09: Sustained Ocean Observations and Information for Society" Conference (Vol. 2),* Venice, Italy, 21–25 September 2009, Hall, J., D.E. Harrison, and D. Stammer, Eds., ESA Publication WPP-306.

McPhaden, M. J., M. Ravichandran, K. Ando, V.S.N. Murty, W. Yu, 2016: RAMA-2.0. 11 pp. Unpublished manuscript available from NOAA/PMEL.

Chapter 21

Centurioni, L., A. Horányi, C. Cardinali, E. Charpentier and R. Lumpkin (2016). "A Global Ocean Observing System for Measuring Sea Level Atmospheric Pressure: Effects and Impacts on Numerical Weather Prediction." Bulletin of the American Meteorological Society **98**(2): 231-238.

Hormann, V., L.R. Centurioni, A. Mahadevan, S. Essink, E.A. D'Asaro, and B. Praveen Kumar. 2016: Variability of near-surface circulation and sea surface salinity observed from Lagrangian drifters in the northern Bay of Bengal during the waning 2015 southwest monsoon. Oceanography, 29(2), 124–133, https://doi.org/10.5670/oceanog.2016.45.

Keeley, R., Pazos, M. and Bradshaw, B., 2010: Data Management System for Surface Drifters. In Proceedings of OceanObs'09: Sustained Ocean Observations and Information for Society (Vol. 2), Venice, Italy, 21-25 September 2009, Hall, J., Harrison, D.E. & Stammer, D., Eds., ESA Publication WPP-306, doi:10.5270/OceanObs09.cwp.47

Lumpkin, R. and M. Pazos, 2007: Measuring surface currents with Surface Velocity Program drifters: the instrument, its data, and some recent results. Chapter 2 of "Lagrangian Analysis and Prediction of Coastal and Ocean Dynamics", ed. A. Griffa, A. D. Kirwan, A. Mariano, T. Özgökmen and T. Rossby, Cambridge University Press.

Lumpkin R., T. Özgökmen, and L. Centurioni, 2016: Advances in the applications of surface drifters. Annu. Rev. Mar. Sci., 9, 59-81, http:/dx.doi.org/10.1146/annurev-marine-010816-060641.

Maximenko, N., R. Lumpkin and L. Centurioni, 2014: Ocean Surface Circulation. Chapter 12 of "Ocean Circulation and Climate, 2nd Ed. A 21st century perspective", ed. G. Siedler, S. Griffies, J. Gould and J. Church, Academic Press, pp. 283-300, http://dx.doi.org/10.1016/B978-0-12-391851-2.000012-X.

Needler, G., N. Smith and A. Villwock, 1999: The Action Plan for GOOS/GCOS (Global Ocean Observing System/Global Climate Observing System) and Sustained Observations for CLIVAR (Climate Variability and Predictability Experiment). Proceedings of the International Conference on the Ocean Observing System for Climate, 18—22 October 1999, St. Raphaël, France.

Niiler, P., 2001: The world ocean surface circulation. Ocean Circulation and Climate, G. Siedler, J. Church, and J. Gould, eds., Academic Press, volume 77 of International Geophysics Series, 193–204.

Niiler, P. P., R. Davis, and H. White, 1987: Water-following characteristics of a mixed-layer drifter. Deep Sea Res., 34, 1867–1882.

Niiler, P. P., A. Sybrandy, K. Bi, P. M. Poulain and D. Bitterman (1995). "Measurements of the water-following capability of holey-sock and TRISTAR drifters." Deep-Sea Research 1 **42**: 1951-1964.

Chapter 22

Andres et al, this report.

Beal, this report.

*Domingues, C. M., J. A. Church, N. J. White, P. J. Gleckler, S. E. Wijffels, P. M. Barker, and J. R. Dunn (2008), Improved estimates of upper-ocean warming and multi-decadal sea-level rise, Nature, **453**, 1090–1095.*

Dong, L., and McPhaden, M.J. (2016). Interhemispheric SST gradient trends in the Indian Ocean prior to and during the recent global warming hiatus. Journal of Climate, doi: http://dx.doi.org/10.1175/JCLI-D-16-0130.1

Donguy, J.-R and G. Meyers (1995), Observations of Geostrophic transport in the tropical Indian Ocean, Deep Sea Research Part I Oceanographic Research Papers 42(6):1007-1028, DOI: 10.1016/0967-0637(95)00047-A

Good, S. A., M. J. Martin and N. A. Rayner, 2013. EN4: quality controlled ocean temperature and salinity profiles and monthly objective analyses with uncertainty estimates, Journal of Geophysical Research: Oceans, 118, 6704-6716, doi:10.1002/2013JC009067

*Han, W., Vialard, J., McPhaden, M. J., Lee, T., Masumoto, Y., Feng, M., & De Ruijter, W. P. (2014). Indian Ocean decadal variability: A review. Bulletin of the American Meteorological Society, **95,** 1679-1703.*

International CLIVAR Project Office, 2006: Understanding The Role Of The Indian Ocean In The Climate System — Implementation Plan For Sustained Observations. January. International CLIVAR Project Office, CLIVAR Publication Series No.100.

*Kosaka, Y., and S.-P. Xie, 2013: Recent global-warming hiatus tied to equatorial Pacific surface cooling. Nature, **501,** 403–407, doi:10.1038/nature12534.*

*Lee, S.-K., W. Park, M. O. Baringer, A. L. Gordon, B. Huber, and Y. Liu, 2015: Pacific origin of the abrupt increase in Indian Ocean heat content during the warming hiatus. Nat. Geosci., **8,** 445–449, doi:10.1038/ngeo2438.*

*Liu, Q. Y., M. Feng, D. Wang, and S. Wijffels (2015), Interannual variability of the Indonesian Throughflow transport: A revisit based on 30 year expendable bathythermograph data, J. Geophys. Res. Oceans, **120**, 8270–8282, doi:10.1002/2015JC011351.*

*Meyers, G. (1996), Variation of Indonesian throughflow and the El Niño-Southern Oscillation, J. Geophys. Res., **101**(C5), 12,255–12,263.*

*Nieves, V., J. K. Willis, and W. C. Patzert, 2015: Recent hiatus caused by decadal shift in Indo-Pacific heating. Science, **349,** 532–535, doi:10.1126/science.aaa4521.*

*Phillips, H. E., S. E. Wijffels, and M. Feng (2005), Interannual variability in the freshwater content of the Indonesian-Australian Basin, Geophys. Res. Lett., **32**, L03603*

Smith, N. R., C. J. Koblinsky Global Ocean Data Assimilation Experiment (2001) Observing the Oceans in the 21st Century: a Strategy for Global Ocean Observations. ISBN 10: 0642706182, ISBN 13: 9780642706188.

Sprintall, J., S. Wijffels, T. Chereskin and N. Bray, (2002). The JADE and WOCE I10/IR6 Throughflow Sections in the Southeast Indian Ocean. Part 2: Velocity and transports. Deep-sea Research Part II, 49, 1363-1389.

Vialard, J., 2015: Hiatus heat in the Indian Ocean, Nature Geoscience, doi:10.1038/ngeo2442.

*Wijffels, S., and G. Meyers (2004), An intersection of oceanic waveguides: Variability in the Indonesian throughflow region, J. Phys. Oceanogr., **34**, 1232–1253.*

*Wijffels, S., G. Meyers, and J. S. Godfrey (2008), A 20-yr average of the Indonesian throughflow: Regional currents and the interbasin exchange, J. Phys. Oceanogr., **38**, 1965–1978.*

*Zhuang, W., M. Feng, Y. Du, A. Schiller, and D. Wang (2013), Low-frequency sea level variability in the southern Indian Ocean and its impacts on the oceanic meridional transports, J. Geophys. Res. Oceans, **118**, 1302–1315, doi:10.1002/jgrc.20129.*

Chapter 23

Holgate, S.J., Matthews, A., Woodworth, P.L., Rickards, L.J., Tamisiea, M.E.,Bradshaw, E., Foden, P.R., Gordon, K.M., Jevrejeva, S. and Pugh, J. 2013.New data systems and products at the Permanent Service for Mean Sea Level. Journal of Coastal Research, 29, 493-504, doi:10.2112/JCOASTRES-D-12-00175.1.

IOC, 2012.The Global Sea Level Observing System (GLOSS) Implementation Plan - 2012.UNESCO/Intergovernmental Oceanographic Commission. 37pp. (IOC Technical Series No. 100). Available fromhttp://unesdoc.unesco.org/images/0021/002178/217832e.pdf.

IOC, 2015. Tsunami warning and mitigation systems to protect coastal communities. Indian Ocean tsunami Warning and Mitigation System 2005-2015. Available from http://unesdoc.unesco.org/images/0023/002336/233627e.pdf.

King, M. 2014. Priorities for installation of continuous Global Navigation Satellite System (GNSS) near to tide gauges. Technical Report. University of Tasmania. October 2014. DOI: 10.13140/RG.2.1.1781.7049.

Nidheesh, A.G., M.Lengaigne, J. Vialard, T. Izumo, A.S. Unnikrishnan, B. Meyssignac, B. Hamlington and C. de Montegut (2017). Robustness of observation-based decadal sea level variability in the Indo-Pacific Ocean, Geophysical Research Letters, 44, doi:10.1002/2017GL073955.

Woodworth, P. L., Wöppelmann, G., Marcos, M., Gravelle, M. and Bingley, R.M. 2017. Why we must tie satellite positioning to tide gauge data. Eos, Transactions of the American Geophysical Union, 98, doi:10.1029/2017EO064037. Published on 03 January 2017. https://eos.org/opinions/why-we-must-tie-satellite-positioning-to-tide-gauge-data.

Chapter 24

Anderson, J.E., and S.C. Riser, 2014. Near-surface variability of temperature and salinity in the near-tropical ocean: Observations from profiling floats, *Journal of Geophysical Research Oceans*, 119, 7433–7448, doi:10.1002/2014JC010112.

Andres, M., V. Mensah, S. Jan, M.-H. Chang, Y.-J. Yang, C.M. Lee, B. Ma, and T.S.B. Sanford, 2017. Downstream evolution of the Kuroshio's time-varying transport and velocity structure, *Journal of Geophysical Research Oceans*, 122 , doi:10.1002/2016JC012519.

Andres, M., S. Jan, T.B. Sanford, V. Mensah, L.R. Centurioni, and J.W. Book. 2015. Mean structure and variability of the Kuroshio from northeastern Taiwan to southwestern Japan. *Oceanography,* 28(4):84–95, http://dx.doi.org/10.5670/oceanog.2015.84.

Beal, L.M. and S. Elipot, 2016. Broadening not strengthening of the Agulhas Current since the early 1990s. *Nature*, 540, 570–573, doi:10.1038/nature19853.

Centurioni and Lumpkin, this report

Centurioni, L., L. Braasch, E. Di Lauro, P. Contestabile, F. De Leo, R. Casotti, L. Franco and D. Vicinanza, 2017. A new strategic wave measurement station off Naples port main breakwater. *Coastal Engineering Proceedings,* **1**(35): 36.

Cheng, L., J. Abraham, G. Goni, T. Boyer, S. Wijffels, R. Cowley, V. Gouretski, F. Reseghetti, S. Kizu, S. Dong, F. Bringas, M. Goes, L. Houpert, J. Sprintall, and J. Zhu, 2016. XBT Science: Assessment of Instrumental Biases and Errors. *Bulletin of the American Meteorological Society*, 97, 924–933, https://doi.org/10.1175/BAMS-D-15-00031.1

Donohue, K.A., D.R. Watts, K.L. Tracey, A.D. Greene and M. Kennelly, 2010. Mapping circulation in the Kuroshio Extension with an array of Current and Pressure recording Inverted Echo Sounders. *Journal of Atmospheric and Oceanic Technology*, 27, 507-527, doi:10.1175/2009JTECHO686.1.

Donohue, K.A., K.L. Tracey, D.R. Watts, M.P. Chidichimo, and T.K. Chereskin, 2016. Mean Antarctic Circumpolar Current transport measured in Drake Passage. *Geophysical Research Letters*, 43(22), 11,760–11,767, doi: 10.1002/2016GL070319.

Eriksen C.C., T.J. Osse, R.D. Light, T. Wen, T.W. Lehman, et al. 2001. Seaglider: a long-range autonomous underwater vehicle for oceanographic research, *IEEE J. Ocean. Eng*. 26:424–36

Feng et al., this report

Fratantoni, D.M., J.K. O'Brien, C. Flagg, and T. Rossby, 2017. AXIS – the Automated eXpendable Instrument System. *Journal of Atmospheric and Oceanic Technology,* under review.

Hormann, V., L.R. Centurioni, A. Mahadevan, S. Essink, E.A. D'Asaro, and B. Praveen Kumar, 2016. Variability of near-surface circulation and sea surface salinity observed from Lagrangian drifters in the northern Bay of Bengal during the waning 2015 southwest monsoon. *Oceanography*, 29 (2),124–133, http://dx.doi.org/10.5670/oceanog.2016.45.

Li, Q., D.M. Farmer, T.F. Duda, and S. Ramp, 2009. Acoustical measurement of nonlinear internal waves using the inverted echo sounder. *Journal of Atmospheric and Oceanic Technology*, 26(10), 2228-2242, doi:10.1175/2009JTECHO652.1.

Lien, R.-C., B. Ma, Y.-H. Cheng, C.R. Ho, B. Qiu, C. M. Lee, and M.-H. Chang, 2014. Modulation of Kuroshio Transport by Mesoscale Eddies at the Luzon Strait Entrance, *Journal of Geophysical Research Oceans*, 119, doi:10.1002/2013JC009548.

Lumpkin and Centurioni, 2017.

Moum, J.N., and J.D. Nash, 2009. Mixing measurements on an equatorial ocean mooring. *Journal of Atmospheric and Oceanic Technology*, 26(2):317–336, http://dx.doi.org/10.1175/2008JTECHO617.1.

2137 Moum, J. N., A. Perlin, J. D. Nash, and M. J. McPhaden, 2013. Seasonal sea surface cooling in
2138 the equatorial Pacific cold tongue controlled by ocean mixing. *Nature* 500 (7460), 64-67..

2139 Ravichandran this report

2140 Rossby, T., R. Curry, and J. Palter, 2017. Packing science into a shipping vessel. *Eos, ,*
2141 https://doi.org/10.1029/2017EO071319. Published on 28 April 2017.

2142 Rudnick D.L., S.T. Cole, 2011. On sampling the ocean using underwater gliders. *Journal of*
2143 *Geophysical Research,* 116, C08010, doi:10.1029/2010JC006849.

2144 Rudnick, D.L., 2016. Ocean Research Enabled by Underwater Gliders. *Annual Review of Marine*
2145 *Science*, 8:9.1-9.23, DOI:10.1146/annurev-marine-122414-033913.

2146 Shroyer, E., D.L. Rudnick, J.T. Farrar, B. Lim, S.K. Venayagamoorthy, L.C. St Laurent, A. Garanaik,
2147 and J. N. Moum, 2016. Modification of upper-ocean temperature structure by subsurface mixing in
2148 the presence of strong salinity stratification. *Oceanography*, 29 (2), 62|-71.

2149 Todd R.E., D.T. Rudnick, R.E. Davis, M.D. Ohman, 2011. Underwater gliders reveal rapid arrival
2150 of El Niño effects off California's coast, *Geophysical Research Letters,* 38: L03609

2151 Toole, J.M., M. Andres, I.A. Le Bras, T.M. Joyce, and M.S. McCartney, 2017. Moored observations
2152 of the Deep Western Boundary Current in the NW Atlantic: 2004-2014, *Journal of Geophysical*
2153 *Research*, under review.

2154 Warner, S.J., J. Becherer, K. Pujiana, E.L. Shroyer, M. Ravichandran, V.P. Thangaprakash, and
2155 J.N. Moum, 2016. Monsoon mixing cycles in the Bay of Bengal: A year-long subsurface mixing
2156 record. *Oceanography* 29(2):158–169, http://dx.doi.org/10.5670/ oceanog.2016.48.

2157 Wijesekera, H., E. Shroyer, A. Tandon, M. Ravichandran, D. Sengupta, S.U.P. Jinadasa, H.
2158 Fernando, et al., ASIRI: An Ocean-Atmosphere Initiative for Bay of Bengal, *Bulletin of the American*
2159 *Meteorological Society*, 2016.

2160 Zaba K.D., D.L. Rudnick, 2016. The 2014-2015 warming anomaly in the Southern California
2161 Current System observed by underwater gliders. *Geophysical Research Letters*, 43, 1241-8.